Studies on Synthesis and Properties of CF$_3$-Substituted π-Conjugated Molecules

Youhei Takeda

2010

Contents

Abbreviations

Ac	acetyl	DTA	differential thermal analysis
aq.	aqueous	EI	electron ionization
Ar	aryl	eq	equivalent
atm	atmospheric pressure	Eq.	equation
BINAP	2,2'-bis(diphenylphosphino)-1,1'-binaphthyl	Et	ethyl
		FAB	fast atom bombardment
Bn	benzyl	GC	gas chromatography
br	broad	*gem*	geminal
bp	boiling point	GPC	gel permeation chromatography
Bpin	4,4,5,5-tetramethyl-1,3,2-dioxaborolan-2-yl		
		h	hour(s)
Bu	butyl	HPLC	high-performance liquid chromatography
c	cyclo		
cat.	catalyst	HRMS	high-resolution mass spectra
CI	chemical ionization	HOMO	highest occupied molecular orbital
conc.	concentrated		
18-Cr-6	18-crown-6	Hz	hertz
Cy	cyclohexyl	*i*	iso
d	doublet	IR	infrared spectroscopy
dba	dibenzylideneacetone	LHMDS	lithium hexamethyldisilazide
DFT	density functional theory		
DIBAL-H	diisobutylaluminium-hydride	LUMO	lowest unoccupied molecular orbital
DMAP	4-dimethylaminopyridine	m	multiplet
DMF	*N*,*N*-dimethylformamide	M	metal
DMSO	dimethyl sulfoxide	Me	methyl
dppb	1,4-bis(diphenylphosphino)-butane	min	minute(s)
		mL	milliliter
dppf	1,1'-bis(diphenylphosphino)-ferrocene	μL	microliter
		mp	melting point

|			
Ms	methanesulfonyl	TBAF	tetrabutylammonium fluoride
MS	mass spectroscopy		
n	normal	TBS	*tert*-butyldimethylsilyl
NMR	nuclear magnetic resonance	Temp.	temperature
NOE	nuclear Overhauser effect	T_d	decomposition temperature
Ph	phenyl	Tf	trifluoromethanesulfonyl
PL	photoluminescence	TG	thermo gravimetry
PMMA	poly(methyl methacrylate)	THF	tetrahydrofuran
q	quartet	TLC	thin layer chromatography
quant.	quantitative	TMEDA	*N*,*N*,*N*',*N*'-tetramethyl-ethylenediamine
ref.	reference		
R_f	retention factor	Ts	*p*-toluenesulfonyl
r.t.	room temperature	UV	ultraviolet
Ruphos	2-dicyclohexylphosphino-2',6'-diisopropoxybiphenyl	vis	visible
		wt%	weight percent
s	singlet	Xphos	2-dicyclohexylphosphino-2',4',6'-triisopropylbiphenyl
t	triplet		
t, *tert*	tertiary		

Chapter 1

Introduction and General Summary
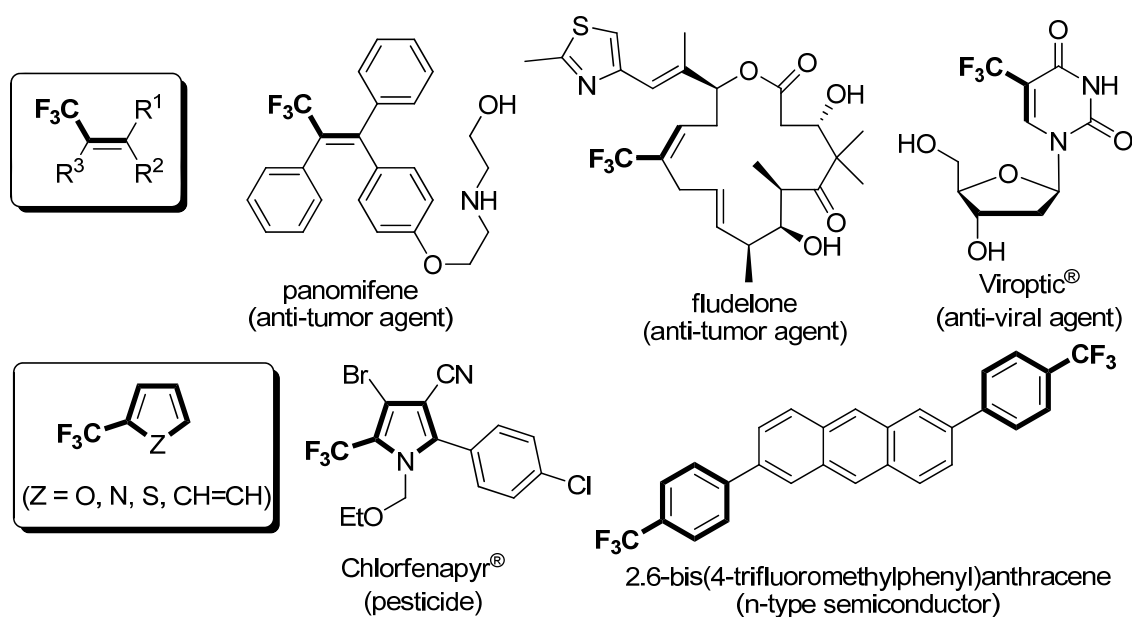
Organofluorine compounds: overview

Fluorine is the most electronegative element [electronegativity: 4.0 (Pauling)] and has a size close to hydrogen (van der Waals radii: F, 1.35 Å; H, 1.20 Å). Due to the unique nature of fluorine, incorporation of fluorine atom(s) into organic molecules often induces dipole moment and rigidity in molecular structure. Based on the profound change in physical, chemical, and biological properties compared to the fluorine-free counterparts, organofluorine compounds have found a wide variety of applications in organic functional materials, pharmaceuticals, and agrochemicals (Figure 1).[1] Fluoropolymers such as Teflon[®] and Fluon[®] have been widely utilized in industry as thermo-plastics, elastomers, membranes, textile finishes, and coatings owing to the low surface tension, and high chemical and thermal stabilities.[2] Trifluorobiphenylcyclohexane is used as a fundamental component for active matrix liquid crystalline displays (LCDs).[3] Furthermore, perfluorinated polycyclic aromatics such as perfluoropentacene[4] are promising materials for organic light-emitting diodes (OLEDs) and organic field-effect transistors (OFETs).[5] Many fluorinated compounds are also found in pharmaceuticals and agrochemicals such as Sevoflurane[®] (anesthetic),[6] Gemcitabine[®] (anti-HIV agent),[7] and Diflubenzuron[®] (insecticide).[8] Indeed, the proportion of partly fluorinated compounds to all pharmaceuticals on market continues to increase from 2% in 1970 to estimates of more than 18% at present.[9]
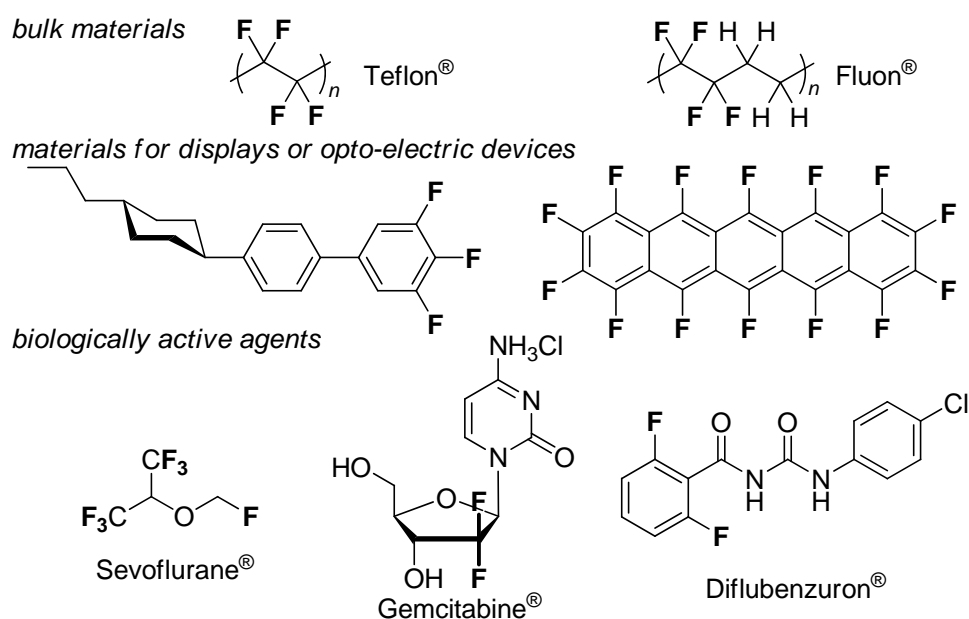
Figure 1. Examples of functional organofluorine compounds.

CF$_3$-containing compounds

A CF$_3$ group can function as a mimic of naturally occurring residues such as a carbonyl group.[9] In addition, incorporation of CF$_3$ group into organic molecules increases their lipophilicity and metabolic stability. Thus, CF$_3$-containing compounds constitute one of the largest classes in functional organofluorine compounds. Especially, CF$_3$-substituted ethenyl and (hetero)aryl moieties are found in many CF$_3$-containing pharmaceuticals and agrochemicals as exemplified with panomifene,[10] fludelone,[11] Viroptic®,[12] and Chlorfenapyr® (Figure 2).[13] Furtheremore, the CF$_3$-substituted compounds are intriguing targets in the field of materials science. For example, 2,6-bis(4-trifluoromethylphenyl)anthracene behaves as a n-type semiconductor.[14] Accordingly, efficient synthesis of CF$_3$-containing compounds is of great importance.


Figure 2. Examples of functional CF$_3$-substituted ethenes and (hetero)arenes.

Synthetic approaches for organofluorine compounds

Synthetic methods for organofluorine compounds are generally classified into two approaches: (1) *direct fluorination approach*, which involves fluorination reaction of organic compounds by a fluorinating reagent such as elemental fluorine (F$_2$) or hydrogen fluoride (HF) in the last stage of a synthetic sequence leading to the target compound; (2) *building block approach*, which includes synthetic transformations

starting from small fluorinated substrates or reagents (building blocks) that are commercially available or readily prepared from commercially sources (Figure 3). Whereas the direct fluorination requires great cares and special equipments to handle hazardous and toxic reagents, the building block strategy does not need such precautions.　Thus, this approach is much familiar to synthetic chemists.
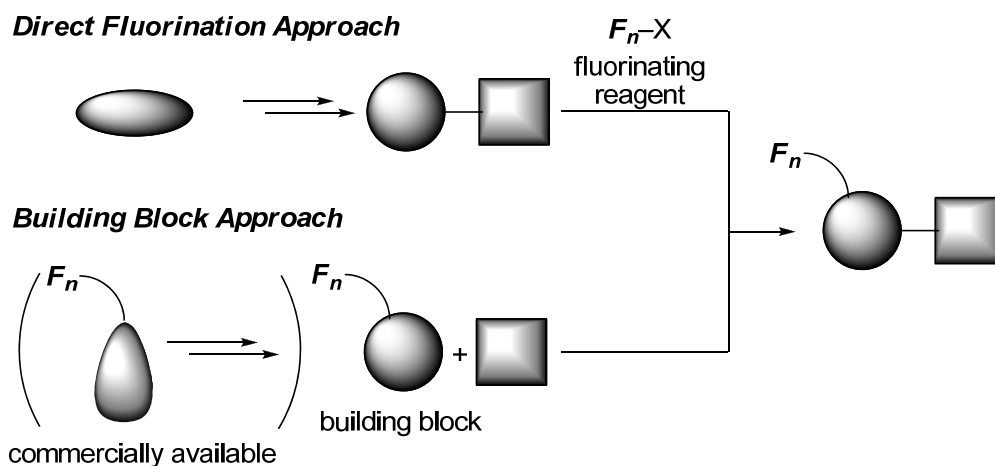

Figure 3.　Synthetic approaches for organofluorine compounds.

Classification of CF$_3$-containing building blocks

　　　Reactive species with CF$_3$-group(s) can be classified into three groups: CF$_3$-containing nucleophiles, electrophiles, and radicals (Figure 4).　Examples of nucleophilic reagents are CF$_3$-substituted organometallic reagents[15] and enolates.[16] These undergo a wide variety of reactions such as carbonyl addition, aldol addition, alkylation, and transition metal-catalyzed cross-coupling reactions.　Electrophilic reagents involve CF$_3$-substituted hypervalent compounds,[17] CF$_3$-containing carbonyl compounds,[18] trifluoropropene and -propyne derivatives,[19,20] and oxiranes.[21]　Radicalic reagents are generated in situ from CF$_3$I and CF$_3$CCl$_3$ by the action of a one-electron reductant, respectively, and add to co-existing alkenes or alkynes to give CF$_3$-substituted alkanes or alkenes, respectively.[22]

CF₃-substituted nucleophilic reagents

·organometallic reagents

CF_3CCl_2ZnCl
$CF_3CCl(ZnCl)CO_2Me$

(M = B, Zn, Sn, Li)

(M = Li, Mg, Zn, Si, Sn)
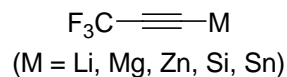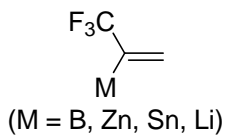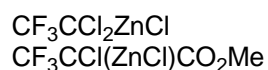
·enolates
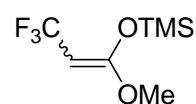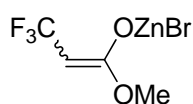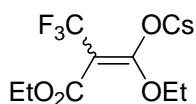
CF₃-substituted electrophilic reagents

·hypervalent compounds

(E = S, Se, Te)
(X = BF₄, OTf)
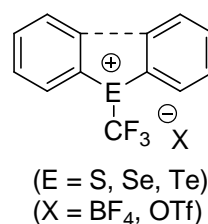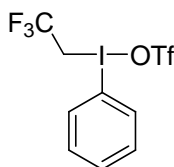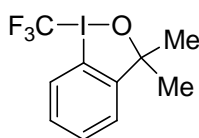
·carbonyl compounds and equivalents

(X = H, OR, SR, NR₂)

(X = H, F)

(X = H, Et)

·propene and propyne derivatives

(X = Cl, Br, I)
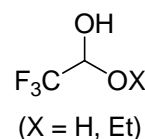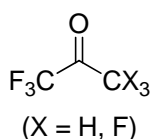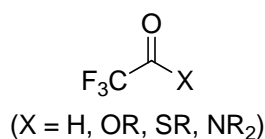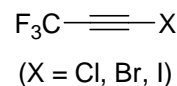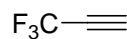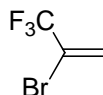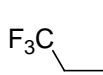
·oxiranes
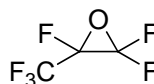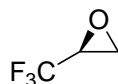
CF₃-substituted radicals
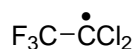
Figure 4.   Classification of CF₃-substituted building blocks.

Synthetic routes to CF₃-substituted ethenes and (hetero)arenes based on building block approach

Retrosynthetic analysis of CF₃-substituted ethenes and (hetero)arenes based on CF₃-containig building blocks is shown in Scheme 1.   Examples of each retrosynthesis will be briefly shown below.
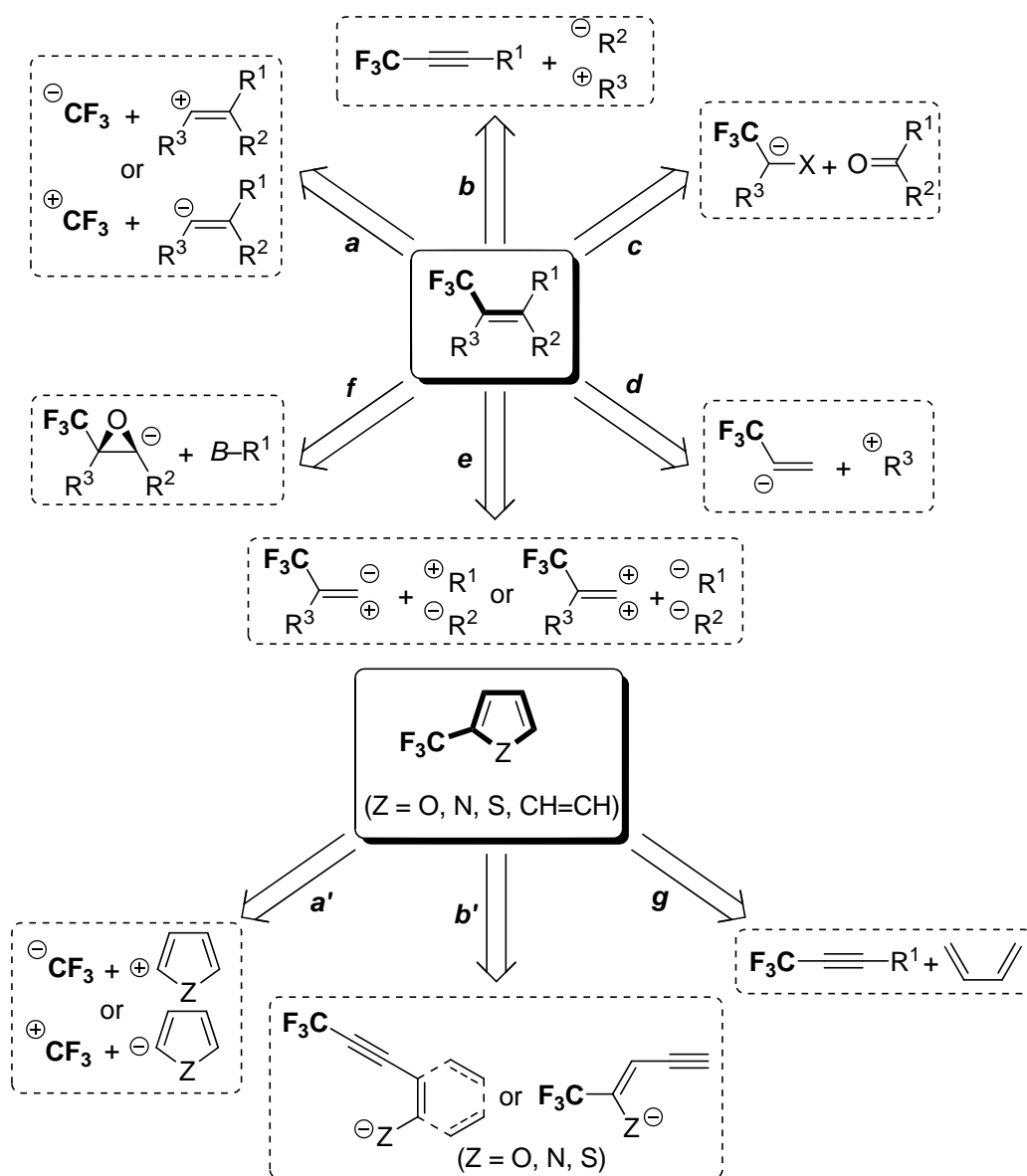
Scheme 1. Retrosynthetic analysis of CF$_3$-substituted ethenes and (hetero)arenes.

Disconnection of CF$_3$–C(sp^2) bond would be the most straightforward route (Scheme 1, route **a** and **a'**). Nucleophilic trifluoromethylation of (hetero)aryl and alkenyl iodides is feasible by using CF$_3$Cu as a CF$_3$ anion equivalent (Eq. 1).[23]
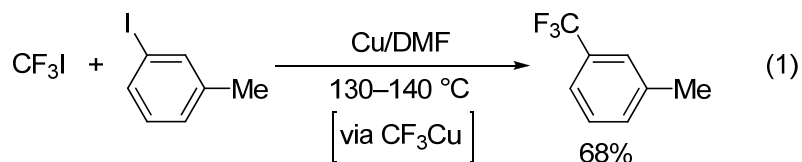
The reaction is also applicable to the corresponding bromides. However, regioisomers of trifluoromethylated products form and are accompanied by pentafluoroethylated products, which are derived from :CF$_2$ species generated in situ.

6

Separation of these is not easy in general (Eq. 2).[23c]

(2)
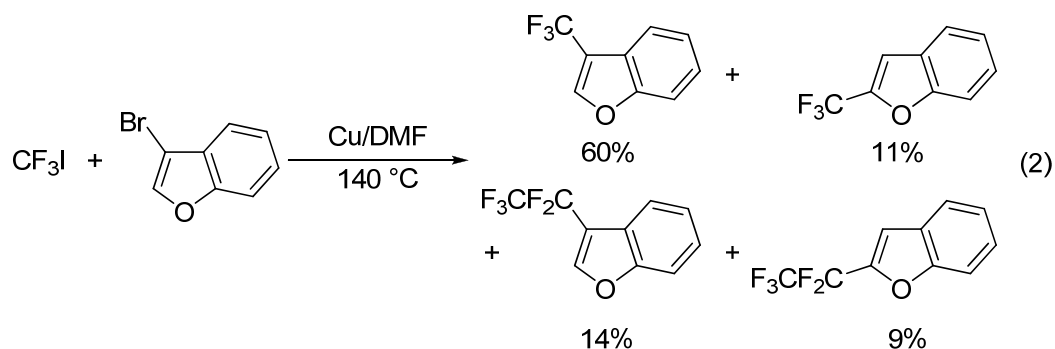
Electrophilic trifluoromethylation of electron-rich aromatics with CF_3-substituted hypervalent reagents is achieved to give a CF_3 cation equivalent (Eq. 3).[17a]   However, narrow scope of aromatic substrates and use of expensive trifluoromethylating reagents in excess limit the versatility of this approach.

(3)
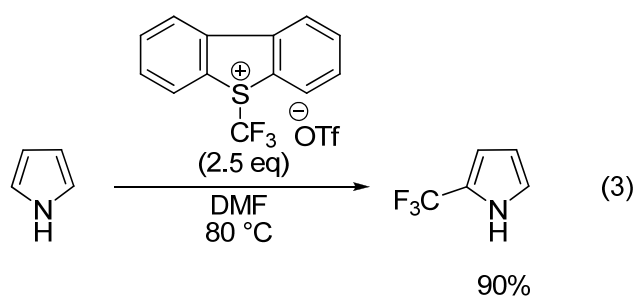
Taking advantage of electron-deficient nature of trifluoropropynes, nucleophilic addition to or cycloaddition reaction of trifluoropropynes are efficient routes to CF_3-containing polysubstituted ethenes and arenes (Scheme 1, route *b*, *b'*, and *g*). Stereoselective carbocupration of CF_3-substituted aryl acetylenes followed by trapping the resultant cuprates with electrophiles gives CF_3-containing tetrasubstituted ethenes as a single stereoisomer (Scheme 2).[24]   Since the nucleophilicity of the resulting alkenyl cuprates is not high enough, the scope of electrophiles is limited to highly reactive ones such as allylic bromides, Br_2, or I_2.
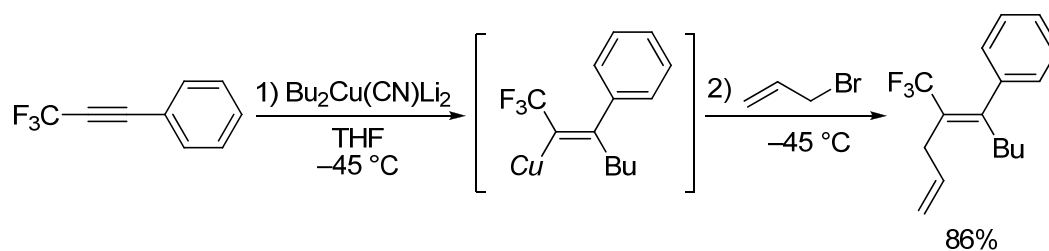
Scheme 2.   Stereoselective synthesis of CF_3-containing tetrasubstituted ethenes.

7

Intramolecular nucleophilic attack of a heteroatom to a trifluoropropynyl moiety is a simple method for the formation of CF$_3$-substituted 5-membered heteroaromatics, although yields are not high enough in general (Scheme 3).[25]
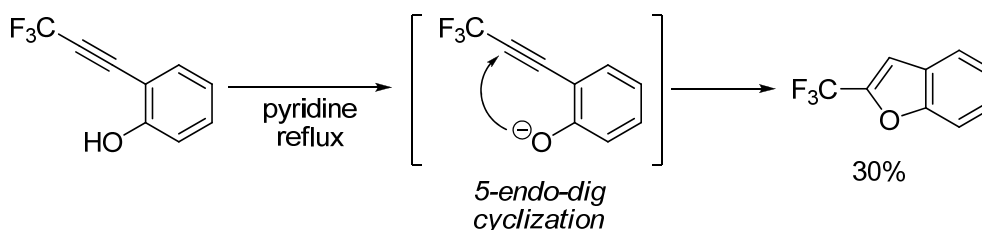
Scheme 3. Intramolecular cyclization of 2-(3,3,3-trifluoropropynyl)phenol.

Bis(trifluoromethyl)-substituted bicyclic dienes are obtained by the Diels–Alder reaction of furans with 1,1,1,4,4,4-hexafluorobutyne (Scheme 4).[26] The adducts are readily transformed into CF$_3$-polysubstituted phenols. Although the present approach is an atom-economical route, hexafluorobutyne is too volatile and hard to handle.
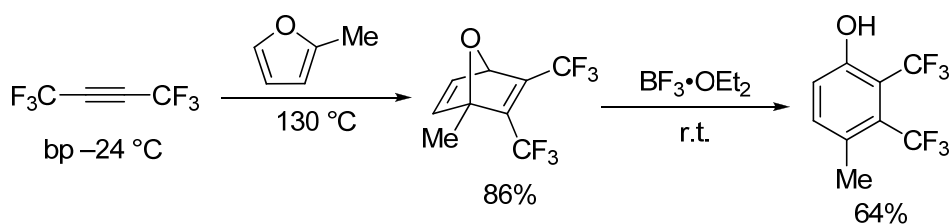
Scheme 4. Diels–Alder reaction of 1,1,1,4,4,4-hexafluorobutyne.

Route *c* (Scheme 1) represents a carbonyl addition of CF$_3$-substituted carbenoid reagents followed by elimination of M–OX (M: metal; X: halogen). Zinc carbenoid CF$_3$CCl$_2$ZnCl serves as a CF$_3$CCl$_2$ carbanion equivalent and its aldehyde addition produces a wide variety of CF$_3$CCl$_2$-substituted alcohols (Scheme 5).[27] The alcohols are readily transformed into 2-chloro-3,3,3-trifluoropropenes with high *Z*-selectivity.[28] One-pot synthesis of polyhalopropenes from aldehydes is also feasible. Synthetic utility is demonstrated by stereocontrolled synthesis of artificial insecticides, bifenthrin and cyhalothrin.[29] CF$_3$CCl$_3$ is now registered as one of Specified Chlorofluorocarbons (CFCs), which are now inhibited by the Montreal Protocol to use as such for heat carrier or cleaning of electric devices due to the possibility of ozone layer destruction.[30]
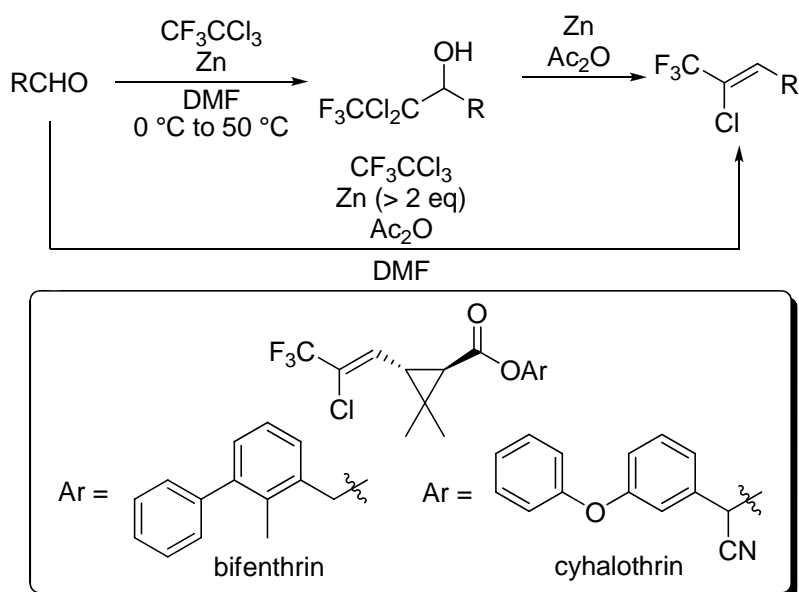
Scheme 5. Stereoselective synthesis of 2-chloro-3,3,3-trifluoropropenes.

Similar transformation using $CF_3CCl_2CO_2Me$ gives CF_3-substituted acrylates (Eq. 4).[31] In view that an ester group can serve as a versatile clue for further transformations, the present method would be an attractive route to functionalized CF_3-containing trisubstituted ethenes, although stereoselectivity remains yet to be improved.
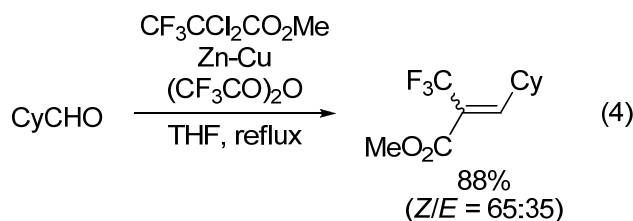
Trifluoropropenylmetals serve as a C_3 nucleophilic reagent (Scheme 1, route ***d***). Versatile examples are 1-(trifluoromethyl)ethenylboron,[32] -zinc,[33] -stannane,[34] and -lithium[35] reagents (Scheme 6). A wide variety of CF_3-containing 1,1-disubstituted ethenes are accessible with these reagents. For instance, the Suzuki-Miyaura cross-coupling of ethenylboronic acid with iodobenzene gives 2-phenyl-3,3,3-trifluoropropene.[32] A limitation of this approach is that ethenes available are restricted only to 2-substituted 3,3,3-trifluoropropenes.
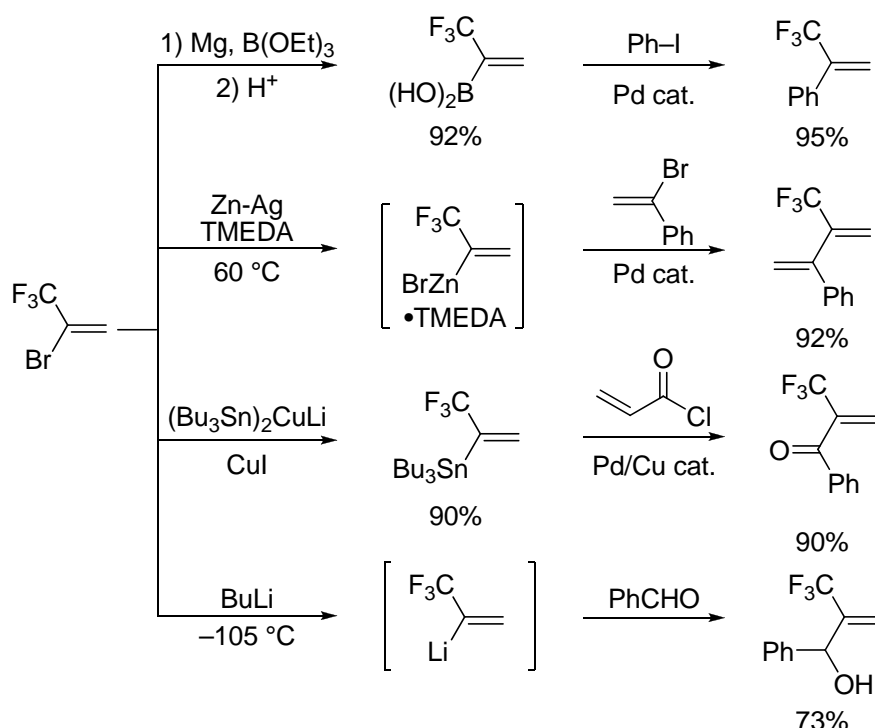
Scheme 6.   Preparation and transformations of 1-(trifluoromethyl)ethenylmetals.

Stereoselective synthesis of CF$_3$-containing tetrasubstituted ethenes and heteroarenes is feasible with 1,1-dibromo-3,3,3-trifluoropropenes CF$_3$RC=CBr$_2$ (R: carbonaceous group) when discrimination of the two bromines is realized (Scheme1, route *e*).   Bromine-lithium exchange of CF$_3$RC=CBr$_2$ in THF predominantly takes place at the *cis* position to the CF$_3$ group.   The stereoselectivity is reversed when the reaction is conducted in hexane.   Trapping the lithium carbenoids with various electrophiles gives stereo-defined CF$_3$-containing trisubstituted alkenyl bromides (Scheme 7).[36]   It should be noted that both (*Z*)- and (*E*)-isomers of alkenyl bromides can be synthesized at will by changing the solvent employed.   However, use of lithium reagents limits the functional compatibility.   The alkenyl bromides are stereospecifically converted into CF$_3$-containing tetrasubstituted ethenes.   Furthermore, CF$_3$-substituted furans are easily synthesized from the ethenes through a nucleophilic cyclization reaction (Scheme1, route *b'*).[36c,d]
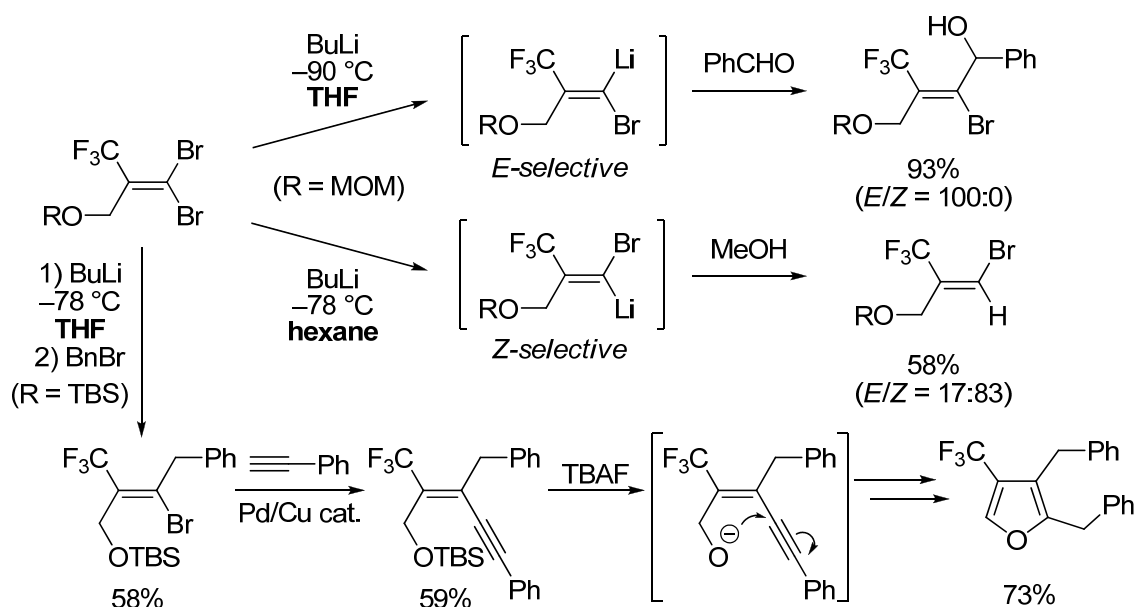
Scheme 7. Stereoselective Br-Li exchange lithiation of *gem*-dibromo olefins and reaction with an electrophile.

Stereocontrolled synthesis of CF$_3$-substituted triarylethenes is achieved via stereoselective generation of CF$_3$-substituted oxiranyllithium from CF$_3$-substituted dichlorohydrins and organolithium reagents (Scheme1, route *f*).[37] Treatment of the oxiranyllithium with bis(pinacolato)diboron gives (*E*)-*β*-CF$_3$-substituted alkenylboronates in a highly stereoselective manner. Cross-coupling reaction of the alkenylboronates produces CF$_3$-substituted triarylethenes as a single stereoisomer (Scheme 8).[38] The synthetic utility is demonstrated by synthesis of a potent anti-tumor agent, panomifene. However, use of organomagnesium and -lithium reagents limits the functional group compatibility.
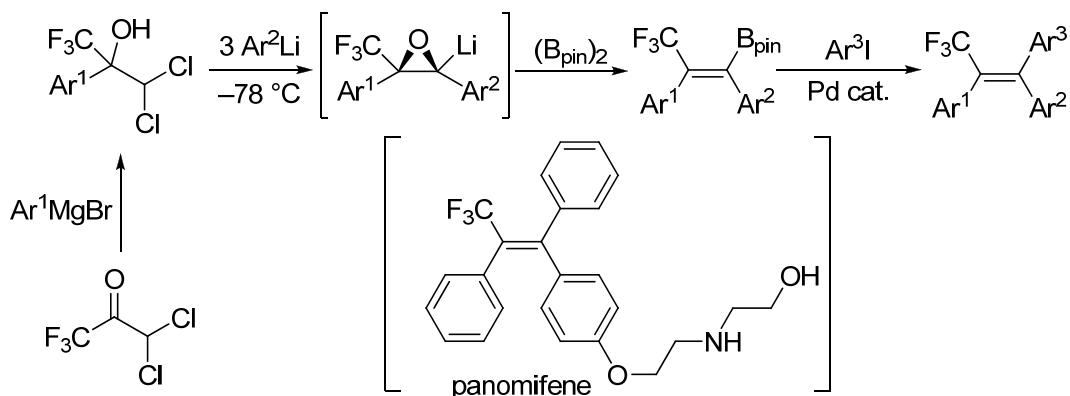
Scheme 8. Stereoselective synthesis of CF$_3$-substituted triarylethenes.

11

Through the overview of synthetic methods for CF$_3$-substituted ethenes and (hetero)arenes, several issues of the building block approach have emerged as summarized below.

(1) Many of CF$_3$-containing organometallic reagents are prepared from Specific Chlorofluorocarbons (CFCs), which are restricted to produce and use in large amounts by the Montreal Protocol because of ozone layer destructive possibility.[30] Therefore, alternative methods that start from non-Specific CFCs are preferred.

(2) Although 3,3,3-trifluoropropyne derivatives can be used as a C$_3$ electrophile, the volatility and instability limit the utility of these reagents. Hence, use of non-volatile and stable 3,3,3-trifluoropropyne derivatives is preferable.

(3) Accessible patterns of CF$_3$-containing ethenes are limited to disubstituted ethenes, and stereoselective synthetic methods for tri- or tetrasubstituted ethenes are rarely available. Furthermore, a few precedents that use lithium- and magnesium reagents lack functional group compatibility. Accordingly, highly flexible and diverse synthesis of CF$_3$-containing multisubstituted ethenes remains to be developed.

Summary of the present Thesis

To develop versatile CF$_3$-containing building blocks and their characteristic reactions for efficient access to CF$_3$-substituted ethenes and (hetero)arenes, the author has chosen 3,3-dihalo-1,1,1-trifluoropropanones as 3,3,3-trifluorine-containing C$_3$ units, because they are multi-functionalized and commercially available. He designed and utilized 1,1-dichloro-3,3,3-trifluoro-2-tosyloxypropene, trifluoropropynyliodonium salt, and 1,1-dibromo-3,3,3-trifluoro-2-tosyloxypropene as novel building blocks, and established efficient synthetic methods for CF$_3$-containing ethenes and (hetero)arenes. In addition, he created dimethoxy- and diaminobis(3,3,3-trifluoropropenyl)benzenes that exhibit fluorescence in a visible light region in the solid state.

In Chapter 2, the author describes new preparation and versatile synthetic reactions of 3,3,3-trifluoropropynyllithim, -borate, and -stannane. Quantitative generation of 3,3,3-trifluoropropynyllithium from 1,1-dichloro-3,3,3-trifluoro-2-tosyl-oxypropene, which is readily prepared from 3,3-dichloro-1,1,1-trifluoropropanone, is demonstrated (Scheme 9).
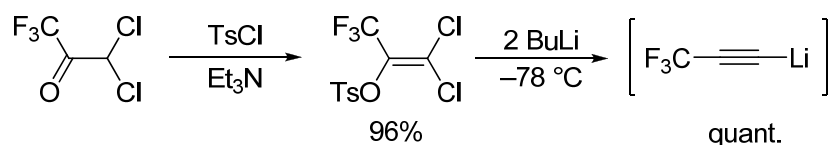
Scheme 9. Facile generation of 3,3,3-trifluoropropynyllithium.

The resulting trifluoropropynyllithium reagent is subsequently trapped with electrophiles like aldehydes, ketones, trimethoxyborane, and chlorostannane to give the corresponding propargyl alcohols, 3,3,3-trifluoropropynylborate, and -stannane, respectively (Scheme 10). Sulfonation of the carbonyl adducts followed by Pd-catalyzed S_N2' reaction with organozinc reagents provides CF_3-containing tetrasubstituted allenes. Pd-catalyzed cross-coupling reactions of the propynylborate and -stannane give rise to a series of 1-aryl-3,3,3-trifluoropropynes. Furthermore, the propynylstannane is found to undergo Pd-catalyzed carbostannylation reaction across alkynes under mild conditions, giving CF_3-substituted enynes as a single stereoisomer in good yields (Scheme 10).
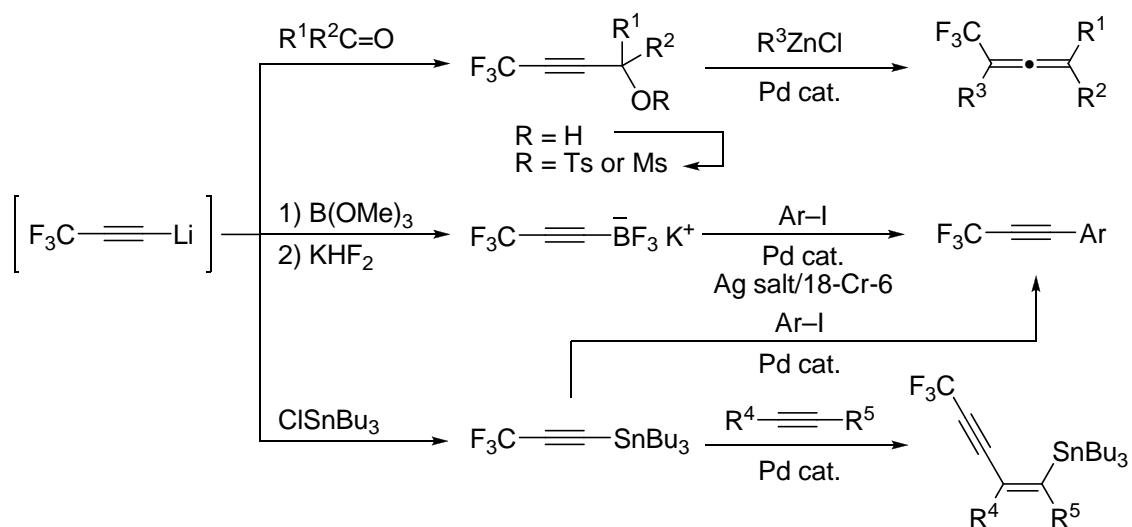
Scheme 10. Preparation and synthetic reactions of 3,3,3-trifluoropropynylmetals.

Demonstrated in Chapter 3 is the preparation of phenyl (3,3,3-trifluoropropynyl)iodonium tirfluoromethanesulfonate and its synthetic applications. The trifluoropropynyliodonium salt is successfully prepared by treatment of trifluoropropynylstannane with PhICN(OTf) for the first time (Scheme 11). The Diels–Alder reaction of the alkynyliodonium salt with 1,3-dienes gives a variety of CF_3-substituted cyclic 1,4-dienyliodonium triflates. The adducts serve as versatile

precursors for CF$_3$-containing polysubstituted arenes and cyclic dienes (Scheme 11).
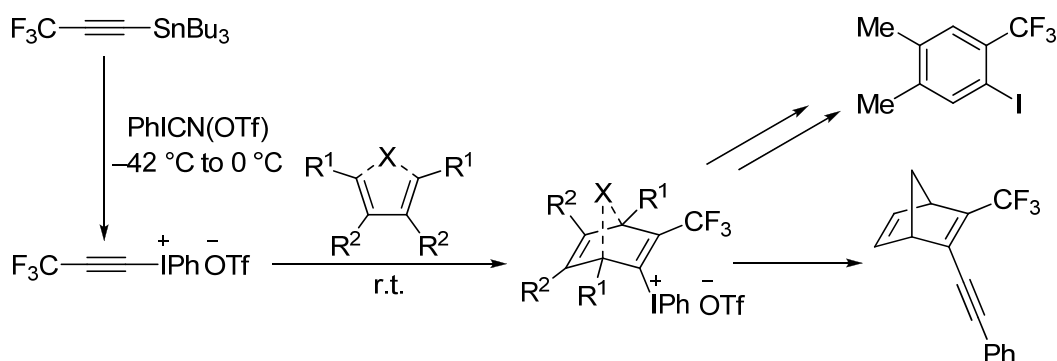
Scheme 11. Synthetic transformations of the trifluoropropynyliodonium salt.
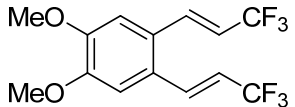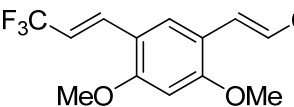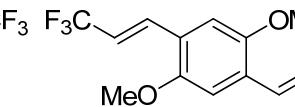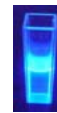
In Chapter 4, the author describes highly stereocontrolled and versatile synthesis of fully substituted 3,3,3-trifluoropropenes, taking advantage of stereoselective cross-coupling reaction of 1,1-dibromo-3,3,3-trifluoro-2-tosyloxypropene. Cross-coupling reaction of the dibromo enol tosylate with an equimolar amount of arylboronic acids and arylstannanes is found to proceed diastereoselectively with high Z-selectivity, the (Z)-mono-coupled products being easily separated from the E/Z mixture (Scheme 12). Two fold chemoselective cross-coupling reactions of the (Z)-mono-arylated products with different two arylboronic acids give CF$_3$-substituted triarylethenes as a single stereoisomer. The advantage of the present method is that any stereoisomers of the triarylethenes can be accessed simply by changing the order of boronic acids employed. Moreover, one-pot synthesis of the triarylethenes and formal synthesis of panomifene are demonstrated (Scheme 12). Taking advantage of the highly stereoselective coupling, the author has synthesized CF$_3$-substituted enynes, which can be transformed into CF$_3$-substituted furans.
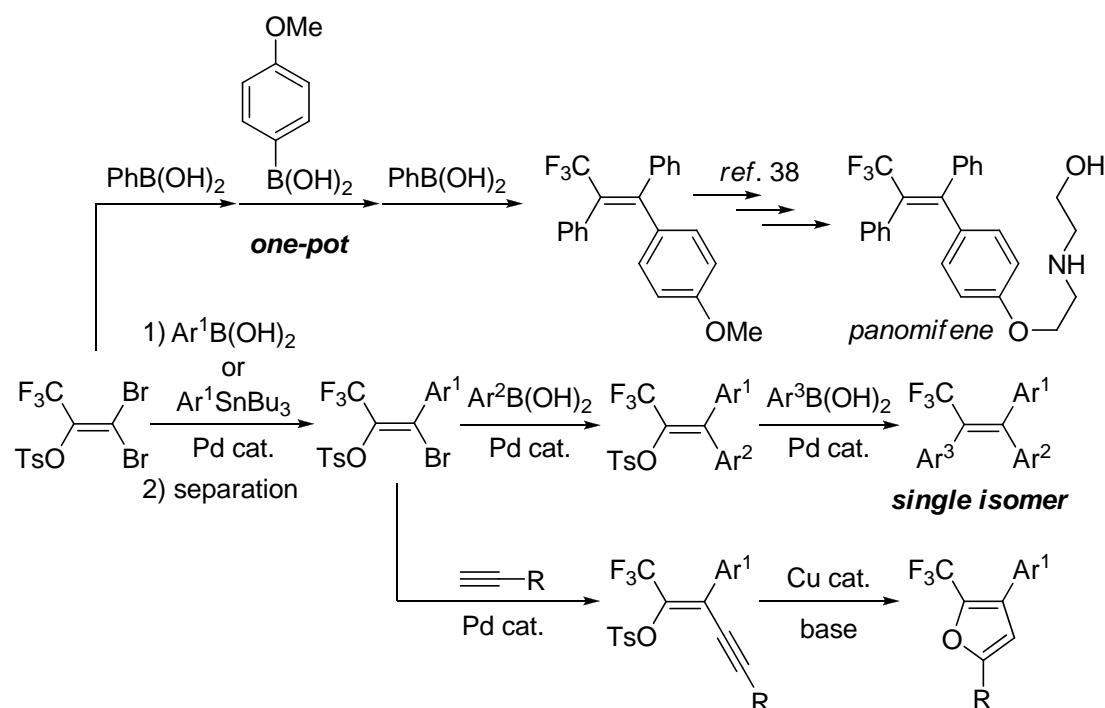
Scheme 12. Stereoselective synthesis of CF$_3$-substituted triarylethenes and enynes.

Demonstrated in Chapter 5 are synthesis, structure, photophysical properties, and theoretical calculations of dimethoxybis(3,3,3-trifluoropropenyl)benzenes. The specifically substituted benzenes are found to emit visible light from violet to blue in solution and in the solid state with absolute quantum yields (Φ_{PL}) of 0.05–0.44 (Table 1). Considering that conventional fluorophores contain multiple aromatic rings and/or polycyclic aromatic hydrocarbon skeletons, it is remarkable that the single benzene aromatic core can emit visible light.
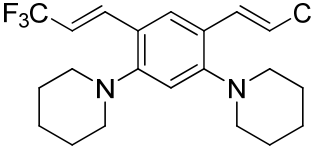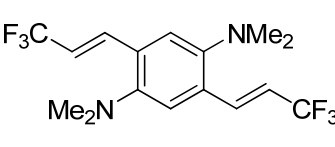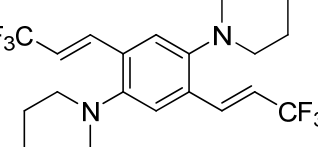
Table 1. Emission properties of dimethoxybis(trifluoropropenyl)benzenes.

solution	λ_{em}: 362 nm Φ_{PL}: 0.22		λ_{em}: 366 nm Φ_{PL}: 0.44	λ_{em}: 407 nm Φ_{PL}: 0.34
solid	λ_{em}: 380 nm Φ_{PL}: 0.05	—	λ_{em}: 397 nm Φ_{PL}: 0.12	λ_{em}: 441 nm Φ_{PL}: 0.31

The author further describes synthesis, structure, photophysical properties, and theoretical calculations of diaminobis(3,3,3-trifluoropropenyl)benzenes in Chapter 6.

It is revealed that 1,4-diamino-2,5-bis(trifluoropropenyl)benzenes emit strong green fluorescence in the solid states such as crystal, powder, thin film, and doped polymer film with extremely high Φ_{PL}, although 1,5-diamino-2,4-bis(trifluoropropenyl)benzenes exhibit low level of Φ_{PL} (Table 2).

Table 2. Emission properties of diaminobis(trifluoropropenyl)benzenes.

solution	λ_{em}: 425 nm Φ_{PL}: 0.17		λ_{em}: 521 nm Φ_{PL}: 0.57		λ_{em}: 523 nm Φ_{PL}: 0.49
solid	λ_{em}: 441 nm Φ_{PL}: 0.21		λ_{em}: 537 nm Φ_{PL}: 0.91		λ_{em}: 523 nm Φ_{PL}: 0.98

The molecular design is found to realize multi-color emission by replacing CF_3 with Me, H, CO_2Et, and acetyl groups (Figure 5). In view that conventional emissive organic solids contain multiply condensed or conjugated aromatic rings, it is remarkable that the 1,4-bis(alkenyl)-2,5-dipiperidinobenzenes exhibit extremely high quantum yields in the solid state with only one benzene ring as an aromatic core.

$(R^1, R^2 = Me, H, CF_3, CO_2Et, C(O)Me)$
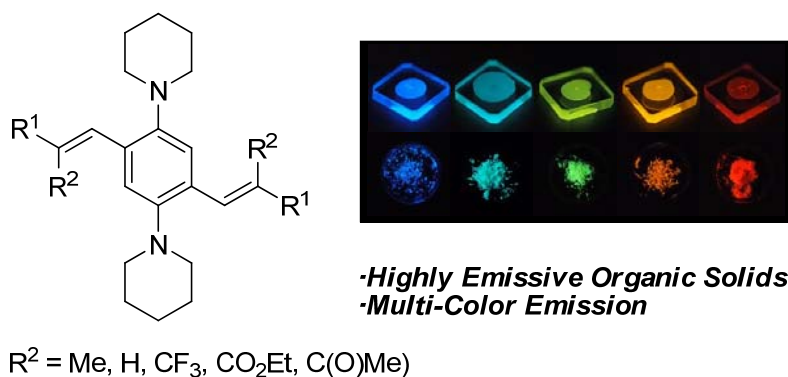
Figure 5. 1,4-Bis(alkenyl)-2,5-dipiperidinobenzenes as highly emissive organic solids.

In summary, the present Thesis demonstrates development of versatile building blocks and stereoselective and efficient synthesis of functionalized CF_3-containing ethenes and (hetero)arenes starting with 3,3-dihalo-1,1,1-trifluoropropanones. Furthermore, the author creates novel benzene-cored fluorophores based on the study of CF_3-substituted π–conjugated compounds.

References and notes

(1) General reviews on organofluorine chemistry: (a) Schlosser, M. *Tetrahedron* **1978**, *34*, 3. (b) Ishikawa, N.; Kobayashi, Y. *Fusso no Kagobutu -Sono Kagaku to Oyo-*; Kodansha: Tokyo, 1979. (c) Welch, J. T. *Tetrahedron* **1987**, *43*, 3123. (d) *Fluorine-Containing Molecules: Structure, Reactivity, Synthesis, and Applications*; Liebman, J. F., Greenberg, A., Dolbier, W. R. J., Eds.; VCH: New York, 1988. (e) Negishi, A. *Fusso no Kagaku -Atarasii Kinosei wo Motomete-*; Maruzen: Tokyo, 1988. (f) *Selective Fluorination in Organic and Bioorganic Chemistry, ACS Symposium Series 456*; Welch, J. T., Ed.; American Chemical Society: Washington, 1991. (g) *Chemistry of Organic Fluorine Compounds*; 2nd ed.; Hudlicky, M., Ed.; Ellis Horwood: New York, 1992. (h) *Organofluorine Chemistry: Principles and Commercial Applications*; Banks, R. E., Smart, B. E., Tatlow, J. C., Eds.; Plenum Press: New York, 1994. (i) *Chemistry of Organic Fluorine Compounds II: A Critical Review, ACS Monograph 187*; Hudlicky, M., Pavlath, A. E., Eds.; American Chemical Society: Washington, 1995. (j) *Biomedical Frontiers of Fluorine Chemistry, ACS Symposium Series 639*; Ojima, I., McCarthy, J. R., Welch, J. T., Eds.; American Chemical Society: Washington, 1996. (k) *Top. Curr. Chem.* **1997**, *192*, 1–244. (l) *Top. Curr. Chem.* **1997**, *193*, 1–252. (m) *Houben-Weyl*; Baasner, B., Hagemann, H., Tatlow, J. C., Eds.; Thieme: Stuttgart, 2000; Vol. E10a. (n) Hiyama, T. *Organofluorine Compounds: Chemistry and Applications*; Springer: Berlin, 2000. (o) *ChemBioChem* **2004**, *5*, 557–726; special issue on "Fluorine in Life Sciences". (p) Chambers, R. D. *Fluorine in Organic Chemistry*; Blackwell Publishing: Oxford, 2004. (q) Kirsch, P. *Modern Fluoroorganic Chemistry: Synthesis, Reactivity, Applications*; Wiley-VCH: Weinheim, 2004. (r) Leroux, F.; Jeschke, P.; Schlosser, M. *Chem. Rev.* **2005**, *105*, 827. (s) Shimizu, M.; Hiyama, T. *Angew. Chem., Int. Ed.* **2005**, *44*, 214. (t) Uneyama, K. *Organofluorine Chemistry*; Blackwell Publishing: Oxford, 2006.

(2) (a) Ref. 1h, Chapter 14–22. p 321. (b) Ref. 1n, Chapter 6.4. p 212. (c) Ref. 1q, Chapter 4.2. p 205.

(3) (a) Ref. 1h, Chapter 12. p 263. (b) Ref. 1n, Chapter 6.3. p 196. (c) Ref. 1q, Chapter 4.4. p 215.

(4) Sakamoto, Y.; Suzuki, T.; Kobayashi, M.; Gao, Y.; Fukai, Y.; Inoue, Y.; Sato, F.; Tokito, S. *J. Am. Chem. Soc.* **2004**, *126*, 8138.

(5) Reviews on recent fluorine-containing (opto)electronic materials: (a) Babudri, F.; Farinola, G. M.; Naso, F.; Ragni, R. *Chem. Commun.* **2007**, 1003. (b) Yamashita, Y. *Chem. Lett.* **2009**, *38*, 870 and references cited therein.

(6) (a) Wallin, R. F.; Regan, B. M.; Napoli, M. D.; Stern, I. J. *Anesth. Analg.* **1975**, *54*, 758. (b) Ref. 1h, Chapter 25. p 543.

(7) (a) Jiang, H. Y.; Hickey, R. J.; Abdel-Aziz, W.; Malkas, L. H. *Cancer Chem. Pharma.* **2000**, *45*, 320. (b) Baker, C. H.; Banzon, J.; Bollinger, J. M.; Stubbe, J.; Samano, V.; Robins, M. J.; Lippert, B.; Jarvi, E.; Resvick, R. *J. Med. Chem.* **2002**, *34*, 1879. (c) Pourquier, P.; Gioffre, C.; Kohlhagen, G.; Urasaki, Y.; Goldwasser, F.; Hertel, L. W.; Yu, S.; Pon, R. T.; Gmeiner, W. H.; Pommier, Y. *Clin. Cancer Res.* **2002**, *8*, 2499.

(8) (a) Robert, F. K. *Pestic. Sci.* **1978**, *9*, 259. (b) Schündehütte, K. H. *Ullmann's Encyklopädie der Technischen Chemie*; 4th ed.; Verlag Chemie: Weinheim, 1981;

Vol. 20, p 113.

(9) Reviews on fluorine in medicinal chemistry: (a) Smart, B. E. *J. Fluorine Chem.* **2001**, *109*, 3. (b) Isanbor, C.; O'Hagan, D. *J. Fluorine Chem.* **2006**, *127*, 303. (c) Bégué, J.-P.; Bonnet-Delpon, D. *J. Fluorine Chem.* **2006**, *127*, 992. (d) Kirk, K. L. *J. Fluorine Chem.* **2006**, *127*, 1013. (e) Thayer, A. M. *Chem. Eng. News* **2006**, *84*, 15. (f) Thayer, A. M. *Chem. Eng. News* **2006**, *84*, 27. (g) Romanenko, V. D.; Kukhar, V. P. *Chem. Rev.* **2006**, *106*, 3868. (h) Müller, K.; Faeh, C.; Diederich, F. *Science* **2007**, *317*, 1881. (i) Hagmann, W. K. *J. Med. Chem.* **2008**, *51*, 4359. (j) Kirk, K. L. *Org. Process. Res. Dev.* **2008**, *12*, 305.

(10) (a) Borvendeg, J. *Drugs Future* **1985**, *10*, 395. (b) Borvendeg, J.; Anheuer, Z. *Exp. Clin. Endocrino.* **1985**, *86*, 368. (c) Borvendeg, J.; Hermann, I.; Csuka, O. *Act. Phys. Hung.* **1996**, *84*, 405. (d) Erdelyi-Tóth, V.; Gyergyay, F.; Szàmel, I.; Pap, E.; Kràlovanszky, J.; Bojti, E.; Csörgo, M.; Drabant, S.; Klebovich, I. *Anti-Cancer Drugs* **1997**, *8*, 603. (e) Monostory, K.; Jemnitz, K.; Vereczkey, L.; Czira, G. *Drug Met. Disp.* **1997**, *25*, 1370.

(11) (a) Rivkin, A.; Yoshimura, F.; Gabarda, A. E.; Cho, Y. S.; Chou, T.-C.; Dong, H.; Danishefsky, S. J. *J. Am. Chem. Soc.* **2004**, *126*, 10913. (b) Cho, Y. S.; Wu, K.-D.; Moore, M. A. S.; Chou, T.-C.; Danishefsky, S. J. *Drugs Future* **2005**, *30*, 737. (c) Chou, T.-C.; Dong, H.; Zhang, X.; Tong, W. P.; Danishefsky, S. J. *Cancer Res.* **2005**, *65*, 9445. (d) Rivkin, A.; Chou, T.-C.; Danishefsky, S. J. *Angew. Chem., Int. Ed.* **2005**, *44*, 2838. (e) Wu, K.-D.; Cho, Y. S.; Katz, J.; Ponomarev, V.; Chen-Kiang, S.; Danishefsky, S. J.; Moore, M. A. S. *Proc. Natl. Acad. Sci. U.S.A.* **2005**, *102*, 10640. (f) Chou, T.-C.; Zhang, X.; Zhong, Z.-Y.; Li, Y.; Feng, L.; Eng, S.; Myles, D. R.; Johnson, R. J.; Wu, N.; Yin, Y. I.; Wilson, R. M.; Danishefsky, S. J. *Proc. Natl. Acad. Sci. U.S.A.* **2008**, *105*, 13157.

(12) (a) Kaufman, H. E.; Heidelberger, C. *Science* **1964**, *145*, 585. (b) Hyndiuk, R. A.; Kaufman, H. E.; Ellison, E.; Centifanto, Y. *Chemotherapy* **1968**, *13*, 139. (c) Wellings, P. C.; Awdry, P. N.; Bors, F. H.; Jones, B. R.; Brown, D. C.; Kaufman, H. E. *Am. J. Ophthalmol.* **1972**, *73*, 932. (d) McGill, J.; Holt-Wilson, A. D.; McKinnon, J. R.; Williams, H. P.; Jones, B. R. *Trans. Ophthalmol. Soc. U.K.* **1974**, *94*, 342. (e) Preben, G.; Kresten, W. *Acta Ophthalmologica* **1980**, *58*, 117. (f) Carmine, A. A.; Brogden, R. N.; Heel, R. C.; Speight, T. M.; Avery, G. S. *Drugs* **1982**, *23*, 329. (g) Kaufman, H. E.; Varnell, E. D.; Thompson, H. W. *Arch. Ophthalmol.* **1998**, *116*, 777.

(13) (a) Kameswaren, V. In *Advances in the Chemistry of Insect Control III*; Briggs, G. G., Ed.; The Royal Society of Chemistry: Cambridge, 1994, p 141. (b) N'Guessan, R.; Boko, P.; Odjo, A.; Akogbéto, M.; Yates, A.; Rowland, M. *Acta Trop.* **2007**, *102*, 69.

(14) Ando, S.; Nishida, J.-i.; Fujiwara, E.; Tada, H.; Inoue, Y.; Tokito, S.; Yamashita, Y. *Chem. Mater.* **2005**, *17*, 1261.

(15) Reviews on fluorinated organometallic reagents: (a) Burton, D. J.; Yang, Z.-Y. *Tetrahedron* **1992**, *48*, 189. (b) Burton, D. J.; Yang, Z.-Y.; Morken, P. A. *Tetrahedron* **1994**, *50*, 2993. (c) Burton, D. J.; Lu, L. *Top. Curr. Chem.* **1997**, *193*, 45.

(16) (a) Ishikawa, N.; Yokozawa, T. *Bull. Chem. Soc. Jpn.* **1983**, *56*, 724. (b) Yokozawa, T.; Nakai, T.; Ishikawa, N. *Tetrahedron Lett.* **1984**, *25*, 3991. (c) Yokozawa, T.; Ishikawa, N.; Nakai, T. *Chem. Lett.* **1987**, *16*, 1971.

(17) (a) Umemoto, T. *Chem. Rev.* **1996**, *96*, 1757. (b) Eisenberger, P.; Gischig, S.; Togni, A. *Chem. Eur. J.* **2006**, *12*, 2579. (c) Kieltsch, I.; Eisenberger, P.; Togni, A. *Angew. Chem., Int. Ed.* **2007**, *46*, 754. (d) Eisenberger, P.; Kieltsch, I.; Armanino, N.; Togni, A. *Chem. Commun.* **2008**, 1575. (e) Stanek, K.; Koller, R.; Togni, A. *J. Org. Chem.* **2008**, *73*, 7678. (f) Koller, R.; Stanek, K.; Stolz, D.; Aardoom, R.; Niedermann, K.; Togni, A. *Angew. Chem., Int. Ed.* **2009**, *48*, 4332.

(18) (a) Creary, X. *J. Org. Chem.* **1987**, *52*, 5026. (b) Burger, K.; Helmreich, B. *J. Chem. Soc., Chem. Commun.* **1992**, 348. (c) Kubota, T.; Iijima, M.; Tanaka, T. *Tetrahedron Lett.* **1992**, *33*, 1351. (d) Schen, Y.; Xiang, Y. *J. Fluorine Chem.* **1992**, *56*, 321. (e) Bégué, J.-P.; Bonnet-Delpon, D.; M'Bida, A. *Tetrahedron Lett.* **1993**, *34*, 7753. (f) Yamazaki, T.; Iwatsubo, H.; Kitazume, T. *Tetrahedron: Asymmetry* **1994**, *5*, 1823.

(19) (a) Fuchikami, T.; Yatabe, M.; Ojima, I. *Synthesis* **1981**, 365. (b) Fuchikami, T.; Ojima, I. *Tetrahedron Lett.* **1982**, *23*, 4099. (c) Ojima, I.; Yatabe, M.; Fuchikami, T. *J. Org. Chem.* **1982**, *47*, 2051. (d) Ojima, I. *Chem. Rev.* **1988**, *88*, 1011. (e) Hu, C.-M.; Hong, F.; Xu, Y.-Y. *J. Fluorine Chem.* **1993**, *64*, 1. (f) Hu, C.-M.; Hong, F.; Xu, Y.-Y. *J. Fluorine Chem.* **1993**, *63*, 1. (g) Hu, C.-M.; Hong, F.; Jiang, B.; Xu, Y. *J. Fluorine Chem.* **1994**, *66*, 215.

(20) (a) Trofimenko, S.; Johnson, R. W.; Doty, J. K. *J. Org. Chem.* **1966**, *43*, 43. (b) Pawlowski, G.; Hanack, M. *Synth. Commun.* **1981**, *11*, 351. (c) Kawada, K.; Kitagawa, O.; Kobayashi, Y. *Chem. Pharm. Bull.* **1985**, *33*, 3670. (d) Stepanova, N. P.; Orlova, N. A.; Galishev, V. A.; Turbanova, E. S.; Petrov, A. A. *Zh. Org. Khim.* **1985**, *21*, 979. (e) Turbanova, E. S.; Orlova, N. A.; Stepanova, N. P.; Petrov, A. A. *Zh. Org. Khim.* **1985**, *21*, 974. (f) Stepanova, N. P.; Orlova, N. A.; Turbanova, E. S.; Petrov, A. A. *Zh. Org. Khim.* **1986**, *22*, 439.

(21) (a) Takahashi, O.; Furuhashi, K.; Fukumasa, M.; Hirai, T. *Tetrahedron Lett.* **1990**, *31*, 7031. (b) Christoph Von Dem, B.-H. n.; Claudio, C.; Dieter, S. *Chemische Berichte* **1992**, *125*, 2795. (c) Katagiri, T.; Obara, F.; Toda, S.; Furuhashi, K. *Synlett* **1994**, *1994*, 507. (d) Katagiri, T. *Enantiocontrolled Synthesis of Fluoro-Organic Compounds: Stereochemical Challenges and Biomedical Targets*; Soloshonok, V. A., Ed.; Wiley: Chichester, 1999, Chapter 5, p 161. (e) Katagiri, T.; Uneyama, K. *J. Fluorine Chem.* **2000**, *105*, 285. (f) Ramachandran, P. V.; Gong, B.; Brown, H. C. *J. Org. Chem.* **2002**, *60*, 41.

(22) (a) Okano, T.; Uekawa, T.; Eguchi, S. *Bull. Chem. Soc. Jpn.* **1989**, *62*, 2575. (b) Cloux, R.; Kavats, E. *Synthesis* **1992**, *1992*, 409. (c) Ma, J.-A.; Cahard, D. *J. Fluorine Chem.* **2007**, *128*, 975.

(23) (a) Kobayashi, Y.; Kumadaki, I. *Tetrahedron Lett.* **1969**, *10*, 4095. (b) Kobayashi, Y.; Yamamoto, K.; Kumadaki, I. *Tetrahedron Lett.* **1979**, *20*, 4071. (c) Kobayashi, Y.; Kumadaki, I. *J. Chem. Soc., Perkin Trans. 1* **1980**, 661.

(24) (a) Konno, T.; Daitoh, T.; Noiri, A.; Chae, J.; Ishihara, T.; Yamanaka, H. *Org. Lett.* **2004**, *6*, 933. (b) Konno, T.; Daitoh, T.; Noiri, A.; Chae, J.; Ishihara, T.; Yamanaka, H. *Tetrahedron* **2005**, *61*, 9391.

(25) Yoneda, N.; Matsuoka, S.; Miyaura, N.; Fukuhara, T.; Suzuki, A. *Bull. Chem. Soc. Jpn.* **1990**, *63*, 2124.

(26) Chambers, R. D.; Roche, A. J.; Rock, M. H. *J. Chem. Soc., Perkin Trans. 1* **1996**, 1095.

(27) (a) Fujita, M.; Morita, T.; Hiyama, T. *Tetrahedron Lett.* **1986**, *27*, 2135. (b) Lang,

R. W. *Helv. Chimi. Acta* **1986**, *69*, 881. (c) Fujita, M.; Hiyama, T. *Bull. Chem. Soc. Jpn.* **1987**, *60*, 4377. (d) Lang, R. W. *Helv. Chim. Acta* **1988**, *71*, 369. Similar reaction using PbBr$_2$/Al system was reported: Tanaka, H.; Yamashita, S.; Katayama1, Y.; Torii, S. *Chem. Lett.* **1986**, *15*, 2043.

(28) Fujita, M.; Hiyama, T. *Tetrahedron Lett.* **1986**, *27*, 3655.

(29) (a) Fujita, M.; Hiyama, T.; Kondo, K. *Tetrahedron Lett.* **1986**, *27*, 2139. (b) Fujita, M.; Kondo, K.; Hiyama, T. *Bull. Chem. Soc. Jpn.* **1987**, *60,* 4385.

(30) Ref. 1h, Chapter 28. P 617.

(31) Allmendinger, T.; Lang, R. W. *Tetrahedron Lett.* **1991**, *32*, 339.

(32) Jiang, B.; Wang, Q.-F.; Yang, C.-G.; Xu, M. *Tetrahedron Lett.* **2001**, *42*, 4083.

(33) (a) Jiang, B.; Xu, Y. *J. Org. Chem.* **1991**, *56*, 7336. (b) Jiang, B.; Xu, Y. *Tetrahedron Lett.* **1992**, *33*, 511. (c) Jin, F.; Xu, Y.; Jiang, B. *J. Fluorine Chem.* **1993**, *65*, 111. (d) Peng, S.; Qing, F.-L.; Guo, Y. *Synlett* **1998**, 859.

(34) (a) Xu, Y.; Jin, F.; Huang, W. *J. Org. Chem.* **1994**, *59*, 2638. (b) Ichikawa, J.; Fujiwara, M.; Okauchi, T.; Minami, T. *Synlett* **1998**, 927.

(35) (a) Drakesmith, F. G.; Stewart, O. J.; Tarrant, P. *J. Org. Chem.* **1968**, *33*, 280. (b) Nadano, R.; Ichikawa, J. *Synthesis* **2006**, 128. (c) Nadano, R.; Ichikawa, J. *Chem. Lett.* **2007**, *36*, 22.

(36) (a) Uno, H.; Nibu, N.; Misobe, N. *Bull. Chem. Soc. Jpn.* **1999**, *72*, 1365. (b) Li, Y.; Lu, L.; Zhao, X. *Org. Lett.* **2004**, *6*, 4467. (c) Zhang, J.; Zhao, X.; Li, Y.; Lu, L. *Tetrahedron Lett.* **2006**, *47*, 4737. (d) Zhang, J.; Zhao, X.; Lu, L. *Tetrahedron Lett.* **2007**, *48*, 1911.

(37) (a) Shimizu, M.; Fujimoto, T.; Minezaki, H.; Hata, T.; Hiyama, T. *J. Am. Chem. Soc.* **2001**, *123*, 6947. (b) Shimizu, M.; Fujimoto, T.; Liu, X.; Minezaki, H.; Hata, T.; Hiyama, T. *Tetrahedron* **2003**, *59*, 9811.

(38) Liu, X.; Shimizu, M.; Hiyama, T. *Angew. Chem., Int. Ed.* **2004**, *43*, 879.

Chapter 2

New Preparation and Synthetic Reactions of
3,3,3-Trifluoropropynyllithium, -borate, and -stannane:
Facile Synthesis of Trifluoromethylallenes, -arylacetylenes, and -enynes

Treatment of 1,1-dichloro-3,3,3-trifluoro-2-tosyloxypropene with two equivalents of butyllithium at –78 °C generated 3,3,3-trifluoropropynyllithium quantitatively, which was trapped with such electrophiles as aldehydes, ketones, trimethoxyborane, chlorosilane, and chlorostannanes, giving rise to the corresponding carbonyl adducts, 3,3,3-trifluoropropynylborate, -silane, -stannanes, respectively, in good yields. These were transformed into trifluoromethylallenes, -arylacetylenes, and -enynes by palladium-catalyzed synthetic reactions.

1. Introduction

In view that a trifluoropropynyl moiety has a carbon–carbon triple bond useful for diverse synthetic transformations leading to various trifluoromethylated benzofurans,[1] indoles,[2] sugars,[3] pyrazoles,[4] isoquinolines,[5] and triarylethenes[6] like panomifene,[7] trifluoropropynylated reagents serve as a class of versatile building blocks (Figure 1). Hence, convenient synthetic methods of trifluoropropynylated reagents are of great significance.
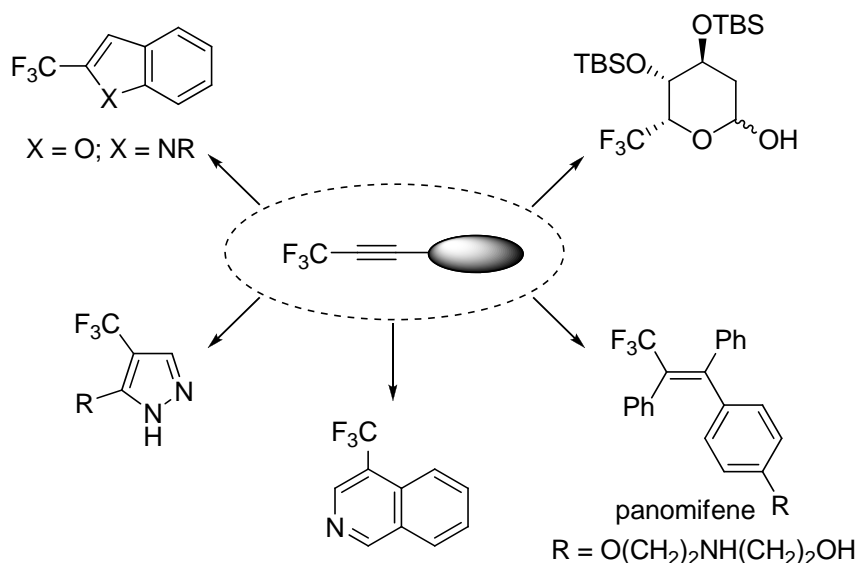
Figure 1. Trifluoromethylated targets derived from trifluoropropynyl building blocks.

Since fluorinated organometallics are highly versatile reagents for direct synthesis of organofluorine compounds, particularly when the reagents are readily accessible from commercially available fluorine-containing organic compounds and exhibit unique reactivity induced by fluorine atom(s),[8] the author has focused his attention on invention of trifluoropropynylmetal reagents. Described in this Chapter is generation of 3,3,3-trifluoropropynyllithium from 1,1-dichloro-3,3,3-trifluoro-2-tosyloxypropene, readily accessible by tosylation of commercially available 3,3-dichloro-1,1,1-trifluoropropanone (Scheme 1). The reagent was successfully employed for preparation of 3,3,3-trifluoropropynylborate and -stannane. These metal reagents are applied to the following three transformations: (1) the lithium reagent: carbonyl addition, sulfonation of the resulting adducts, and coupling reaction of the sulfonates with organozinc reagents; (2) the alkynylborate reagent: cross-coupling

reaction with aryl iodides; (3) the alkynylstannane reagent: cross-coupling reaction with aryl iodides and carbostannylation across alkynes.[9,10]
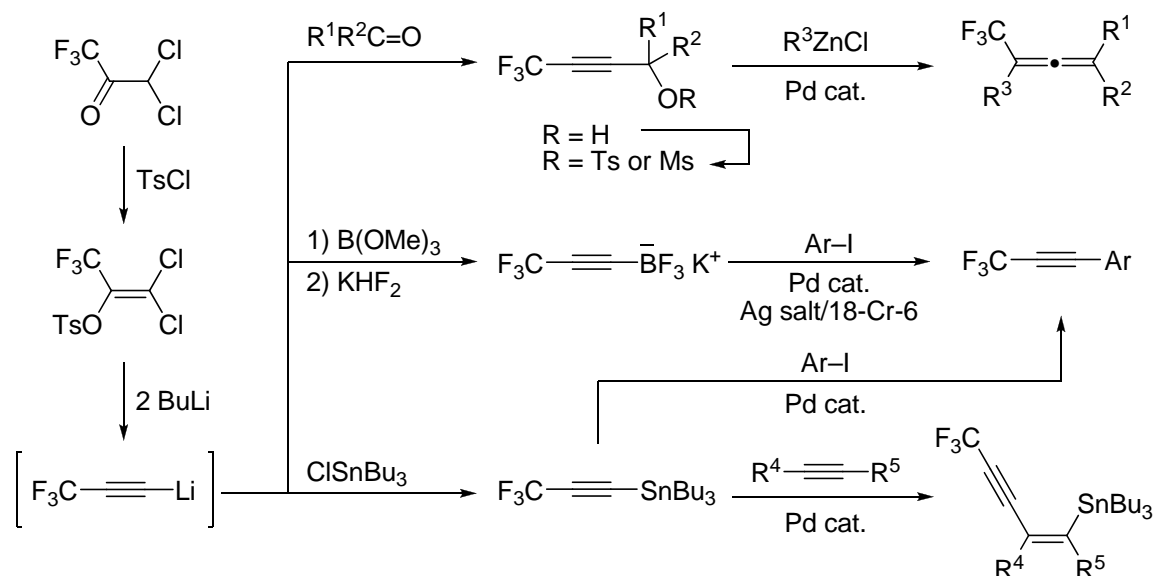
Scheme 1. Synthesis and transformations of trifluoropropynylmetal reagents.

2. Results and Discussion

2–1. Generation of 3,3,3-trifluoropropynyllithium and reaction with electrophiles

For installation of a trifluoropropynyl group into substrates, the most simple and straightforward reagent is 3,3,3-trifluoropropynyllithium (**1**). Preparative methods of **1** so far reported involve (1) deprotonation of 3,3,3-trifluoropropyne (bp –48 °C) with BuLi;[11] (2) treatment of 2-bromo-3,3,3-trifluoropropene (bp 33 °C) with two molar amounts of LDA;[3,12] (3) double dehydrofluorination and a deprotonation of 1,1,1,3,3-pentafluoropropane (bp 15 °C) with LDA;[13] (4) treatment of (Z)-2,3,3,3-tetrafluoro-1-iodopropene with two equivalents of BuLi (Scheme 2).[14] In view that these protocols start with volatile materials or require multi-step transformations, a facile method for generation of the alkynyllithium **1** is highly desired.
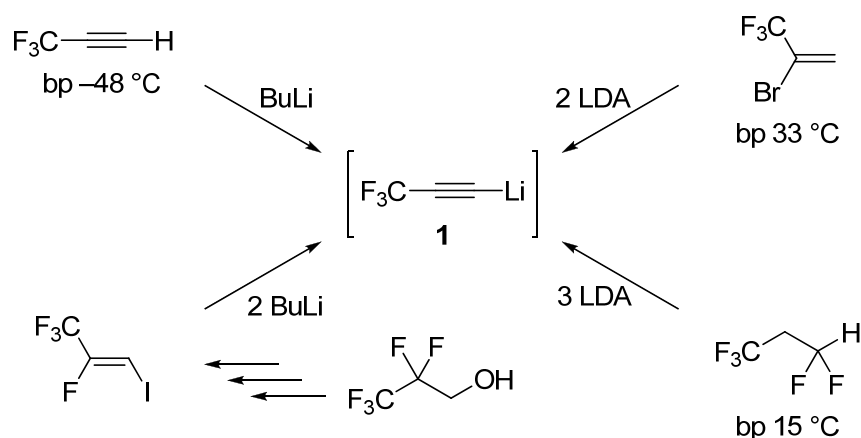
Scheme 2. Methods for generation of 3,3,3-trifluoropropynyllithium.

Recently, Shimizu and Hiyama have disclosed 3,3-dichloro-1,1,1-trifluoro-propanone (**2**) is a versatile C_3 building block for CF_3-containing compounds.[15] The present author focused his attention on a route for novel generation of **1** from 1,1-dichloro-3,3,3-trifluoro-2-(sulfonyloxy)propene (**3**), an enol sulfonate of **2**. Thus, the author considered that treatment of **3** with two molar equivalents of an organolithium reagent would generate **1** through chlorine–lithium exchange of **3** followed by β-elimination of $LiOSO_2R$ from **4**, and the second chlorine–lithium exchange of resulting **5** (Scheme 3).
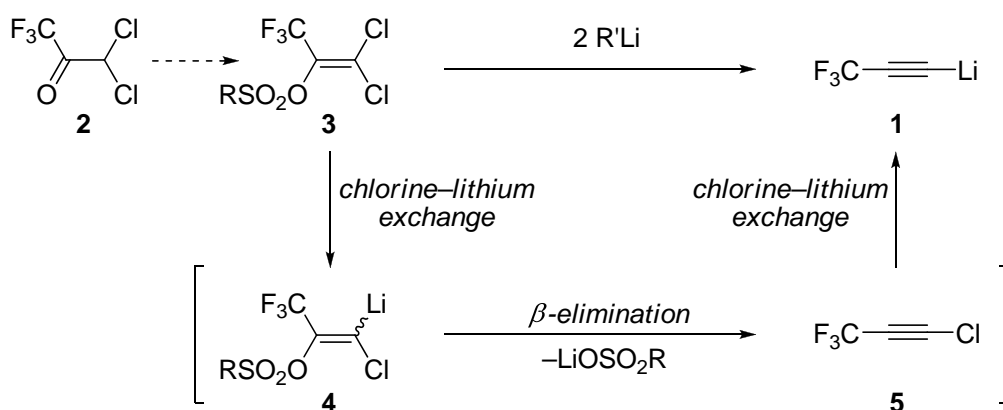
Scheme 3. Plan for the generation of **1**.

Considering that most sulfonates are solids and stable enough to handle with, the author chose a tosyl group as the substituent SO_2R in **3**. Treatment of **2** with TsCl in the presence of Et_3N gave enol tosylate **6** in high yield (Scheme 4). Tosylate **6** was easily isolated by distillation under reduced pressure (bp 122 °C/2 Torr) and a

gram-scale preparation was readily carried out.   Treatment of THF solution of **6** with two equivalents of BuLi at –78 °C for 10 min followed by addition of benzaldehyde gave propargyl alcohol **7a** in almost quantitative yield.   This result clearly indicates that the hypothetical transformation shown in Scheme 3 works well and that the alkynyllithium **1** is quantitatively generated under the conditions.   When the amount of BuLi was decreased to one equivalent, **7a** was produced in 50% yield along with 50% recovery of **6**.   This implies that the first chlorine–lithium exchange is the rate-determining step in the generation of **1** from **6** (Scheme 4).
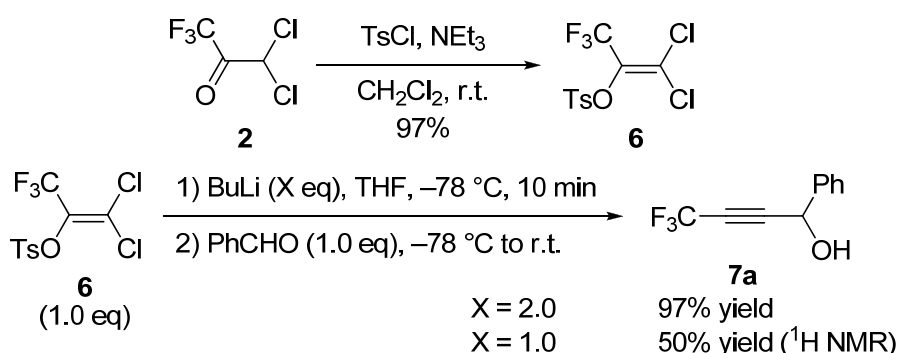
Scheme 4.   Generation of **1** from **6**.

The scope of the carbonyl addition is summarized in Scheme 5.   Both aliphatic and aromatic aldehydes as well as ketones gave the corresponding propargyl alcohols **7** in good to excellent yields.
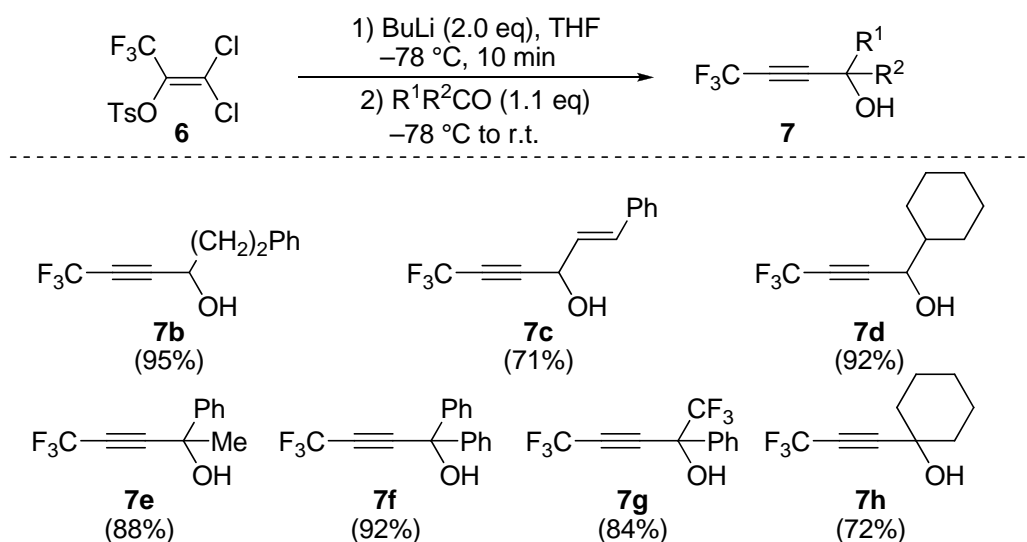
Scheme 5.   Carbonyl addition of **1**.

25

Treatment of **1** with chlorotriethylsilane, trimethoxyborane/KHF$_2$, or chlorostannanes gave 3,3,3-trifluoropropynylsilane **8**, -borate **9**,[16] or -stannanes **10** and **11**,[4,17] respectively, in moderate to high yields as illustrated in Scheme 6.

Conditions: a) Et$_3$SiCl (1.1 eq), −78 °C to r.t. (82%); b) B(OMe)$_3$, −78 °C to 0 °C, and then KHF$_2$/HF, 0 °C to r.t. (54%); c) Ph$_3$SnCl (1.2 eq), −78 °C to r.t. (50%); d) Bu$_3$SnCl, −78 °C to r.t. (64%).
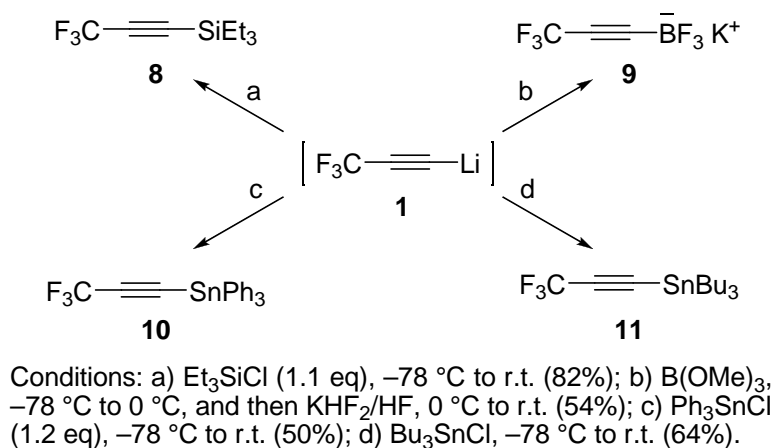
Scheme 6. Trapping of **1** with metalloid electrophiles.

2–2. Palladium-catalyzed coupling reaction of propargyl/allenyl sulfonates with organozinc reagents: facile synthesis of trifluoromethylallenes

Allenes serve as versatile substrates and/or intermediates in organic synthesis.[18] In addition, there are many allenic natural products and pharmaceuticals.[19] Therefore, fluorinated allenes can serve as not only useful intermediates for fluorinated substances but also attractive candidates for exploration and modification of biologically active allenes. On the other hand, examples of trifluoromethylallenes are quite a few so far.[20] Accordingly, novel synthetic methods for trifluoromethylallenes are indispensable for enhancement of the importance of allenes in medicinal chemistry. As palladium-catalyzed reaction of propargylic (pseudo)halides is an efficient approach to allenes,[21] the author scrutinized the Pd-catalyzed reaction of trifluoromethylated propargyl sulfonates **12**, which are readily available by sulfonation of alcohols **7**. Some of **7** were treated with TsCl or MsCl in the presence of Et$_3$N and DMAP in CH$_2$Cl$_2$ at 0 °C to room temperature. Propargyl alcohols **7b**, **7g**, and **7h** were converted into the corresponding sulfonates (**12b**, **12g**, and **12h**) in good yields, whereas sulfonyloxyallenes **13a** and **13f** were unexpectedly produced from **7a** and **7f**, respectively (Scheme 7).[22] The allene formation was confirmed by ^{13}C NMR and IR analysis. Namely, ^{13}C signals of 201.2 ppm for **13a** and 193.4 ppm for **13f** are

characteristic of the central sp carbon of an allenic moiety.   In addition, IR absorption
bands at 1973 cm^{-1} for **13a** and 1952 cm^{-1} for **13f** are assignable to stretching vibration
modes of C=C=C moiety.   Since mesylation of γ,γ-difluoroallylic alcohols was
reported to produce α,α-difluoroallylic mesylates via allylic rearrangement of the
mesyloxy group,[22a] the production of **13a** and **13f** may be ascribed to the similar
rearrangement.
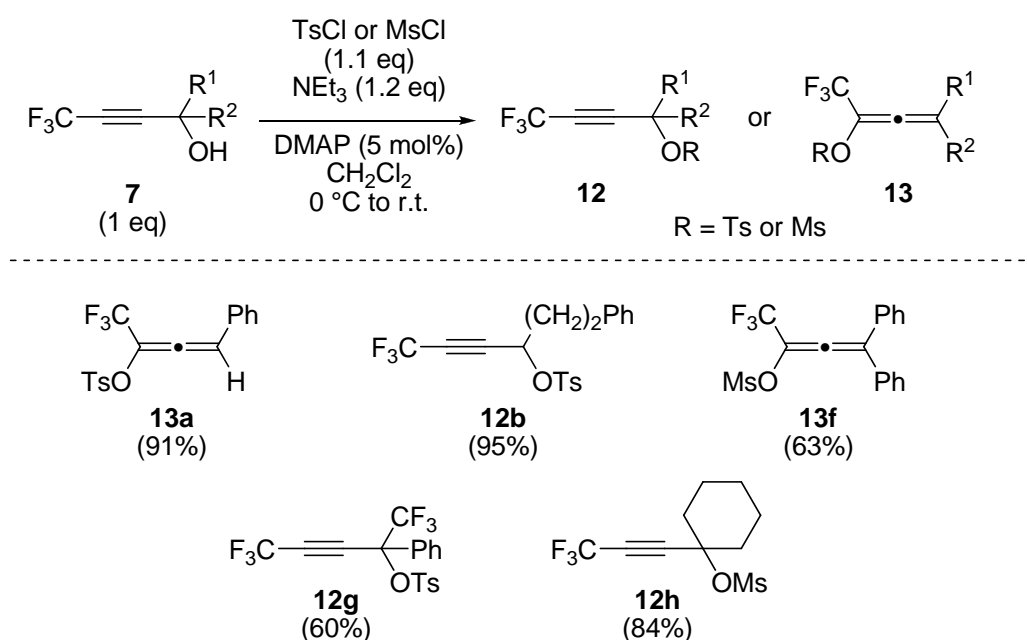
Scheme 7.   Preparation of sulfonates **12** or **13** from **7**.

Coupling reaction of these sulfonates with organozinc reagents was carried out in
the presence of Pd(PPh$_3$)$_4$ (5 mol%) in THF at 0 °C to room temperature.   The results
are summarized in Table 1.   Allenyl tosylate **13a** reacted with PhZnCl (**14a**) to give
15aa in a low yield probably due to the instability of **13a** under the reaction conditions
(entry 1).   Propargyl tosylate **12b**, in contrast, coupled with arylzinc chlorides **14a–c**
smoothly to give trifluoromethylallenes **15ba**, **15bb**, and **15bc** in moderate to high
yields, respectively (entries 2–4).   When **12b** was treated with Et$_2$Zn (**14d**), hydride
incorporation took place, giving rise to **15bd** in 86% yield (entry 5).   Formation of
such a reduced product may be ascribed to (1) oxidative addition of **12b** to Pd(0), (2)
transmetalation with Et$_2$Zn, (3) β-elimination from an ethylpalladium intermediate, and
(4) reductive elimination of the resulting hydridopalladium(II) complex.
(Trimethylsilyl)methylzinc chloride (**14e**) also reacted with **12b** to give allylic silane
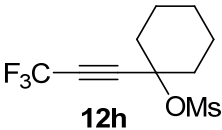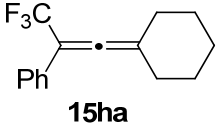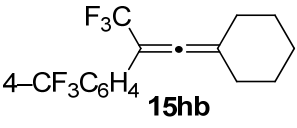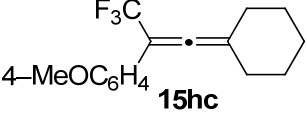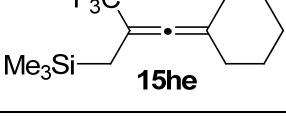
15be in a low yield (entry 6).   Both allenyl mesylate **13f** and propargyl sulfonate **12g** gave rise to the corresponding allenic products in moderate to high yields (entries 7 and 8).   The S_N2' type coupling took place with **12h** to give allenes **15a–15e** (entries 9–12).

Table 1.   Pd-catalyzed coupling reaction of **12/13** with **14**.
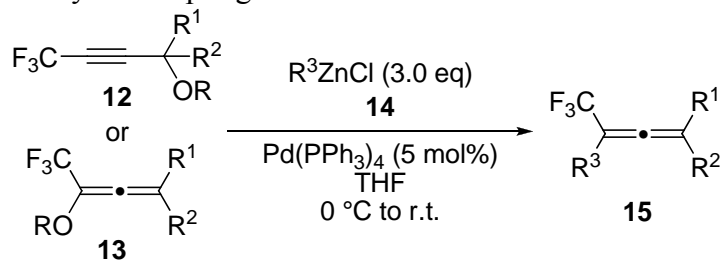
Entry	**12** or **13**	**14**	**15**	Yield (%)
1	**13a**	PhZnCl (**14a**)	**15aa**	21
2	**12b**	**14a**	**15ba**	69
3	**12b**	4–CF$_3$C$_6$H$_4$ZnCl (**14b**)	**15bb**	62
4	**12b**	4–MeOC$_6$H$_4$ZnCl (**14c**)	**15bc**	84
5	**12b**	Et$_2$Zn (**14d**)	**15bd**	86
6	**12b**	Me$_3$SiCH$_2$ZnCl (**14e**)	**15be**	31
7	**13f**	**14a**	**15fa**	94
8	**12g**	**14a**	**15ga**	65

28

9	$F_3C\text{—}\!\!\equiv\!\!\text{—}$ **12h** OMs	**14a**	F_3C, Ph $>\!=\!\bullet\!=\!<$ **15ha**	69
10	**12h**	**14b**	F_3C, $4\text{–}CF_3C_6H_4$ $>\!=\!\bullet\!=\!<$ **15hb**	59
11	**12h**	**14c**	F_3C, $4\text{–}MeOC_6H_4$ $>\!=\!\bullet\!=\!<$ **15hc**	66
12	**12h**	**14e**	F_3C, Me_3Si $>\!=\!\bullet\!=\!<$ **15he**	61

2–3. Palladium-catalyzed cross-coupling reaction of 9 and 11 with aryl iodides: facile synthesis of 3,3,3-trifluoropropynylarenes

The cross-coupling reaction of organoboron reagents with organic halides, so-called Suzuki–Miyaura coupling, is an efficient method for stereospecific bond forming reactions between sp^2 and sp carbons with a wide range of functional group compatibility.[23] The most commonly used reagents are boronic acids and boronates. Recently potassium organotrifluoroborates (RBF_4K) are emerging as a new entry of reagents for the coupling reactions, because the borates are readily available, easy to handle, and very stable toward air and moisture, keeping superior nucleophilicity.[24] Whereas preparation of potassium trifluoro(3,3,3-trifluoropropynyl)borate (**9**) has been already reported,[16] to the best of his knowledge, its Pd-catalyzed cross-coupling reaction has remained to be studied.[25] Accordingly, the author examined the coupling reaction with aryl iodides. At first, the author chose 1-iodo-4-methoxybenzene (**16a**) as a coupling partner and attempted the reaction under the conditions optimized by Molander and coworkers for Pd-catalyzed cross-coupling reaction of fluorine-free potassium alkynyltrifluoroborates with aryl halides/triflates.[26] However, no trace of desired product **17a** was obtained (Table 2, entry 1). This failure suggested the nucleophilicity of **9** might be much lower than those of fluorine-free counterparts presumably due to the strong electron-withdrawing nature of a CF_3 group. Addition of Ag_2O is reported to efficiently accelerate some Pd-catalyzed cross-coupling reactions of organoboron[27] and silicon reagents.[28] Indeed, Ag_2O (1.2 eq) upon addition to the

reaction system was effective to produce **17a** in 41% GC yield (entry 2).　Furthermore, 18–crown–6 (1.2 eq) was also used as an additive for complexation of the potassium cation with the crown ether to increase the nucleophilicity of **9**.[29]　Gratifyingly, GC yield of **17a** increased up to 59% and isolation yield was 63% yield (entry 3). Isolation yield of **17a** remained invariable even when the amount of 18–crown–6 was diminished to 0.1 equivalent (entry 5).　Under the conditions, Pd(PPh₃)₄ also worked well (entry 6).　On the other hand, decrease in the amount of Ag₂O resulted in a lower yield of **17a** (entry 7).

Table 2.　Pd-catalyzed Cross-coupling reaction of **9** with **16a**.[a]
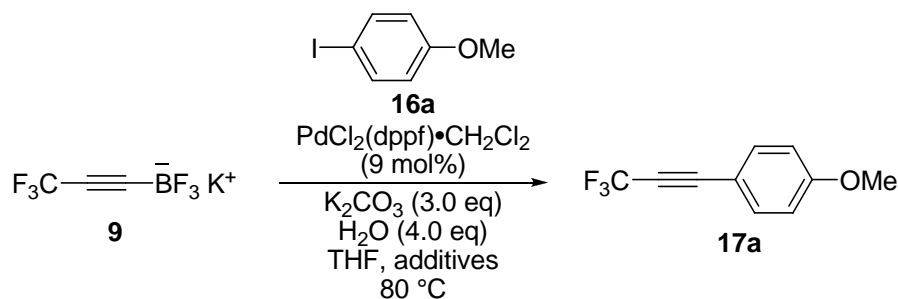
Entry	Ag$_2$O (eq)	18–crown–6 (eq)	GC yield (%)[b]
1	–	–	0
2	1.2	–	41
3	1.2	1.2	59 (63)
4	1.2	0.6	56 (60)
5	1.2	0.1	55 (60)
6[c]	1.2	0.1	– (60)
7	0.6	0.1	35

[a] Typical conditions: **9** (1.2 eq), **16a** (1.0 eq), PdCl$_2$(dppf)•CH$_2$Cl$_2$ (9 mol%), K$_2$CO$_3$ (3.0 eq), H$_2$O (4.0 eq), THF, and additives at 80 °C.　[b] Values in parentheses are isolated yields.　[c] Pd(PPh$_3$)$_4$ (10 mol%) was used in place of PdCl$_2$(dppf)•CH$_2$Cl$_2$.

　　　The scope of Pd-catalyzed/Ag-promoted coupling reaction of **9** with aryl iodides **16** is summarized in Table 3.　Iodotoluene **16b** and iodobenzene **16c** reacted with **9** to give **17b** and **17c** both in 65% yields (entries 1 and 2), whereas the reaction with iodobenzenes **16d–16f** bearing an electron-withdrawing group turned out less efficient (entries 3–5).　Yields of **17d–17f** were fairly improved when Pd(PPh₃)₄ was used as a Pd catalyst.　Nitro and formyl-substituted iodobenzenes **16g** and **16h** also underwent the coupling in moderate yields (entries 6 and 7).　It is noteworthy that the present reaction tolerated a formyl group that was not compatible with organozinc reagents

upon heating, although **17h** was isolated in a low yield due to its instability under the reaction conditions.

Table 3. Pd-catalyzed/Ag-promoted Coupling reaction of **9** with **16**.[a]

Entry	16	R	17	Yield (%) of 17[b]	
				$PdCl_2(dppf)\bullet CH_2Cl_2$	$Pd(PPh_3)_4$
1	**16b**	Me	**17b**	65	not examined
2	**16c**	H	**17c**	65	not examined
3	**16d**	CN	**17d**	43	54 (53)
4	**16e**	Ac	**17e**	30	60 (56)
5	**16f**	CO_2Et	**17f**	16	42 (43)
6	**16g**	NO_2	**17g**	not examined	43 (43)
7	**16h**	CHO	**17h**	not examined	25 (48)

[a] **9** (1.2 eq), **16** (1.0 eq), $PdCl_2(dppf)\bullet CH_2Cl_2$ (9 mol%) or $Pd(PPh_3)_4$ (10 mol%), K_2CO_3 (3.0 eq), H_2O (4.0 eq), THF, 80 °C. [b] Isolated yields. The values in parentheses are ^{19}F NMR yields.

An alternative metal reagent, stannane **11**, reacted smoothly at room temperature in the presence of $Pd_2(dba)_3$ (5 mol%) in toluene, giving rise to **17** in good to high yields as shown in Scheme 8.

17a (R = OMe, 77%)
17c (R = H, 74%)
17f (R = CO_2Et, 80%)
17g (R = NO_2, 85%)
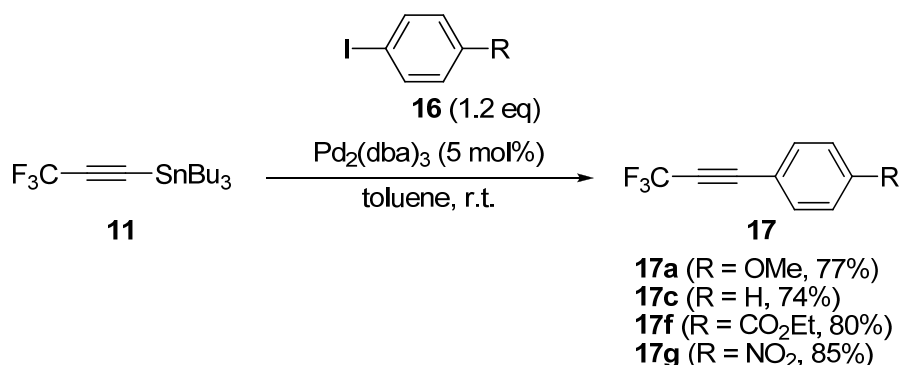
Scheme 8. Pd-catalyzed cross-coupling of **11** with **16**.

2–4. Carbostannylation of alkynes with tributyl(3,3,3-trifluoropropynyl)-stannane: stereoselective synthesis of doubly trifluoromethylated enynes

Transition metal-catalyzed carbostannylation of alkynes with alkynylstannanes produces stannylated enynes stereoselectively.[30]   This new reaction has emerged as a highly valuable carbometalation reaction, because the resulting alkenylstannane functionality serves as a clue for further synthetic transformations with a wide functional group tolerance.   Therefore, fluorinated alkynylstannanes that can efficiently undergo carbostannylation are quite attractive reagents for efficient and stereoselective preparation of fluorinated enynes/multi-substituted olefins.   During the screening study on the coupling reaction of trifluoropropynylstannane **11** with **16c**, the author found that the catalyst system consisting of 5 mol% of $Pd_2(dba)_3$ and 10 mol% of t-Bu$_3$P gave alkenylstannane **18c** in 40% yield as a single stereoisomer.   The product was ascribed to carbostannylation of the cross-coupled product **17c** with **11** (Scheme 9). Indeed, after a toluene solution of **11** (1.0 eq) and **16e** (1.0 eq) was stirred at room temperature for 8 h in the presence of $Pd_2(dba)_3$ (5 mol%), and consumption of both **11** and **16e** as well as production of cross-coupled product **17e** were confirmed by TLC monitoring, addition of t-Bu$_3$P (10 mol%) and another equivalent of **11** to the solution at room temperature gave alkenylstannane **18e** as a single stereoisomer.   These results clearly indicate that **11** can undergo carbostannylation across alkynes with the catalyst system of $Pd_2(dba)_3$ and t-Bu$_3$P.
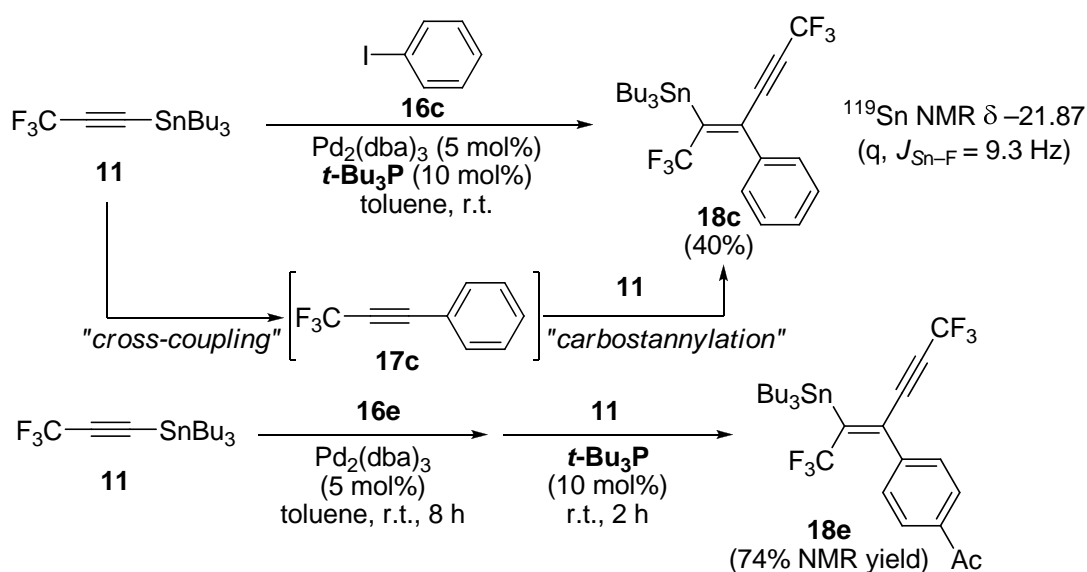
Scheme 9.   Discovery of Pd-catalyzed carbostannylation of alkynes with **11**.

Then, the author examined the generality of the alkyne-carbostannylation reaction of **11**. Initially, the reaction with terminal alkynes was investigated. Under the same conditions, arylethynes **19a–19d** were carbostannylated with **11** at room temperature to give **20a–20d** as a stereochemically pure form in high yields (Scheme 10), respectively. The stereochemistry of **20b** was determined as *Z* by NOE experiment of the *ortho*-aromatic hydrogen with the olefinic hydrogen, and the protonolysis of the C–Sn bond leading to the formation of 1,1-disubstituted ethene **23b**. This result indicates a general rule: the reaction proceeds via *syn*-addition, and the Bu₃Sn group that is bulkier than the CF₃CC group connects to a less hindered *sp* carbon. Meanwhile, methyl propiolate (**21a**) and *N,N*-dimethylpropiolamide (**21b**) also reacted with **11** to give **22a** and **22b** as a single stereoisomer, respectively. The opposite regiochemistry in the formation of **22** was confirmed by the protonolysis of **22** to give *trans*-olefins **24**.
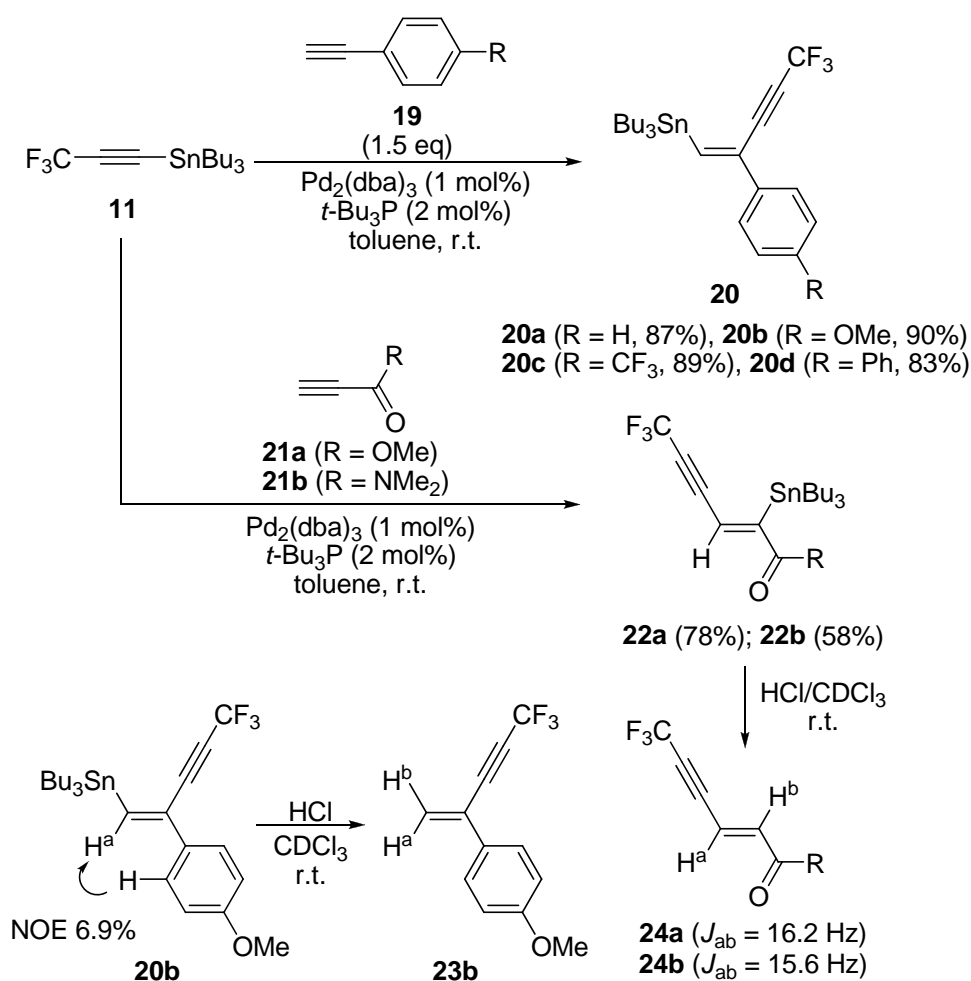
Scheme 10. Carbostannylation of terminal alkynes.

33

The carbostannylation reaction across internal alkynes was next examined using **11**. The addition of **11** across 1-aryl-3,3,3-trifluoropropynes **17** took place at room temperature under the same conditions to give **18** as a sole product (Scheme 11).
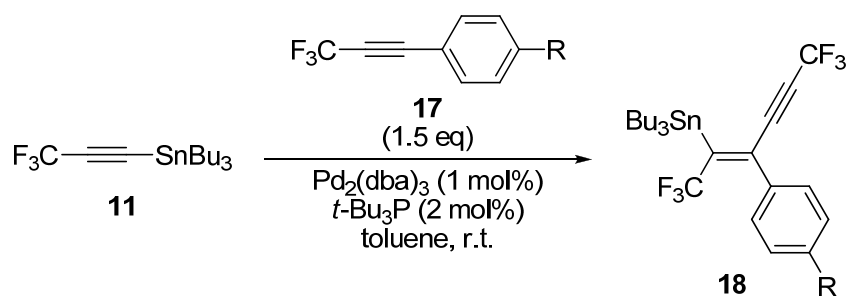
18a (R = OMe, 67%), **18b** (R = Me, 52%), **18c** (R = H, 76%), **18e** (R = Ac, 68%),
18f (R = CO$_2$Et, 57%), **18g** (R = NO$_2$, 58%),**18i** (R = CF$_3$, 67%), **18k** (R = Cl, 62%)

Scheme 11.   Carbostannylation across internal alkynes.

It should be noted that CF$_3$-substituted alkynylstannane **11** undergoes carbostannylation across internal alkynes, in sharp contrast to fluorine-free alkynylstannanes.   Various functional groups such as methoxy, acetyl, ethoxycarbonyl, nitro, and chloro tolerated the reaction conditions.   Methyl- and phenyl-substituted propiolate derivatives **25** and **27** as well as acetylenedicarboxylate **29** reacted with **11** to give **26**, **28**, and **30** as a single stereoisomer in good to high yields, respectively (Scheme 12).   The Michael-type addition of a trifluoropropynyl group was confirmed by the reduction of the ethoxycarbonyl group of **26** leading to **31** in which vicinal coupling between the methylene (H^a) and olefinic hydrogens (H^b) was observed by ^{1}H NMR.   Since diphenylacetylene and oct-4-yne did not react with **11** at all, the presence of such an electron-withdrawing group as CF$_3$ and CO$_2$R appears to be essential for the successful transformation.

Scheme 12.

Me——≡——CO$_2$Et
25

Ph——≡——CO$_2$Et
27

MeO$_2$C——≡——CO$_2$Me
29

F$_3$C——≡——SnBu$_3$
11

Pd$_2$(dba)$_3$ (1 mol%)
t-Bu$_3$P (2 mol%)
toluene, r.t.

26 (77%)

28 (87%)

30 (71%)

26 → DIBAL-H, toluene, −78 °C → HCl, CDCl$_3$, r.t. → **31**

H^a : δ 4.29 (d, J = 6.6 Hz, 2H)
H^b : δ 6.27 (t, J = 6.6 Hz, 1H)
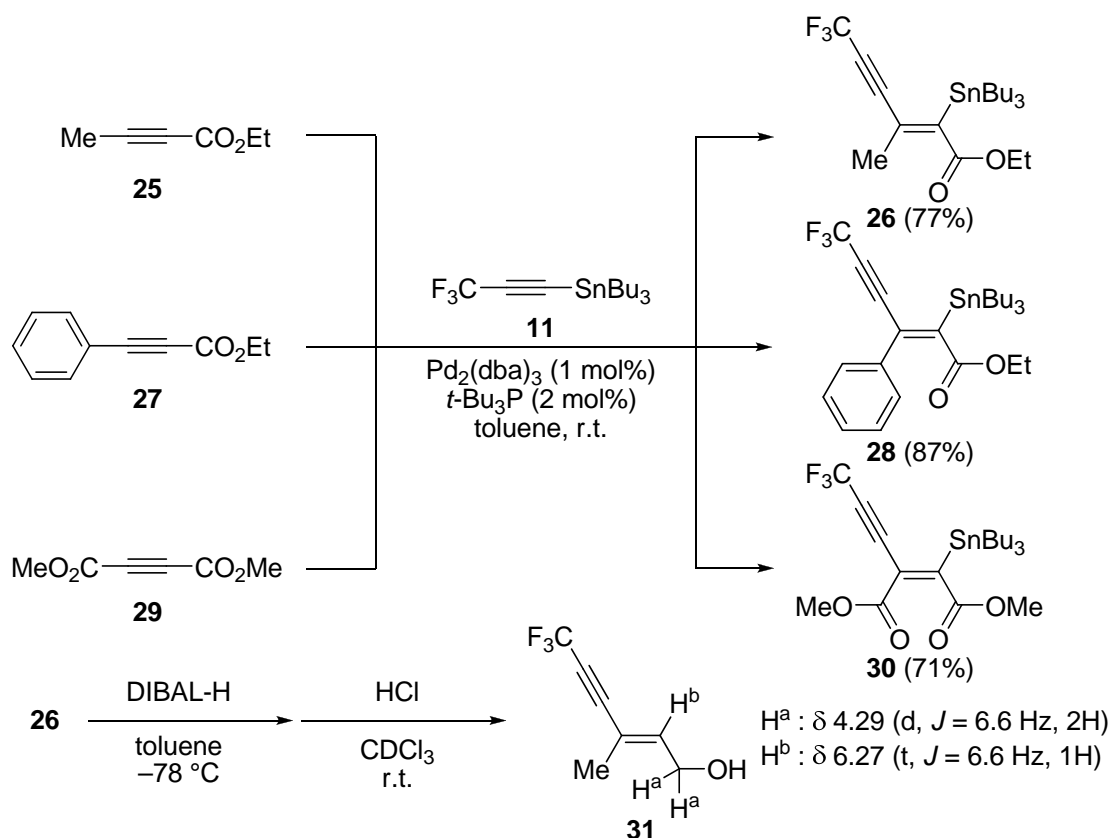
Scheme 12. Carbostannylation of alkynoates.

Since stereochemical outcome observed in this study is consistent with the typical alkynylstannylation, the present reaction is considered to proceed via a well-accepted reaction mechanism shown in Scheme 13. Thus, oxidative addition of **11** to the Pd(0) complex would generate complex **A**. Since t-Bu$_3$P was essential for this carbostannylation, the phosphine should accelerate the oxidative addition step. In the case of arylacetylenes, insertion of an alkyne into the Pd–C bond of **A** proceeds in a manner that a bulkier stannylpalladium moiety connects to the less hindered sp carbon. The following reductive elimination of the alkenyl moiety and the stannyl group from complex **B** results in formation of the alkenylstannanes and regeneration of the Pd(0) species. On the other hand, Michael-type addition of **A** to ynones proceeds possibly due to the nucleophilic nature of the palladium complex, giving complex **C**, and successive reductive elimination would complete the catalytic cycles for **25**, **27**, and **29**. The fact that all the reactions took place at *room temperature* definitely shows that reactivity of **11** is remarkably higher than those of common alkynylstannanes, which require heating to perform the carbostannylation reaction. Strong

electron-withdrawing nature of a CF$_3$ group probably induces acceleration of the oxidative addition step to achieve the reaction at room temperature, which, as a result, leads to perfect stereoselectivity.
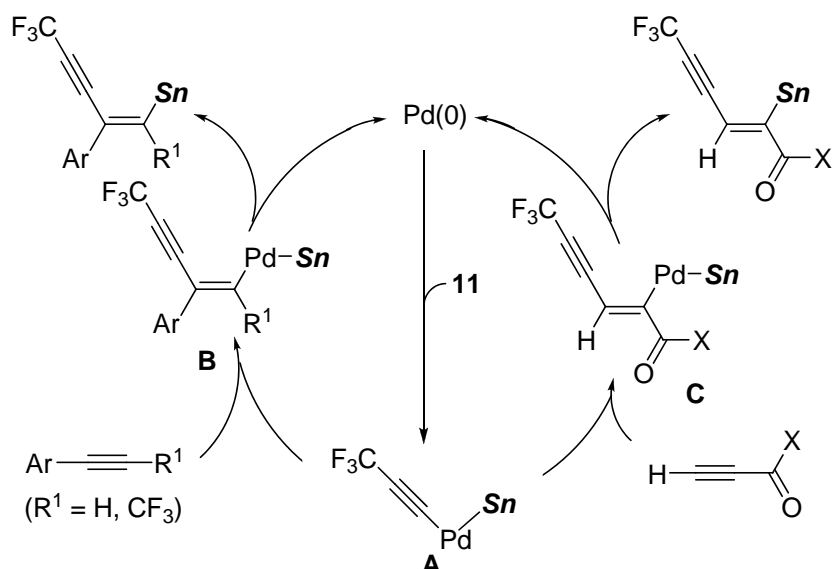
Scheme 13. Plausible mechanism for the carbostannylation.

Various transformations of the carbostannylated products are feasible by taking advantage of the resulting stannyl group. Representative examples are demonstrated in Scheme 14. Palladium-catalyzed cross-coupling reaction of **20a** with aryl and alkenyl iodides gave CF$_3$-substituted enyne **32** and dienyne **33**, while iodinated enyne **34** was prepared by treatment of **20a** with I$_2$ in THF.
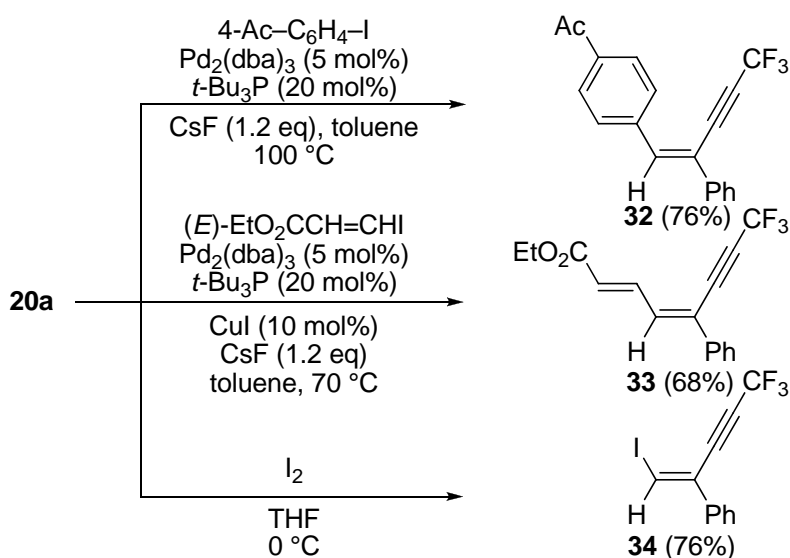
Scheme 14. Synthetic transformations of **20a**.

3. Conclusion

In summary, the author has developed a facile two-step protocol for generation of 3,3,3-trifluoropropynyllithium starting from 3,3-dichloro-1,1,1-trifluoropropanone. Its carbonyl adducts were converted into CF_3-substituted allenes via sulfonates formation followed by the Pd-catalyzed coupling with organozinc reagents. Trifluoropropynylborate and -stannane derived from the lithium reagent also cross-coupled with aryl iodides in the presence of Pd-catalysts. Moreover, the stannane reagent is disclosed to exhibit superior reactivity for Pd-catalyzed carbostannylation across alkynes, giving rise to trifluoromethylated enynes as a single stereoisomer.

4. Experimental Section

General Remarks: *The following experimentation applies to all the Chapters of the present Thesis.* Melting points were determined using a Yanagimoto Micro Melting Point Apparatus. ^{1}H NMR spectra were measured on a Varian Mercury 200 (200 MHz), 300 (300 MHz), and 400 (400 MHz) spectrometers. The chemical shifts of ^{1}H NMR are expressed in parts per million downfield relative to the internal tetramethylsilane (δ = 0 ppm) or chloroform (δ = 7.26 ppm). Splitting patterns are indicated as s, singlet; d, doublet; t, triplet; q, quartet; brs, broad singlet; m, multiplet. ^{13}C NMR spectra were measured on a Varian Mercury 400 (100 MHz), 300 (75 MHz), and JEOL EX–270 (67.8 MHz) spectrometers with tetramethylsilane as an internal standard (δ = 0 ppm) or CDCl$_3$ (δ = 77.0 ppm) with Proton-decoupled conditions. ^{19}F NMR spectra were measured on a Varian Mercury 200 (188 MHz) and 300 (282 MHz) spectrometers with CFCl$_3$ as an internal standard (δ = 0 ppm). ^{119}Sn NMR spectra were measured on a JEOL EX–270 (101 MHz) spectrometer with tetramethyltin (δ = 0 ppm) as an internal standard. Infrared spectra (IR) were recorded on a Shimadzu FTIR-8400 spectrometer. GC-MS analyses were performed with a JEOL JMS–700 spectrometer by electron ionization at 70 eV. FAB-MS analyses were performed with a JEOL-HX110A spectrometer. Elemental analyses were carried out with a YANAKO MT2 CHN CORDER machine at Elemental Analysis Center of Kyoto University. TLC analyses were performed by means of Merck Kieselgel 60 F$_{254}$ and column chromatography was carried out using Merck Kieselgel 60 (230–400 mesh), Merck aluminum oxide 90 active neutral (activity stage I), or Kishida Chemical Florisil (50–60 mesh). Preparative HPLC was carried out with a Japan Analytical Industry Co., Ltd, LC–908 chromatograph using a JAIGEL–1H and –2H GPC columns. Toluene, THF, hexane, Et$_2$O, and CH$_2$Cl$_2$ were passed through two packed columns of neutral alumina and copper oxide under a nitrogen atmosphere before use. All reactions were carried out under an argon atmosphere.

Preparation of enol tosylate 6. To a solution of **2** (13.6 g, 75 mmol) and TsCl (15.7 g, 82 mmol) in CH$_2$Cl$_2$ (100 mL) was added Et$_3$N (9.1 g, 90 mmol) at room temperature. The reaction mixture was stirred at room temperature for 1 h before dilution with Et$_2$O (50 mL). The resulting solution was washed with water and then sat. aq. NaCl, and dried over anhydrous MgSO$_4$. Removal of organic solvent *in vacuo* followed by distillation under reduced pressure (122 °C/2 Torr) gave 1,1-dichloro-3,3,3-trifluoro-2-tosyloxypropene (**6**, 24.4 g, 97% yield) as a colorless oil. R$_f$ 0.33 (hexane/AcOEt 10:1). ^{1}H NMR (200 MHz, CDCl$_3$) δ 2.49 (s, 3H), 7.39 (d, *J* = 8.6 Hz, 2H), 7.87 (d, *J* = 8.6 Hz, 2H); ^{13}C NMR (100 MHz, CDCl$_3$) δ 21.9, 119.0 (q, *J* = 273.8 Hz), 128.3, 129.9, 130.0 (q, *J* = 2.8 Hz), 132.4, 134.0 (q, *J* = 38.9 Hz), 146.4; ^{19}F NMR (188 Hz, CDCl$_3$) δ –63.1. IR (neat): ν 1618, 1394, 1196, 1153, 972 cm^{-1}. MS (EI): *m/z* (%) 180 (10, M$^+$–Ts), 160 (12), 111 (33), 91 (23), 74 (100). Anal. Calcd for C$_{10}$H$_7$Cl$_2$F$_3$O$_3$S: C, 35.84; H, 2.11. Found: C, 36.03, H, 2.22.

Representative procedure for generation and carbonyl addition of 1.

To a THF solution of **6** (10.0 g, 30 mmol) was added BuLi (41 mL, 66 mmol, 1.6 M in hexane) at –78 °C. The solution was stirred at –78 °C for 10 min before addition of 3-phenylpropanal (4.0 g, 30 mmol) in THF (20 mL) at –78 °C. The resulting solution was stirred at –78 °C for 1 h and at room temperature for 1 h. The reaction

mixture was quenched with sat. aq. NH$_4$Cl (40 mL) at 0 °C and extracted with AcOEt (40 mL × 3 times).   The combined organic layer was dried over anhydrous MgSO$_4$ and concentrated by a rotary evaporator.   The residue was purified by column chromatography on silica gel (hexane/AcOEt 15:1) to give **7b** (6.5 g, 95% yield) as a colorless oil.

4,4,4-Trifluoro-1-phenylbut-2-ynol (7a).[3]   Purified by silica gel column chromatography (hexane/AcOEt 15:1).   Yield: 97%, a colorless oil.

6,6,6-Trifluoro-1-phenylhex-4-yn-3-ol (7b).[3]   Purified by silica gel column chromatography (hexane/AcOEt 15:1).   Yield: 95%, a colorless oil.
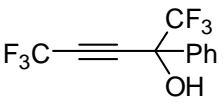
(*E*)-6,6,6-Trifluoro-1-phenylhexen-4-yn-3-ol (7c).[3]   Purified by silica gel column chromatography (hexane/AcOEt 15:1).   Yield: 71%, a colorless oil.

4,4,4-Trifluoro-1-cyclohexylbut-2-ynol (7d).[3]   Purified by silica gel column chromatography (hexane/AcOEt 15:1).   Yield: 92%, a colorless oil.

5,5,5-Trifluoro-2-phenylpent-3-yn-2-ol (7e).[3]   Purified by silica gel column chromatography (hexane/AcOEt 15:1).   Yield: 88%, a colorless solid.

4,4,4-Trifluoro-1,1-diphenylbut-2-ynol (7f).[12]   Purified by silica gel column chromatography (hexane/AcOEt 15:1).   Yield: 92%, a colorless solid.

1,1,1,5,5,5-Hexafluoro-2-phenylpent-3-yn-2-ol (7g).   Purified by silica gel column chromatography (hexane/AcOEt 15:1).   Yield: 84%, a colorless oil.   R$_f$ 0.47 (hexane/AcOEt 4:1). ^{1}H NMR (400 MHz, CDCl$_3$): δ 3.79–3.91 (m, 1H), 7.46–7.48 (m, 3H), 7.69–7.71 (m, 2H); ^{13}C NMR (100 MHz, CDCl$_3$): δ 72.9 (q, *J* = 33.0 Hz), 74.5 (q, *J* = 53.9 Hz), 82.3, (q, *J* = 6.4 Hz), 113.5 (q, *J* = 258.7 Hz), 122.4 (q, *J* = 285.2 Hz), 126.6, 128.5, 130.2, 132.8; ^{19}F NMR (282 MHz, CDCl$_3$): δ −51.9, −80.4.   IR (neat): ν 3422, 2270, 1709, 1454, 1283, 1252, 1157, 1043, 737, 698 cm^{-1}.   MS (EI): *m/z* (%) 268 (10, M$^+$), 199 (100), 151 (40), 121 (100).   HRMS Calcd for C$_{11}$H$_6$F$_6$O: M$^+$: 268.0323.   Found: 268.0311.

1-(3,3,3-Trifluoropropynyl)cyclohexanol (7h).[3]   Purified by silica gel column chromatography (hexane/AcOEt 15:1).   Yield: 72%, a colorless oil.

Triethyl(3,3,3-trifluoropropynyl)silane (8).[17]   Purified by distillation under reduced pressure (50 °C/17 Torr bath temperature).   Yield: 82%, a colorless oil.

Potassium trifluoro(3,3,3-trifluoropropynyl)borate (9).[16]   A 250–mL Schlenk tube was charged with **6** (5.03 g, 15 mmol) and THF (38 mL), and was cooled at −78 °C. To this solution was added BuLi (21 mL, 33 mmol, 1.60 M in hexane) over a period of 40 min at −78 °C.   The resulting solution was stirred at −78 °C for 10 min before the addition of (MeO)$_3$B (1.84 mL, 17 mmol) over a period of 20 min.   The solution was stirred at −78 °C for 30 min and allowed to warm to 0 °C over a period of 3 h.   The

organic solvents were partly removed under reduced pressure until the volume of solvents decreased to 50 mL.   Another Schlenk tube was charged with potassium hydrogenfluoride (3.52 g, 45 mmol), water (9.3 mL), and hydrogen fluoride (1.56 mL, 38 mmol, 48wt% in water).   To this Schlenk tube was added the THF solution of trimethoxy(trifluoropropynyl)borate via a cannula at 0 °C over a period of 30 min. The mixture was stirred at room temperature overnight.   The reaction mixture was quenched with water (9 mL), and the resulting solution was neutralized with K_2CO_3 and treated with sat. aq. KF (20 mL).   The aqueous layer was extracted with CH_3CN (50 mL × 2 times).   The combined organic layer was washed with sat. aq. KF, dried over anhydrous $MgSO_4$, and concentrated by a rotary evaporator to give a brown solid.   The crude solid was washed with toluene (20 mL × 3 times) and hexane (20 mL × 2 times) on a glass filter.   The residue was dried at 40 °C under reduced pressure to give **9** (1.62 g, 8.1 mmol, 54%) as a colorless solid.

Triphenyl(3,3,3-trifluoropropynyl)stannane (10).[13]   Purified by GPC.   Yield: 50%, a yellow solid.

Tributyl(3,3,3-trifluoropropynyl)stannane (11).[17]   Purified by distillation under reduced pressure (120 °C/6 Torr bath temperature).   Yield: 64%, a pale yellow oil.

Representative procedure for preparation of 12/13.
   To a solution of **7b** (1.5 g, 6.6 mmol), TsCl (1.4 g, 7.2 mmol), DMAP (40 mg, 0.33 mmol) in CH_2Cl_2 (26 mL) was added Et_3N (1.1 mL, 7.9 mmol) at 0 °C.   The resulting solution was stirred at room temperature for 2 h before quenching with sat. aq. NH_4Cl (20 mL) at 0 °C.   The aqueous layer was extracted with CH_2Cl_2 (20 mL × 3 times), and the combined organic solvent was washed with sat. aq. NaCl (60 mL), dried over anhydrous $MgSO_4$, and concentrated *in vacuo*.   The residue was purified by silica gel column chromatography (hexane/AcOEt 15:1) to give 1,1,1-trifluoro-6-phenyl-4-tosyloxyhex-2-yne (**12b**, 2.4 g, 95% yield) as a colorless solid.   Mp: 47.8–49.0 °C. R_f 0.45 (hexane/AcOEt 4:1).   ^{1}H NMR (400 MHz, $CDCl_3$): δ 2.13–2.28 (m, 2H), 2.46 (s, 3H), 2.74–2.82 (m, 2H), 5.07–5.11 (m, 1H), 7.15 (d, *J* = 8.0 Hz, 2H), 7.21–7.32 (m, 3H), 7.35 (d, *J* = 8.4 Hz, 2H), 7.80 (d, *J* = 8.4 Hz, 2H); ^{13}C NMR (100 MHz, $CDCl_3$): δ 21.5, 30.5, 36.3, 68.3, 74.3 (q, *J* = 52.9 Hz), 81.9 (q, *J* = 6.4 Hz), 113.2 (q, *J* = 257.9 Hz), 126.3, 127.9, 128.2, 128.4, 129.7, 132.7, 138.9, 145.5; ^{19}F NMR (282 MHz, $CDCl_3$): δ −51.8.   IR (KBr): ν 2361, 2341, 1364, 1271, 1159, 953, 746, 677 cm^{-1}. MS (EI): *m/z* (%) 382 (1, M$^+$), 210 (30), 141 (90), 91 (100).   Anal. Calcd for $C_{19}H_{17}F_3O_3S$: C, 59.68; H, 4.48.   Found: C, 59.60; H, 4.60.

4,4,4-Trifluoro-1-phenyl-3-tosyloxybuta-1,2-diene (13a).   Purified by Florisil column chromatography (hexane/AcOEt 20:1).   Yield: 91%, a colorless oil. R_f 0.62 (hexane/AcOEt 4:1).   ^{1}H NMR (400 MHz, $CDCl_3$): δ 2.43 (s, 3H), 6.14–6.19 (m, 1H), 7.32–7.36 (m, 7H), 7.83 (d, *J* = 8.4 Hz, 2H); ^{13}C NMR (100 MHz, $CDCl_3$): δ 21.7, 98.8 (q, *J* = 39.6 Hz), 120.4 (q, *J* = 272.2 Hz), 125.3, 128.3, 128.5, 128.8, 129.7, 130.2, 132.0, 134.0, 145.8, 201.2 (q, *J* = 6.1 Hz); ^{19}F NMR (282 MHz, $CDCl_3$): δ −62.2.   IR (neat): ν 3065, 1973, 1597, 1381, 1265, 1128, 995, 816, 691 cm^{-1}.   MS (EI): *m/z* (%) 354 (1, M$^+$), 335

(2), 290 (48), 105 (100). Calcd for C$_{17}$H$_{13}$F$_3$O$_3$S: M$^+$ 354.0538. Found: 354.0538.

4,4,4-Trifluoro-3-mesyloxy-1,1-diphenylbuta-1,2-diene (13f). Purified by Florisil column chromatography (hexane/AcOEt 20:1). Yield: 63%, a colorless oil. R$_f$ 0.56 (hexane/AcOEt 4:1). ^{1}H NMR (400 MHz, CDCl$_3$): δ 3.14 (s, 3H), 7.44 (s, 10H); ^{13}C NMR (100 MHz, CDCl$_3$): δ 38.5, 114.5 (q, J = 43.4 Hz), 120.0 (q, J = 273.0 Hz), 128.7, 129.0, 129.3, 129.8, 132.9, 193.4; ^{19}F NMR (282 MHz, CDCl$_3$): δ –67.9. IR (neat): ν 3026, 1952, 1383, 1271, 1190, 833, 696 cm^{-1}. MS (EI): m/z (%) 354 (23, M$^+$), 291 (100), 275 (81), 259 (45), 225 (81). HRMS Calcd for C$_{17}$H$_{13}$F$_3$O$_3$S: M$^+$: 354.0538. Found: 354.0522.

1,1,1,5,5,5-Hexafluoro-4-phenyl-4-tosyloxypent-2-yne (12g). Purified by Florisil column chromatography (hexane/AcOEt 20:1). Yield: 60%, a colorless solid. Mp: 85.8–86.3 °C. R$_f$ 0.49 (hexane/AcOEt 4:1). ^{1}H NMR (400 MHz, CDCl$_3$): δ 2.48 (s, 3H), 7.34 (d, J = 8.8 Hz, 2H), 7.47–7.52 (m, 3H), 7.69 (d, J = 8.0 Hz, 2H), 7.77 (d, J = 8.0 Hz, 2H); ^{13}C NMR (100 MHz, CDCl$_3$): δ 21.6, 77.0 (q, J = 6.5 Hz), 78.6 (q, J = 54.6 Hz), 80.2 (q, J = 33.4 Hz), 113.1 (q, J = 259.5 Hz), 120.9 (q, J = 285.5 Hz), 127.2, 127.7, 128.6, 129.8, 130.2, 130.9, 133.9, 145.7; ^{19}F NMR (282 MHz, CDCl$_3$): δ –52.2, –78.5. IR (KBr): ν 2359, 1375, 1286, 1248, 1200, 727, 696, 667 cm^{-1}. MS (EI): m/z (%) 422 (3, M$^+$), 251 (100). Anal. Calcd for C$_{18}$H$_{12}$F$_6$O$_3$S: C, 51.11; H, 2.86. Found: C, 50.92; H, 2.98.

1-Mesyloxy-1-(3,3,3-trifluoropropynyl)cyclohexane (12h). Purified by Florisil column chromatography (hexane/AcOEt 20:1). Yield: 84%, a colorless oil. R$_f$ 0.33 (hexane/AcOEt 4:1). ^{1}H NMR (400 MHz, CDCl$_3$): δ 1.37–1.44 (m, 2H), 1.56–1.65 (m, 2H), 1.76–1.83 (m, 2H), 2.05–2.11 (m, 2H), 2.17–2.21 (m, 2H), 3.12 (s, 3H); ^{13}C NMR (100 MHz, CDCl$_3$): δ 22.4, 24.2, 37.7, 40.5, 75.9 (q, J = 53.2 Hz), 81.7, 85.0 (q, J = 6.13 Hz), 113.7 (q, J = 257.7 Hz); ^{19}F NMR (282 MHz, CDCl$_3$): δ –51.3. IR (neat): ν 2945, 2868, 2268, 1369, 1265, 1148, 928, 797, 686 cm^{-1}. MS (EI): m/z (%) 270 (1, M$^+$), 174 (19), 105 (20), 79 (100). HRMS Calcd for C$_{10}$H$_{13}$F$_3$O$_3$S: M$^+$: 270.0538. Found: 270.0533.

Representative procedure for the preparation of 15.

To a THF (2.6 mL) solution of **12b** (0.10 g, 0.26 mmol) and Pd(PPh$_3$)$_4$ (15 mg, 13 μmol) was added PhZnCl (0.79 mL, 0.79 mmol, 1.0 M in THF prepared from PhMgCl and ZnCl$_2$•TMEDA) at 0 °C. The solution was stirred at room temperature for 2 h before quenching with sat. aq. NH$_4$Cl (2 mL) at 0 °C. The aqueous layer was extracted with AcOEt (2 mL × 3 times). The combined organic solvent was washed with sat. aq. NaCl (6 mL), dried over anhydrous MgSO$_4$, and concentrated by a rotary evaporator. The residue was purified by column chromatography on silica gel (hexane/AcOEt 20:1), giving 1,1,1-trifluoro-2,6-diphenylhexa-2,3-diene (**15ba**, 52 mg, 69% yield) as a colorless solid. Mp: 28.4–30.1 °C. R$_f$ 0.67 (hexane/AcOEt 4:1). ^{1}H NMR (400 MHz, CDCl$_3$): δ 2.54–2.67 (m, 2H), 2.80–2.91 (m, 2H), 5.96–6.01 (m, 1H), 7.21–7.34 (m,

10H); ^{13}C NMR (100 MHz, CDCl$_3$): δ 29.9, 34.9, 99.2, 102.1 (q, J = 34.5 Hz), 123.3 (q, J = 273.2 Hz), 126.1, 126.8, 126.8, 127.8, 128.4, 128.5, 129.8, 140.5, 204.0 (q, J = 4.6 Hz); ^{19}F NMR (282 MHz, CDCl$_3$): δ −60.9.   IR (KBr): ν 3030, 2926, 1958, 1497, 1303, 1168, 1121, 934, 694 cm^{-1}.   MS (EI): m/z (%) 288 (30, M$^+$), 219 (20), 129 (45), 91 (100).   HRMS Calcd for C$_{18}$H$_{15}$F$_3$: M$^+$: 288.1126.   Found: 288.1124.
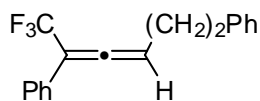
4,4,4-Trifluoro-1,3-diphenylbuta-1,2-diene (15aa).   Purified by silica gel column chromatography (hexane/AcOEt 15:1).   Yield: 21%, a colorless solid.   Mp: 58.5–59.7 °C.   R$_f$ 0.62 (hexane/AcOEt 4:1). ^{1}H NMR (400 MHz, CDCl$_3$): δ 5.96–6.00 (m, 1H), 7.35–7.43 (m, 10H); ^{13}C NMR (100 MHz, CDCl$_3$): δ 88.5 (q, J = 39.1 Hz), 116.8, 122.4 (q, J = 270.7 Hz), 128.4, 128.54 (2C), 128.58 (3C), 133.7 (2C), 206.2 (q, J = 6.1 Hz); ^{19}F NMR (282 MHz, CDCl$_3$): δ −60.5.   IR (KBr): ν 3020, 2359, 1955, 1456, 1151, 839, 772, 694 cm^{-1}. MS (EI): m/z (%) 260 (52, M$^+$), 191 (100).   Anal. Calcd for C$_{16}$H$_{11}$F$_3$: C, 73.84; H, 4.26.   Found: C, 73.62; H, 4.43.

1,1,1-Trifluoro-6-phenyl-2-(4-trifluoromethylphenyl)hexa-2,3-diene   (15bb). Purified by preparative TLC (hexane/AcOEt 5:1).   Yield: 62%, a colorless solid.   Mp: 49.4–51.0 °C.   R$_f$ 0.72 (hexane/AcOEt 4:1). ^{1}H NMR (400 MHz, CDCl$_3$): δ 2.52–2.69 (m, 2H), 2.72–2.92 (m, 2H), 6.00–6.05 (m, 1H), 7.17–7.29 (m, 5H), 7.32 (d, J = 8.4 Hz, 2H), 7.53 (d, J = 8.4 Hz, 2H); ^{13}C NMR (100 MHz, CDCl$_3$): δ 29.7, 34.8, 100.0, 101.3 (q, J = 34.5 Hz), 123.0 (q, J = 272.9 Hz), 123.8 (q, J = 270.6 Hz), 125.4 (q, J = 3.9 Hz), 126.2, 126.9, 128.3, 128.4, 129.7 (q, J = 32.4 Hz), 133.6, 140.1, 204.6 (q, J = 3.0 Hz); ^{19}F NMR (282 MHz, CDCl$_3$): δ −60.9, −63.3.   IR (KBr): ν 3026, 2361, 1958, 1331, 1182, 1124, 845, 700 cm^{-1}.   MS (EI): m/z (%) 356 (55, M$^+$), 287 (39), 91 (100).   Anal. Calcd for C$_{19}$H$_{17}$F$_3$O: C, 64.05; H, 3.96. Found: C, 63.80; H, 3.96.

1,1,1-Trifluoro-2-(4-methoxyphenyl)-6-phenylhexa-2,3-diene (15bc).   Purified by preparative TLC (hexane/AcOEt 5:1).   Yield: 84%, a colorless solid.   Mp: 40.4–41.0 °C.   R$_f$ 0.63 (hexane/AcOEt 4:1). ^{1}H NMR (400 MHz, CDCl$_3$): δ 2.48–2.63 (m, 2H), 2.77–2.89 (m, 2H), 3.82 (s, 3H), 5.91–5.95 (m, 1H), 6.85 (d, J = 8.8 Hz, 2H), 7.19–7.30 (m, 7H); ^{13}C NMR (100 MHz, CDCl$_3$): δ 30.0, 34.9, 55.3, 99.1, 101.6 (q, J = 34.0 Hz), 113.9, 122.0, 123.4 (q, J = 273.2 Hz), 126.0, 128.0, 128.3 (2C), 140.5, 159.1, 203.4 (q, J = 3.8 Hz); ^{19}F NMR (282 MHz, CDCl$_3$): δ −61.1.   IR (KBr): ν 2957, 2932, 2341, 1962, 1512, 1306, 1258, 1175, 1103, 831, 700 cm^{-1}.   MS (EI): m/z (%) 318 (71, M$^+$), 249 (22), 359 (3), 207 (100). HRMS Calcd for C$_{19}$H$_{17}$F$_3$ O: M$^+$: 318.1232.   Found: 318.1217.

1,1,1-Trifluoro-6-phenylhexa-2,3-diene (15bd).   Purified by silica gel column chromatography (hexane/AcOEt 15:1).   Yield: 86%, a colorless oil.   R$_f$ 0.60 (hexane/AcOEt 4:1).

1,1,1-Trifluoro-6-phenyl-2-[(trimethylsilyl)methyl]hexa-2,3-diene (15be). Purified by Florisil column chromatography (hexane only) followed by GPC. Yield: 31%, a colorless oil. R_f 0.67 (hexane/AcOEt 4:1). ^{1}H NMR (400 MHz, CDCl$_3$): δ 0.07 (s, 9H), 1.40–1.41 (m, 2H), 2.36–2.47 (m, 2H), 2.73–2.76 (m, 2H), 5.55–5.58 (m, 1H), 7.19–7.32 (m, 5H); ^{13}C NMR (100 MHz, CDCl$_3$): δ −1.34, 15.0, 30.3, 35.1, 96.2 (q, J = 34.6 Hz), 96.8, 123.9 (q, J = 272.7 Hz), 125.9, 128.3 (2C), 140.8, 202.3 (q, J = 3.6 Hz); ^{19}F NMR (282 MHz, CDCl$_3$): δ −65.6. IR (neat): ν 2957, 1969, 1306, 1250, 1151, 1115, 853, 698 cm^{-1}. MS (EI): m/z (%) 298 (1, M$^+$), 225 (3), 206 (17), 155 (20), 73 (100). HRMS Calcd for C$_{16}$H$_{21}$F$_3$Si: M$^+$: 298.1365. Found: 298.1361.

4,4,4-Trifluoro-1,1,3-triphenylbuta-1,2-diene (15fa). Purified by silica gel column chromatography (hexane/AcOEt 15:1). Yield: 94%, a colorless solid. Mp: 59.8–60.4 °C. R_f 0.62 (hexane/AcOEt 4:1). ^{1}H NMR (400 MHz, CDCl$_3$): δ 7.33–7.56 (m, 15H); ^{13}C NMR (100 MHz, CDCl$_3$): δ 104.3 (q, J = 33.8 Hz), 118.1, 123.2 (q, J = 274.5 Hz), 126.9, 127.0, 128.3, 128.5, 128.7, 128.8, 129.5, 134.0, 206.5 (q, J = 3.8 Hz); ^{19}F NMR (282 MHz, CDCl$_3$): δ −60.4. IR (KBr): ν 3028, 1949, 1491, 1298, 1169, 928, 770, 694 cm^{-1}. MS (EI): m/z (%) 336 (100, M$^+$), 267 (99). Anal. Calcd for C$_{22}$H$_{16}$F$_3$: C, 78.56; H, 4.50. Found: C, 78.74; H, 4.47.
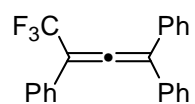
2,4-Diphenylperfluoropenta-2,3-diene (15ga). Purified by preparative TLC (hexane/AcOEt 5:1). Yield: 42%, a colorless oil. R_f 0.62 (hexane/AcOEt 4:1). ^{1}H NMR (400 MHz, CDCl$_3$): δ 7.41–7.49 (m, 10H); ^{13}C NMR (100 MHz, CDCl$_3$): δ 109.8 (q, J = 35.1 Hz), 122.2 (q, J = 277.6 Hz), 127.2, 127.4, 129.1, 129.6, 205.5; ^{19}F NMR (282 MHz, CDCl$_3$): δ −60.9. IR (KBr): ν 3074, 3033, 1967, 1497, 1204, 11142, 934, 764, 691 cm^{-1}. MS (EI): m/z (%) 328 (62, M$^+$), 259 (100). Anal. Calcd for C$_{17}$H$_{10}$F$_6$: C, 62.20; H, 3.07. Found: C, 62.44; H, 3.23.

1-Cyclohexylidene-3,3,3-trifluoro-2-phenylpropene (15ha). Purified by preparative TLC (hexane/AcOEt 5:1). Yield: 69%, a colorless oil. R_f 0.65 (hexane/AcOEt 4:1). ^{1}H NMR (400 MHz, CDCl$_3$): δ 1.60–1.65 (m, 2H), 1.70–1.76 (m, 4H), 2.30–2.34 (m, 4H), 7.28–7.29 (m, 1H), 7.34–7.35 (m, 2H), 7.42–7.43 (m, 2H); ^{13}C NMR (100 MHz, CDCl$_3$): δ 25.9, 27.3, 30.7, 98.9 (q, J = 34.6 Hz), 111.6, 123.5 (q, J = 273.2 Hz), 126.8, 127.4, 128.4, 131.2, 198.7 (q, J = 3.8 Hz); ^{19}F NMR (282 MHz, CDCl$_3$): δ −60.8. IR (neat): ν 2936, 1948, 1302, 1155, 1115, 932, 692 cm^{-1}. MS (EI): m/z (%) 252 (100, M$^+$), 183 (65). Anal. Calcd for C$_{15}$H$_{15}$F$_3$: C, 71.41; H, 5.99. Found: C, 71.62; H, 6.05.
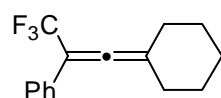
1-Cyclohexylidene-3,3,3-trifluoro-2-(4-trifluoromethylphenyl)propene (15hb). Purified by preparative TLC (hexane/AcOEt 5:1). Yield: 59%, a colorless oil. R_f 0.67 (hexane/AcOEt 4:1). ^{1}H NMR (400 MHz, CDCl$_3$): δ 1.62–1.66 (m, 2H), 1.71–1.77 (m, 4H),
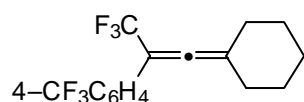
2.32–2.36 (m, 4H), 7.52 (d, J = 8.3 Hz, 2H), 7.60 (d, J = 8.3 Hz, 2H); ^{13}C NMR (100 MHz, CDCl$_3$): δ 25.8, 27.3, 30.5, 98.3 (q, J = 34.5 Hz), 112.6 (q, J = 272.9 Hz), 123.9 (q, J = 271.4 Hz), 125.4, 125.4, 126.9, 129.4 (q, J = 32.4 Hz), 135.0, 199.4 (q, J = 3.8 Hz); ^{19}F NMR (282 MHz, CDCl$_3$): δ –60.9, –63.2.   IR (neat): ν 2937, 1949, 1620, 1329, 1130, 1115, 845, 721 cm^{-1}.   MS (EI): m/z (%) 320 (80, M$^+$), 251 (25), 209 (100). Anal. Calcd for C$_{16}$H$_{14}$F$_6$: C, 60.00; H, 4.41.   Found: C, 60.28; H, 4.57.
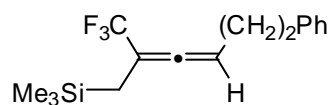
1-Cyclohexylidene-3,3,3-trifluoro-2-(4-methoxyphenyl)propene (15hc).   Purified by preparative TLC (hexane/AcOEt 5:1).   Yield: 66%, a colorless solid.   R$_f$ 0.58 (hexane/AcOEt 4:1). ^{1}H NMR (400 MHz, CDCl$_3$): δ 1.59–1.63 (m, 2H), 1.68–1.74 (m, 4H), 2.28–2.32 (m, 4H), 3.82 (s, 3H), 6.89 (d, J = 8.8 Hz, 2H), 7.34 (d, J = 8.8 Hz, 2H); ^{13}C NMR (100 MHz, CDCl$_3$): δ 25.9, 27.4, 30.8, 55.3, 98.4 (q, J = 33.7 Hz), 111.4, 113.9, 123.4, 123.6 (q, J = 273.2 Hz), 128.0, 158.9, 198.0 (q, J = 3.9 Hz); ^{19}F NMR (282 MHz, CDCl$_3$): δ –61.1.   IR (KBr): ν 2936, 1961, 1514, 1304, 1155, 930, 831 cm^{-1}.   MS (EI): m/z (%) 282 (100, M$^+$), 213 (35).   Anal. Calcd for C$_{19}$H$_{17}$F$_3$O: C, 68.07; H, 6.07.   Found: C, 68.20; H, 6.17.

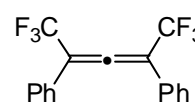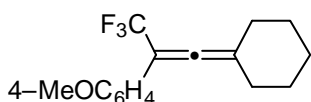**1-Cyclohexylidene-3,3,3-trifluoro-2-[(trimethylsilyl)methyl]propene (15he).**   Purified by Florisil column chromatography (hexane only).   Yield: 61%, a colorless oil.   R$_f$ 0.70 (hexane/AcOEt 4:1). ^{1}H NMR (400 MHz, CDCl$_3$): δ 0.06 (s, 9H), 1.43–1.66 (m, 8H), 2.10–2.23 (m, 4H); ^{13}C NMR (100 MHz, CDCl$_3$): δ –1.4, 15.1, 26.0, 27.0, 31.1, 92.8 (q, J = 34.3 Hz), 108.8, 124.2 (q, J = 272.7 Hz), 196.9 (q, J = 4.6 Hz); ^{19}F NMR (282 MHz, CDCl$_3$): δ –65.8.   IR (neat): ν 2934, 2858, 1959, 1448, 1296, 1163, 1111, 858, 696 cm^{-1}.   MS (EI): m/z (%) 262 (5, M$^+$), 170 (7), 73 (100).   HRMS Calcd for C$_{13}$H$_{21}$F$_3$Si: M$^+$: 262.1365.   Found: 262.1357.
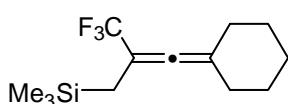
Typical procedure for cross-coupling reaction of 9 with aryl iodides 16.

   A THF (1 mL) solution of borate salt **9** (24 mg, 0.12 mmol), 1-iodo-4-methoxybenzene (**16a**, 23 mg, 0.10 mmol), PdCl$_2$(dppf)•CH$_2$Cl$_2$ (7.3 mg, 9.0 mmol), H$_2$O (7.2 mg, 0.40 mmol), K$_2$CO$_3$ (42 mg, 0.30 mmol), Ag$_2$O (17 mg, 0.12 mmol), and 18-crown-6 (2.6 mg, 10 μmol) was stirred at 80 °C for 10 h before dilution with Et$_2$O (20 mL).   The resulting solution was washed with water and then sat. aq. NaCl, and then dried over anhydrous MgSO$_4$.   Removal of organic solvent in $vacuo$ followed by column chromatography (hexane/AcOEt 8:1) on silica gel gave **17a**[14] (12 mg, 60%) as a colorless oil.

3,3,3-Trifluoro-1-(4-methylphenyl)propyne (17b).[14]   Purified by preparative TLC (hexane/AcOEt 8:1).   Yield: 65%, a colorless oil.

3,3,3-Trifluoro-1-phenylpropyne (17c).[14]   Purified by preparative TLC (hexane/AcOEt 8:1).   Yield: 65%, a colorless oil.

1-(4-Cyanophenyl)-3,3,3-trifluoropropyne (17d).   Purified by preparative TLC (hexane/AcOEt 8:1).   Yield: 54%, a colorless solid.   Mp: 43.6–44.0 °C.   R$_f$ 0.31 (hexane/AcOEt 8:1). ^{1}H NMR (300
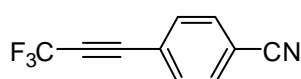
MHz, CDCl$_3$): δ 7.65–7.73 (m, 4H); ^{13}C NMR (100 MHz, CDCl$_3$): δ 78.9 (q, J = 52.9 Hz), 84.0 (q, J = 6.5 Hz), 114.3 (q, J = 256.2 Hz), 114.5, 117.5, 123.0, 132.2, 132.8; ^{19}F NMR (282 MHz, CDCl$_3$): δ −51.0.   IR (KBr); ν 2259, 2228, 1505, 1314, 1190, 1167, 1144, 843 cm^{-1}.   MS (EI): m/z (%) 195 (100, M$^+$), 194 (26, M$^+$−H), 176 (41).   HRMS Calcd for C$_{10}$H$_4$F$_3$N: M$^+$ 195.0300.   Found: 195.0296.

1-(4-Acetylphenyl)-3,3,3-trifluoropropyne (17e).   Purified by preparative TLC (hexane/AcOEt 8:1).   Yield: 60%, a colorless solid.   Mp: 55.3–55.6 °C.   R$_f$ 0.44 (hexane/AcOEt 4:1). ^{1}H NMR (400 MHz, CDCl$_3$): δ 2.62 (s, 3H), 7.66 (d, J = 8.4 Hz, 2H), 7.97 (d, J = 8.4 Hz, 2H); ^{13}C NMR (100 MHz, CDCl$_3$): δ 26.7, 77.9 (q, J = 51.9 Hz), 85.1 (q, J = 6.1 Hz), 114.6 (q, J = 255.4 Hz), 122.9, 128.3, 132.6, 138.3, 196.9; ^{19}F NMR (188 MHz, CDCl$_3$): δ −50.7.   IR (KBr): ν 2260, 1682, 1315, 1265, 1134, 839 cm^{-1}.   MS (EI): m/z (%) 212 (37, M$^+$), 197 (100), 169 (68).   Anal. Calcd for C$_{11}$H$_7$F$_3$O: C, 62.27; H, 3.33.   Found: C, 62.13; H, 3.35.

1-(4-Ethoxycarbonylphenyl)-3,3,3-trifluoropropyne (17f).[14]   Purified by preparative TLC (hexane/AcOEt 8:1).   Yield: 42%, a colorless oil.

3,3,3-Trifluoro-1-(4-nitrophenyl)propyne (17g).[14]   Purified by preparative TLC (hexane/AcOEt 8:1).   Yield: 43%, a colorless oil.

1-(4-Formylphenyl)-3,3,3-trifluoropropyne (17h).   Purified by Florisil column chromatography (hexane/AcOEt 8:1) followed by GPC. Isolated yield: 25%; ^{19}F NMR yield: 48%, a colorless solid. R$_f$ 0.25 (hexane/AcOEt 8:1). ^{1}H NMR (300 MHz, CDCl$_3$): δ 7.73 (d, J = 8.2 Hz, 2H), 7.92 (d, J = 8.2 Hz, 2H), 10.06 (s, 1H); ^{13}C NMR (100 MHz, CDCl$_3$): δ 78.4 (q, J = 52.6 Hz), 84.8 (q, J = 6.3 Hz), 114.4 (q, J = 256.2 Hz), 124.1, 129.4, 132.9 (d, J = 1.5 Hz), 137.2, 190.7; ^{19}F NMR (282 MHz, CDCl$_3$): δ −50.8.   MS (EI): m/z (%) 198 (96, M$^+$), 197 (100), 179 (41), 170 (43), 169 (93).   HRMS Calcd for C$_{10}$H$_4$F$_3$O: M$^+$−H 197.0218.   Found: 197.0215.

A general procedure for carbostannylation of alkynes.

To a stirring toluene (0.6 mL) solution of alkynes **19** (0.92 mmol), Pd$_2$(dba)$_3$ (5.5 mg, 6.1 μmol), t-Bu$_3$P (36 mg, 12 μmol) was slowly added **11** (0.23 g, 0.61 mmol) in toluene (1.0 mL) over a period of 0.5 h.   The mixture was stirred at room temperature for 1 h and then filtered through a Florisil pad.   Removal of the organic solvent using a rotary evaporator afforded a crude solid, which was purified by flash column chromatography on silica gel (hexane/AcOEt with 5.0 wt% of Et$_3$N), giving rise to the corresponding carbostannylation product.

(Z)-5,5,5-Trifluoro-2-phenyl-1-(tributylstannyl)penten-3-yne (20a). Yield: 87%, a pale yellow oil. R_f 0.58 (hexane only). ^{1}H NMR (200 MHz, CDCl$_3$): δ 0.90 (t, J = 7.0 Hz, 9H), 1.10 (t, J = 7.6 Hz, 6H), 1.28–1.43 (m, 6H), 1.49–1.61 (m, 6H), 7.31–7.38 (m, 3H), 7.44 (s, 1H), 7.56–7.66 (m, 2H); ^{13}C NMR (67.8 MHz, CDCl$_3$): δ 10.4, 13.7, 27.4, 29.2, 75.7 (q, J = 52.4 Hz), 88.0 (q, J = 6.7 Hz), 114.9 (q, J = 256.6 Hz), 125.5, 128.4, 128.5, 135.4 137.5, 149.2; ^{19}F NMR (188 MHz, CDCl$_3$): δ –50.1; ^{119}Sn NMR (101 MHz, CDCl$_3$): δ –51.6. IR (neat): ν 2923, 2852, 2231, 1238, 1139, 758 cm^{-1}. MS (EI): m/z (%) 429 (48, M$^+$–Bu), 427 (38), 425 (21), 157 (100). HRMS (FAB) Calcd for C$_{19}$H$_{24}$F$_3$Sn: M$^+$–Bu, 429.0852. Found: 429.0861.
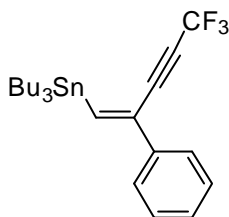
(Z)-5,5,5-Trifluoro-2-(4-methoxyphenyl)-1-(tributylstannyl)penten-3-yne (20b). Yield: 90%, a colorless oil. R_f 0.50 (hexane/AcOEt 10:1). ^{1}H NMR (200 MHz, CDCl$_3$): δ 0.88 (t, J = 7.4 Hz, 9H), 1.06 (t, J = 7.6 Hz, 6H), 1.25–1.40 (m, 6H), 1.49–1.58 (m, 6H), 3.80 (s, 3H), 6.87 (d, J = 8.8 Hz, 2H), 7.23 (s, 1H), 7.49 (d, J = 8.8 Hz, 2H); ^{13}C NMR (67.8 MHz, CDCl$_3$): δ 10.3, 13.8, 27.3, 29.2, 55.4, 75.4 (q, J = 52.4 Hz), 88.1 (q, J = 6.7 Hz), 113.8, 114.8 (q, J = 255.5 Hz), 126.7, 130.2, 134.6, 146.1, 159.8; ^{19}F NMR (188 MHz, CDCl$_3$): δ –50.0; ^{119}Sn NMR (101 MHz, CDCl$_3$): δ –51.8. IR (neat): ν 2926, 2232, 1607, 1240, 1140, 818 cm^{-1}. MS (EI): m/z (%) 459 (18, M$^+$–Bu), 457 (14), 455 (8), 187 (100). Anal. Calcd for C$_{24}$H$_{35}$OF$_3$Sn: C, 55.95; H, 6.85. Found: C, 56.20; H, 6.55.
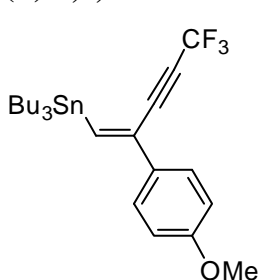
(Z)-5,5,5-Trifluoro-1-tributylstannyl-2-(4-trifluoromethylphenyl)penten-3-yne (20c). Yield: 89%, a colorless oil. R_f 0.58 (hexane). ^{1}H NMR (200 MHz, CDCl$_3$): δ 0.91 (t, J = 7.2 Hz, 9H), 1.12 (t, J = 7.8 Hz, 6H), 1.28–1.36 (m, 6H), 1.50–1.62 (m, 6H), 7.57 (s, 1H), 7.60–7.71 (m, 4H); ^{13}C NMR (67.8 MHz, CDCl$_3$): δ 10.4, 13.7, 27.4, 29.2, 76.1 (q, J = 52.4 Hz), 87.1 (q, J = 6.7 Hz), 114.7 (q, J = 256.6 Hz), 124.0 (q, J = 271.1 Hz), 125.5, 125.8, 130.8 (J = 32.3 Hz), 134.1, 140.6, 152.7; ^{19}F NMR (188 MHz, CDCl$_3$): δ –50.2, –63.1; ^{119}Sn NMR (101 MHz, CDCl$_3$): δ –50.0. IR (neat): ν 2926, 2233, 1618, 1240, 1144, 824 cm^{-1}. MS (EI): m/z (%) 497 (12, M$^+$–Bu), 495 (9), 493 (5), 225 (100), 177 (21). Anal. Calcd for C$_{24}$H$_{32}$F$_3$Sn: C, 52.11; H, 5.83. Found: C, 52.18; H, 5.75.
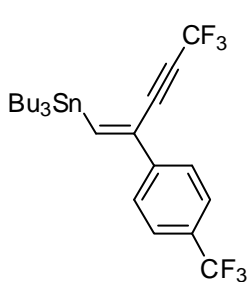
(Z)-5,5,5-Trifluoro-2-(4-phenylphenyl)-1-(tributylstannyl)penten-3-yne (20d). Yield: 83%, a colorless oil. R_f 0.45 (hexane). ^{1}H NMR (200 MHz, CDCl$_3$): δ 0.91 (t, J = 7.2 Hz, 9H), 1.12 (t, J = 7.6 Hz, 6H), 1.29–1.40 (m, 6H), 1.54–1.63 (m, 6H), 7.39–7.50 (m, 4H), 7.59–7.69 (m, 6H); ^{13}C NMR (67.8 MHz, CDCl$_3$): δ 10.3, 13.8, 27.4, 29.2, 75.7 (q, J = 51.3 Hz), 87.8 (q, J = 6.7 Hz), 114.8 (q, J = 256.6 Hz), 125.9, 126.9, 127.1, 127.5 128.8, 134.9, 136.2, 140.2, 141.2, 149.1; ^{19}F NMR (188 MHz, CDCl$_3$): δ –50.1; ^{119}Sn NMR
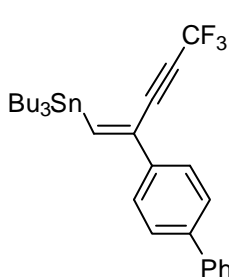
(101 MHz, CDCl$_3$): δ −51.1.   IR (neat): ν 3305, 2231, 1600, 1458, 1240, 1143, 758 cm^{-1}.   MS (EI): *m/z* (%) 505 (28, M$^+$−Bu), 503 (20), 501 (11), 181 (100).   Anal. Calcd for C$_{29}$H$_{37}$F$_3$Sn: C, 62.05; H, 6.64.   Found: C, 61.80; H, 6.64.

Methyl (*Z*)-6,6,6-trifluoro-2-(tributylstannyl)hex-2-en-4-ynoate (22a).   Yield: 78%, a colorless oil.   R$_f$ 0.68 (hexane/AcOEt 4:1). ^{1}H NMR (200 MHz, CDCl$_3$): δ 0.89 (t, *J* = 7.2 Hz, 9H), 1.12 (t, *J* = 7.6 Hz, 6H), 1.26–1.37 (m, 6H), 1.44–1.57 (m, 6H), 3.76 (s, 3H), 7.13 (q, *J* = 3.3 Hz, 1H); ^{13}C NMR (100 MHz, CDCl$_3$): δ 11.3, 13.6, 27.2, 28.9, 52.3, 81.3 (q, *J* = 52.9 Hz), 85.0 (q, *J* = 6.1 Hz), 114.4 (q, *J* = 256.8 Hz), 127.5, 159.9, 170.3; ^{19}F NMR (188 MHz, CDCl$_3$): δ −50.9 (d, *J* = 3.3 Hz); ^{119}Sn NMR (101 MHz, CDCl$_3$): δ −32.2.   IR (neat): ν 2956, 2854, 2235, 1717, 1570, 1288, 1146, 1053 cm^{-1}.   MS (EI): *m/z* (%) 411 (100, M$^+$−Bu), 409 (75), 407 (40), 151 (43).   Anal. Calcd for C$_{19}$H$_{31}$O$_2$F$_3$Sn: C, 48.85; H, 6.69.   Found: C, 49.10; H, 6.43.
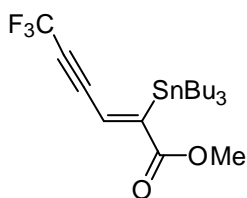
(*Z*)-*N,N*-Dimethyl-6,6,6-trifluoro-2-(tributylstannyl)hex-2-en-4-ynamide   (22b).   Yield: 58%, a colorless oil.   R$_f$ 0.53 (hexane/AcOEt 1:1). ^{1}H NMR (200 MHz, CDCl$_3$): δ 0.89 (t, *J* = 7.2 Hz, 9H), 1.12 (t, *J* = 7.8 Hz, 6H), 1.27–1.38 (m, 6H), 1.47–1.58 (m, 6H), 2.92 (s, 3H), 2.97 (s, 3H), 6.21 (q, *J* = 2.8 Hz, 1H); ^{13}C NMR (67.8 MHz, CDCl$_3$): δ 11.0, 13.6, 27.2, 28.9, 34.4, 38.1, 77.6 (q, *J* = 52.2 Hz), 85.7 (q, *J* = 6.7 Hz), 114.4 (q, *J* = 252.1 Hz), 116.3, 167.1, 172.1; ^{19}F NMR (188 MHz, CDCl$_3$): δ −50.5 (d, *J* = 2.8 Hz); ^{119}Sn NMR (101 MHz, CDCl$_3$): δ −33.3.   IR (neat): ν 2925, 2854, 2229, 1627, 1390, 1288, 1141, 1047 cm^{-1}.   MS (EI): *m/z* (%) 482 (23, M$^+$+1), 424 (100, M$^+$−Bu), 422 (72), 420 (42), 154 (100).   HRMS (FAB) Calcd for C$_{16}$H$_{25}$ONF$_3$Sn: M$^+$−Bu, 429.0910.   Found: *m/z*, 429.0909.   Anal. Calcd for C$_{20}$H$_{34}$ONF$_3$Sn: C, 50.02; H, 7.14.   Found: C, 49.88; H, 7.07.
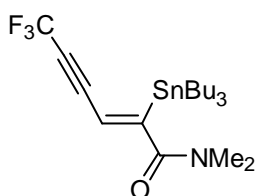
5,5,5-Trifluoro-2-(4-methoxyphenyl)penten-3-yne (23b). ^{1}H NMR (200 MHz, CDCl$_3$): δ 3.83 (s, 3H), 5.83 (s, 1H), 6.07 (s, 1H), 6.91 (d, *J* = 8.6 Hz, 2H), 7.52 (d, *J* = 8.6 Hz, 2H); ^{19}F NMR (188 MHz, CDCl$_3$): δ −50.2.
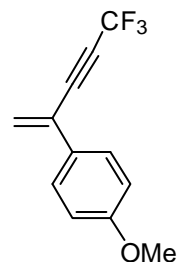
Methyl (*E*)-6,6,6-trifluorohex-2-en-4-ynoate (24a). ^{1}H NMR (200 MHz, CDCl$_3$): δ 3.81 (s, 3H), 6.50 (d, *J* = 16.2 Hz, 1H), 6.76 (dq, *J* = 16.2, 2.8 Hz, 1H); ^{19}F NMR (188 MHz, CDCl$_3$): δ −51.2 (d, *J* = 2.8 Hz).
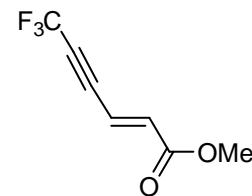
(*E*)-*N,N*-Dimethyl-6,6,6-trifluorohex-2-en-4-ynamide   (24b). ^{1}H NMR (200 MHz, CDCl$_3$): δ 3.05 (s, 3H), 3.12 (s, 3H), 6.74 (dq, *J* = 15.6, 2.6 Hz, 1H), 7.05 (d, *J* = 15.6 Hz, 1H); ^{19}F NMR (188 MHz, CDCl$_3$): δ −50.8 (d, *J* = 2.6 Hz).
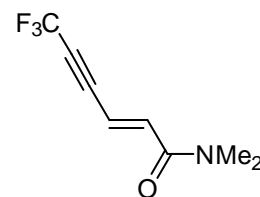
(Z)-1,1,1,6,6,6-Hexafluoro-3-(4-methoxyphenyl)-2-(tributylstannyl)hex-2-en-4-yne
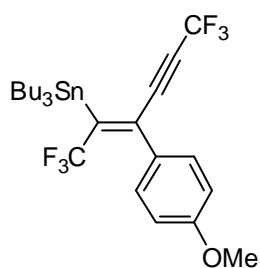
(18a).   Yield: 67%, a pale yellow oil. R_f 0.71 (hexane/AcOEt 4:1). ^{1}H NMR (400 MHz, CDCl$_3$): δ 0.92 (t, J = 7.6 Hz, 9H), 1.18–1.22 (m, 6H), 1.33–1.38 (m, 6H), 1.52–1.59 (m, 6H), 3.82 (s, 3H), 6.88 (d, J = 8.4 Hz, 2H), 7.23 (d, J = 8.4 Hz, 2H); ^{13}C NMR (67.8 MHz, CDCl$_3$): δ 11.8, 13.7, 27.2, 28.6, 55.3, 79.1 (q, J = 52.4 Hz), 87.1 (q, J = 6.7 Hz), 114.0 (2C), 114.5 (q, J = 256.6 Hz), 125.7 (q, J = 273.3 Hz), 129.4, 137.5 (q, J = 10.0 Hz), 149.4 (q, J = 32.3 Hz), 160.0; ^{19}F NMR (188 MHz, CDCl$_3$): δ –50.8, –52.1; ^{119}Sn NMR (101 MHz, CDCl$_3$): δ –22.7 (q, J = 5.5 Hz).   IR (neat): ν 2959, 2924, 2854, 2241, 1607, 1508, 1288, 1146, 837 cm^{-1}.   MS (FAB): m/z (%) 583 (2, M$^+$–1), 581 (2, M$^+$–3), 527 (51, M$^+$–Bu), 255 (100).   Anal. Calcd for C$_{25}$H$_{34}$ClF$_6$Sn: C, 51.48; H, 5.88. Found: C, 51.67; H, 6.09.

(Z)-1,1,1,6,6,6-Hexafluoro-3-(4-methylphenyl)-2-(tributylstannyl)hex-2-en-4-yne
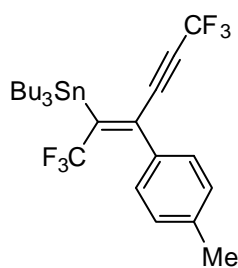
(18b).   Yield: 52%, a pale yellow oil. R_f 0.83 (hexane/AcOEt 4:1). ^{1}H NMR (400 MHz, CDCl$_3$): δ 0.92 (t, J = 7.6 Hz, 9H), 1.19–1.23 (m, 6H), 1.33–1.39 (m, 6H), 1.53–1.59 (m, 6H), 2.37 (s, 3H), 7.17 (s, 4H); ^{13}C NMR (67.8 MHz, CDCl$_3$): δ 11.7, 13.7, 21.4, 27.2, 28.6, 79.3 (q, J = 53.5 Hz), 86.9 (q, J = 6.7 Hz), 114.4 (q, J = 257.7 Hz), 125.5 (q, J = 273.3 Hz), 127.7, 128.9, 134.3, 137.9 (q, J = 6.7 Hz), 138.9, 150.0 (q, J = 31.2 Hz); ^{19}F NMR (188 MHz, CDCl$_3$): δ –50.8, –52.1; ^{119}Sn NMR (101 MHz, CDCl$_3$): δ –22.4 (q, J = 9.3 Hz).   IR (neat): ν 2959, 2924, 2856, 2241, 1508, 1300, 1148, 825 cm^{-1}.   MS (FAB): m/z (%) 567 (2, M$^+$–1), 511 (74, M$^+$–Bu), 509 (59), 442 (4), 253 (53), 239 (100). Anal. Calcd for C$_{25}$H$_{34}$F$_6$OSn: C, 52.94; H, 6.04.   Found: C, 52.77; H, 5.92.

(Z)-1,1,1,6,6,6-Hexafluoro-3-phenyl-2-(tributylstannyl)hex-2-en-4-yne   **(18c).**
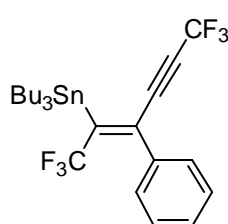
Yield: 76%, a pale yellow oil. R_f 0.70 (hexane/AcOEt 4:1). ^{1}H NMR (400 MHz, CDCl$_3$): δ 0.93 (t, J = 7.3 Hz, 9H), 1.16–1.26 (m, 6H), 1.30–1.49 (m, 6H), 1.52–1.61 (m, 6H), 7.24–7.37 (m, 5H); ^{13}C NMR (67.8 MHz, CDCl$_3$): δ 11.8, 13.7, 27.2, 28.8, 79.6 (q, J = 53.6 Hz), 86.8 (q, J = 6.7 Hz), 114.4 (q, J = 256.6 Hz), 125.5 (q, J = 273.4 Hz), 127.8, 128.2, 128.8, 137.1, 137.8 (q, J = 6.6 Hz), 150.7 (q, J = 36.8 Hz); ^{19}F NMR (188 MHz, CDCl$_3$): δ –50.8, –52.2; ^{119}Sn NMR (101 MHz, CDCl$_3$): δ –21.9 (q, J = 9.3 Hz).   IR (neat): ν 2957, 2924, 2856, 2241, 1570, 1466, 1296, 1148, 877 cm^{-1}.   MS (FAB): m/z (%) 554 (3, M$^+$), 497 (57, M$^+$–Bu), 495 (45), 444 (13), 253 (100).   Anal. Calcd for C$_{24}$H$_{32}$F$_6$Sn: C, 52.11; H, 5.83. Found: C, 52.21; H, 5.78.

(Z)-3-(4-Acetylphenyl)-1,1,1,6,6,6-hexafluoro-2-(tributylstannyl)hex-2-en-4-yne
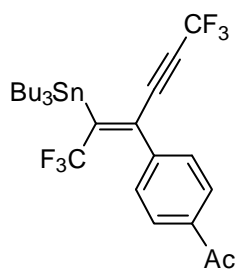
(18e). Yield: 68%, a brown oil. R_f 0.59 (hexane/AcOEt 4:1). ^{1}H NMR (400 MHz, CDCl$_3$): δ 0.93 (t, J = 7.2 Hz, 9H), 1.22–1.26 (m, 6H), 1.34–1.40 (m, 6H), 1.54–1.60 (m, 6H), 2.62 (s, 3H), 5.37 (d, J = 8.4 Hz, 2H), 7.96 (d, J = 8.4 Hz, 2H); ^{13}C NMR (67.8 MHz, CDCl$_3$): δ 11.9, 13.7, 26.7, 27.2, 28.8, 80.2 (q, J = 52.4 Hz), 86.0 (q, J = 6.7 Hz), 114.3 (q, J = 257.7 Hz), 125.3 (q, J = 273.4 Hz), 128.1, 128.3, 136.5 (q, J = 6.6 Hz), 137.1, 141.7, 152.5 (q, J = 33.4 Hz), 197.0; ^{19}F NMR (188 MHz, CDCl$_3$): δ −51.0, −52.3; ^{119}Sn NMR (101 MHz, CDCl$_3$): δ −19.8 (q, J = 5.6 Hz). IR (neat): ν 2959, 2924, 2856, 2241, 1691, 1265, 1149, 847 cm^{-1}. MS (FAB): m/z (%) 597 (65, M$^+$+1), 595 (49, M$^+$−1), 539 (58, M$^+$−Bu), 537 (46), 253 (100), 251 (79). Anal. Calcd for C$_{26}$H$_{34}$F$_6$OSn: C, 52.46; H, 5.76. Found: C, 52.38; H, 5.68.

(Z)-3-(4-Ethoxycarbonylphenyl)-1,1,1,6,6,6-hexafluoro-2-(tributylstannyl)hex-2-en-4-yne (18f). Yield: 57%, a brown oil. R_f 0.74 (hexane/AcOEt 4:1). ^{1}H NMR (400 MHz, CDCl$_3$): δ 0.93 (t, J = 7.2 Hz, 9H), 1.21–1.26 (m, 6H), 1.32–1.42 (m, 9H), 1.43–1.62 (m, 6H), 4.39 (q, J = 6.8 Hz, 2H), 7.34 (d, J = 8.4 Hz, 2H), 8.05 (d, J = 8.4 Hz, 2H); ^{13}C NMR (67.8 MHz, CDCl$_3$): δ 11.8, 13.6, 14.4, 27.2, 28.8, 61.2, 80.1 (q, J = 52.4 Hz), 86.0 (q, J = 6.7 Hz), 114.3 (q, J = 257.7 Hz), 125.3 (q, J = 273.4 Hz), 127.8, 129.5, 130.8, 136.7 (q, J = 8.9 Hz), 141.4, 152.4 (q, J = 33.5 Hz), 165.7; ^{19}F NMR (188 MHz, CDCl$_3$): δ −49.9, −51.0; ^{119}Sn NMR (101 MHz, CDCl$_3$): δ −20.1 (q, J = 9.3 Hz). IR (neat): ν 2959, 2924, 2856, 2243, 1728, 1273, 1149, 862, 710 cm^{-1}. MS (FAB): m/z 627 (13, M$^+$+1), 569 (26, M$^+$−Bu), 567 (21), 253 (79), 251 (55), 136 (100). Anal. Calcd for C$_{27}$H$_{36}$F$_6$O$_2$Sn: C, 51.86; H, 5.80. Found: C, 51.63; H, 5.77.
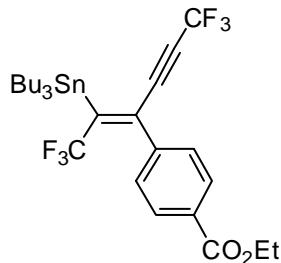
(Z)-1,1,1,6,6,6-Hexafluoro-3-(4-nitrophenyl)-2-(tributylstannyl)hex-2-en-4-yne
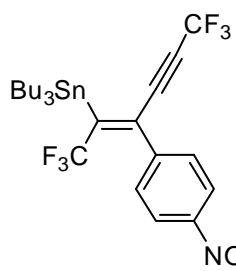
(18g). Yield: 58%, a pale yellow oil. R_f 0.78 (hexane/AcOEt 4:1). ^{1}H NMR (400 MHz, CDCl$_3$): δ 0.93 (t, J = 7.2 Hz, 9H), 1.23–1.27 (m, 6H), 1.35–1.40 (m, 6H), 1.54–1.58 (m, 6H), 7.44 (d, J = 8.8 Hz, 2H), 8.24 (d, J = 8.8 Hz, 2H); ^{13}C NMR (100 MHz, CDCl$_3$): δ 11.8, 13.5, 27.4, 28.7, 80.7 (q, J = 53.4 Hz), 85.3 (q, J = 6.8 Hz), 114.2 (q, J = 257.0 Hz), 123.7, 125.3 (q, J = 273.0 Hz), 128.9, 135.2 (q, J = 6.1 Hz), 143.5, 148.0, 154.3 (q, J = 33.5 Hz); ^{19}F NMR (188 MHz, CDCl$_3$): δ −51.1, −52.4; ^{119}Sn NMR (101 MHz, CDCl$_3$): δ −17.7 (q, J = 7.5 Hz). IR (neat): ν 2959, 2926, 2856, 2243, 1529, 1352, 1304, 1151, 856 cm^{-1}. MS (FAB): m/z (%) 600 (4, M$^+$+1), 542 (15, M$^+$−Bu), 540 (11), 253 (100), 251 (81). Anal. Calcd for C$_{24}$H$_{31}$F$_6$NO$_2$Sn: C, 48.19; H, 5.22; N, 2.34. Found: C, 48.06; H, 5.40; N, 2.27.

(Z)-1,1,1,6,6,6-Hexafluoro-2-(tributylstannyl)-3-(4-trifluoromethylphenyl)hex-2-en-4-yne (18i). Yield: 67%, a brown oil. R_f 0.84 (hexane/AcOEt 4:1). ^{1}H NMR (400 MHz, CDCl$_3$): δ 0.93 (t, J = 7.2 Hz, 9H), 1.22–1.26 (m, 6H), 1.34–1.40 (m, 6H), 1.54–1.60 (m, 6H), 7.39 (d, J = 8.0 Hz, 2H), 7.63 (d, J = 8.0 Hz, 2H); ^{13}C NMR (67.8 MHz, CDCl$_3$): δ 11.9, 13.7, 27.2, 28.8, 80.3 (q, J = 54.7 Hz), 85.9 (q, J = 6.7 Hz), 114.3 (q, J = 256.5 Hz), 123.7 (q, J = 271.1 Hz), 125.3 (q, J = 273.3 Hz), 125.4, 128.2, 130.9 (q, J = 33.5 Hz), 136.1 (q, J = 6.7 Hz), 140.6, 152.9 (q, J = 34.6 Hz); ^{19}F NMR (188 MHz, CDCl$_3$): δ −51.1, −52.3, −63.3; ^{119}Sn NMR (101 MHz, CDCl$_3$): δ −19.4 (q, J = 9.3 Hz). IR (neat): ν 2960, 2928, 2858, 2243, 1325, 1151, 849 cm^{-1}. MS (CI): m/z (%) 603 (96, M$^+$–F), 565 (90, M$^+$–Bu), 291 (100), 253 (45). Anal. Calcd for C$_{25}$H$_{31}$F$_9$Sn: C, 48.34; H, 5.03. Found: C, 48.13; H, 4.97.
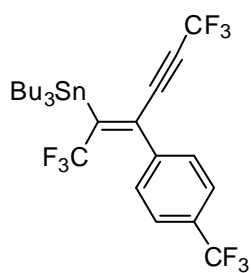
(Z)-3-(4-Chlorophenyl)-1,1,1,6,6,6-hexafluoro-2-(tributylstannyl)hex-2-en-4-yne (18k). Yield: 62%, a pale yellow oil. R_f 0.73 (hexane/AcOEt 4:1). ^{1}H NMR (400 MHz, CDCl$_3$): δ 0.93 (t, J = 7.2 Hz, 9H), 0.95–1.24 (m, 6H), 1.34–1.39 (m, 6H), 1.53–1.59 (m, 6H), 7.21 (d, J = 8.4 Hz, 2H), 7.35 (d, J = 8.4 Hz, 2H); ^{13}C NMR (67.8 MHz, CDCl$_3$): δ 11.8, 13.7, 27.2, 28.8, 79.8 (q, J = 47.5 Hz), 86.3 (q, J = 5.9 Hz), 114.3 (q, J = 231.7 Hz), 125.4 (q, J = 246.2 Hz), 128.5, 129.1, 135.0, 135.5, 136.5 (q, J = 6.6 Hz), 151.8 (q, J = 32.4 Hz); ^{19}F NMR (188 MHz, CDCl$_3$): δ −50.7, −51.9; ^{119}Sn NMR (101 MHz, CDCl$_3$): δ −20.7 (q, J = 7.4 Hz). IR (neat): ν 2959, 2924, 2856, 2241, 1489, 1298, 1149, 1016, 837 cm^{-1}. MS (CI): m/z (%) 89 (5, M$^+$+1), 569 (16, M$^+$–F), 531 (84, M$^+$–Bu), 291 (100), 253 (46). Anal. Calcd for C$_{24}$H$_{31}$ClF$_6$Sn: C, 49.05; H, 5.32. Found: C, 49.32; H, 5.34.
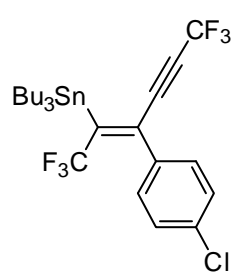
Ethyl (Z)-6,6,6-trifluoro-3-methyl-2-(tributylstannyl)hex-2-en-4-ynoate (26). Yield: 77%, a colorless oil. R_f 0.70 (hexane/AcOEt 4:1). ^{1}H NMR (400 MHz, CDCl$_3$): δ 0.89 (t, J = 7.2 Hz, 9H), 1.08 (t, J = 8.0 Hz, 6H), 1.22–1.37 (m, 9H), 1.44–1.55 (m, 6H), 2.02 (s, 3H), 4.20 (q, J = 7.2 Hz, 2H); ^{13}C NMR (100 MHz, CDCl$_3$): δ 11.0, 13.5, 14.3, 21.4, 27.1, 28.7, 60.6, 76.1 (q, J = 52.3 Hz), 88.4 (q, J = 6.8 Hz), 114.6 (q, J = 256.8 Hz), 129.0, 153.7, 170.9; ^{19}F NMR (188 MHz, CDCl$_3$): δ −50.5; ^{119}Sn NMR (101 MHz, CDCl$_3$): δ −30.8. IR (neat): ν 2923, 2855, 2237, 1712, 1582, 1300, 1142, 1040 cm^{-1}. MS (EI): m/z (%) 439 (100, M$^+$–Bu), 437 (75), 435 (45), 179 (55). Anal. Calcd for C$_{21}$H$_{35}$O$_2$F$_3$Sn: C, 50.93; H, 7.12. Found: C, 51.20; H, 7.03.
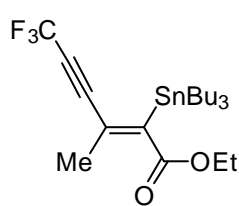
Ethyl (Z)-6,6,6-trifluoro-3-phenyl-2-(tributylstannyl)hex-2-en-4-ynoate (28). Yield: 87%, a colorless oil. R_f 0.65 (hexane/AcOEt 4:1). ^{1}H NMR (200 MHz, CDCl$_3$): δ 0.92 (t, J = 7.2 Hz, 9H), 1.08 (t, J = 7.2 Hz, 6H), 1.15–1.63 (m, 15H), 4.04 (q, J = 7.2 Hz, 2H), 7.31–7.40 (m, 5H); ^{13}C NMR (67.8 MHz, CDCl$_3$): δ 11.4, 13.7, 14.1, 27.2, 28.8, 60.6, 76.9 (q, J = 52.5 Hz), 87.6 (q, J = 6.7 Hz), 114.6 (q, J =
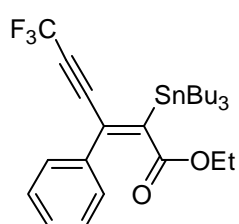
256.6 Hz), 127.3, 128.3, 128.7, 131.6, 137.0, 156.4, 170.9; ^{19}F NMR (188 MHz, CDCl$_3$): δ –50.4; ^{119}Sn NMR (101 MHz, CDCl$_3$): δ –23.7. IR (neat): ν 2958, 2923, 2231, 1709, 1558, 1299, 1195, 1143 cm^{-1}. MS (EI): m/z (%) 501 (100, M$^+$–Bu), 499 (75), 497 (43), 179 (24). HRMS (FAB) Calcd for C$_{22}$H$_{28}$O$_2$F$_3$Sn: M$^+$–Bu, 501.1063. Found: m/z, 501.1062. Anal. Calcd for C$_{26}$H$_{37}$O$_2$F$_3$Sn: C, 56.04; H, 6.69. Found: C, 56.00; H, 6.46.

Dimethyl (Z)-5,5,5-trifluoro-1-(tributylstannyl)penten-3-yne-1,2-dicarboxylate (30).
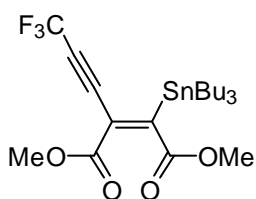
Yield: 71%, a yellow oil. R$_f$ 0.44 (hexane/AcOEt 4:1). ^{1}H NMR (200 MHz, CDCl$_3$): δ 0.89 (t, J = 7.2 Hz, 9H), 1.08 (t, J = 8.0 Hz, 6H), 1.22–1.37 (m, 6H), 1.44–1.55 (m, 6H), 3.801 (s, 3H), 3.809 (s, 3H); ^{13}C NMR (67.8 MHz, CDCl$_3$): δ 11.3, 13.6, 27.2, 28.6, 51.9, 53.1, 78.7 (q, J = 52.3 Hz), 83.4 (q, J = 5.6 Hz), 114.3 (q, J = 256.6 Hz), 121.0, 160.8, 170.9, 173.3; ^{19}F NMR (188 MHz, CDCl$_3$): δ –50.9; ^{119}Sn NMR (101 MHz, CDCl$_3$): δ –16.5. IR (neat): ν 2957, 2926, 2854, 2247, 1745, 1732, 1313, 1226, 1146 cm^{-1}. MS (EI): m/z 469 (100, M$^+$–Bu), 441 (36), 403 (40). Anal. Calcd for C$_{21}$H$_{33}$O$_4$F$_3$Sn: C, 48.03; H, 6.33. Found: C, 48.10; H, 6.13.

Cross-coupling reaction of 20a with 4-iodoacetophenone. To a stirring toluene (3.0 mL) solution of 4-iodoacetophenone (**16e**, 0.96 mmol), Pd$_2$(dba)$_3$ (37 mg, 40 μmol), t-Bu$_3$P (32 mg, 160 μmol), CsF (0.30 g, 2.0 mmol) was slowly added **20a** (0.39 g, 0.80 mmol). The solution was stirred at 100 °C for 3 h and then filtered through a Celite pad. Evaporation of the organic solvent followed by flash column chromatography on silica gel (hexane/AcOEt 4:1) gave (Z)-1-(4-acetylphenyl)-5,5,5-trifluoro-2-phenyl-penten-3-yne (**32**, 0.19 g, 76% yield) as a colorless solid. Mp: 61.9–62.3 °C. R$_f$ 0.50 (hexane/AcOEt 4:1). ^{1}H NMR (200 MHz, CDCl$_3$): δ (s, 3H), 7.41–7.48 (m, 4H), 7.63–7.68 (m, 2H), 7.90 (d, J = 8.6 Hz, 2H), 8.02 (d, J = 8.6 Hz, 2H); ^{13}C NMR (67.8 MHz, CDCl$_3$): δ 85.0 (q, J = 6.1 Hz), 114.6 (q, J = 256.2 Hz), 120.0, 126.3, 128.5, 128.9, 129.1, 136.6, 137.2, 139.0, 139.3, 143.3, 197.3; ^{19}F NMR (188 MHz, CDCl$_3$): δ –50.1. IR (KBr): ν 2956, 2224, 1605, 1512, 1153 cm^{-1}. MS (EI): m/z (%) 302 (100, M$^+$), 287 (13), 259 (10), 233 (15), 189 (25). Anal. Calcd for C$_{18}$H$_{13}$OF$_3$: C, 71.52; H, 4.33. Found: C, 71.23; H, 4.41.
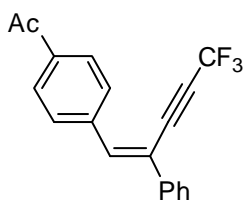
Cross-coupling reaction of 20a with ethyl (E)-3-iodopropenoate. To a stirring toluene (2.0 mL) solution of ethyl (E)-3-iodopropenate (68 mg, 0.30 mmol), Pd$_2$(dba)$_3$ (9.2 mg, 10 μmol), t-Bu$_3$P (4.0 mg, 20 μmol), CuI (19 mg, 0.10 mmol), CsF (46 mg, 0.30 mmol) was slowly added **20a** (97 mg, 0.20 mmol). The solution was stirred at 70 °C for 20 h and then filtered through a Celite pad. Evaporation of the organic solvent followed by flash column chromatography on aluminum oxide (hexane/AcOEt 4:1) gave ethyl (2E,4Z)-8,8,8-trifluoro-5-phenylocta-2,4-dien-6-ynoate (**33**, 40 mg, 68% yield) as a pale yellow solid. Mp: 54.8–55.7 °C. R$_f$ 0.50 (hexane/AcOEt 4:1). ^{1}H NMR (400 MHz, CDCl$_3$): δ 1.34 (t, J = 7.2 Hz, 3H), 4.27 (q, J = 7.2 Hz, 2H), 6.21 (d, J = 15.2 Hz, 1H), 7.38–7.45 (m, 3H), 7.62–7.64 (m, 3H), 7.80 (dd, J = 15.2, 12.0 Hz, 1H);
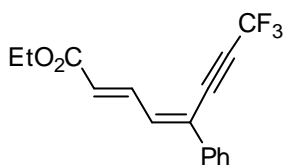
^{13}C NMR (67.8 MHz, CDCl$_3$): δ 14.2, 60.8, 82.5 (q, J = 6.8 Hz), 84.6 (q, J = 52.9 Hz), 114.6 (q, J = 257.6 Hz), 126.1, 126.3, 126.8, 129.0, 129.9, 134.7, 136.1, 139.7, 166.2; ^{19}F NMR (188 MHz, CDCl$_3$): δ −50.4.   IR (KBr): ν 2956, 2237, 1705, 1612, 1256, 1140 cm^{-1}.   MS (EI): m/z (%) 294 (13, M$^+$), 249 (21), 221 (100), 201 (93), 152 (85). HRMS Calcd for C$_{16}$H$_{13}$O$_2$F$_3$: M$^+$, 294.0866.   Found: m/z, 294.0861.

Iododestannylation of 20a.   To a round–bottom flask, **20a** (0.38 g, 0.77 mmol) and THF (10 mL) were charged.   The resulting solution was stirred at room temperature for 3 min, and then cooled to 0 °C.   A solution of I$_2$ (0.27 g, 1.10 mmol) in THF (29 mL) was added dropwise to the solution of **20a** over a period of 20 min.   The mixture was stirred at 0 °C for 40 min before quenching with sat. aq. Na$_2$S$_2$O$_3$.   The aqueous layer was extracted with Et$_2$O.   The combined organic layer was dried over anhydrous MgSO$_4$ and concentrated *in vacuo*.   Removal of the solvent followed by flash column chromatography on silica gel gave (*Z*)-5,5,5-trifluoro-1-iodo-2-phenylpenten-3-yne (**34**, 0.19 g, 76% yield) as a colorless oil.   R$_f$ 0.67 (hexane). ^{1}H NMR (200 MHz, CDCl$_3$): δ 7.37–7.41 (m, 3H), 7.48–7.53 (m, 2H), 7.58 (s, 1H); ^{13}C NMR (67.8 MHz, CDCl$_3$): δ 81.5 (q, J = 52.6 Hz), 86.2 (q, J = 6.9 Hz), 92.6, 114.7 (q, J = 256.2 Hz), 126.0, 128.9, 129.4, 133.6, 136.0; ^{19}F NMR (188 MHz, CDCl$_3$): δ −50.6.   IR (neat): ν 2927, 2855, 2243, 1240, 1139 cm^{-1}.   MS (EI): m/z (%) 323 (16, M$^+$+1), 322 (100, M$^+$), 195 (75), 175 (31).   Anal. Calcd for C$_{11}$H$_6$F$_3$I: C, 41.02; H, 1.88.   Found: C, 41.04; H, 2.13.
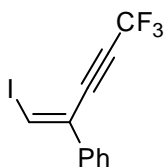
References

(1)   (a) Yoneda, N.; Matsuoka, S.; Miyaura, N.; Fukuhara, T.; Suzuki, A. *Bull. Chem. Soc. Jpn.* **1990**, *63*, 2124. (b) Konno, T.; Chae, J.; Ishihara, T.; Yamanaka, H. *Tetrahedron* **2004**, *60*, 11695.

(2)   Chae, J.; Konno, T.; Ishihara, T.; Yamanaka, H. *Chem. Lett.* **2004**, *33*, 314.

(3)   Yamazaki, T.; Mizutani, K.; Kitazume, T. *J. Org. Chem.* **1995**, *60*, 6046.

(4)   (a) Hanamoto, T.; Hakoshima, Y.; Egashira, M. *Tetrahedron Lett.* **2004**, *45*, 7573. (b) Hanamoto, T.; Egashira, M.; Ishizuka, K.; Furuno, H.; Inanaga, J. *Tetrahedron* **2006**, *62*, 6332.

(5)   Konno, T.; Chae, J.; Miyabe, T.; Ishihara, T. *J. Org. Chem.* **2005**, *70*, 10172.

(6)   (a) Konno, T.; Daitoh, T.; Noiri, A.; Chae, J.; Ishihara, T.; Yamanaka, H. *Org. Lett.* **2004**, *6*, 933. (b) Konno, T.; Daitoh, T.; Noiri, A.; Chae, J.; Ishihara, T.; Yamanaka, H. *Tetrahedron* **2005**, *61*, 9391.

(7)   (a) Borvendeg, J. *Drugs Future* **1985**, *10*, 395. (b) Borvendeg, J.; Anheuer, Z. *Exp. Clin. Endocrinol.* **1985**, *86*, 368. (c) Borvendeg, J.; Hermann, I.; Csuka, O. *Acta Physiol. Hung.* **1996**, *84*, 405. (d) Erdelyi-Toth, V.; Gyergyay, F.; Szamel, I.; Pap, E.; Kralovanszky, J.; Bojti, E.; Csorgo, M.; Drabant, S.; Klebovich, I. *Anti-Cancer Drugs* **1997**, *8*, 603. (e) Monostory, K.; Jemnitz, K.; Vereczkey, L.; Czira, G. *Drug Metab. Dispos.* **1997**, *25*, 1370.

(8)   (a) Burton, D. J.; Yang, Z.-Y. *Tetrahedron* **1992**, *48*, 189. (b) Burton, D. J.; Yang, Z.-Y.; Morken, P. A. *Tetrahedron* **1994**, *50*, 2993. (c) Burton, D. J.; Yang, Z.-Y.; Qiu, W. *Chem. Rev.* **1996**, *96*, 1641.

(9)   Shimizu, M.; Higashi, M.; Takeda, Y.; Jiang, G.; Murai, M.; Hiyama, T. *Synlett* **2007**, 1163.

(10)   Shimizu, M.; Jiang, G.; Murai, M.; Takeda, Y.; Nakao, Y.; Hiyama, T.; Shirakawa, E. *Chem. Lett.* **2005**, *34*, 1700.

(11)   Drakesmith, F. G.; Stewart, O. J.; Tarrant, P. *J. Org. Chem.* **1968**, *33*, 280.

(12)   Katritzky, A. R.; Qi, M.; Wells, A. P. *J. Fluorine Chem.* **1996**, *80*, 145.

(13)   Brisdon, A. K.; Crossley, I. R. *Chem. Commun.* **2002**, 2420.

(14)   Konno, T.; Chae, J.; Kanda, M.; Nagai, G.; Tamura, K.; Ishihara, T.; Yamanaka, H. *Tetrahedron* **2003**, *59*, 7571.

(15)   (a) Shimizu, M.; Fujimoto, T.; Minezaki, H.; Hata, T.; Hiyama, T. *J. Am. Chem. Soc.* **2001**, *123*, 6947. (b) Shimizu, M.; Fujimoto, T.; Liu, X.; Minezaki, H.; Hata, T.; Hiyama, T. *Tetrahedron* **2003**, *59*, 9811. (c) Liu, X.; Shimizu, M.; Hiyama, T. *Angew. Chem., Int. Ed.* **2004**, *43*, 879. (d) Shimizu, M.; Fujimoto, T.; Liu, X.; Hiyama, T. *Chem. Lett.* **2004**, *33*, 438. (e) Takeda, Y.; Shimizu, M.; Hiyama, T. *Angew. Chem., Int. Ed.* **2007**, *46*, 8659. (f) Shimizu, M.; Fujimoto, T.; Liu, X.; Takeda, Y.; Hiyama, T. *Heterocycles* **2008**, *76*, 329.

(16)   Bardin, V. V.; Adonin, N. Y.; Frohn, H.-J. *Organometallics* **2005**, *24*, 5311.

(17)   Brisdon, A. K.; Crossley, I. R.; Pritchard, R. G.; Sadiq, G. Warren, J. E. *Organometallics* **2003**, *22*, 5534.

(18)   (a) Zimmer, R.; Dinesh, C. U.; Nandanan, E.; Khan, F. A. *Chem. Rev.* **2000**, *100*, 3067. (b) Hashmi, A. S. K. *Angew. Chem., Int. Ed.* **2000**, *39*, 3590. (c) Ma, S. *Chem. Rev.* **2005**, *105*, 2829. (d) Brummond, K. M.; DeForrest, J. E. *Synthesis* **2007**, 795.

(19)   (a) Hoffmann-Röder, A.; Krause, N. *Angew. Chem., Int. Ed.* **2004**, *43*, 1196. (b) Dembitsky, V. M.; Maoka, T. *Prog. Lipid Res.* **2007**, *46*, 328.

(20) (a) Bosbury, P. W. L.; Fields, R.; Haszeldine, R. N.; Moran, D. *J. Chem. Soc, Perkin Trans. 1* **1976**, 1173. (b) Bosbury, P. W. L.; Fields, R.; Haszeldine, R. N. *J. Chem. Soc, Perkin Trans. 1* **1978**, 422. (c) Dolbier, Jr. W. R.; Burkholder, C. R.; Piedrahita, C. A. *J. Fluorine Chem.* **1982**, *20*, 637. (d) Hanzawa, Y.; Kawagoe, K.-i.; Yamada, A.; Kobayashi, Y. *Tetrahedron Lett.* **1985**, *26*, 219. (e) Burton, D. J.; Hartgraves, G. A.; Hsu, J. A. *Tetrahedron Lett.* **1990**, *31*, 3699. (f) Hung, M.-H. *Tetrahedron Lett.* **1990**, 31, 3703. (g) Konno, T.; Tanikawa, M.; Ishihara, T.; Yamanaka, H. *Chem. Lett.* **2000**, *29*, 1360. (h) Lentz, D.; Willemsen, S. *Angew. Chem., Int. Ed.* **2001**, *40*, 2087. (i) Shen, Q.; Hammond, G. B. *J. Am. Chem. Soc.* **2002**, *124*, 6534. (j) Lentz, D. *J. Fluorine Chem.* **2004**, *125*, 853. (k) Han, H. Y.; Kim, M. S.; Son, J. B.; Jeong, I. H. *Tetrahedron Lett.* **2006**, *47*, 209. (l) Yamazaki, T.; Yamamoto, T.; Ichihara, R. *J. Org. Chem.* **2006**, *71*, 6251. (m) Watanabe, Y.; Yamazaki, T.; *Synlett* **2009**, 3352.

(21) (a) Tsuji, J.; Mandai, T. *Angew. Chem., Int. Ed. Engl.* **1996**, *34*, 2589. (b) Ogasawara, M.; Hayashi, T. In *Modern Allene Chemistry;* Krause, N.; Hashmi, A. S. K., Eds.; Wiley-VCH: Weinheim, 2004, pp. 93–140.

(22) (a) Yamazaki, T.; Hiraoka, S.; Sakamoto, J.; Kitazume, T. *Org. Lett.* **2001**, *3*, 743. (b) Schwier, T.; Sromek, A. W.; Yap, D. M. L.; Chernyak, D.; Gevorgyan, V. *J. Am. Chem. Soc.* **2007**, *129*, 9868.

(23) (a) Miyaura, N.; Suzuki, A. *Chem. Rev.* **1995**, *95*, 2457. (b) Suzuki, A. *J. Organomet. Chem.* **1999**, *576*, 147. (c) Miyaura, N. *Top. Curr. Chem.;* Miyaura, N., Ed.; Springer: Berlin, 2002, pp. 11–59.

(24) (a) Batey, R. A.; Quach, T. D.; Shen, M.; Thadani, A. N.; Smil, D. V.; Li, S.-W.; MacKay, D. B. *Pure Appl. Chem.* **2002**, *74*, 43. (b) Darses, S.; Genet, J.-P. *Eur. J. Org. Chem.* **2003**, 4313. (c) Molander, G. A.; Figueroa, R. *Aldrichim. Acta* **2005**, *38*, 49. (d) Molander, G. A.; Ellis, N. *Acc. Chem. Res.* **2007**, *40*, 275. (e) Stefani, H. A.; Cella, R.; Vieira, A. S. *Tetrahedron* **2007**, *63*, 3623. (f) Darses, S.; Genet, J.-P. *Chem. Rev.* **2008**, *108*, 288.

(25) Bunch, J. E.; Bumgardner, C. L. *J. Fluorine Chem.* **1987**, *36*, 313.

(26) Molander, G. A.; Katona, B. W.; Machrouhi, F. *J. Org. Chem.* **2002**, *67*, 8416.

(27) (a) Uenishi, J.-i.; Beau, J.-M.; Armstrong, R. W; Kishi, Y. *J. Am. Chem. Soc.* **1987**, *109*, 4756. (b) Gillmann, T.; Weeber, T. *Synlett* **1994**, 649. (c) Chen, H.; Deng, M.-Z. *Org. Lett.* **2000**, *2*, 1649. (d) Frohn. H.-J.; Adonin, N. Y.; Bardin, V. V.; Starichenko, V. F. *Tetrahedron Lett.* **2002**, *43*, 8111.

(28) Hirabayashi, K.; Mori, A.; Kawashima, J.; Suguro, M.; Nishihara, Y.; Hiyama, T. *J. Org. Chem.* **2000**, *65*, 5342.

(29) Fei, Z.; Zhao, D.; Geldbach, T. J.; Scopelliti, R.; Dyson, P. J. *Eur. J. Inorg. Chem.* **2005**, 860.

(30) (a) Shirakawa, E.; Yoshida, H.; Kurahashi, T.; Nakao, Y.; Hiyama, T. *J. Am. Chem. Soc.* **1998**, *120*, 2975. (b) Shirakawa, E.; Yoshida, H.; Nakao, Y.; Hiyama, T. *J. Am. Chem. Soc.* **1999**, *121*, 4290. (c) Shirakawa, E.; Hiyama, T. *J. Organomet. Chem.* **1999**, *576*, 169. (d) Shirakawa, E.; Yamasaki, K.; Yoshida, H.; Hiyama, T. *J. Am. Chem. Soc.* **1999**, *121*, 10221. (e) Shirakawa, E.; Yoshida, H.; Nakao, Y.; Hiyama, T. *Org. Lett.* **2000**, *2*, 2209. (f) Shirakawa, E.; Nakao, Y.; Yoshida, H.; Hiyama, T. *J. Am. Chem. Soc.* **2000**, *122*, 9030. (g) Shirakawa, E.; Nakao, Y.; Hiyama, T. *Chem. Commun.* **2001**, 263. (h) Shirakawa E, Hiyama T. *Bull. Chem. Soc. Jpn.* **2002**, *75*, 1435. (i) Shirakawa, E.; Nakao, Y.; Tsuchimoto,

T.; Hiyama, T. *Chem. Commun.* **2002**, *8*, 1962. (j) Shirakawa, E.; Hiyama, T. *J. Organomet. Chem.* **2002**, *653*, 114. (k) Shirakawa, E.; Yamamoto, Y.; Nakao, Y.; Oda, S.; Tsuchimoto, T.; Hiyama, T. *Angew. Chem., Int. Ed.* **2004**, *43*, 344.

Chapter 3

Preparation, Structure, and Diels-Alder Reaction of
Phenyl(3,3,3-trifluoropropynyl)iodoium Trifluoromethanesulfonate

Phenyl(3,3,3-trifluoropropynyl)iodonium trifluoromethanesulfonate was prepared from tributyl(3,3,3-trifluoropropynyl)stannane and PhI(CN)OTf. The molecular structure, as determined by X-ray diffraction crystallographic analysis, was shown to have a T-shape geometry with a hypervalent iodine as the central atom. The iodonium salt underwent smoothly the Diels–Alder reaction with 1,3-dienes, furans, and pyrrole, respectively, to give trifluoromethylated cyclohexadienyliodonium salts in good to high yields.

1. Introduction

As described in Chapter 2, 3,3,3-trifluoropropynylmetals serve as useful nucleophilic reagents for facile incorporation of a 3,3,3-trifluorine-substituted C_3 moiety into organic molecules.[1] In contrast, electrophilic reagents consisting of a 3,3,3-trifluoropropynyl group remain to be explored.[2] A sole example is 1-chloro- and 1-bromo-3,3,3-trifluoropropynes, which have boiling point of 3 °C and 24 °C, respectively, and readily polymerize even below their boiling points.[2c] Thus, non-volatile and stable trifluoropropynylated electrophilic reagents, if available, definitely open a new entry to CF_3-containing compounds. In view that alkynyl(aryl)iodonium salts are generally stable, highly reactive, and widely utilized in various organic reactions,[3] the author considered preparation and reactions of 3,3,3-trifluoropropynyliodonium salts would facilitate synthesis of CF_3-containing target molecules. Described in this Chapter are preparation, structure, the Diels–Alder reaction, and theoretical calculations of phenyl(3,3,3-trifluoropropynyl)iodonium trifluoromethanesulfonate (**1**). The iodonium salt is stable and easy to handle, and its cycloaddition with dienes smoothly proceeds even at room temperature to give the corresponding CF_3-containing cyclohexadienyliodonium salts in good to high yields.

1
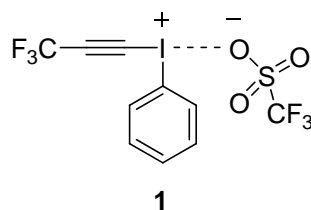
2. Results and Discussion

2–1. Preparation of phenyl(3,3,3-trifluoropropynyl)iodonium triflate (1)

At the outset, the author attempted to prepare **1** according to the protocol reported for functionalized alkynyl(phenyl)iodonium triflates.[4] Thus, to a CH_2Cl_2 solution of PhI(CN)OTf [5] was added tributyl(3,3,3-trifluoropropynyl)stannane (see Chapter 2) at –42 °C, and the resulting mixture was stirred for 1 h at the same temperature. Addition of hexane to the reaction mixture at –42 °C was found only to recover starting materials (Table 1, entry 1). These results may be attributed to low nucleophilic nature of 3,3,3-trifluoropropynylstannane owing to the highly electronegative CF_3 group. Slow elevation of the reaction temperature from –42 to –20 °C over 1 h resulted in

formation of colorless precipitates, which were purified by recrystallization from hexane/CH$_2$Cl$_2$ at –30 °C to give colorless microcrystals of **1** (mp 110–111 °C) in 20% yield (entry 2). The structure was characterized by ^{1}H, ^{13}C, and ^{19}F NMR, IR, and elementary analysis, and unambiguously confirmed by X-ray crystallographic analysis of its single crystal (vide infra). Infrared spectra showed a weak peak at 2222 cm^{-1}, suggesting the presence of carbon–carbon triple bond, and ^{13}C NMR spectra exhibited two signals at 41.2 and 89.4 ppm assignable to *sp*-hybridized carbons at α- and β-position relative to the iodonium center, respectively. Since C$_\beta$ signal of fluorine-free alkynyliodonium salts is typically observed at δ 110–120 ppm,[3a] the large upfield shift (20–30 ppm) is worth noting. This phenomenon might be rationalized by contribution of negative-fluorine resonance structure of **1** (vide infra). The hypervalent iodonium salt (**1**) is soluble in CH$_3$CN and CH$_2$Cl$_2$, and can be stored without decomposition under argon atmosphere at –30 °C for at least 3 months. To improve isolation yield, the reaction mixture was warmed up to room temperature in 0.5 h (entry 3). However, the alkynyliodonium salt was obtained in less than 20% yield and accompanied by inseparable impurities presumably derived from decomposition of **1** under the reaction conditions. When the reaction mixture was gradually warmed from –42 to 0 °C over 2 h, **1** was isolated in 60% yield (entry 4). Under the same conditions, neither PhI(CN)OTs[6] nor PhI(CN)OMs[7] afforded **1** at all (entries 5 and 6).

Table 1. Preparation of phenyl(3,3,3-trifluoropropynyl)iodonium triflate (**1**).

Entry	X	Temp. (°C)	Time (h)	Yield (%)[a]
1	OTf	–42	1	0
2	OTf	–42 to –20	1	20
3	OTf	–42 to 25	0.5	<20[b]
4	OTf	–42 to 0	2	60
5	OTs	–42 to 0	2	0
6	OMs	–42 to 0	2	0

[a] Isolated yields. [b] Not isolated as a pure form.

2–2. X-ray crystallographic analysis of 1

Single crystal of **1** was obtained by recrystallization from hexane/CH$_2$Cl$_2$ at –30 °C and analyzed by the X-ray crystallography to reveal the molecular structure of **1** shown in Figure 1a. Salt **1** adopted a T-shape geometry with bond angles being 92.67(14)° for C(3)–I(1)–C(4) and 84.33(11)° for O(2)–I(1)–C(4). The atomic distance between I(1) and O(2) was 2.596(3) Å, much longer than the sum of covalent bond radii of iodine and oxygen (2.07 Å), but shorter than sum of the van der Walls radii (3.50 Å).[8] These structural characteristics are clearly consistent with the hypervalent nature of the iodine atom. Packing diagram of **1** showed a dimeric structure where one TfO⁻ cross-links adjacent two iodonium centers (Figure 1b). Namely, one oxygen atom coordinates to an I⁺ at the apical position, and the other at the pseudo-equatorial position of the adjacent iodonium center with the distance of 2.91(9) Å, which is longer than that of I–O (apical). The closest contact of F···F (2.90 Å) was shorter than the sum of van der Waals radii (2.94 Å) and is responsible for the 2D molecular column.[9]
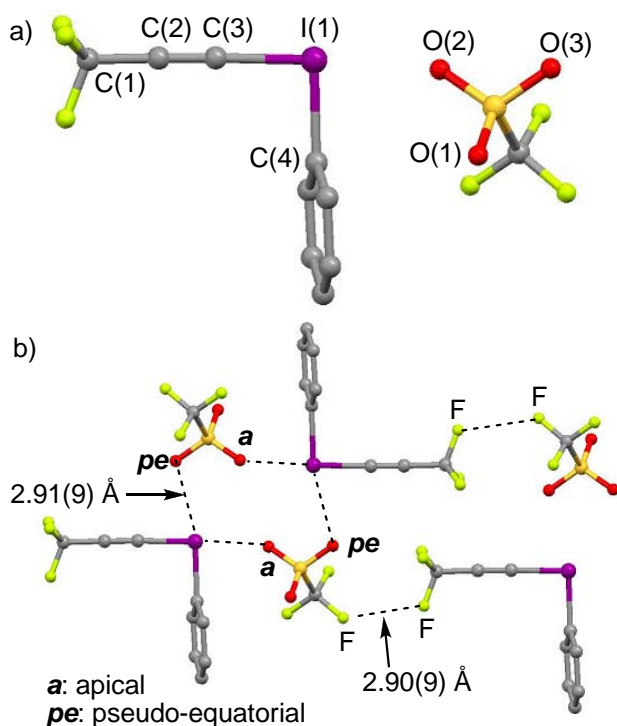
Figure 1. (a) Molecular structure and (b) packing diagram of **1**.
Selected bond lengths (Å) and angles (°): C(1)–C(2) 1.451(1), C(2)–C(3) 1.176(5), C(3)-I(1) 2.022(3), I(1)–C(4) 2.109(3), I(1)–O(2) 2.596(3); C(1)–C(2)–C(3) 179.2(4), C(2)–C(3)–I(1) 178.3(3), C(3)–I(1)–O(2) 176.99(12), C(3)–I(1)–C(4) 92.67(14), C(4)–I(1)–O(2) 84.33(11).

60

2–3. Diels–Alder reaction with 1,3-cyclic dienes

To demonstrate the synthetic utility of **1**, the author carried out the Diels–Alder reaction with 2,3-dimethylbuta-1,3-diene (**2a**) (Scheme 1).   Treatment of **1** with diene **2a** in CH$_3$CN at room temperature was found to give the corresponding adduct **3a** as a microcrystalline colorless solid in 87% yield.   Since phenyl(propynyl)iodonium trifluoromethanesulfonate (**4**), which is fluorine-free counterpart of **1**, did not react with **2a** at all under the similar conditions, the high reactivity of **1** is ascribed to the presence of three fluorine atoms.
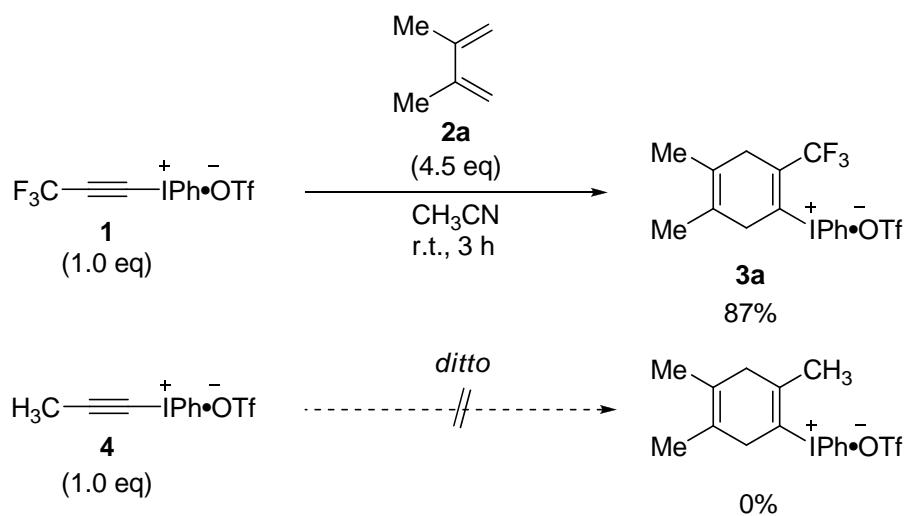
Scheme 1.   Diels–Alder reaction with 2,3-dimethylbuta-1,3-diene (**2a**).

The molecular structure and packing diagram of **3a** were clarified by single-crystal X-ray crystallography as shown in Figure 2.   Single crystal of **3a** was obtained by recrystallization from hexane/CH$_2$Cl$_2$ at −30 °C.   Like **1**, alkenyliodonium salt **3a** adopted a T-shape geometry with the hypervalent iodine atom as the central point (Figure 2a).   It should be noted that the bond length of C(1)–I was slightly longer (2.13 Å) than that of fluorine-free typical cyclic alkenyliodonium salt **5** (2.07 Å),[4] which might be attributed to steric repulsion between a CF$_3$ group and a iodine atom.   Crystal packing of **3a** adopted polymeric structure in which one iodine atom was coordinated by two adjacent triflate counter ion, in turn one triflate ion serving as a divalent ligand with two iodine atoms (Figure 2b).
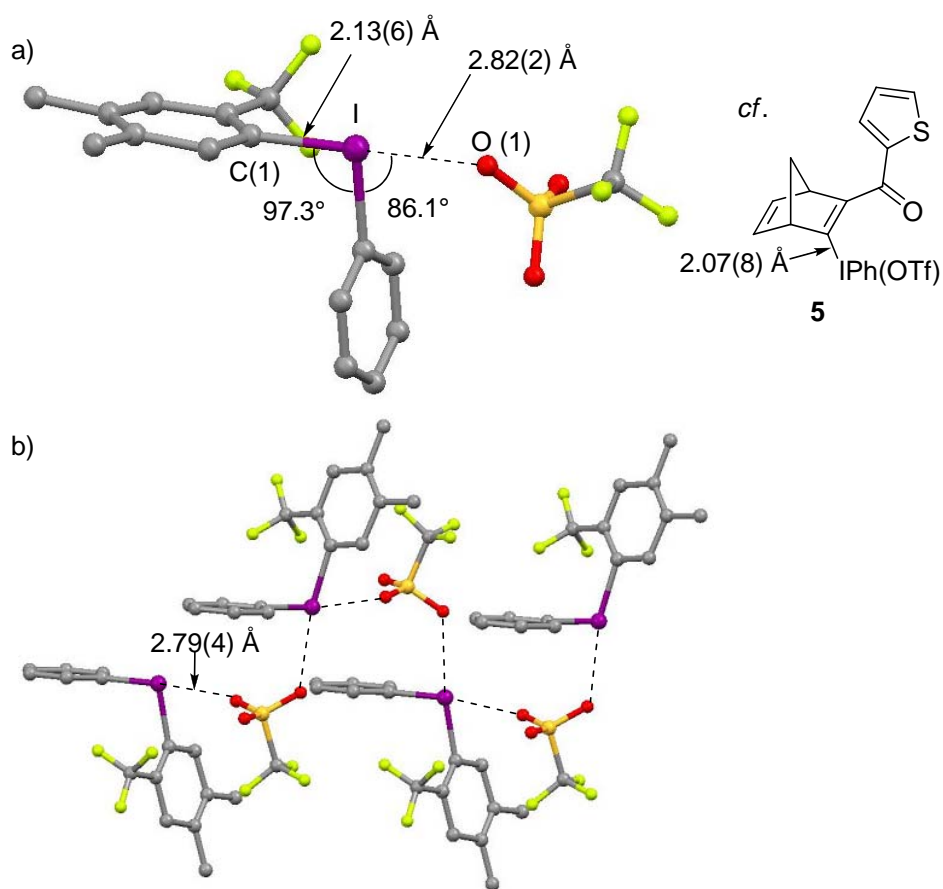
Figure 2. (a) Molecular structure and (b) packing diagram of **3a**.

The scope of the Diels–Alder reaction with cyclic 1,3-dienes is summarized in Table 2. Dienes **2b** and **2c** also underwent the cycloaddition to give alkenyliodonium salts **3b** and **3c** in good yields (entries 1 and 2). Trifluoromethylated 7-oxabicyclo[2.2.1]heptanes **3d** and **3e** were prepared from **1** with furans **2d** and **2e**, respectively (entries 3 and 4). It is noteworthy that **1** underwent the Diels-Alder reaction even with *N*-methylpyrrole (**2f**) which rarely undergoes cycloadditions (entry 5).[10] Acyclic 1,3-dienes such as *trans*-1-methoxy-3-(trimethylsilyloxy)buta-1,3-diene (Danishefsky's diene)[11] gave intractable complex mixtures of products presumably due to polymerization of the dienes.

Table 2.   Diels–Alder reaction of **1** with cyclic 1,3-dienes **2**.

Entry	Diene	Product		Yield (%)
1	**2b**	**3b**		78
2	**2c**	**3c**		63
3	**2d**	**3d**		81
4	**2e**	**3e**		81
5	**2f**	**3f**		72

Versatile alkenyliodonium functionality in the Diels–Alder adducts allows various transformations.[12]   For example, treatment of **3a** with CuI/KI gave iodocyclohexadiene **6**, which was converted into CF_3-containing polysubstituted iodobenzene **7** by dehydrogenation with *p*-chloranil (Scheme 2).[12d]
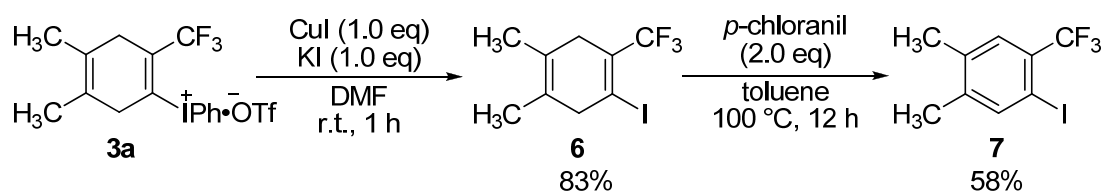
Scheme 2.   Transformation of **3a** into CF_3-substituted iodobenzene **7**.

Furthermore, CF$_3$-containing enyne **8** was synthesized by the Pd/Cu-catalyzed coupling reaction of **3b** with phenylethenylstannane (Eq. 1).[12e]

(1)
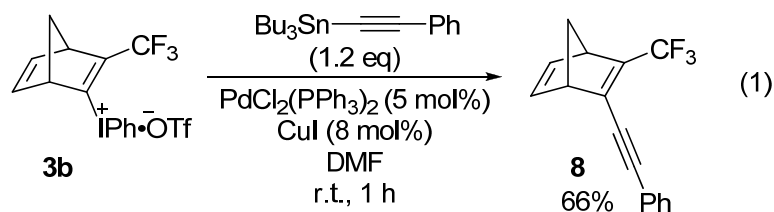
2–4. Theoretical calculations

To gain further insights into the structure of **1**, theoretical calculations were carried out by a DFT method using Gaussian 03 package.[13] The optimized structure obtained by the calculation at a B3LYP/LanL2DZ+dp, 6-31++G(d,p) level clearly showed a T-shape geometry with bond angles being 91.14(75)° for C(1)–I–C(3) and 86.92(51)° for O(1)–I–C(3) (Figure 3), a quite similar structure as observed by X-ray analysis. It should be noted that the I–O(1) distance is much shorter (2.34 Å) than that observed by X-ray analysis (2.59 Å), which may reflect much stronger coordination of a triflate to iodonium center in the gas phase than in the solid state, or possibly due to the assumption of monomeric structure in the calculation contrast to the dimeric structure in the solid state. Other representative bond lengths and angles were close to those observed by X-ray crystallographic analysis.
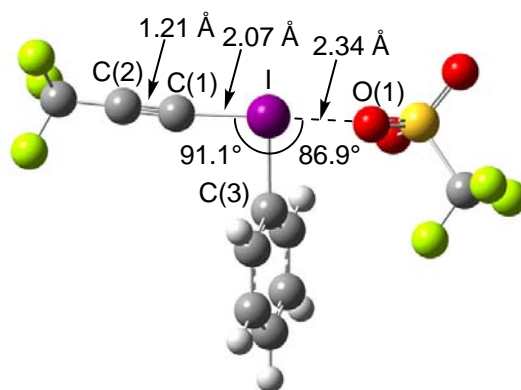
Figure 3. Optimized structure of **1** at B3LYP/LanL2DZ+dp,6-31++G(d,p) level.

Molecular orbital shapes of HOMO and LUMO of **1** are drawn in Figure 4 along with those of fluorine-free counterpart **4** for comparison. HOMOs of both compounds dominantly localize on three oxygen atoms of TfO⁻, while LUMOs mainly lie on the iodobenzene moiety and even expand to the carbon–carbon triple bond. Notably,

LUMO of **1** is more expanded onto the alkynyl moiety including a CF_3 group than that of **4** does.
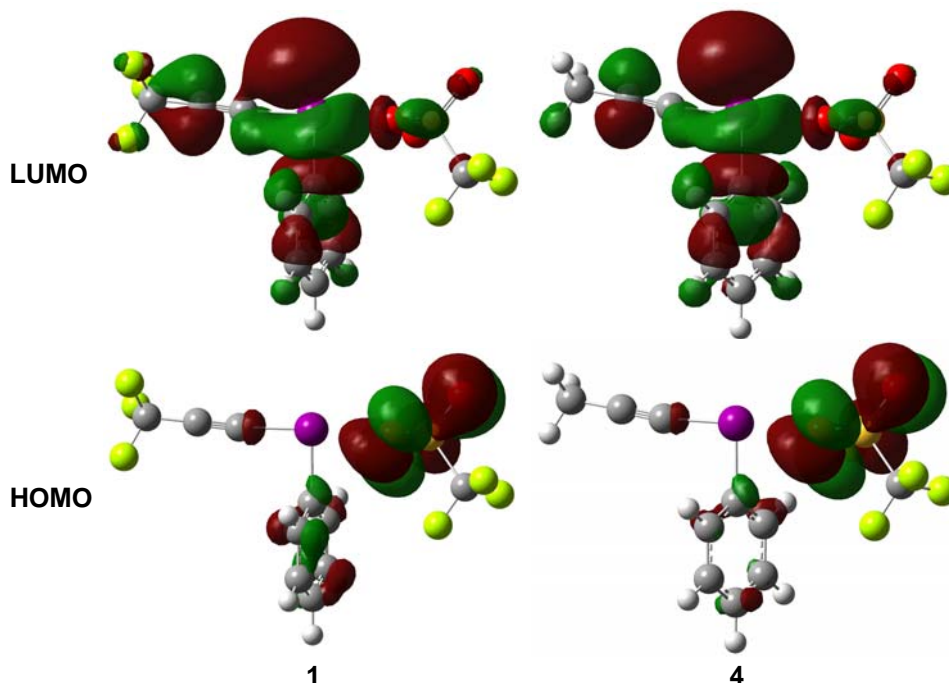
Figure 4. Molecular orbital drawings of **1** and **4** at B3LYP/LanL2DZ+dp, 6-31++G(d,p) level.

To consider the difference in reactivity of **1** and **4** for the Diels–Alder reaction with **2a**, the author has calculated their orbital energy levels and summarizes the results in Table 3. Substitution of CH_3 in **4** with CF_3 decreases both of HOMO and LUMO energy levels by 0.53 eV and 0.47 eV, respectively. Energy differences (ΔE) between HOMO of butadiene **2a** and LUMO of trifluoropropynyliodonium salt **1** was found smaller (2.98 eV) than that for **4** (3.45 eV), supporting the experimental outcomes that **1** undergoes the Diels–Alder reaction more easily than **4** (Scheme 1).

Table 3. Comparison of calculated energy levels of **1** and **4**.

Compound	E_{HOMO} (eV)	E_{LUMO} (eV)	ΔE (eV)^a
2a	−6.14	−0.09	—
1	−7.95	−3.16	2.98
4	−7.42	−2.69	3.45

^{a} $\Delta E = E_{HOMO(2a)} - E_{LUMO(1 \text{ or } 4)}$.

Charge distributions in the iodonium salts **1** and **4** were evaluated by natural bonding orbital (NBO) analysis[14] as illustrated in Figure 5. As expected, the hyper

iodine atom in both compounds has a large positive charge (+1.238 for **1**, +1.227 for **4**). Whereas a positive charge (+1.062) is localized at the CF$_3$ carbon due presumably to three electronegative fluorine atoms, the charge distribution of **4** is markedly reversed where the CH$_3$ carbon has a negative charge (–0.729). Due probably to the such contrasting charge distribution, **1** has a negative charge (–0.109) on the C$_\beta$ atom; in contrast, **4** has a positive charge (+0.054). These results are consistent with the experimental observation that NMR signal of C$_\beta$ in **1** shifted to upper field region than that of the fluorine-free alkynyliodonium salt **4**.
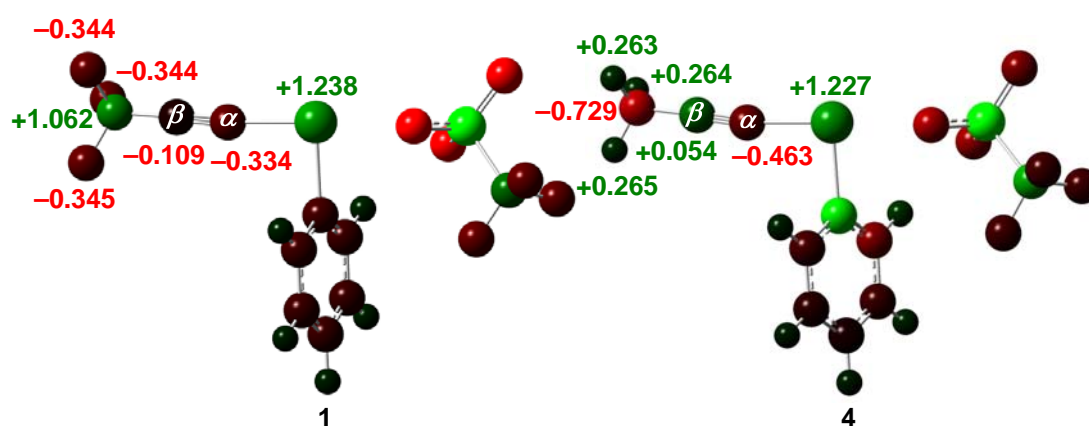
Figure 5. Summary of atomic charge distributions of **1** and **4** by NBO analysis at B3LYP/LanL2DZ+dp, 6-31++G(d,p) level.

This charge inversion at the alkynyl β-carbons would be rationalized by resonance structures of **1** and **4** as shown in Figure 6. As for **1**, contribution of structure **1'** can be considered because **1'** should be stabilized by negative hyperconjugation.[15] On the contrary, fluorine-free alkynyliodonium salt **4** should favor resonance structure **4'** and **4''** probably due to the electron-donating nature of CH$_3$ group through hyperconjugation.
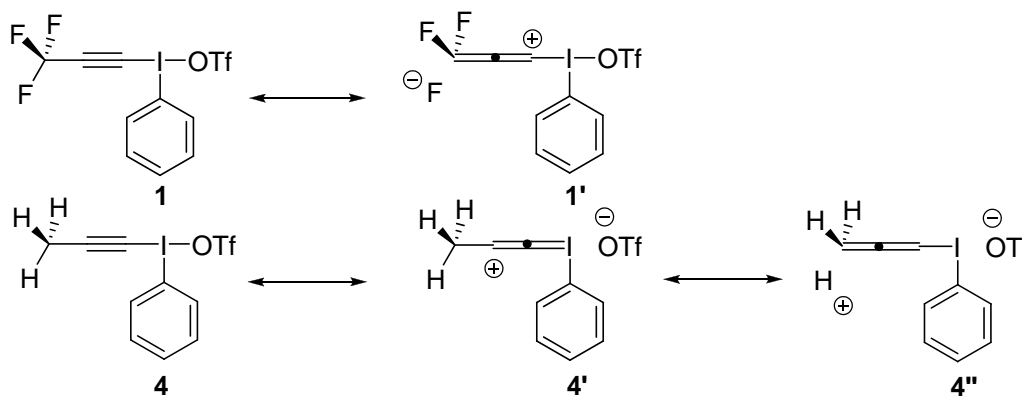
Figure 6. Resonance structures of **1** (top) and **4** (bottom).

3. Conclusion

In summary, the author has succeeded in preparation of phenyl(3,3,3-trifluoropropynyl)iodonium triflate (**1**) for the first time, and its structure was disclosed to have a T-shape geometry as revealed by X-ray crystallographic analysis. The Diels–Alder reaction of **1** provides CF$_3$-substituted cyclohexadienyliodonium salts, which can further serve as versatile synthetic precursors.

4. Experimental Section

Preparation of phenyl(3,3,3-trifluoropropynyl)iodonium trifluoromethanesulfonate (1). To a three-necked round-bottomed flask (500 mL) equipped with a magnetic stirring bar were added PhI(CN)OTf (6.7 g, 18 mmol) and CH_2Cl_2 (180 mL) under an argon atmosphere. The solution was cooled to –42 °C and stirred for 10 min before dropwise addition of a CH_2Cl_2 solution (50 mL) of tributyl(3,3,3-trifluoropropynyl)stannane (7.1 g, 19 mmol) with a syringe over a period of 20 min. The resulting solution was warmed to 0 °C over a period of 2 h. The resulting mixture was cooled again to –42 °C, and then hexane (200 mL) was added to the flask with keeping the temperature at –42 °C. After 10 min, colorless solid precipitated, which was filtered through a sintered glass under an argon atmosphere. The precipitates were washed with cold hexane (100 mL), dried under reduced pressure, and dissolved in CH_2Cl_2 (150 mL). Filtration of insoluble impurities followed by

$$F_3C \!-\!\!\!\equiv\!\!\!-\! \overset{+}{I}Ph \cdot \overset{-}{O}Tf$$

dilution with hexane (200 mL) gave precipitates which were recrystallized from CH_2Cl_2/hexane to give **1** (4.7 g, 60% yield) as colorless microcrystals. Mp: 110.0–111.0 °C (dec). ^{1}H NMR (400 MHz, CD_3CN): δ 7.61–7.65 (m, 2H), 7.78–7.82 (m, 1H), 8.22–8.24 (m, 2H); ^{13}C NMR (100 MHz, CD_3CN): δ 41.2 (q, J = 8.8 Hz), 89.4 (q, J = 54.1 Hz), 114.1 (q, J = 258.5 Hz), 118.4, 121.5 (q, J = 317.2 Hz), 134.2, 135.1, 136.7; ^{19}F NMR (282 MHz, CD_3CN): δ –51.6, –78.0. IR (KBr): ν 3070, 2222, 1649, 1595, 1564, 1471, 1442, 1261, 1180, 1165, 1151, 1028, 989, 916, 732, 644, 580, 520, 451 cm^{-1}. MS (FAB): m/z 298 (56, [M^+–OTf+H]), 297 (100, [M^+–OTf]), 204 (16), 201 (38), 170 (98), 77 (87). Anal. Calcd for $C_{10}H_5F_6IO_3S$: C, 26.92; H, 1.13. Found: C, 26.90; H, 1.39.

General procedure for Diels-Alder reaction of alkynyliodonium salt 1 with 1,3-dienes.

To a vial tube (15 mL) equipped with a magnetic stirring bar was added **1** (0.22 g, 0.50 mmol). The vial tube was then capped with a rubber septum, evacuated for 5 min, and charged with argon. The evacuation–purge operation was repeated twice. Acetonitrile (5 mL) was added to the vial at room temperature under an argon atmosphere to completely dissolve **1**. To the mixture was added a 1,3-diene (2.3 mmol) dropwise at room temperature. The resulting solution was stirred at room temperature for 3 h. Removal of organic solvent under reduced pressure followed by recrystallization of the residue from CH_2Cl_2/hexane at –30 °C gave **3**.

(4,5-Dimethyl-2-(trifluoromethyl)cyclohexa-1,4-dienyl)(phenyl)iodonium trifluoromethanesulfonate (3a). Yield: 87%, colorless microcrystals. Mp: 179.0–180.0 °C (dec). ^{1}H NMR (400 MHz, CD_3CN): δ 1.57 (s, 3H), 1.62 (s, 3H), 3.19–3.23 (m, 2H), 3.36–3.38 (m, 2H), 7.58–7.62 (m, 2H), 7.77–7.81 (m, 1H), 8.07–8.09 (m, 2H); ^{13}C NMR (100 MHz, CD_3CN): δ 18.1, 18.3, 36.0, 44.5, 112.1, 118.3 (q, J = 3.0 Hz), 122.2 (q, J = 317.9 Hz), 122.3, 122.7 (q, J = 273.8 Hz), 124.3, 133.9, 134.9, 137.1 (q, J = 32.1 Hz), 137.7; ^{19}F NMR (282 MHz, CD_3CN): δ –61.7, –78.0. IR (KBr): ν 3057, 2922, 1705, 1668, 1579, 1562, 1471, 1444, 1415, 1367, 1286, 1230, 1292, 1174, 1165, 1138, 1124, 1105, 1028, 989, 856, 759, 748, 680, 636, 570, 515, 457 cm^{-1}. MS (FAB): m/z 380 (100, [M^+–OTf+H]), 379 (11, [M^+–OTf]), 204 (7), 175 (88), 77 (21). Anal. Calcd

for $C_{16}H_{15}F_6IO_3S$: C, 36.38; H, 2.86. Found: C, 36.30; H, 3.13.

Phenyl(3-(trifluoromethyl)bicyclo[2.2.1]hepta-2,5-dien-2-yl)iodonium trifluoro-methanesulfonate (3b). Yield: 78%, colorless microcrystals. Mp: 168.0–169.0 °C (dec). ^{1}H NMR (400 MHz, CD₃CN): δ 2.16 (d, J = 7.6 Hz, 1H), 2.39 (d, J = 7.6 Hz, 1H), 4.00 (bs, 1H), 4.04 (bs, 1H), 6.61 (dd, J = 4.8, 3.2 Hz, 1H), 6.86–6.88 (m, 1H), 7.50–7.60 (m, 2H), 7.76–7.80 (m, 1H), 8.00–8.02 (m, 2H); ^{13}C NMR (100 MHz, CD₃CN): δ 54.5, 61.6, 76.4, 112.7, 122.1 (q, J = 317.9 Hz), 122.9 (q, J = 266.9 Hz), 127.2 (q, J = 5.1 Hz), 133.8, 134.6, 137.4, 142.4, 142.8, 155.3 (q, J = 35.1 Hz); ^{19}F NMR (282 MHz, CD₃CN): δ −63.8, −78.0. IR (KBr): ν 3007, 2991, 1626, 1579, 1560, 1467, 1444, 1303, 1288, 1265, 1249, 1168, 1139, 1126, 1033, 1026, 989, 885, 804, 738, 731, 704, 680, 651, 642, 576, 518, 451 cm^{−1}. MS (FAB): m/z 364 (100, [M[+]–OTf+H]), 204 (7), 159 (27), 77 (25). Anal. Calcd for $C_{15}H_{11}F_6IO_3S$: C, 35.17; H, 2.16. Found: C, 34.98; H, 2.21.
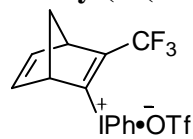
Phenyl(3-(trifluoromethyl)bicyclo[2.2.2]octa-2,5-dien-2-yl)iodonium trifluoro-methanesulfonate (3c). Yield: 63%, colorless microcrystals. Mp: 168.0–169.0 °C (dec). ^{1}H NMR (400 MHz, CD₃CN): δ 1.37–1.54 (m, 4H), 4.20–4.22 (m, 1H), 4.30–4.31 (m, 1H), 6.22 (t, J = 6.6 Hz, 1H), 6.40 (t, J = 6.6 Hz, 1H), 7.57–7.62 (m, 2H), 7.77–7.81 (m, 1H), 8.03–8.07 (m, 2H); ^{13}C NMR (100 MHz, CD₃CN): δ 25.6, 26.4, 42.4, 50.2, 113.2, 116.3 (q, J = 3.8 Hz), 122.0 (q, J = 317.3 Hz), 122.2 (q, J = 269.1 Hz), 133.6, 133.8, 134.6, 135.2, 137.4, 145.7 (q, J = 33.5 Hz); ^{19}F NMR (282 MHz, CD₃CN): δ −64.2, −79.0. IR (KBr): ν 3051, 2953, 1643, 1604, 1579, 1564, 14665, 1444, 1330, 1288, 1261, 1242, 1176, 1172, 1159, 1122, 1105, 1033, 1012, 989, 860, 837, 819, 740, 704, 684, 644, 576, 518, 449 cm^{−1}. MS (FAB): m/z 378 (100, [M[+]–OTf+H]), 350 (100), 222 (13), 204 (5), 77 (38). Anal. Calcd for $C_{16}H_{13}F_6IO_3S$: C, 36.52; H, 2.49. Found: C, 36.47; H, 2.41.
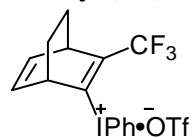
Phenyl(3-(trifluoromethyl)-7-oxabicyclo[2.2.1]hepta-2,5-dien-2-yl)iodonium tri-fluoromethanesulfonate (3d). Yield: 81%, gray microcrystals. Mp: 129.0–130.0 °C (dec). ^{1}H NMR (400 MHz, CD₃CN): δ 5.73 (bs, 1H), 5.80 (bs, 1H), 6.98 (dd, J = 5.2, 2.0 Hz, 1H), 7.19 (dd, J = 5.2, 2.0 Hz, 1H), 7.58–7.62 (m, 2H), 7.77–7.81 (m, 1H), 8.04–8.06 (m, 2H); ^{13}C NMR (100 MHz, CD₃CN): δ 86.0, 90.3, 113.1, 122.0 (q, J = 325.9 Hz), 122.4 (q, J = 266.8 Hz), 128.8 (q, J = 5.4 Hz), 134.1, 134.9, 137.5, 143.5, 144.4, 156.5 (q, J = 37.4 Hz); ^{19}F NMR (282 MHz, CD₃CN): δ −63.7, −78.0. IR (KBr): ν 3032, 1639, 1564, 1471, 1442, 1307, 1286, 1265, 1178, 1165, 1120, 1035, 1028, 989, 871, 740, 727, 682, 642, 518, 447 cm^{−1}. MS (FAB): m/z 366 (100, [M[+]–OTf+H]), 297 (100), 204 (9), 161 (57), 77 (50). Anal. Calcd for $C_{14}H_9F_6IO_4S$: C, 32.70; H, 1.76. Found: C, 32.41; H, 1.95.
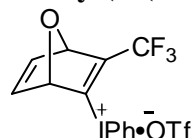
(1,4-Dimethyl-3-(trifluoromethyl)-7-oxabicyclo[2.2.1]hepta-2,5-dien-2-yl)(phenyl)-iodonium trifluoromethanesulfonate (3e). Yield: 81%, colorless microcrystals. Mp: 114.0–115.0 °C (dec). ^{1}H NMR (400 MHz, CD₃CN): δ 1.70 (s, 3H), 1.79 (s, 3H), 6.69 (d, J = 5.2 Hz, 1H), 6.92 (d, J = 5.2 Hz, 1H), 7.57–7.61 (m, 2H), 7.75–7.79 (m, 1H), 7.95–7.98
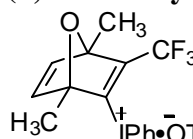
(m, 2H); ^{13}C NMR (100 MHz, CD$_3$CN): δ 16.3, 17.2, 95.4, 96.9, 112.8, 122.1 (q, *J* = 268.3 Hz), 122.2 (q, *J* = 315.6 Hz), 134.1, 134.9, 135.4 (q, *J* = 5.4 Hz), 137.2, 146.8, 148.3, 159.1 (q, *J* = 35.1 Hz); ^{19}F NMR (282 MHz, CD$_3$CN): δ −63.3, −78.0.   IR (KBr): ν 3051, 1641, 1577, 1566, 1469, 1438, 1386, 1307, 1290, 1269, 1249, 1157, 1132, 1033, 989, 898, 889, 869, 858, 736, 719, 653, 518, 449 cm^{-1}.   MS (FAB): *m/z* 394 (100, [M$^+$−OTf+H]), 204 (7), 189 (100), 77 (25).   Anal. Calcd for C$_{16}$H$_{13}$F$_6$IO$_4$S: C, 35.44; H, 2.49. Found: C, 35.26; H, 2.44.

(7-Methyl-3-(trifluoromethyl)-7-azabicyclo[2.2.1]hepta-2,5-dien-2-yl)(phenyl)-iodonium trifluoromethanesulfonate (3f).   Yield: 72%, yellow microcrystals.   Mp: 100.0–101.0 °C (dec). ^{1}H NMR (400 MHz, CD$_3$CN): δ 3.42 (s, 3H), 6.23–6.24 (m, 1H), 6.63–6.37 (m, 1H), 6.94–6.95 (m, 1H), 7.53–7.57 (m, 2H), 7.74–7.78 (m, 2H), 7.85–7.87 (m, 2H), 8.00–8.01 (m, 1H); ^{13}C NMR (100 MHz, CD$_3$CN): δ 35.9, 110.4, 113.4, 115.5, 121.3 (q, *J* = 4.6 Hz), 121.9 (q, *J* = 274.5 Hz), 122.2 (q, *J* = 316.6 Hz), 124.6, 129.2, 133.6, 134.6, 137.5, 138.5 (q, *J* = 34.3 Hz); ^{19}F NMR (282 MHz, CD$_3$CN): δ −63.1, −78.0.   IR (KBr): ν 3107, 1622, 1608, 1562, 1527, 1469, 1321, 1273, 1244, 1178, 1141, 1028, 989, 804, 742, 731, 678, 638, 574, 516, 451 cm^{-1}.   MS (FAB): *m/z* 379 (100, [M$^+$−OTf+H]), 364 (16), 174 (69), 77 (13).   Anal. Calcd for C$_{15}$H$_{12}$F$_6$INO$_3$S: C, 34.17; H, 2.29. Found: C, 34.39; H, 2.42.
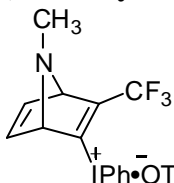
1-Iodo-4,5-dimethyl-2-(trifluoromethyl)cyclohexa-1,4-diene (6).[12d]   To a Schlenk tube (80 mL) equipped with a magnetic stirring bar were added KI (0.66 g, 4.0 mmol), CuI (0.76 g, 4.0 mmol) and DMF (25 mL) at room temperature under argon atmosphere, and the mixture was stirred until it gave a clear solution.   Alkenyliodonium salt **3a** (0.21 g, 0.39 mmol) was added portionwise to the reaction mixture.   The resulting mixture was stirred at room temperature for 1 h and diluted with hexane (30 mL) and water (100 mL).   The aqueous layer was extracted with hexane (30 mL × 3 times). The combined organic layer was washed with sat. aq. NaCl (50 mL × 2 times), dried over anhydrous MgSO$_4$, and concentrated under reduced pressure to give **6** (0.10 g, 83% yield) as a analytically pure and colorless solid.   Mp: 71.3–72.1 °C. ^{1}H NMR (400 MHz, CDCl$_3$): δ 1.60 (s, 3H), 1.65 (s, 3H), 2.85 (t, *J* = 8.0 Hz, 2H), 3.29 (bs, 2H); ^{13}C NMR (100 MHz, CDCl$_3$): δ 17.2, 18.0, 34.3 (q, *J* = 3.1 Hz), 50.5, 98.0 (q, *J* = 4.6 Hz), 121.1, 122.1 (q, *J* = 272.9 Hz), 123.3, 130.8 (q, *J* = 29.8 Hz); ^{19}F NMR (282 MHz, CDCl$_3$): δ −63.9. IR (KBr): ν 2914, 1701, 1654, 1423, 1386, 1367, 1290, 1269, 1184, 1161, 1122, 1101, 1033, 866, 738, 653, 644, 594 cm^{-1}.   MS (EI): *m/z* 303 (71, [M$^+$+H]), 302 (100, M$^+$), 287 (67), 175 (82), 160 (78), 127 (64), 91 (71).   Anal. Calcd for C$_9$H$_{10}$F$_3$I: C, 35.78; H, 3.34. Found: C, 35.51; H, 3.20.
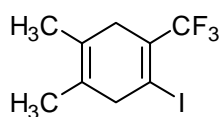
1-Iodo-4,5-dimethyl-2-(trifluoromethyl)benzene (7).[16]   In a vial tube (5 mL) equipped with a magnetic stirring bar were placed **5** (30 mg, 0.10 mmol) and *p*-chloranil (49 mg, 0.20 mmol).   The vial tube was then capped with a rubber septum, evacuated for 5 min, and charged with argon.   The evacuation–purge operation was repeated twice.   Toluene (1 mL) was added to the mixture in the vial at room temperature under an argon atmosphere.   The reaction mixture was stirred at room temperature for 5 min

and then heated at 100 °C for 12 h. The reaction mixture was cooled to room temperature, diluted with hexane (3 mL) and filtered through a silica gel pad. Removal of the organic solvent under reduced pressure followed by silica gel column chromatography (eluent: hexane) of the residue gave **7** (17 mg, 58% yield) as a colorless solid. R_f 0.60 (hexane). ^{19}F NMR (282 MHz, CDCl$_3$): δ −62.7.

Palladium-catalyzed cross-coupling reaction of alkenyliodonium salt 3b with tributyl(2-phenylethynyl)stannane.   In a vial tube (5 mL) equipped with a magnetic stirring bar were placed PdCl$_2$(PPh$_3$)$_2$ (7.0 mg, 10 μmol) and CuI (3.0 mg, 16 μmol). The vial tube was then capped with a rubber septum, evacuated for 5 min, and charged with argon.   The evacuation–purge operation was repeated twice.   To the mixture in the vial DMF (1 mL) and tributyl(2-phenylethynyl)stannane (94 mg, 0.24 mmol) were added at room temperature under an argon atmosphere.   The mixture was stirred at room temperature for 5 min before **3b** (0.10 g, 0.20 mmol) was added portionwise. The resulting mixture was stirred at room temperature for 1 h and diluted with Et$_2$O (3 mL) and water (5 mL).   The aqueous layer was extracted with Et$_2$O (3 mL × 3 times). The combined organic layer was washed with sat. aq. NaCl (10 mL × 2 times), dried over anhydrous MgSO$_4$, and evaporated under reduced pressure.   Purification of the residue by silica gel column chromatography (hexane/AcOEt 8:1) followed by GPC gave 2-(2-phenylethynyl)-3-(trifluoromethyl)bicyclo[2.2.1]hepta-2,5-diene (**8**, 34 mg, 66% yield) as a colorless oil. R_f 0.64 (hexane/AcOEt 8:1). ^{1}H NMR (400 MHz, CDCl$_3$): δ 2.16 (d, J = 6.8 Hz, 1H), 2.30 (dt, J = 6.8, 1.6 Hz, 1H), 3.81–3.82 (m, 2H), 6.88–6.92 (m, 2H), 7.33–7.35 (m, 3H), 7.45–7.47 (m, 2H); ^{13}C NMR (100 MHz, CDCl$_3$): δ 50.6, 57.5, 72.3, 82.4, 103.7, 122.5, 123.3 (q, J = 266.1 Hz), 128.2, 128.8, 131.4, 140.8 (q, J = 5.3 Hz), 141.6, 141.9, 145.7 (q, J = 33.6 Hz); ^{19}F NMR (282 MHz, CDCl$_3$): δ −64.6. IR (KBr): ν 3001, 2195, 1631, 1489, 1442, 1367, 1296, 1271, 1253, 1244, 1168, 1147, 1109, 1041, 952, 833, 802, 756, 731, 707, 688, 599 cm^{-1}.   MS (FAB): m/z 261 (23, [M$^+$+H]), 260 (100, M$^+$), 191 (21), 77 (19).   Anal. Calcd for C$_{16}$H$_{11}$F$_3$: C, 73.84; H, 4.26. Found: C, 73.84; H, 4.26.
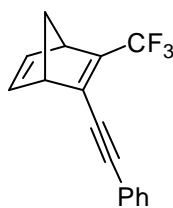
Crystallographic data for 1 and 3a.
Table 4.   Crystal data and structure refinement for **1** (see Figure 1, CCDC–701842).

Empirical formula	C$_{10}$H$_5$F$_6$IO$_3$S
Formula weight	446.10
Temperature	293(2) K
Wavelength	0.71073 Å
Crystal system	Triclinic
Space group	P–1
Unit cell dimensions	a = 7.8469(18) Å, α = 96.561(4)°
	b = 8.3777(19) Å, β = 96.976(4)°
	c = 11.898(3) Å, γ = 109.404(3)°
Volume	722.2(3) Å^3
Z	2
Density (calculated)	2.051 Mg/m^3

Absorption coefficient	2.433 mm^{-1}
F(000)	424
Crystal size	0.50 × 0.20 × 0.20 mm^3
Theta range for data collection	1.75 to 26.96°
Index ranges	−8<=h<=9, −10<=k<=10, −15<=l<=8
Reflections collected	4363
Independent reflections	3028 [R(int) = 0.0176]
Completeness to theta = 26.96°	96.6 %
Absorption correction	Empirical
Max. and min. transmission	0.6418 and 0.3759
Refinement method	Full-matrix least-squares on F^2
Data / restraints / parameters	3028 / 0 / 190
Goodness-of-fit on F^2	1.070
Final R indices [I>2sigma(I)]	R_1 = 0.0296, wR_2 = 0.0783
R indices (all data)	R_1 = 0.0312, wR_2 = 0.0794
Largest diff. peak and hole	0.500 and −0.630 e.Å^{-3}

Table 5. Crystal data and structure refinement for **3a** (see Figure 2).

Empirical formula	$C_{16} H_{15} F_6 I O_3 S$
Formula weight	528.24
Temperature	300(2) K
Wavelength	0.71073 Å
Crystal system	Monoclinic
Space group	P2(1)/c
Unit cell dimensions	a = 13.1787(8) Å, α = 90°
	b = 9.3954(5) Å, β = 102.2150(10)°
	c = 16.0128(9) Å, γ = 90°
Volume	1937.80(19) Å^3
Z	4
Density (calculated)	1.811 Mg/m^3
Absorption coefficient	1.829 mm^{-1}
F(000)	1032
Crystal size	0.50 × 0.50 × 0.50 mm^3
Theta range for data collection	1.58 to 25.50°
Index ranges	−8<=h<=15, −11<=k<=11, −19<=l<=19
Reflections collected	10228
Independent reflections	3609 [R(int) = 0.0204]
Completeness to theta = 25.50°	99.9 %
Absorption correction	None
Max. and min. transmission	0.4615 and 0.4615
Refinement method	Full-matrix least-squares on F^2
Data / restraints / parameters	3609 / 36 / 274
Goodness-of-fit on F^2	1.145
Final R indices [I>2sigma(I)]	R_1 = 0.0263, wR_2 = 0.0697

R indices (all data)	$R_1 = 0.0296$, $wR_2 = 0.0712$
Largest diff. peak and hole	0.424 and −0.413 e.Å^{-3}

Molecular orbital calculations. Molecular structures were optimized by DFT methods at the B3LYP level with a LANL2DZ+dp ECP for iodine and 6-31++G(d,p) for other atoms using Gaussian 03 package.[13] The Cartesian coordinates of the initial structure were set based on the data obtained from X-ray crystallography of **1** (Table 6). The initial structure of **4** was obtained by substituting a CF$_3$ group of initial structure of **1** with a CH$_3$ group (Table 7). The initial coordinates of **2a** are listed in Table 8. The coordinates of the optimized structures of **1**, **4**, and **2a** are listed in Table 9–11. Energy levels of molecular orbitals were calculated at the B3LYP/LANL2DZ+dp, 6-31++G(d,p) level. Absolute energies are as follows: −1618.191697 hartree for **1**, −1320.476136 hartree for **4**, and −234.622760 hartree for **2a**. Natural bonding orbital (NBO) analysis was performed at B3LYP level of theory with the NBO 5.0[14] included in Gaussian 03; LANL2DZ+dp ECP basis set was employed for iodine, 6-31++G(d,p) for the other atoms. The charge distributions of **1** and **4** are shown in Table 12 and 13, respectively.

Table 6. Cartesian coordinates of the initial structure of **1**.

I	0.333974	0.292218	−0.883491	C	5.079801	0.419040	−1.011407	C	0.545182	−3.157610	1.781062
C	2.409407	0.292218	−0.883491	F	5.634492	−0.598351	−0.314757	C	0.004624	−1.254445	3.185071
O	−3.802099	1.886314	−0.883491	S	−2.917108	1.078602	−0.049368	C	0.271216	−2.618038	3.041409
O	−2.012264	0.134636	−0.868097	C	−4.031321	−0.175554	0.798930	H	0.765829	−2.749383	−0.330908
C	0.299277	−0.980884	0.838015	F	−3.298525	−1.034608	1.532634	H	0.743459	−4.218947	1.667931
C	3.617622	0.359316	−0.954496	F	−4.884610	0.457760	1.615336	H	−0.232802	0.644697	2.167622
O	−2.158074	1.726061	1.035584	F	−4.732733	−0.876554	−0.100828	H	−0.221909	−0.838187	4.161686
F	5.549083	1.574230	−0.491021	C	0.014347	−0.405796	2.072189	H	0.258201	−3.265229	3.912928
F	5.525062	0.335031	−2.284724	C	0.559593	−2.336191	0.649839				

Table 7. Cartesian coordinates of the initial structure of **4**.

I	0.352387	−1.025306	1.101317	C	−0.115385	0.657115	−3.263976	H	−2.689214	−0.472724	1.533172
C	0.352387	−1.025306	3.176751	F	−0.974440	1.390818	−2.531181	H	−4.158778	1.526115	1.510802
O	1.946483	−1.025307	−3.034755	F	0.517928	1.473521	−4.117266	H	0.704866	2.025806	0.534542
O	0.194805	−1.009912	−1.244920	F	−0.816385	−0.242644	−3.965389	H	−0.778019	4.019871	0.545435
C	−0.920715	0.696199	1.066621	C	−0.345628	1.930374	0.781691	H	−3.205060	3.771112	1.025545
C	0.419485	−1.096312	4.384966	C	−2.276021	0.508023	1.326937	H	0.412609	−2.161297	6.199654
O	1.786230	0.893768	−1.390730	C	−3.097440	1.639247	1.312526	H	−0.325935	−0.601907	6.286117
C	0.479208	−1.153223	5.847145	C	−1.194277	3.043256	0.771968	H	1.394053	−0.741106	6.218790
S	1.138771	−0.191183	−2.149764	C	−2.557870	2.899594	1.038559				

Table 8. Cartesian coordinates of the initial structure of **2a**.

C	−1.843778	−0.570715	−0.175718	H	2.049155	−0.173669	0.895343	C	0.290913	−1.851288	0.198560
C	−0.528306	−0.564011	−0.009768	H	2.049251	−0.173764	−0.914556	H	0.966948	−1.980339	−0.620721
H	−2.428009	0.347318	−0.324308	C	0.304071	0.731655	−0.009732	H	0.845693	−1.777329	1.110507
H	−2.437395	−1.494729	−0.175740	C	−0.183075	1.964838	−0.009789	H	−0.370708	−2.690601	0.250641
C	1.771509	0.419603	−0.009653	H	0.458252	2.856404	−0.009841				
H	2.375652	1.359170	−0.009687	H	−1.260561	2.177451	−0.009781				

Table 9. Cartesian coordinates of the optimized structure of **1**.

I	0.302459	−0.865735	0.342981	F	0.466953	−2.322534	5.499445	C	−0.376291	2.095638	0.047275
C	0.292428	−0.863593	2.418650	C	0.426778	−1.036298	5.086226	C	−2.328370	0.671805	0.502942
O	1.907265	−0.843599	−3.800144	F	−0.652441	−0.455128	5.656838	C	−3.145093	1.806224	0.479138
O	0.166074	−0.878579	−2.001478	S	1.073006	−0.031846	−2.918972	C	−1.220068	3.211870	0.027452
C	−0.964247	0.858781	0.292214	C	−0.219222	0.754802	−4.035204	C	−2.592464	3.068932	0.245038
C	0.361382	−0.951790	3.625669	F	−1.097996	1.469941	−3.307498	H	−2.751880	−0.310480	0.678501
O	1.681463	1.085237	−2.174904	F	0.378130	1.578494	−4.907235	H	−4.212941	1.693929	0.639183
F	1.526596	−0.418094	5.569737	F	−0.894025	−0.180402	−4.715942	H	0.682020	2.191483	−0.161991

H	−0.793096	4.190450	−0.168528		H	−3.235908	3.943077	0.224627

Table 10. Cartesian coordinates of the optimized structure of **4**.

I	0.311189	−0.980636	1.170133		C	−0.006592	0.604328	−3.365992		H	−2.688917	−0.397992	1.808180
C	0.298197	−1.021753	3.213265		F	−0.878705	1.404289	−2.720341		H	−4.180268	1.584361	1.729761
O	2.023449	−1.074609	−2.959893		F	0.675269	1.352649	−4.246696		H	0.572507	2.005753	0.282134
O	0.197120	−0.955276	−1.250347		F	−0.704085	−0.320875	−4.040359		H	−0.928713	3.987193	0.237603
C	−0.983323	0.725277	1.076239		C	−0.451641	1.930517	0.629392		H	−3.300938	3.777322	0.952285
C	0.409485	−1.175130	4.414606		C	−2.308483	0.560315	1.473194		H	0.349202	−2.365637	6.158511
O	1.810240	0.929009	−1.434653		C	−3.141861	1.681913	1.427960		H	−0.226617	−0.701686	6.368061
C	0.518294	−1.325155	5.861834		C	−1.311897	3.034585	0.590288					
S	1.178781	−0.198484	−2.148525		C	−2.644683	2.913045	0.989263					

Table 11. Cartesian coordinates of the optimized structure of **2a**.

C	−1.732714	−0.555947	−0.547809		H	2.334723	−0.106886	0.342379		C	0.113180	−1.832963	0.526200
C	−0.497226	−0.563486	−0.027065		H	1.915760	0.100069	−1.356482		H	0.990807	−2.145624	−0.054079
H	−2.159063	0.339065	−0.991020		C	0.334969	0.673399	0.012624		H	0.451323	−1.694501	1.561550
H	−2.350307	−1.450799	−0.556876		C	−0.186753	1.852598	0.379917		H	−0.608072	−2.655341	0.509463
C	1.796027	0.543087	−0.359051		H	0.411820	2.760265	0.388302					
H	2.290738	1.518869	−0.357091		H	−1.221949	1.944380	0.694799					

Table 12. Atomic charges of **1** calculated by NBO analysis.

atom	atomic charge					
I	+1.238	C	+1.062	C	−0.210
C	−0.334	F	−0.345	C	−0.204
O	−0.919	S	+2.327	H	+0.261
O	−1.033	C	+0.849	H	+0.254
C	−0.245	F	−0.362	H	+0.286
C	−0.109	F	−0.349	H	+0.257
O	−0.973	F	−0.348	H	+0.252
F	−0.344	C	−0.219		
F	−0.344	C	−0.232		
		C	−0.216		

Table 13. Atomic charges of **4** calculated by NBO analysis.

atom	atomic charge					
I	+1.227	C	+0.843	H	+0.251
C	−0.463	F	−0.364	H	+0.290
O	−0.931	F	−0.352	H	+0.255
O	−1.037	F	−0.353	H	+0.249
C	−0.239	C	−0.223	H	+0.263
C	+0.054	C	−0.235	H	+0.265
O	−0.982	C	−0.220	H	+0.264
C	−0.729	C	−0.211		
S	+2.331	C	−0.211		
		H	+0.259		

References

 (1) (a) Henne, A. L.; Nager, M. *J. Am. Chem. Soc.* **1952**, *74*, 650. (b) Drakesmith, F. G.; Stewart, O. J.; Tarrant, P. *J. Org. Chem.* **1968**, *33*, 280. (c) Bunch, J. E.; Bumgardner, C. L. *J. Fluorine Chem.* **1987**, *36*, 313. (d) Yoneda, N.; Matsuoka, S.; Miyaura, N.; Fukuhara, T.; Suzuki, A. *Bull. Chem. Soc. Jpn.* **1990**, *63*, 2124. (e) Bobrovnikov, M. N.; Turbanova, E. S.; Petrov, A. A. *Russ. J. Org. Chem.* **1993**, *29*, 1445. (f) Yamazaki, T.; Mizutani, K.; Kitazume, T. *J. Org. Chem.* **1995**, *60*, 6046. (g) Katritzky, A. R.; Qi, M.; Wells, A. P. *J. Fluorine Chem.* **1996**, *80*, 145. (h) Brisdon, A. K.; Crossley, I. R. *Chem. Commun.* **2002**, 2420. (i) Konno, T.; Chae, J.; Kanda, M.; Nagai, G.; Tamura, K.; Ishihara, T.; Yamanaka, H. *Tetrahedron* **2003**, *59*, 7571. (j) Bardin, V. V.; Adonin, N. Y.; Frohn, H. J. *Organometallics* **2005**, *24*, 5311. (k) Shimizu, M.; Jiang, G.; Murai, M.; Takeda, Y.; Nakao, Y.; Hiyama, T.; Shirakawa, E. *Chem. Lett.* **2005**, *34*, 1700. (l) Shimizu, M.; Higashi, M.; Takeda, Y.; Jiang, G.; Murai, M.; Hiyama, T. *Synlett* **2007**, 1163. (m) Shimizu, M.; Higashi, M.; Takeda, Y.; Murai, M.; Jiang, G.; Asai, Y.; Nakao, Y.; Shirakawa, E.; Hiyama, T. *Future Med. Chem.* **2009**, *1*, 921.

 (2) (a) Norris, W. P.; Finnegan, W. G. *J. Org. Chem.* **1966**, *31*, 3292. (b) Augdahl, E.; Kloster-Jensen, E.; Devarajan, V.; Cyvin, S. J. *Spectrochimica Acta Part A: Molecular Spectroscopy* **1973**, *29*, 1329. (c) Trofimenko, S.; Johnson, R. W.; Doty, J. K. *J. Org. Chem.* **1978**, *43*, 43. (d) Bieri, G.; Heilbronner, E.; Hornung, V.; Kloster-Jensen, E.; Maier, J. P.; Thommen, F.; Niessen, W. V. *Chem. Phys.* **1979**, *36*, 1. (e) Stepanova, N. P.; Orlova, N. A.; Turbanova, E. S.; Petrov, A. A. *Zh. Org. Khim.* **1986**, *22*, 439.

 (3) Reviews on alkynyl(aryl)iodonium salts: (a) Stang, P. J. *Angew. Chem. Int. Ed. Engl.* **1992**, *31*, 274. (b) Stang, P. J. *Russ. Chem. Bull* **1993**, *42*, 20. (c) Stang, P. J.; Zhdankin, V. V. *Chem. Rev.* **1996**, *96*, 1123. (d) Zhdankin, V. V.; Stang, P. J. *Tetrahedron* **1998**, *54*, 10927. (e) Zhdankin, V. V.; Stang, P. J. *Chem. Rev.* **2002**, *102*, 2523.

 (4) Williamson, B. L.; Stang, P. J.; Arif, A. M. *J. Am. Chem. Soc.* **1993**, *115*, 2590. According to the original protocol, the solvent for the precipitation was Et_2O.

 (5) Zhdankin, V. V.; Scheuller, M. C.; Stang, P. J. *Tetrahedron Lett.***1993**, *34*, 6853.

 (6) Zhdankin, V. V.; Crittell, C. M.; Stang, P. J. *Tetrahedron Lett.* **1990**, *31*, 4821.

 (7) Wipf, P.; Venkatraman, S. *J. Org. Chem.* **1996**, *61*, 8004.

 (8) Emsley, J. *The Elements,* 3rd ed.; Oxford University Press: Oxford, 2000.

 (9) Reichenbächer, K.; Süss, H. I.; Hulliger, J. *Chem. Soc. Rev.* **2005**, *34*, 22.

 (10) Fringuelli, F.; Taticchi, A. *Dienes in the Diels-Alder Reaction*; John Wiley & Sons, Ltd.: New York, 1990.

 (11) Danishefsky, S. J.; Kitahara, T. *J. Am. Chem. Soc.* **1974**, *96*, 7807.

 (12) (a) Varvoglis, A. *Tetrahedron* **1997**, *53*, 1179. (b) Okuyama, T. *Acc. Chem. Res.* **2002**, *35*, 12. (c) Deprez, N. R.; Sanford, M. S. *Inorg. Chem.* **2007**, *46*, 1924. (d) Ochiai, M.; Sumi, K.; Takaoka, Y.; Kunishima, M.; Nagao, Y.; Shiro, M.; Fujita, E. *Tetrahedron* **1988**, *44*, 4095. (e) Ryan, J. H.; Stang, P. J. *J. Org. Chem.* **1996**, *61*, 6162. (f) Lin, S.-H.; Li, F.; Cheng, S. Z. D.; Harris, F. W. *Macromolecules*, **1998**, *31*, 2080.

 (13) Frisch, M. J.; Trucks, G. W.; Schlegel, H. B.; Scuseria, G. E.; Robb, M. A.; Cheeseman, J. R.; Montgomery, J. A., Jr.; Vreven, T.; Kudin, K. N.; Burant, J. C.; Millam, J. M.; Iyengar, S. S.; Tomasi, J.; Barone, V.; Mennucci, B.; Cossi, M.;

Scalmani, G.; Rega, N.; Petersson, G. A.; Nakatsuji, H.; Hada, M.; Ehara, M.; Toyota, K.; Fukuda, R.; Hasegawa, J.; Ishida, M.; Nakajima, T.; Honda, Y.; Kitao, O.; Nakai, H.; Klene, M.; Li, X.; Knox, J. E.; Hratchian, H. P.; Cross, J. B.; Bakken, V.; Adamo, C.; Jaramillo, J.; Gomperts, R.; Stratmann, R. E.; Yazyev, O.; Austin, A. J.; Cammi, R.; Pomelli, C.; Ochterski, J. W.; Ayala, P. Y.; Morokuma, K.; Voth, G. A.; Salvador, P.; Dannenberg, J. J.; Zakrzewski, V. G.; Dapprich, S.; Daniels, A. D.; Strain, M. C.; Farkas, O.; Malick, D. K.; Rabuck, A. D.; Raghavachari, K.; Foresman, J. B.; Ortiz, J. V.; Cui, Q.; Baboul, A. G.; Clifford, S.; Cioslowski, J.; Stefanov, B. B.; Liu, G.; Liashenko, A.; Piskorz, P.; Komaromi, I.; Martin, R. L.; Fox, D. J.; Keith, T.; Al-Laham, M. A.; Peng, C. Y.; Nanayakkara, A.; Challacombe, M.; Gill, P. M. W.; Johnson, B.; Chen, W.; Wong, M. W.; Gonzalez, C.; Pople, J. A. *Gaussian 03*, revision C.02; Gaussian, Inc.: Wallingford, CT, 2004.

(14) Glendening, E. D.; Badenhoop, J. K.; Reed, A. E.; Carpenter, J. E.; Bohmann, J. A.; Morales, C. M.; Weinhold, F. Theoretical Chemistry Institute, University of Wisconsin, Madison, 2001.

(15) Dixon, D. A.; Fukunaga, T.; Smart, B. E. *J. Am. Chem. Soc.* **1986**, *108*, 4027.

(16) Lin, S.-H.; Li, F.; Cheng, S. Z. D.; Harris, F. W. *Macromolecules* **1998**, *31*, 2080.

Chapter 4

Stereocontrolled Synthesis of CF$_3$-containing Triarylethenes and Enynes: Palladium-catalyzed Stereoselective Cross-coupling Reaction of 1,1-Dibromo-3,3,3-trifluoro-2-tosyloxypropene

Cross-coupling reaction of 1,1-dibromo-3,3,3-trifluoro-2-tosyloxypropene with arylboronic acids and -stannanes proceeded stereoselectively by the aid of a palladium catalyst to give (*Z*)-1-aryl-1-bromo-3,3,3-trifluoro-2-tosyloxypropenes. Successive two-fold cross-coupling reactions of the stereochemically pure *Z*-propenes with two different arylboronic acids provided CF$_3$-substituted triarylethenes as a single diastereomer. The other coupling reaction of mono-arylated ethenes with terminal alkynes gave CF$_3$-substituted enynes, which was led to CF$_3$-substituted furans.

1. Introduction

Tetrasubstituted ethenes including trifluoromethyl are highly important targets as biologically active agents. For example, panomifene,[1] which is a fluorinated analog of anti-tumor agent tamoxifen,[2] exhibits better activity than tamoxifen. In view that the bioactivities of tetrasubstituted ethenes often depend on the configuration of the carbon–carbon double bond, stereoselective synthesis of ethenes substituted by CF_3 and three other groups is essential for exploration and discovery of novel fluorinated bioactive agents.

panomifene   tamoxifen
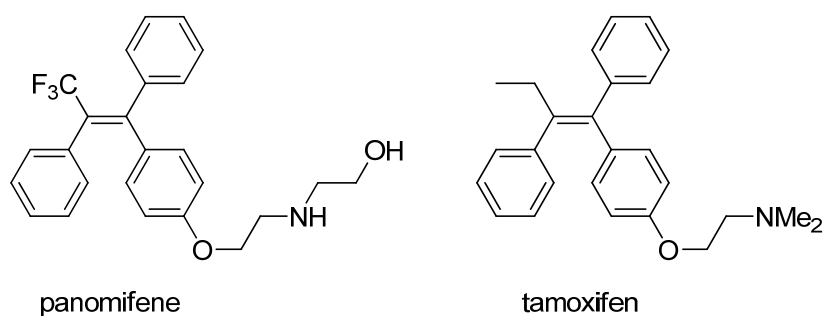
From synthetic viewpoint, stereoselective synthesis of ethenes substituted by CF_3 and three other groups are, however, quite a few.[3] An example is reported recently by Konno and co-workers who developed a protocol including stereoselective preparation of α-CF_3 substituted iodoethenes by carbocupration of 1-aryl-3,3,3-trifluoropropynes followed by iodination of the resulting cuprates and successive cross-coupling with arylboronic acids.[3g, i]
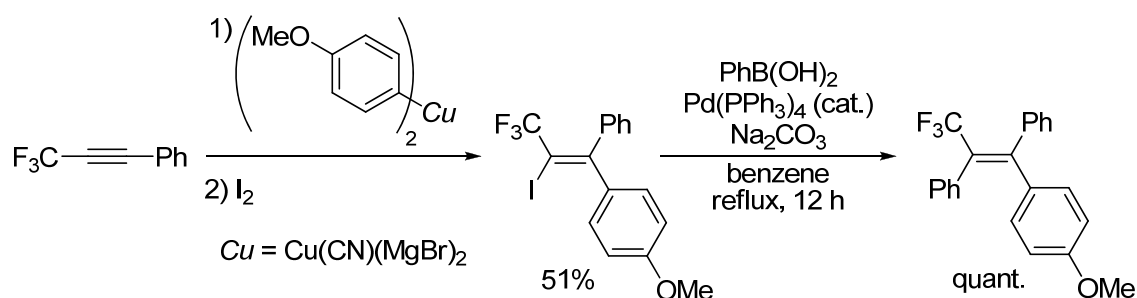
Another example is reported by Shimizu and Hiyama who disclosed stereocontrolled synthesis of CF_3-substituted triarylethenes via stereoselective generation of CF_3-substituted oxiranyllithium from CF_3-substituted dichlorohydrins and organolithium reagents.[3c,d] Treatment of CF_3-substituted oxiranyllithium with a bis(pinacolato)diboron gives (*E*)-β-CF_3-substituted alkenylboronates in a highly

stereoselective manner.   Cross-coupling reaction of the alkenylboronates produces CF$_3$-substituted triarylethenes as a single stereoisomer.[3f]
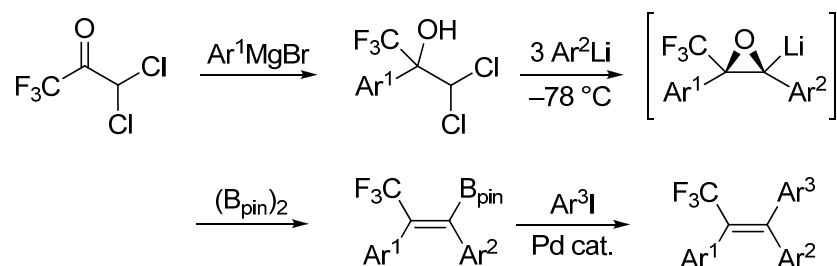
In addition to scarcity in precedents, the scope of these methods is severely limited by little availability of CF$_3$-containing starting material and/or use of organolithium or organomagnesium reagents.   Moreover, these methods require multi steps of different reaction conditions.   To overcome these issues and to establish a truly efficient and general synthetic method for the desired CF$_3$-substituted ethenes, the author conceived three-fold cross-coupling reactions of (pseudo)trihaloethenes with organometalloid reagents (Scheme 1), because transition metal-catalyzed cross-coupling is one of the most reliable reactions to form Csp_2–C bond stereospecifically[4] and such organometalloid reagents as organoboron and -tin compounds are compatible with a variety of functional groups.   Furthermore, this strategy may allow one-pot synthesis of the ethenes, because the same or similar reagents and/or reaction conditions can be applied sequentially.

X^1, X^2, X^3 = (pseudo)halogens
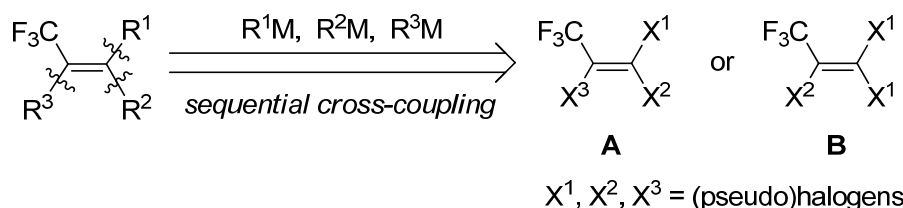
Scheme 1.   Three-fold coupling reactions of CF$_3$-substituted tri(pseudo)haloethene.

A question to be solved first is a choice of starting trihalide.   If an ethene substituted by three different halogens (type **A**), discrimination of the halogens in coupling reactions would be easy, but the stereocontrolled preparation of such ethene is extremely difficult.   On the other hand, when germinal dihalogens are the same (type **B**), such stereocontrol is not necessary.   An intrinsic issue of this approach is whether discrimination between two leaving groups X^1 is possible or not.   Although

cross-coupling reaction of $R(R^1)C=C(X^1)_2$ leading to unsymmetrical tetrasubstituted alkenes has no precedent[5] except for the coupling reaction of γ-(dibromomethylene)butenolide[5c] due presumably to the difficulty in discrimination of two X^1, the author envisioned that the steric and/or electronic nature of a CF_3 group might overcome this difficulty.[6] Described in this Chapter is stereocontrolled and versatile synthesis of CF_3-containing tetrasubstituted ethenes, based on stereoselective cross-coupling reaction of 1,1-dibromo-3,3,3-trifluoro-2-tosyloxypropene (Scheme 2). Cross-coupling reaction of the dibromoenol tosylate with 1 equivalent of arylboronic acids and –stannanes was found to proceed in a stereoselective manner, giving (*Z*)-mono-arylated enol tosylates as a major product. Stereochemically pure (*Z*)-isomer was easily separated from (*E*)-isomer by column chromatography or recrystallization of the *E/Z* mixture. Successive two-fold cross-coupling reactions of the tosylates provided CF_3-containing triarylethenes as a single diastereoisomer. Moreover, one-pot synthesis of the triaylethenes and formal synthesis of panomifene were demonstrated.
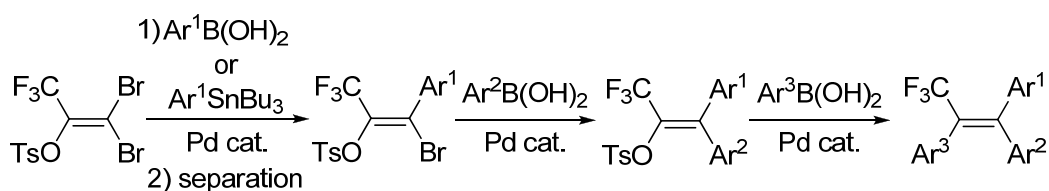
Scheme 2. Stereoselective synthesis of CF_3-containing triarylethenes.

2. Results and Discussion

2–1. Preparation of 1,1-dibromo-3,3,3-trifluoro-2-tosyloxypropene (2)

Dibromoenol tosylate **2** was readily prepared by treatment of freshly distilled 3,3-dibromo-1,1,1-trifluoropropanone (**1**) with TsCl in the presence of Et_3N in 60% yield as a colorless solid (Eq. 1). The tosylate is stable to air and moisture, and well soluble to common organic solvents such as CH_2Cl_2, toluene, and THF.

(1)
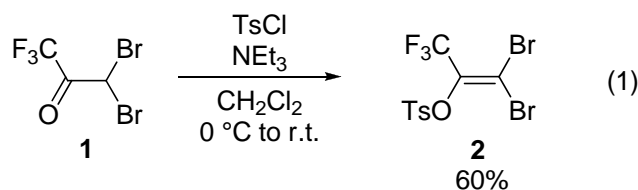
2–2. Stereoselective cross-coupling reaction of 2

At the outset, a series of phenylmetals as a coupling partner was scrutinized (Table 1). Treatment of **2** with PhMgBr in the presence of 5 mol% of PdCl$_2$(dppb)[7a] at 40 °C was found to give dibromoketone **1** quantitatively as a sole fluorine-containing product (entry 1). The production of **1** is probably explained by nucleophilic attack of PhMgBr at the sulfur atom of the Ts group followed by protonation of the resulting dibromoenolate in aqueous work-up. When PhZnCl[7a] was employed in THF at 80 °C, the reaction proceeded stereoselectively to produce mono-coupled product **5a** with good diastereoselectivity (83:17) (entry 2). However, conversion of **2** and yield (NMR) of **5a** would not be improved to a meaningful degree. The Z-configuration of the major stereoisomer was unambiguously confirmed by X-ray analysis of the single crystal obtained by recrystallization of the crude product from hexane (Table 10 in Experimental Section). Considering that A values of CF$_3$ and OTs groups being 2.4–2.5 and 0.5 kcal/mol, respectively,[8] it should be noted that the coupling occurred at more hindered site. Use of PhB(OH)$_2$[7b] and PhSuBu$_3$[7c] gave **5a** in moderate yields with high Z-selectivity along with di-coupled product **6aa** in 1% and 15% yields, respectively (entries 3 and 4). Taking account of functional group compatibility and the availability of reagents, boronic acids were chosen as a phenylmetal for further screening experiments.

Table 1. Screening of phenylmetals.

Entry	Ph–Metal	Pd cat. (X mol%)	Solvent	Temp. (°C)	Conv. (%)[a]	5a (%, Z:E)[a]	6aa (%)[a]
1	PhMgBr	PdCl$_2$(dppb) (5)	Et$_2$O	40	100[b]	0	0
2	PhZnCl	PdCl$_2$(dppb) (5)	THF	80	12	6 (83:17)	0
3[c]	PhB(OH)$_2$ (**3a**)	Pd(PPh$_3$)$_4$ (5)	toluene	80	100	86 (86:14)	1
4	PhSnBu$_3$ (**4a**)	Pd$_2$(dba)$_3$ (2.5) P(2-furyl)$_3$ (15)	toluene	100	100	54 (92:8)	15

[a] Determined by ^{19}F NMR analysis of the crude products. [b] Quantitative production of **1** was observed by ^{19}F NMR. [c] 2 M aq. K$_2$CO$_3$ (2.0 eq) was used as a base.

To improve the chemical yield and diastereoselectivity of **5a**, base, solvent, temperature, Pd catalyst, and ligand were extensively screened. Representative results are summarized in Table 2. Aqueous Cs_2CO_3 was found the most effective base with respect to yield and diastereoselectivity (entries 1–4). Strong base such as KOH gave no product due presumably to hydrolysis of sulfonate (entry 2). Toluene was the best solvent to suppress the formation of di-coupled product **6aa** (entries 4 and 5). Other solvents such as DMSO, DMF, CH_3CN, and Et_2O did not give **5a** at all. Reaction temperature of 80 °C was necessary to attain high yield (entries 4, 6 and 7). Screening of Pd pre-catalysts and ligands revealed the combination of 5 mol% of $PdCl_2(PPh_3)_2$/P(m-tolyl)$_3$ gave **5a** with the highest Z-selectivity (94:6) in good yield (81%) without formation of **6aa** (entries 8–12). When the reaction time was extended to 24 h under the best conditions, **5a** was isolated in 94% yield (entry 13).

Table 2. Optimization study of stereoselective cross-coupling of **2** with PhB(OH)$_2$.
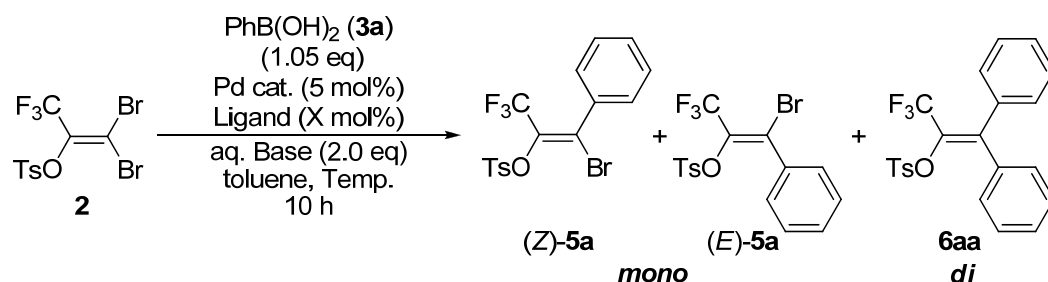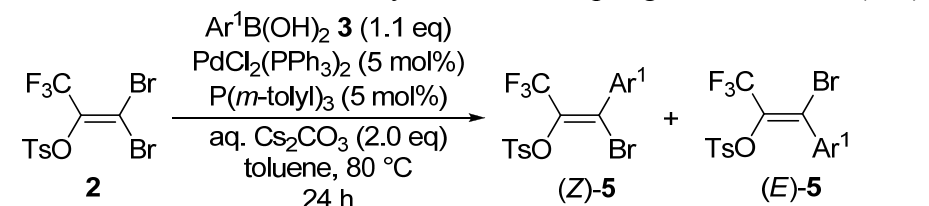
Entry	Pd cat.	Ligand (X mol%)	aq. Base	Temp. (°C)	5a (%, Z:E)[a]	6aa (%)[a]
1	Pd(PPh$_3$)$_4$	none	K$_2$CO$_3$	80	86 (86:14)	1
2	Pd(PPh$_3$)$_4$	none	KOH	80	0	0
3	Pd(PPh$_3$)$_4$	none	Ag$_2$CO$_3$	80	28 (79:21)	0
4	Pd(PPh$_3$)$_4$	none	Cs$_2$CO$_3$	80	99 (89:11)	1
5[b]	Pd(PPh$_3$)$_4$	none	Cs$_2$CO$_3$	80	19 (100:0)	29
6	Pd(PPh$_3$)$_4$	none	Cs$_2$CO$_3$	60	34 (91:9)	0
7	Pd(PPh$_3$)$_4$	none	Cs$_2$CO$_3$	70	56 (89:11)	0
8	PdCl$_2$(PPh$_3$)$_2$	PPh$_3$ (5)	Cs$_2$CO$_3$	80	99 (90:10)	0
9	PdCl$_2$(PPh$_3$)$_2$	P(o-tolyl)$_3$ (5)	Cs$_2$CO$_3$	80	55 (98:2)	6
10	PdCl$_2$(PPh$_3$)$_2$	PCy$_3$ (5)	Cs$_2$CO$_3$	80	78 (87:13)	5
11	PdCl$_2$(PPh$_3$)$_2$	P(t-Bu)$_3$ (5)	Cs$_2$CO$_3$	80	61 (93:7)	21
12	PdCl$_2$(PPh$_3$)$_2$	P(m-tolyl)$_3$ (5)	Cs$_2$CO$_3$	80	81 (94:6)	0
13[c]	**PdCl$_2$(PPh$_3$)$_2$**	**P(m-tolyl)$_3$ (5)**	**Cs$_2$CO$_3$**	**80**	**94[d] (92:8)**	**0**
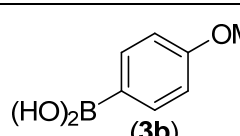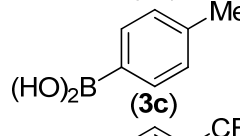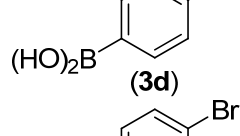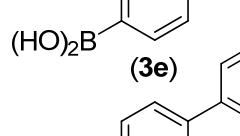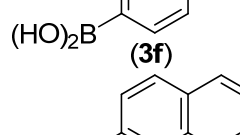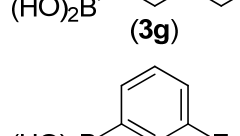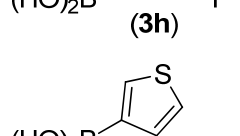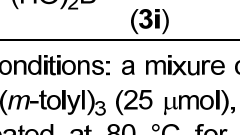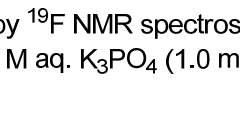
[a] Determined by ^{19}F NMR spectroscopic analysis of the crude products. [b] In THF. [c] The reaction was effected for 24 h. [d] Isolated yield.

With the optimized conditions in hand, scope of arylboronic acids **3** was investigated (Table 3).   A variety of *para*-substituted arylboronic acids bearing electron-donating or –withdrawing functional groups coupled with **2** stereoselectively, giving rise to the corresponding mono-arylated products (**5b–5f**) in good to excellent yields with high *Z*-selectivity (entries 1–5).   In particular, it should be noted that reaction with *p*-bromophenylboronic acid (**3e**) gave the desired product **5e** with the bromine atom on the phenyl ring intact.   This indicates that the bromine atom *cis* to the CF$_3$ group in **2** is more reactive than the one on the phenylboronic acid.   Naphthyl-(**3g**) and *m*-fluorophenylboronic acid (**3h**) also gave the corresponding mono-coupled products **5g** and **5h** stereoselectively in good yields (entries 6 and 7).   In the case of 3-thienylboronic acid (**3i**), use of aq. K$_3$PO$_4$ in place of aq. Cs$_2$CO$_3$ (26%, entry 8) gave higher yield (80%, entry 9).   The configuration of (*Z*)-**5c** was confirmed by X-ray crystallographic analysis of its single crystal (Table 11 in Experimental Section). Based on the fact that ^{19}F NMR chemical shifts of (*Z*)-**5a** and (*Z*)-**5c** were observed in down field (–60.5 ppm for (*Z*)-**5a** and –60.4 ppm for (*Z*)-**5c**) relative to those of (*E*)-isomers (–62.6 ppm for (*E*)-**5a** and –62.5 ppm for (*E*)-**3c**), respectively, the configurations of **5b** and **5d–5i** were determined similarly.   In all cases, the *Z*/*E* selectivity was almost constant (~9:1) regardless of the nature of substituents on the phenylboronic reagent, and *E*/*Z* isomers of **5** were easily separated by silica gel column chromatography or recrystallization from hexane.   In contrast, *p*-(*N*,*N*-dimethylamino)phenylboronic acid gave the corresponding mono-coupled product in only 28% yield, and *p*-formylphenyl- and 2-furylboronic acids were not applicable to the reaction, due possibly to instability of the reagents under the basic aqueous conditions leading to protodeborylated compounds.[9]

Table 3. Stereoselective Suzuki-Miyaura cross-coupling of **2** with $Ar^1B(OH)_2$.[a]

Ar^{1}B(OH)$_2$ **3** (1.1 eq)
PdCl$_2$(PPh$_3$)$_2$ (5 mol%)
P(*m*-tolyl)$_3$ (5 mol%)
aq. Cs$_2$CO$_3$ (2.0 eq)
toluene, 80 °C
24 h

F$_3$C, Br, TsO, Br **2** → F$_3$C, Ar^1, TsO, Br (*Z*)-**5** + F$_3$C, Br, TsO, Ar^1 (*E*)-**5**

Entry	3	5	Yield (%)[b]	Z:E[c]
1	(HO)$_2$B—C$_6$H$_4$—OMe **(3b)**	**5b**	74	90:10
2	(HO)$_2$B—C$_6$H$_4$—Me **(3c)**	**5c**	73	89:11
3	(HO)$_2$B—C$_6$H$_4$—CF$_3$ **(3d)**	**5d**	89	87:13
4	(HO)$_2$B—C$_6$H$_4$—Br **(3e)**	**5e**	85	88:12
5	(HO)$_2$B—C$_6$H$_4$—C$_6$H$_5$ **(3f)**	**5f**	96	88:12
6	(HO)$_2$B—naphthyl **(3g)**	**5g**	78	89:11
7	(HO)$_2$B—C$_6$H$_4$—F **(3h)**	**5h**	87	89:11
8	(HO)$_2$B—thienyl **(3i)**	**5i**	26	94:6
9[d]			80	90:10

[a] Reaction conditions: a mixure of **2** (0.50 mmol), **3** (0.55 mmol), PdCl$_2$(PPh$_3$)$_2$ (25 μmol), P(*m*-tolyl)$_3$ (25 μmol), and 5 M aq. Cs$_2$CO$_3$ (1.0 mmol) in toluene (5 mL) was heated at 80 °C for 24 h. [b] Isolated yield. [c] The Z:E ratio was determined by ^{19}F NMR spectroscopic analysis of the crude products. [d] **3i** (0.75 mmol) and 5 M aq. K$_3$PO$_4$ (1.0 mmol) as a base were employed.

In view that PhSnBu$_3$ (**4a**) gave results comparable to PhB(OH)$_2$ (**3a**) in the screening experiments (Table 1, entry 4) and that heteroatom-containing arylstannanes are more stable than the corresponding boronic acids, the author screened reaction

84

conditions for cross-coupling of **2** with arylstannanes, and the results are summarized in Table 4. As the ratio of ligand/Pd was increased from 1 to 4, diastereoselectivity of **5** increased at the expense of yield (entries 1–3); when the reaction time was extended from 10 h to 24 h, yield increased (entry 4); the reaction at 90 °C resulted in excellent yield and at high *Z*-diastereoselectivity (entry 5); the reaction at 100 °C produced 3% of di-coupled product **6aa** (entry 6).

Table 4. Optimization study of stereoselective cross-coupling of **2** with PhSnBu₃.[a]
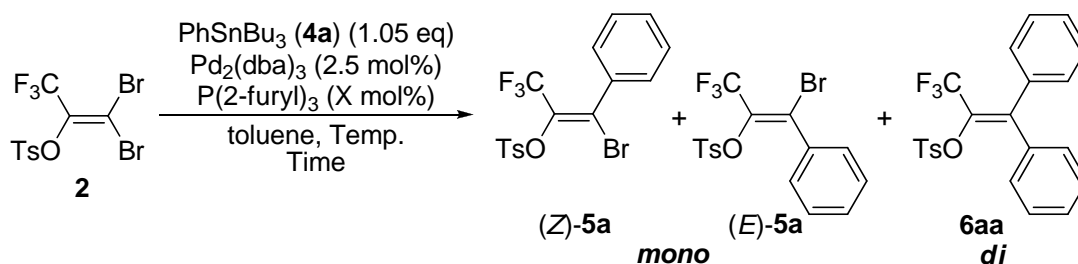
Entry	P(2-furyl)₃ (X mol%)	Temp. (°C)	Time (h)	5a (%, Z:E)[a]	6aa (%)[a]
1	5	80	10	71 (83:17)	0
2	10	80	10	67 (85:15)	0
3	20	80	10	33 (88:12)	0
4	20	80	24	80 (88:12)	0
5	**20**	**90**	**24**	**96 (88:12)**	**0**
6	20	100	24	93 (86:14)	3

[a] Determined by ^{19}F NMR spectroscopic analysis of the crude products.

The optimum conditions (Table 4, entry 5) were applicable to various arylstannanes **4**, and the results are summarized in Table 5. Arylstannanes bearing a strong electron-donating NMe₂ group (**4j**) or an electrophilic CHO group (**4k**) tolerated the reaction conditions to give the corresponding mono-arylated products (**5j**) and (**5k**), respectively (entries 1 and 2). Heteroarylstannanes were also applicable to this reaction (entries 3–5). It is noteworthy that the reaction using **4m** afforded (*Z*)-**5m** as a sole product without any trace of *E* isomer. X-Ray crystallographic analysis of **5n** confirmed *Z*-configuration of the major stereoisomer (Table 12 in Experimental Section). Configuration of **5j–m** as well as **5b** and **5d–5i** was assigned based on ^{19}F NMR. Considering that boronic acids corresponding to **4k**, **4l**, and **4j** did not gave products at all or gave at best low yield of **5**, the Migita–Kosugi–Stille reaction is complementary to the Suzuki-Miyaura coupling of **2**.

Table 5. Stereoselective Migita-Kosugi-Stille cross-coupling of **2** with Ar^{1}SnBu$_3$.[a]

Entry	4	5	Yield (%)[b]	Z:E[c]
1	Bu$_3$Sn—⬡—NMe$_2$ **(4j)**	**5j**	76	90:10
2	Bu$_3$Sn—⬡—CHO **(4k)**	**5k**	93	88:12
3	Bu$_3$Sn—furyl-O **(4l)**	**5l**	84	87:13
4	Bu$_3$Sn—benzofuryl-O **(4m)**	**5m**	62	>99:1
5	Bu$_3$Sn—thienyl-S **(4n)**	**5n**	87	93:7

[a] Reaction conditions: a mixture of **2** (0.50 mmol), **4** (0.525 mmol), Pd$_2$(dba)$_3$ (12.5 μmol), and P(2-furyl)$_3$ (100 μmol) in toluene (5 mL) was heated at 90 °C for 24 h. [b] Isolated yield. [c] The Z:E ratio was determined by ^{19}F NMR spectroscopic analysis of the crude products.

2–3. Trifluoromethyl substituent effect on the cross-coupling reaction

To gain insight into the CF$_3$ effect on the selectivity of the first coupling, the author carried out the reaction of dibromo-olefins **7a–c** with PhB(OH)$_2$ under the optimal conditions for **2** (Table 6). Reaction of fluorine-free dibromoalkene **7a** resulted in lower isolated yield and Z/E selectivity of mono-coupled product **8a** (entry 1). Ethoxycarbonyl-substituted ethene **7b** in place of CF$_3$ gave mono-coupled product **8b** in moderate yield with excellent Z-selectivity (entry 2), di-coupled product **9b** and acetylene **10** being accompanied as byproducts. Thus, the high diastereoselectivity may not represent the real one. In the case of **7c**, di-phenylated ethene **9c** became the major product (entry 3). The configuration of **8** was confirmed in each case by X-ray crystallography of single crystals (Tables 13–15 in Experimental Section). Thus, these

results indicate the high *Z* selectivity of **2** is attributed to the presence of a CF$_3$ group, while both CF$_3$ and TsO groups are apparently indispensable for suppressing the second coupling.

Table 6. Cross-coupling reaction of dibromoalkenes **7**.[a]

Entry	7	R^1	R^2	8 (%, *Z:E*)[b]	9 (%)[b]	10 (%)[b]
1	**7a**	CH$_3$	OTs	70 (68:32)	0	—
2	**7b**	EtO$_2$C	OTs	57 (96:4)	16	21
3	**7c**	CF$_3$	(CH$_2$)$_2$Ph	15 (81:19)[c]	47	—

[a] Reaction conditions: **7** (1.0 eq), PhB(OH)$_2$ (1.1 eq), PdCl$_2$(PPh$_3$)$_2$ (5 mol%), P(*m*-tolyl)$_3$ (5 mol%), 5 M aq. Cs$_2$CO$_3$ (2.0 eq), toluene, 80 °C, 24 h. [b] Isolated yield. [c] **7c** was recovered in 31% yield.

2–4. Mechanistic studies

Based on a typical catalytic cycle for Pd-catalyzed cross-coupling reaction shown in Scheme 3, it is reasonable to assume that diastereoselectivity of **5** is determined in the oxidative addition step, because the stereoselectivity was almost constant (*Z/E*~9:1) regardless of electronic or steric nature of substituents on organometallic reagents.
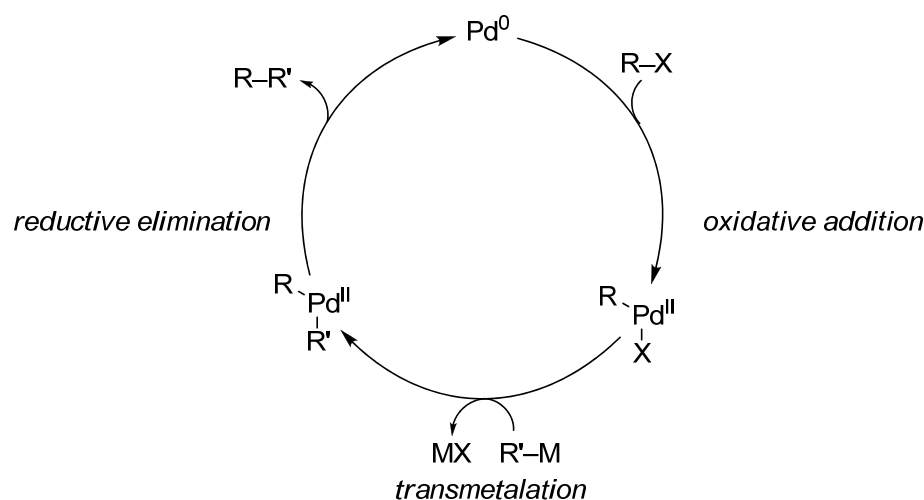
Scheme 3. Typical catalytic cycle for cross-coupling reaction.

Reaction of **2** with stoichiometric amounts of Pd(PPh$_3$)$_4$ in toluene at 80 °C was found to give pale-yellow precipitates, which were collected and recrystallized from EtOH/CH$_2$Cl$_2$ to give a colorless prism crystal of oxidative adduct *trans*-(*E*)-**11** in 68% yield (Eq. 2).
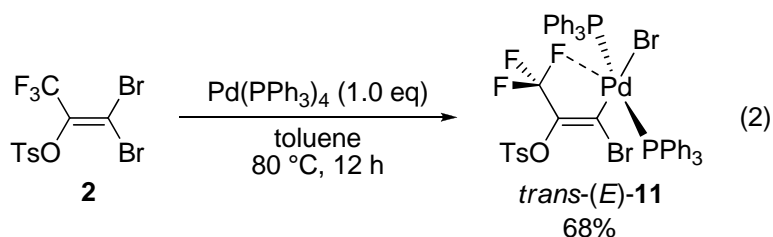
The complex **11** was fully characterized by ^{1}H, ^{13}C, ^{31}P, and ^{19}F NMR, IR, mass spectrometry, and elementary analysis. Furthermore, the molecular structure was unambiguously confirmed by X-ray crystallographic analysis of its single crystal as shown in Figure 1. The complex adopted a square-planar geometry with the Pd atom as a central point, the bond angles being 91.4(7)° for Br(1)–Pd–P(1), 88.4(6)° for Br(1)–Pd–P(2), 91.4(3)° for P(1)–Pd–C(1), and 88.5(3)° for P(2)–Pd–C(1) (Figure 1b). The *trans* geometry of two PPh$_3$ was also evidenced by the presence of a single resonance at 22.6 ppm in the ^{31}P NMR spectrum. Bond lengths for Pd–Br(1), Pd–P(1), Pd–P(2), and Pd–C(1) were nearly the same as those reported for the oxidative adduct of Br$_2$C=C(H)Fc (Fc: ferrocenyl) to Pd(0).[10] The most notable feature of the Pd complex was the distance between F(1) and Pd (2.95 Å, Figure 1a), which is longer than the sum of covalent bond radii of F and Pd (1.86 Å),[11] but shorter than the sum of the van der Walls radii (3.10 Å),[12] suggesting that some electronic interaction between F and Pd exists. To the best of his knowledge, Pd complex with such a short F⋯Pd contact has not been reported so far except for one literature.[13]
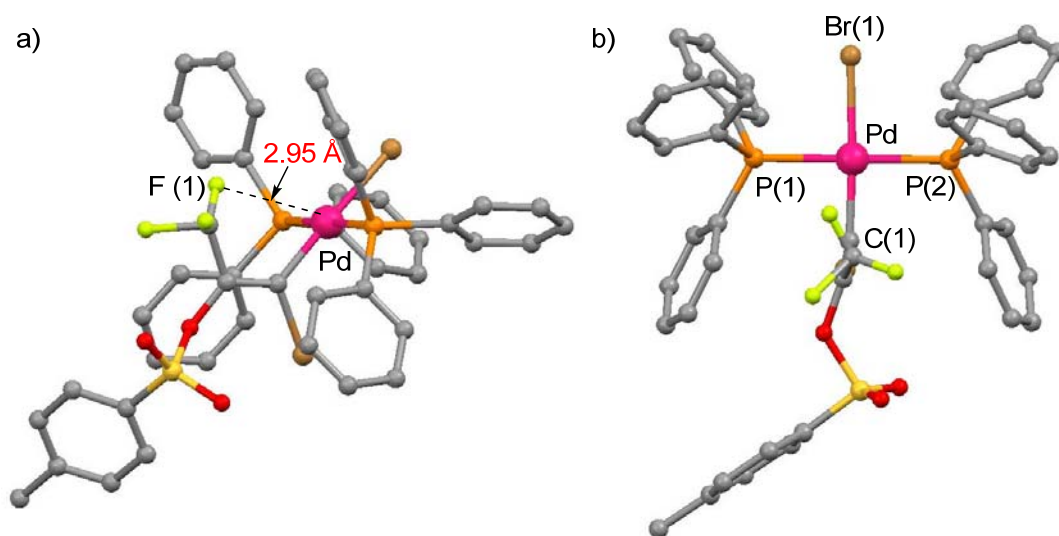
Figure 1. Molecular structure of *trans*-(*E*)-**11**: (a) side view; (b) top view. Selected bond lengths (Å) and angles (°): F(1)–Pd 2.95(9), Br(1)–Pd 2.48(0), P(1)–Pd 2.36(0), P(2)–Pd 2.33(7), Pd–C(1) 1.97(8); Br(1)–Pd–P(1) 91.4(7), Br(1)–Pd–P(2) 88.4(6), P(1)–Pd–C(1) 91.4(3), P(2)–Pd–C(1) 88.5(3), Br(1)–Pd–C(1) 175.7(1), P(1)–Pd–P(2) 177.9(3).

The Pd complex *trans*-(*E*)-**11** catalyzed cross-coupling reaction of **2** with PhB(OH)$_2$ to give **5a** with diastereoselectivity essentially the same as that obtained with Pd(PPh$_3$)$_4$ catalyst (Table 2, entry 4), although the yield was moderate (Eq. 3). This result indicates that oxidative adduct **11** would be involved in the catalytic cycle.
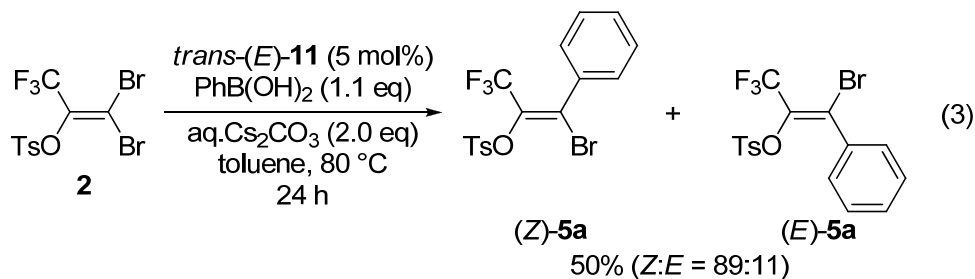
To gain further information into the oxidative addition step, the reaction was monitored by ^{31}P and ^{19}F NMR (Scheme 4). Upon mixing **2** and 10 mol% of Pd(PPh$_3$)$_4$ in C$_6$D$_6$ at room temperature, a resonance in ^{31}P NMR spectrum at 16.9 ppm corresponding to Pd(PPh$_3$)$_4$ completely disappeared within 15 min. At the same time, ^{31}P NMR exhibited a new resonance assignable to free PPh$_3$ (–4.2 ppm)[14] and two pairs of resonances at 20.2 ppm (d, *J* = 29.6 Hz) and 28.1 ppm (dq, *J* = 29.6, 5.5 Hz) as major peak, and at 19.6 ppm (d, *J* = 26.0 Hz) and 29.6 ppm (d, *J* = 26.0 Hz) as minor one. Meanwhile, ^{19}F NMR showed two new resonances at –59.4 ppm (d, *J* = 5.5 Hz) coupled

with one P atom as a major and at −59.2 ppm (s) as a minor. The ratio of the two components was estimated to be 8.2:1 based on integration in ^{31}P and ^{19}F NMR spectra. After heating the mixture at 50 °C for 3 h, the two pairs of resonances in ^{31}P NMR spectrum completely disappeared, and, instead, two new resonances appeared at 22.7 ppm (q, J = 5.6 Hz) as a major and at 23.3 ppm (s) as a minor one. Similarly, ^{19}F NMR spectrum showed advent of two new resonances at −60.3 ppm coupled with two P atoms (t, J = 5.6 Hz) as a major and at −59.9 (s) as a minor, while two resonances at −59.4 and −59.2 ppm observed at room temperature perfectly disappeared. The ratio of the two resonances was calculated as 8.9:1. This conversion was very sluggish at room temperature as evidenced by the fact that almost no change was observed in ^{31}P and ^{19}F NMR spectra after 4 h. Since chemical shifts and the coupling constants of the major resonance were identical with those of the isolated Pd complex *trans*-(*E*)-**11** in C$_6$D$_6$, the major resonance was assigned to *trans*-(*E*)-**11**. Assuming that the P–F coupling of *trans*-(*E*)-**11** reflect the close disposition of the CF$_3$ and two PPh$_3$, the observation that the minor resonance did not show any P–F coupling indicates that the CF$_3$ and two PPh$_3$ are far from each other, in other word, the CF$_3$ and Pd are positioned *trans* to each other. The geometry of two PPh$_3$ of minor resonance could be assigned as *trans*, because ^{31}P NMR spectrum showed only one resonance, indicating the two PPh$_3$ was chemically equivalent. Thus, minor resonance observed after heating was attributed to *trans*-(*Z*)-**11**. In a similar manner, initially observed two species can be assigned. Since the major component showed P–F coupling (J = 5.5 Hz) and the minor one did not show any coupling, the configuration of the major and minor should be *E* and *Z*, respectively. In addition, judging from non-equivalent PPh$_3$ resonances and the coupling constants (J = 29.6 Hz and 26.0 Hz), two PPh$_3$ should coordinate to the Pd atom in a *cis* fashion.[15] Thus, the major and minor pairs of resonances were tentatively assigned to *cis*-(*E*)-**11** and *cis*-(*Z*)-**11**, respectively, as shown in Scheme 4.
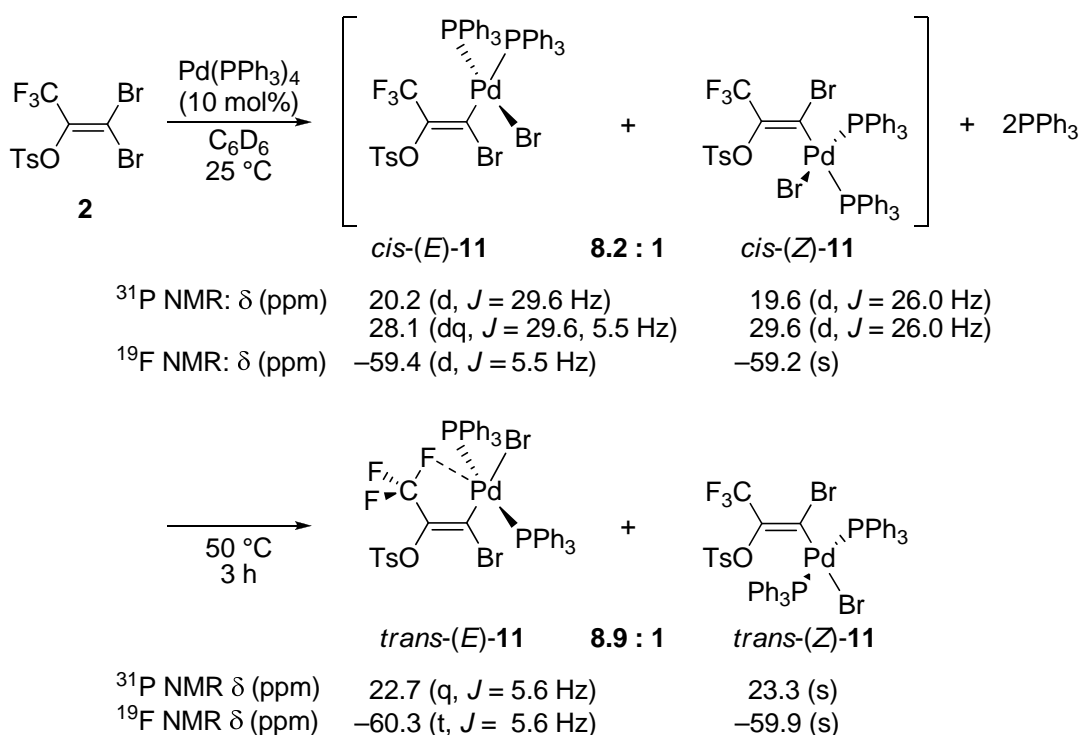
Scheme 4. Oxidative addition study of **2**.

On the basis of the experimental results, catalytic cycle of the cross-coupling reaction of **2** is proposed in Scheme 5. Oxidative addition of **2** to Pd(0) proceeds very fast and stereoselectively, giving rise to oxidative adduct *cis*-**11** with the stereoselectivity of 8.2:1. Following *cis-trans* isomerization should give *trans*-**11**. The *E*/*Z* ratio of *trans*-**11** was slightly higher (8.9:1) than that of *cis*-**11**, due possibly to the reversibility of oxidative addition and/or *cis-trans* isomerization step(s). Thermodynamic preference of *E*-**11** as compared with *Z*-**11** is rationalized by the presence of F···Pd chelation which allows Pd to fulfill 18-electron rule. Transmetalation of **11** with R–M would give diorganopalladium *trans*-**12**, which then undergoes *cis-trans* isomerization and reductive elimination, producing mono-coupled products **5** with the *Z*/*E* ratio of approximately 9:1. Considering that the smooth reaction required heating at 80 °C, higher than oxidative addition (25 °C) and *cis-trans* isomerization step (50 °C), the rate-determing step should be transmetalation or reductive elimination step(s). This is consistent with the fact that the stereoisomer ratio of **5** was almost identical with that of *trans*-**11**.

91
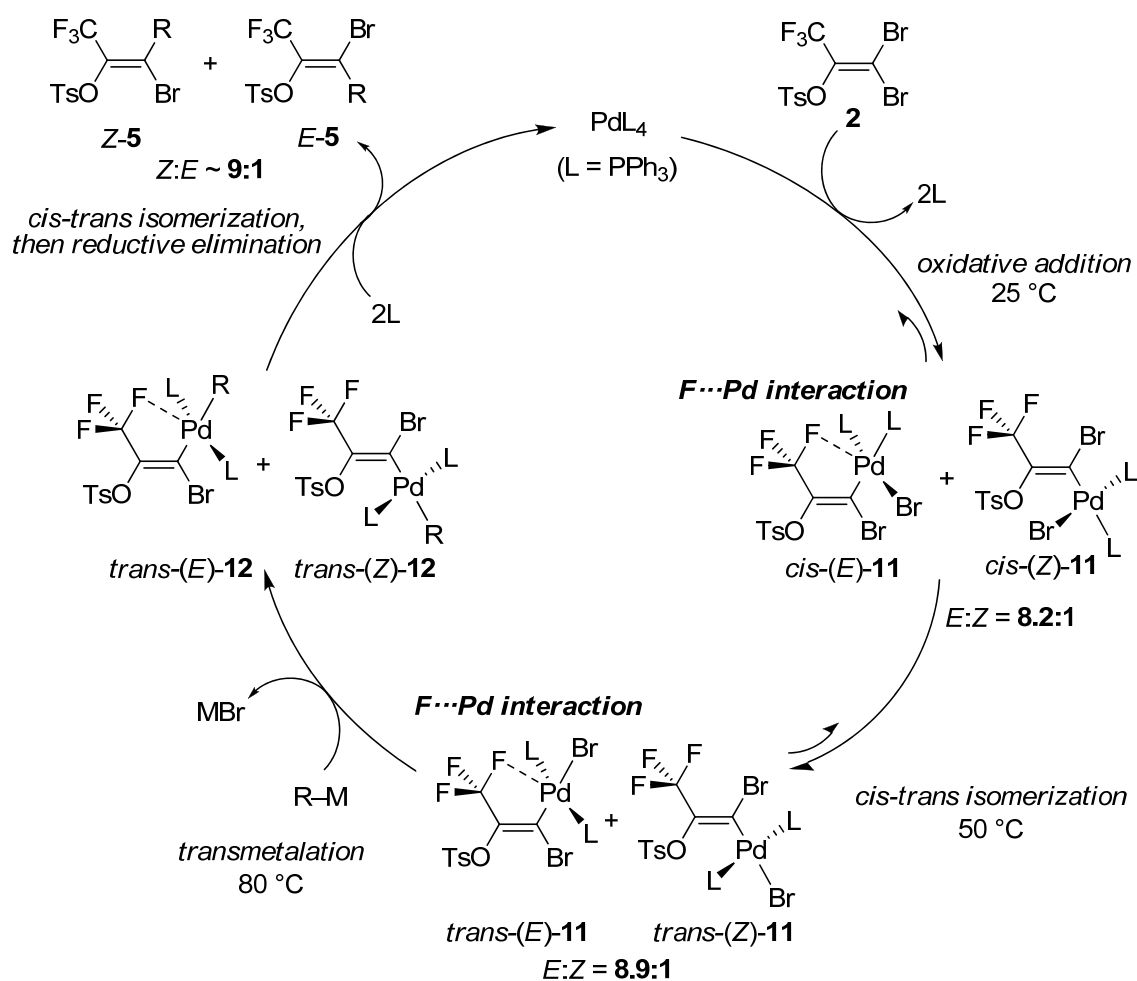
Scheme 5. Proposed catalytic cycle of stereoselective cross-coupling reaction of **2**.

2–4. Stereoselective synthesis of CF₃-substituted triarylethenes

With stereochemically pure (*Z*)-**5** in hand, the second cross-coupling with Ar²B(OH)₂ using 5 mol% of Pd(PPh₃)₄ and aqueous Cs₂CO₃ in toluene was carried out. The reaction proceeded at 100 °C chemoselectively at the remaining Br atom rather than the TsO group to give rise to CF₃-substituted diarylenol tosylates **6** as a single diastereomer in good to excellent yields (Table 7). Retention of C=C configuration was confirmed by X-ray crystallographic analysis of the single crystal of **6ab** (Table 17 in Experimental Section). Since slightly higher temperature was required for the second coupling than the first coupling, the reaction rate of the second coupling should be slower than the first one.

Table 7. Chemoselective cross-coupling reaction of (Z)-**5** with Ar²B(OH)₂.[a]

$$\text{(Z)-5} \xrightarrow[\substack{\text{aq. Cs}_2\text{CO}_3\text{ (2.0 eq)} \\ \text{toluene, 100 °C} \\ \text{24 h}}]{\substack{\text{Ar}^2\text{B(OH)}_2\ \mathbf{3}\ \text{(1.2 eq)} \\ \text{Pd(PPh}_3)_4\ \text{(5 mol\%)}}} \mathbf{6}$$

Entry	(Z)-**5**	**3**	**6**	Yield (%)[b]
1	**5a**	(3a)	**6aa**	97
2	**5a**	(3b)	**6ab**	88
3	**5a**	(3d)	**6ad**	83
4[c]	**5a**	(3i)	**6ai**	60
5	**5b**	**3a**	**6ba**	82
6	**5b**	**3d**	**6bd**	70

93

| 7 | 5d (F₃C, TsO, Br, CF₃) | 3a | 6da | 97 |

Entry	5	3	6	Yield
7	**5d**	**3a**	**6da**	97
8	**5h**	**3b**	**6hb**	90
9	**5i**	**(3g)**	**6ig**	88

Final coupling of **6** with Ar³B(OH)₂ **3** leading to **13** was accomplished with the aid of a catalytic system of Pd(OAc)₂ (2 mol%) and sterically bulky phosphine Xphos (5 mol%) in the presence of K₃PO₄ as a base.[16] Diverse substitution patterns of **13** were successfully isolated as a single stereoisomer in high to excellent yields (Table 8). Striking versatility of the present strategy is that both of *E* and *Z* isomers as well as any olefinic constitutional isomers of **13** can be synthesized at will simply by changing the order of three arylboronic acids employed as demonstrated in preparation of **13abd**, **13adb**, and **13bad** (entries 2, 3, and 4, respectively).

Table 8. Synthesis of CF$_3$-substituted triarylethenes **13**.[a]

Entry	6	3	13	Yield (%)[b]
1	6ab	(HO)$_2$B– (3a)	13aba	95
2	6ab	(HO)$_2$B–C$_6$H$_4$–CF$_3$ (3d)	13abd	96
3	6ad	(HO)$_2$B–C$_6$H$_4$–OMe (3b)	13adb	96
4	6ba	3d	13bad	95
5	6ig	3b	13igb	95

95

6 **6ai** (3i) **13aii** 91

7 **6hb** OMe (3g) **13hbg** OMe 90

8[c] **6aa** B(OH)₂ (3h) **13aah** 45

---
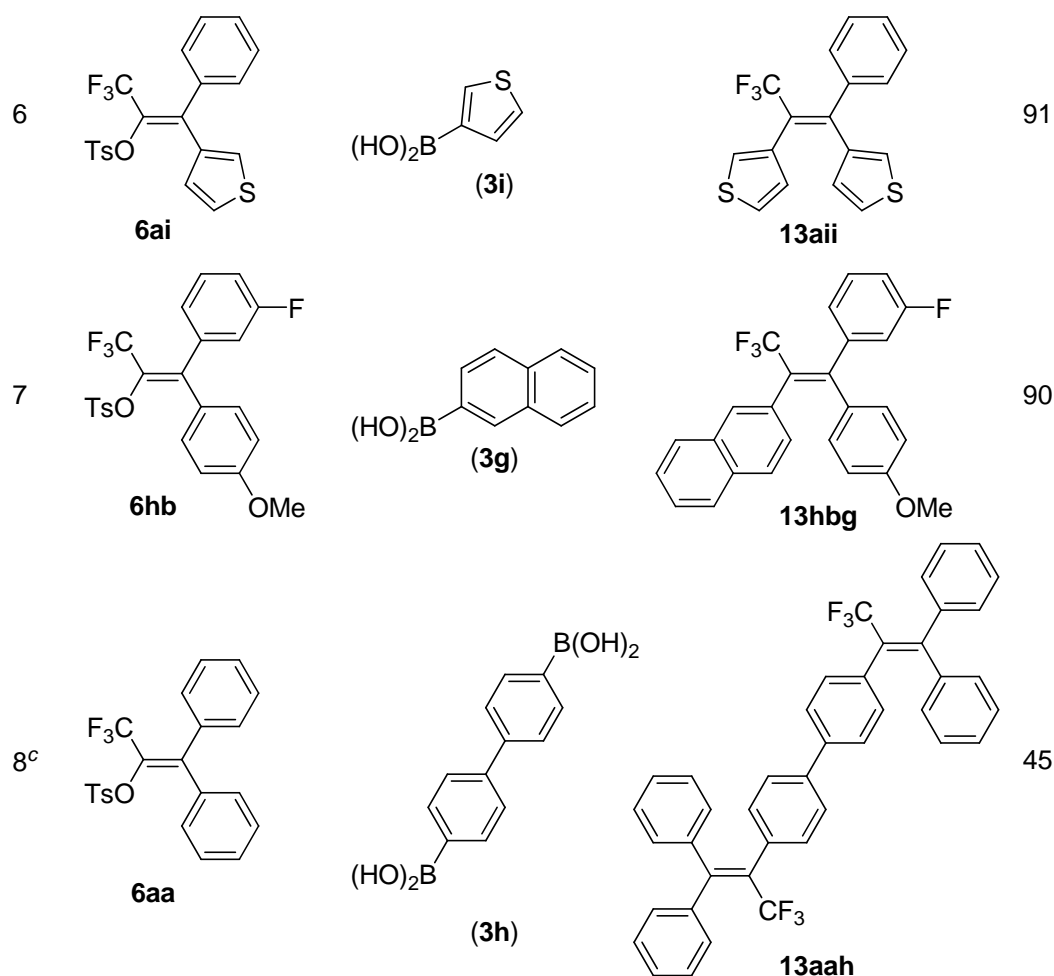
[a] Reaction conditions: a mixture of **6** (0.10 mmol), **3** (0.20 mmol), Pd(OAc)₂ (2 μmol), Xphos (5 μmol), and 2 M aq. K₃PO₄ (0.30 mmol) in THF (0.5 mL) was heated at 80 °C for 2 h. [b] Isolated yield. [c] **6aa** (0.20 mmol) and **3h** (0.10 mmol) were used and the reaction time was 6 h.

An advantage of the present approach is the realization of one-pot triarylethene synthesis (Scheme 6).   Namely, PhB(OH)₂ and aq. Cs₂CO₃ were added to a toluene solution of **2** in the presence of PdCl₂(PPh₃)₂/P(*m*-tolyl)₃.   After the solution was heated at 80 °C for 24 h, *p*-MeOC₆H₄B(OH)₂ and aq. Cs₂CO₃ were added to the reaction mixture, and then the resulting mixture was heated at 100 °C for additional 24 hours. Finally, PhB(OH)₂ and 2 M aq. K₃PO₄, Pd(OAc)₂, Xphos and THF were added to the reaction mixture, and the resulting solution was heated at 80 °C for 12 h.   Usual workup and purification gave the desired triarylethene **13aba** in 69% overall yield as a single diastereomer.   Since Shimizu and Hiyama have previously demonstrated that **13aba** can be transformed to panomifene in three steps,[3f] the result shown here is equivalent to a formal synthesis of panomifene, that is much more efficient than the

previous ones.[3a,b,f–i]
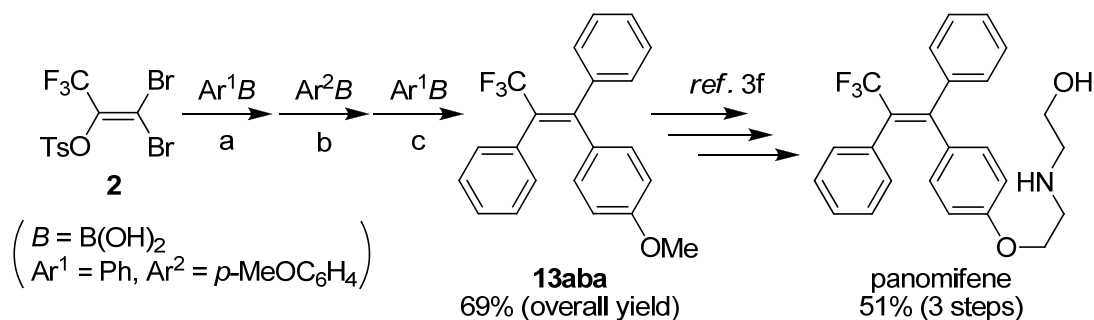
Reagents and conditions: (a) PdCl$_2$(PPh$_3$)$_2$ (5 mol%), P(m-tolyl)$_3$ (5 mol%), 5 M aq. Cs$_2$CO$_3$, toluene, 80 °C, 24 h; (b) 5 M aq. Cs$_2$CO$_3$, toluene, 100 °C, 24 h; (c) Pd(OAc)$_2$ (5 mol%), Xphos (10 mol%), 2 M aq. K$_3$PO$_4$, THF, 80 °C, 12 h.

Scheme 6. One-pot formal synthesis of panomifene.

2–5. Stereoselective synthesis of CF$_3$-substituted enynes

Making use of stereo-defined (Z)-**5**, synthesis of CF$_3$-containing enynes was demonstrated. Bégué and co-workers reported the Sonogashira cross-coupling of β-CF$_3$-substituted vinyl bromides with terminal alkynes (2.0 eq) proceeded in the presence of Pd(PPh$_3$)$_4$ as a catalyst in refluxing Et$_3$N.[17] Similar conditions were found applicable to the reaction of (Z)-**5**, giving stereospecifically CF$_3$-substituted enynes **15** in moderate to good yields (Table 9). A variety of *para*-substituted arylacetylenes **14a–c** (entries 1–3, and 6–8), silylacetylenes such as trimethylsilylacetylene (**14d**) (entries 4 and 9) and dimethylphenylsilylacetylene (**14e**) (entry 5) were applicable to the reaction. Diacetylene **14f** and **14g** gave double-coupled products **15af** and **15ag** in moderate yields (entries 10 and 11).

Table 9. Synthesis of CF$_3$-substituted enynes **15**.[a]

$$\underset{(Z)\text{-}5}{\overset{\displaystyle F_3C \qquad Ar^1}{\underset{\displaystyle TsO \qquad Br}{}}} \xrightarrow[\substack{NEt_3 \\ 100\ ^\circ C,\ 3\ h}]{\substack{\equiv\!-R \quad \mathbf{14}\ (1.2\ eq) \\ Pd(PPh_3)_4\ (5\ mol\%)}} \underset{\mathbf{15}}{\overset{\displaystyle F_3C \qquad Ar^1}{\underset{\displaystyle TsO}{}}} \quad R$$

Entry	(Z)-5	14	15	Yield (%)[b]
1	**5a** F$_3$C, TsO, Br (Ph)	phenylacetylene (**14a**)	**15aa**	80
2	**5a**	═⟨⟩–OMe (**14b**)	**15ab**	99
3	**5a**	═⟨⟩–CF$_3$ (**14c**)	**15ac**	87
4	**5a**	═–SiMe$_3$ (**14d**)	**15ad**	88
5	**5a**	═–SiMe$_2$Ph (**14e**)	**15ae**	75

98

| 6 | | **5c** | **14a** | | **12ca** | 83 |

| 7 | | **5k** | **14a** | | **15ka** | 72 |

| 8 | | **5n** | **14a** | | **15na** | 62 |

| 9 | | **5d** | **14d** | | **15dd** | 81 |

| 10[c] | | **5a** | (**14f**) | | **15af** | 54 |

| 11[c] | | **5a** | (**14g**) | | **15ag** | 44 |

---

[a] Reaction conditions: a mixture of (Z)-**5** (0.10 mmol), **14** (0.12 mmol), and Pd(PPh$_3$)$_4$ (5 μmol) in Et$_3$N (2 mL) was heated at 100 °C for 3 h. [b] Isolated yield. [c] **5a** (0.20 mmol) and **14** (0.10 mmol) were used.

99

Synthetic utility of the enynes **15** was demonstrated by transformation of **15aa** into 2-CF$_3$-substituted furan **16** (Scheme 7). Treatment of **15aa** with two equivalents of Cs$_2$CO$_3$ in the presence of catalytic amount of CuI gave 3,5-diphenyl-2-(trifluoromethyl)furan (**16**) in 69% yield. A possible mechanism is suggested below: (1) coordination of copper catalyst to carbon–carbon triple bond to form complex **A**. (2) nucleophilic attack of enol ether oxygen onto *sp*-carbon activated by Cu coordination to cyclize in *5-endo-dig* fashion, giving intermediate **B**. (3) S–O$^+$ bond cleavage by nucleophilic attack of Cs$_2$CO$_3$ followed by protonation of the resulting **C** by solvent leading to furan **16**, and Cu catalyst regenerates.
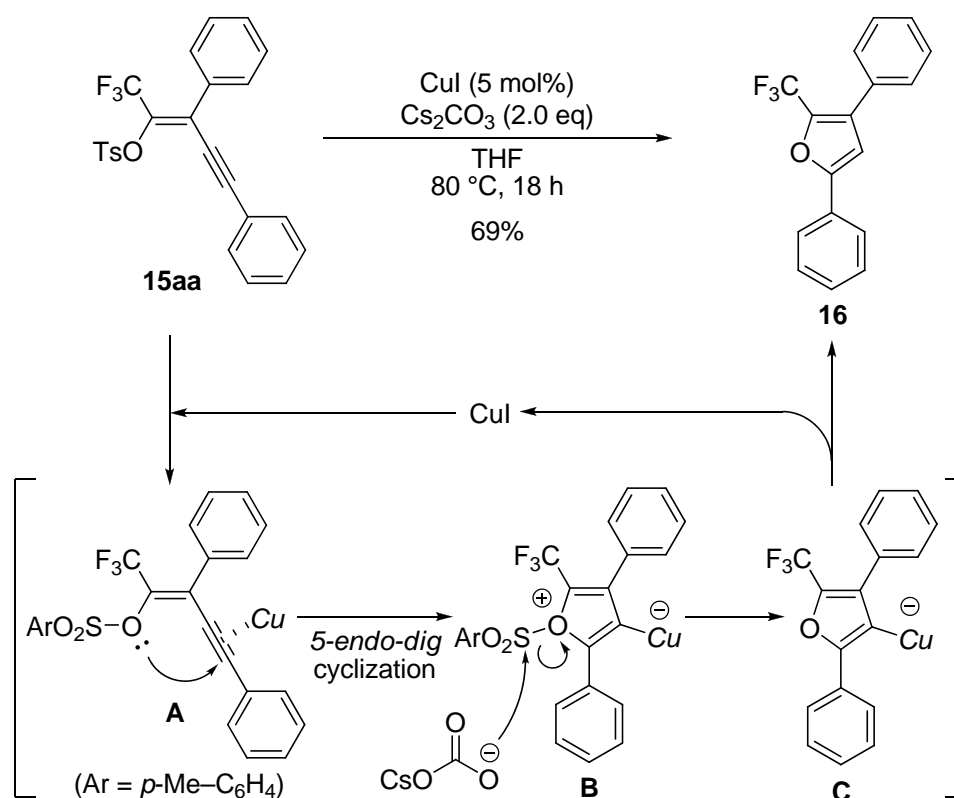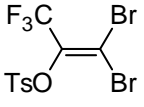
Scheme 7. Transformation of **15aa** into 2-CF$_3$-substituted furan **16**.

3. Conclusion

In summary, the author has achieved stereocontrolled synthesis of CF$_3$-substituted triarylethenes and enynes by taking advantage of stereoselective cross-coupling reaction of 1,1-dibromo-3,3,3-trifluoro-2-tosyloxypropene. The key to the high stereoselectivity is found to be attributable to fluorine coordination to Pd in oxidative addition step.

4. Experimental Section

A hydrate form of 3,3-dibromo-1,1,1-trifluoropropanone was purchased from SynQuest Laboratories, Inc. and dehydrated in conc. H_2SO_4 at 100 °C for 1 h, and then distilled under reduced pressure (57 °C/36 Torr) before use to give an anhydrous reagent. All boronic acids were purchased from Aldrich and used without any further purification. Ethyl 3,3-dibromo-2-oxopropanoate[18] and 1,1,1-trifluoro-4-phenylbutan-2-one[19] were prepared according to the literature.

Preparation of 1,1-dibromo-3,3,3-trifluoro-2-tosyloxypropene (2). To a two-necked round-bottomed flask (50 mL) equipped with a magnetic stirring bar and a dropping funnel were added TsCl (1.7 g, 9.0 mmol), freshly distilled 3,3-dibromo-1,1,1-trifluoropropanone (1.2 mL, 10 mmol), and CH_2Cl_2 (20 mL) under an argon atmosphere. The solution was cooled to 0 °C and stirred for 10 min before dropwise addition of Et_3N (1.3 mL, 9.0 mmol). The resulting solution was warmed to room temperature and stirred for 3 h. Saturated aq. NH_4Cl (5 mL) was added to the reaction mixture, and the aqueous layer was extracted with CH_2Cl_2 (20 mL × 3 times). The combined organic layer was washed with sat. aq. NaCl (15 mL), dried over anhydrous $MgSO_4$, and evaporated under reduced pressure. Recrystallization of the residue from hexane gave **2** (2.3 g, 60% yield) as colorless plates. Mp: 64.0–65.5 °C.

R_f 0.50 (hexane/AcOEt 4:1). ^1H NMR (400 MHz, $CDCl_3$): δ 2.48 (s, 3H), 7.38 (d, J = 8.4 Hz, 2H), 7.87 (d, J = 8.4 Hz, 2H); ^{13}C NMR (75 MHz, $CDCl_3$): δ 21.7, 99.7 (q, J = 2.7 Hz), 119.3 (q, J = 275.5 Hz), 128.5, 130.0, 132.8, 137.4 (q, J = 38.2 Hz), 146.5; ^{19}F NMR (282 MHz, $CDCl_3$): δ –62.1. IR (KBr): ν 2964, 2929, 1596, 1492, 1382, 1296, 1205, 1180, 1141, 1080, 1141, 1080, 906, 819, 719, 692, 678, 559, 543 cm^{-1}. MS (FAB): m/z (%) 427 (2, [M$^+$+H]+4), 425 (5, [M$^+$+H]+2), 423 (2, [M$^+$+H]), 407 (5), 405 (9), 403 (5). Anal. Calcd for $C_{10}H_7Br_2F_3O_3S$: C, 28.33; H, 1.66. Found: C, 28.44; H, 1.78.

General procedure for cross-coupling reaction of 2 with arylboronic acids.

A Schlenk tube (20 mL) equipped with a magnetic stirring bar was charged with $PdCl_2(PPh_3)_2$ (18 mg, 25 μmol), P(m-tolyl)$_3$ (7.5 mg, 25 μmol), **2** (0.21 g, 0.50 mmol), and arylboronic acid (0.55 mmol). The tube was then capped with a rubber septum, evacuated for 5 min and purged with argon. The evacuation–purge operation was repeated twice. Toluene (5 mL) and 5 M aq. Cs_2CO_3 (0.20 mL, 1.0 mmol) were added to the mixture at room temperature. The solution was stirred for 5 min and heated at 80 °C for 24 h. The reaction was monitored by TLC. Upon completion of the reaction, the mixture was allowed to cool to room temperature, diluted with AcOEt (5 mL), and filtered through a Florisil pad. The filtrate was washed with water (10 mL), and the aqueous layer was extracted with AcOEt (15 mL × 3 times). The combined organic layer was washed with sat. aq. NaCl (15 mL), dried over anhydrous $MgSO_4$, and concentrated *in vacuo*. The residue was purified by column chromatography on silica gel followed by preparative HPLC or recrystallization.

(Z)-1-Bromo-3,3,3-trifluoro-1-phenyl-2-tosyloxypropene   [(Z)-5a].   Purified by silica gel column chromatography (hexane/AcOEt 8:1) followed by recrystallization from hexane.   Yield: 86%, colorless prisms.   Mp: 90.0–91.9 °C. R_f 0.45 (hexane/AcOEt 4:1). ^{1}H NMR (400 MHz, CDCl$_3$): δ 2.47 (s, 3H), 7.37–7.42 (m, 7H), 7.94 (d, J = 8.8 Hz, 2H); ^{13}C NMR (100 MHz, CDCl$_3$): δ 21.9, 119.1 (q, J = 274.5 Hz), 128.2, 128.3, 129.4 (q, J = 3.1 Hz), 129.6, 130.2, 133.2, 134.2 (q, J = 36.6 Hz), 134.5, 145.9; ^{19}F NMR (282 MHz, CDCl$_3$): δ −60.5.   IR (KBr): ν 3057, 2029, 1641, 1595, 1492, 1446, 1382, 1301, 1230, 1193, 1180, 1145, 1080, 918, 821, 767, 734, 698, 680, 661, 563, 543, 524 cm^{-1}.   MS (FAB): m/z (%) 423 (12, [M$^+$+H]+2), 421 (12, [M$^+$+H]), 343 (71), 342 (11), 341 (68).   Anal. Calcd for C$_{16}$H$_{12}$BrF$_3$O$_3$S: C, 45.62; H, 2.87.   Found: C, 45.36; H, 2.90.
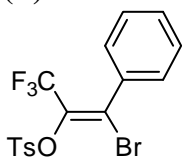
(E)-1-Bromo-3,3,3-trifluoro-1-phenyl-2-tosyloxypropene   [(E)-5a].   Purified by silica gel column chromatography (hexane/AcOEt 8:1) followed by recrystallization from hexane.   Yield: 8%, colorless prisms.   Mp: 87.5–88.6 °C. R_f 0.35 (hexane/AcOEt 8:1). ^{1}H NMR (400 MHz, CDCl$_3$): δ 2.39 (s, 3H), 7.07 (d, J = 8.0 Hz, 2H), 7.20–7.27 (m, 5H) 7.40 (d, J = 8.0 Hz, 2H); ^{13}C NMR (100 MHz, CDCl$_3$): δ 21.7, 119.8 (q, J = 273.7 Hz), 126.1 (q, J = 2.4 Hz), 127.9, 129.0, 129.5, 129.7, 131.9, 133.0, 133.5 (q, J = 36.2 Hz), 135.0, 145.3; ^{19}F NMR (282 MHz, CDCl$_3$): δ −62.6.   IR (KBr): ν 3058, 2922, 1627, 1596, 1490, 1444, 1386, 1298, 1195, 1184, 1176, 1145, 1074, 910, 767, 707, 692, 557 cm^{-1}.   MS (FAB): m/z (%) 423 (15, [M$^+$+H]+2), 421 (15, [M$^+$+H]).   Anal. Calcd for C$_{16}$H$_{12}$BrF$_3$O$_3$S: C, 45.62; H, 2.87.   Found: C, 45.57; H, 2.78.
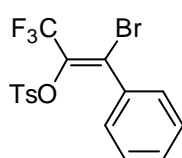
(Z)-1-Bromo-3,3,3-trifluoro-1-(4-methoxyphenyl)-2-tosyloxypropene   [(Z)-5b].   Purified by silica gel column chromatography (hexane/AcOEt 8:1) followed by recrystallization from hexane.   Yield: 67%, colorless prisms.   Mp: 80.0–82.3 °C. R_f 0.23 (hexane/AcOEt 8:1). ^{1}H NMR (400 MHz, CDCl$_3$): δ 2.48 (s, 3H), 3.84 (s, 3H), 6.89 (d, J = 8.8 Hz, 2H), 7.33 (d, J = 8.8 Hz, 2H), 7.38 (d, J = 8.4 Hz, 2H), 7.93 (d, J = 8.4 Hz, 2H); ^{13}C NMR (100 MHz, CDCl$_3$): δ 21.8, 55.3, 113.7, 119.2 (q, J = 273.8 Hz), 126.6, 128.3, 129.6, 129.8 (q, J = 3.1 Hz), 130.1 (d, J = 1.5 Hz), 133.2, 133.5 (q, J = 36.6 Hz), 145.8, 160.9; ^{19}F NMR (282 MHz, CDCl$_3$): δ −60.3.   IR (KBr): ν 3060, 2937, 1624, 1604, 1512, 1394, 1296, 1267, 1199, 1174, 1145, 1078, 916, 810, 723, 692, 680, 663, 597, 545 cm^{-1}.   MS (FAB): m/z (%) 453 (69, [M$^+$+H]+2), 451 (69, [M$^+$+H]), 371 (27).   Anal. Calcd for C$_{17}$H$_{14}$BrF$_3$O$_4$S: C, 45.25; H, 3.13.   Found: C, 45.48; H, 3.10.

(E)-1-Bromo-3,3,3-trifluoro-1-(4-methoxyphenyl)-2-tosyloxypropene   [(E)-5b].   Purified by silica gel column chromatography (hexane/AcOEt 8:1) followed by HPLC.   Yield: 7%, a colorless solid.   Mp: 87.0–88.6 °C. R_f 0.21 (hexane/AcOEt 8:1). ^{1}H NMR (300 MHz, CDCl$_3$): δ 2.38 (s, 3H), 3.80 (s, 3H), 6.66 (d, J = 9.0 Hz, 2H), 7.08 (d, J = 8.4 Hz, 2H), 7.21 (d, J = 9.0 Hz, 2H), 7.43 (d, J = 8.4 Hz, 2H); ^{13}C NMR (100 MHz, CDCl$_3$): δ 21.7, 55.3, 113.3, 120.0 (q, J =
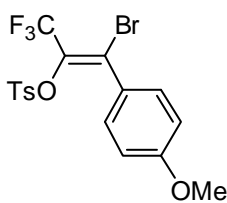
273.0 Hz), 126.2 (q, J = 3.0 Hz), 127.0, 127.9, 129.3, 130.8, 132.40, 132.45 (q, J = 37.3 Hz), 145.2, 160.6; ^{19}F NMR (282 MHz, CDCl$_3$): δ −62.2.   IR (KBr): ν 3062, 2956, 1622, 1604, 1508, 1382, 1303, 1261, 1182, 1157, 1066, 1028, 914, 833, 812, 731, 709, 696, 655, 596, 545, 522 cm^{-1}.   MS (FAB): m/z (%) 453 (60, [M$^+$+H]+2), 451 (60, [M$^+$+H]), 371 (2), 297 (100), 295 (100).   Anal. Calcd for C$_{17}$H$_{14}$BrF$_3$O$_4$S: C, 45.25; H, 3.13.   Found: C, 45.30; H, 3.25.

(Z)-1-Bromo-3,3,3-trifluoro-1-(p-tolyl)-2-tosyloxypropene   [(Z)-5c].   Purified by silica gel column chromatography (hexane/AcOEt 8:1) followed by recrystallization from hexane.   Yield: 65%, colorless plates.   Mp: 91.5–92.7 °C.   R$_f$ 0.28 (hexane/AcOEt 8:1).   ^{1}H NMR (400 MHz, CDCl$_3$): δ 2.39 (s, 3H), 2.48 (s, 3H), 7.19 (d, J = 8.0 Hz, 2H), 7.27 (d, J = 8.0 Hz, 2H), 7.38 (d, J = 8.4 Hz, 2H), 7.94 (d, J = 8.4 Hz, 2H); ^{13}C NMR (100 MHz, CDCl$_3$): δ 21.5, 21.9, 119.1 (q, J = 274.4 Hz), 128.35, 128.37, 128.9, 129.6, 129.8 (q, J = 3.0 Hz), 131.6, 133.2, 133.9 (q, J = 37.4 Hz), 140.6, 145.8; ^{19}F NMR (282 MHz, CDCl$_3$): δ −60.4.   IR (KBr): ν 3060, 2925, 1625, 1606, 1595, 1396, 1294, 1199, 1182, 1149, 1080, 918, 812, 800, 721, 692, 680, 663, 596, 545 cm^{-1}.   MS (FAB): m/z (%) 437 (19, [M$^+$+H]+2), 435 (19, [M$^+$+H]), 355 (6). Anal. Calcd for C$_{17}$H$_{14}$BrF$_3$O$_3$S: C, 46.91; H, 3.24.   Found: C, 47.02; H, 3.30.

(E)-1-Bromo-3,3,3-trifluoro-1-(p-tolyl)-2-tosyloxypropene   [(E)-5c].   Purified by silica gel column chromatography (hexane/AcOEt 8:1) followed by HPLC.   Yield: 8%, a colorless solid.   Mp: 58.0–58.9 °C.   R$_f$ 0.36 (hexane/AcOEt 4:1).   ^{1}H NMR (300 MHz, CDCl$_3$): δ 2.32 (s, 3H), 2.39 (s, 3H), 6.98 (d, J = 8.4 Hz, 2H), 7.07 (d, J = 8.1 Hz, 2H), 7.15 (d, J = 8.1 Hz, 2H), 7.41 (d, J = 8.4 Hz, 2H); ^{13}C NMR (100 MHz, CDCl$_3$): δ 21.5, 21.8, 119.9 (q, J = 273.8 Hz), 126.3 (q, J = 2.8 Hz), 127.9, 128.6, 129.0, 129.3, 132.1, 132.3, 132.9 (q, J = 37.0 Hz), 140.2, 145.2; ^{19}F NMR (282 MHz, CDCl$_3$): δ −62.5.   IR (KBr): ν 3062, 2922, 1622, 1608, 1595, 1386, 1294, 1193, 1180, 1157, 1068, 916, 812, 725, 707, 655, 543, 536 cm^{-1}.   MS (FAB): m/z (%) 437 (31, [M$^+$+H]+2), 435 (31, [M$^+$+H]), 355 (30), 281 (30), 221 (38), 207 (36).   Anal. Calcd for C$_{17}$H$_{14}$BrF$_3$O$_3$S: C, 46.91; H, 3.24.   Found: C, 46.75; H, 3.24.
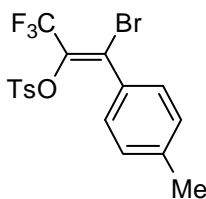
(Z)-1-Bromo-3,3,3-trifluoro-2-tosyloxy-1-(4-trifluoromethylphenyl)propene   [(E)-5d].   Purified by silica gel column chromatography (hexane/AcOEt 8:1) followed by HPLC.   Yield: 77%, a colorless solid.   Mp: 57.0–58.3 °C.   R$_f$ 0.50 (hexane/AcOEt 4:1).   ^{1}H NMR (400 MHz, CDCl$_3$): δ 2.48 (s, 3H), 7.40 (d, J = 8.4 Hz, 2H), 7.50 (d, J = 8.4 Hz, 2H), 7.67 (d, J = 8.4 Hz, 2H), 7.94 (d, J = 8.4 Hz, 2H); ^{13}C NMR (100 MHz, CDCl$_3$): δ 21.9, 118.9 (q, J = 274.5 Hz), 123.3 (q, J = 269.9 Hz), 125.4 (q, J = 3.8 Hz), 127.2 (q, J = 2.3 Hz), 128.3, 128.8 (d, J = 1.5 Hz), 129.7, 132.1 (q, J = 38.8 Hz), 133.0, 135.2 (q, J = 39.3 Hz), 138.1 (d, J = 1.8 Hz), 146.1; ^{19}F NMR (282 MHz, CDCl$_3$): δ −60.6, −63.5.   IR (KBr): ν 3070, 2931, 1624, 1593, 1396, 1330, 1294, 1201, 1149, 1080, 1066, 923, 850, 812, 727, 667, 642, 555, 547 cm^{-1}.   MS (FAB): m/z (%) 491 (8, [M$^+$+H]+2), 489 (8, [M$^+$+H]), 423 (30), 422 (100).   Anal. Calcd for C$_{17}$H$_{11}$BrF$_6$O$_3$S: C, 41.74; H, 2.27.   Found: C, 41.85; H, 2.25.
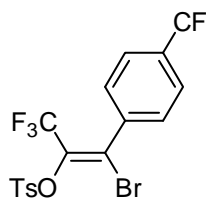
(*E*)-1-Bromo-3,3,3-trifluoro-2-tosyloxy-1-(4-trifluoromethylphenyl)propene
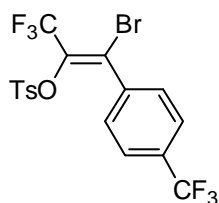
[(*E*)-5d]. Purified by silica gel column chromatography (hexane/AcOEt 8:1) followed by HPLC. Yield: 12%, a colorless oil. R_f 0.50 (hexane/AcOEt 4:1). ^{1}H NMR (400 MHz, CDCl$_3$): δ 2.38 (s, 3H), 7.07 (d, *J* = 8.4 Hz, 2H), 7.35–7.39 (m, 4H), 7.42 (d, *J* = 8.4 Hz, 2H); ^{13}C NMR (100 MHz, CDCl$_3$): δ 21.6, 119.5 (q, *J* = 274.5 Hz), 122.2 (q, *J* = 265.5 Hz), 124.9 (q, *J* = 3.0 Hz), 126.6 (d, *J* = 1.5 Hz), 127.8, 129.4, 129.6, 131.4 (q, *J* = 32.8 Hz), 132.1, 134.7 (q, *J* = 35.9 Hz), 138.5, 147.1; ^{19}F NMR (282 MHz, CDCl$_3$): δ –63.0, –63.5. IR (neat): ν 3070, 2929, 1616, 1596, 1392, 1325, 1299, 1195, 1180, 1149, 1132, 1068, 923, 835, 813, 731, 711, 657, 561 cm^{-1}. MS (FAB): *m/z* (%) 491 (8, [M$^+$+H]+2), 489 (8, [M$^+$+H]), 471 (19), 469 (19), 427 (16), 425 (16). Anal. Calcd for C$_{17}$H$_{11}$BrF$_6$O$_3$S: C, 41.74; H, 2.27. Found: C, 41.70; H, 2.39.

(*Z*)-1-Bromo-1-(4-bromophenyl)-3,3,3-trifluoro-2-tosyloxypropene [(*Z*)-5e].
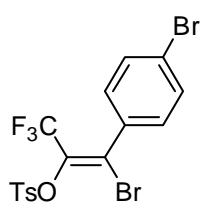
Purified by silica gel column chromatography (hexane/AcOEt 8:1) followed by recrystallization from hexane. Yield: 75%, colorless prisms. Mp: 91.5–92.7 °C. R_f 0.31 (hexane/AcOEt 8:1). ^{1}H NMR (400 MHz, CDCl$_3$): δ 2.48 (s, 3H), 7.25 (d, *J* = 8.8 Hz, 2H), 7.39 (d, *J* = 8.4 Hz, 2H), 7.54 (d, *J* = 8.8 Hz, 2H), 7.93 (d, *J* = 8.4 Hz, 2H); ^{13}C NMR (100 MHz, CDCl$_3$): δ 21.9, 119.0 (q, *J* = 274.5 Hz), 124.8, 128.0 (q, *J* = 2.8 Hz), 128.3, 129.7, 129.9, 131.6, 133.1, 133.4, 134.6 (q, *J* = 37.3 Hz), 146.0; ^{19}F NMR (282 MHz, CDCl$_3$): δ –60.5. IR (KBr): ν 2960, 2931, 1593, 1583, 1485, 1396, 1290, 1199, 1180, 1147, 1080, 1012, 918, 804, 734 669, 644, 557, 547 cm^{-1}. MS (FAB): *m/z* (%) 503 (11, [M$^+$+H]+4), 501 (17, [M$^+$+H]+2), 499 (11, [M$^+$+H]), 421 (3), 419 (3). Anal. Calcd for C$_{16}$H$_{11}$Br$_2$F$_3$O$_3$S: C, 38.42; H, 2.22. Found: C, 38.67; H, 2.39.

(*E*)-1-Bromo-1-(4-bromophenyl)-3,3,3-trifluoro-2-tosyloxypropene [(*E*)-5e].
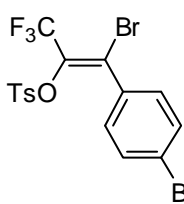
Purified by silica gel column chromatography (hexane/AcOEt 8:1) followed by HPLC. Yield: 10%, a colorless solid. Mp: 118.5–119.0 °C. R_f 0.31 (hexane/AcOEt 8:1). ^{1}H NMR (400 MHz, CDCl$_3$): δ 2.45 (s, 3H), 7.11 (d, *J* = 8.8 Hz, 2H), 7.13 (d, *J* = 8.8 Hz, 2H), 7.28 (d, *J* = 8.4 Hz, 2H), 7.40 (d, *J* = 8.4 Hz, 2H); ^{13}C NMR (100 MHz, CDCl$_3$): δ 21.9, 119.7 (q, *J* = 273.8 Hz), 124.3 (q, *J* = 3.0 Hz), 124.6, 127.8, 129.5, 130.5, 131.1, 131.6, 132.4, 133.8, 137.8 (q, *J* = 36.0 Hz), 145.8; ^{19}F NMR (282 MHz, CDCl$_3$): δ –62.9. IR (KBr): ν 2962, 2925, 1595, 1583, 1483, 1379, 1303, 1288, 1193, 1172, 1149, 1072, 918, 810, 732, 711, 563, 540 cm^{-1}. MS (FAB): *m/z* (%) 503 (6, [M$^+$+H]+4), 501 (9, [M$^+$+H]+2), 499 (6, [M$^+$+H]), 347 (6), 345 (9), 343 (6). Anal. Calcd for C$_{16}$H$_{11}$Br$_2$F$_3$O$_3$S: C, 38.42; H, 2.22. Found: C, 38.71; H, 2.16.

(Z)-1-Bromo-3,3,3-trifluoro-1-(4-phenylphenyl)-2-tosyloxypropene   **[(Z)-5f].**
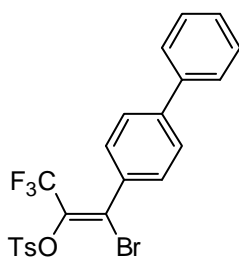
Purified by silica gel column chromatography (hexane/AcOEt 8:1). Yield: 84%, a colorless solid. Mp: 135.5–137.7 °C. R_f 0.35 (hexane/AcOEt 8:1). ^{1}H NMR (400 MHz, CDCl$_3$): δ 2.49 (s, 3H), 7.39–7.41 (m, 3H), 7.44–7.48 (m, 4H), 7.59–7.63 (m, 4H), 7.96 (d, J = 8.0 Hz, 2H); ^{13}C NMR (100 MHz, CDCl$_3$): δ 21.9, 119.1 (q, J = 274.5 Hz), 126.9, 127.0, 127.9, 128.3, 128.7, 128.9, 129.3 (q, J = 3.1 Hz), 129.7, 133.2, 133.3, 134.2 (q, J = 37.4 Hz), 139.5, 143.0, 145.9; ^{19}F NMR (282 MHz, CDCl$_3$): δ –60.3. IR (KBr): ν 3066, 3033, 1639, 1595, 1404, 1369, 1298, 1207, 1193, 1176, 1136, 1076, 921, 819, 812, 769, 756, 717, 690, 680, 623, 563 cm^{-1}. MS (FAB): m/z (%) 499 (30, [M$^+$+H]+2), 497 (30, [M$^+$+H]), 417 (5), 343 (69), 341 (69). Anal. Calcd for C$_{22}$H$_{16}$BrF$_3$O$_3$S: C, 53.13; H, 3.24. Found: C, 52.86; H, 2.97.

(E)-1-Bromo-3,3,3-trifluoro-1-(4-phenylphenyl)-2-tosyloxypropene   **[(E)-5f].**
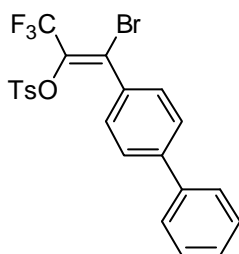
Purified by silica gel column chromatography (hexane/AcOEt 8:1). Yield: 12%, a colorless solid. Mp: 129.4–130.2 °C. R_f 0.28 (hexane/AcOEt 8:1). ^{1}H NMR (300 MHz, CDCl$_3$): δ 2.48 (s, 3H), 7.38–7.48 (m, 7H), 7.59–7.64 (m, 4H), 7.96 (d, J = 8.7 Hz, 2H); ^{13}C NMR (100 MHz, CDCl$_3$): δ 21.9, 119.1 (q, J = 274.5 Hz), 126.9, 127.0, 127.9, 128.3, 128.7, 128.9 (d, J = 1.6 Hz), 129.3 (q, J = 3.1 Hz), 129.7, 133.2, 133.3, 134.2 (q, J = 36.6 Hz), 139.5, 143.0, 145.9; ^{19}F NMR (282 MHz, CDCl$_3$): δ –60.4. IR (KBr): ν 3053, 3035, 1647, 1596, 1386, 1303, 1203, 1180, 1132, 1083, 925, 813, 756, 723, 711, 690, 659, 621, 563, 538 cm^{-1}. MS (FAB): m/z (%) 499 (25, [M$^+$+H]+2), 497 (25, [M$^+$+H]), 343 (60), 341 (60). Anal. Calcd for C$_{22}$H$_{16}$BrF$_3$O$_3$S: C, 53.13; H, 3.24. Found: C, 53.02; H, 3.14.

(Z)-1-Bromo-3,3,3-trifluoro-1-(2-naphthyl)-2-tosyloxypropene **[(Z)-5g].** Purified by silica gel column chromatography (hexane/AcOEt 8:1). Yield: 69%, a colorless solid. Mp: 78.5–79.0 °C. R_f 0.31 (hexane/AcOEt 8:1). ^{1}H NMR (400 MHz, CDCl$_3$): δ 2.49 (s, 3H), 7.40 (d, J = 8.0 Hz, 2H), 7.45 (d, J = 8.8 Hz, 1H), 7.55–7.57 (m, 2H), 7.85-7.88 (m, 4H), 7.98 (d, J = 8.0 Hz, 2H); ^{13}C NMR (100 MHz, CDCl$_3$): δ 21.9, 119.2 (q, J = 274.5 Hz), 126.8, 127.60, 127.64, 128.33, 128.34, 128.38, 128.4, 129.6 (q, J = 3.1 Hz), 129.7, 131.7, 132.2, 133.2, 133.5, 134. 3 (q, J = 37.4 Hz), 145.9; ^{19}F NMR (282 MHz, CDCl$_3$): δ –60.3. IR (KBr): ν 3060, 2931, 1595, 1380, 1298, 1197, 1178, 1134, 1074, 925, 835, 825, 794, 750, 715, 688, 657, 592, 569, 561 cm^{-1}. MS (FAB): m/z (%) 473 (16, [M$^+$+H]+2), 471 (16, [M$^+$+H]), 391 (3), 317 (34), 315 (34). Anal. Calcd for C$_{20}$H$_{14}$BrF$_3$O$_3$S: C, 50.97; H, 2.99. Found: C, 50.96; H, 3.00.
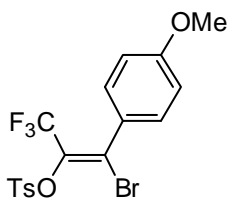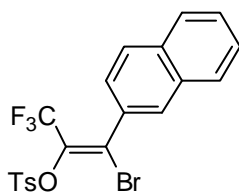
105

(*E*)-1-Bromo-3,3,3-trifluoro-1-(2-naphthyl)-2-tosyloxypropene [(*E*)-5g]. Purified by silica gel column chromatography (hexane/AcOEt 8:1) followed by recrystallization from hexane. Yield: 9%, colorless plates. Mp: 111.6–112.5 °C. R_f 0.24 (hexane/AcOEt 8:1). ^{1}H NMR (400 MHz, CDCl$_3$): δ 2.05 (s, 3H), 6.63 (d, *J* = 8.0 Hz, 2H), 7.23 (d, *J* = 4.0 Hz, 2H), 7.35 (dd, *J* = 4.0, 2.0 Hz, 1H), 7.47–7.56 (m, 2H), 7.61–7.65 (m, 3H), 7.77 (d, *J* = 8.0 Hz, 1H); ^{13}C NMR (100 MHz, CDCl$_3$): δ 21.5, 119.9 (q, *J* = 273.8 Hz), 125.6, 125.7 (q, *J* = 3.0 Hz), 126.5, 127.3, 127.5, 127.6, 127.7, 128.3, 128.9, 129.4, 132.05, 132.08, 132.3, 133.4, 134.5 (q, *J* = 32.0 Hz), 145.2; ^{19}F NMR (282 MHz, CDCl$_3$): δ –62.7. IR (KBr): ν 3060, 2923, 1629, 1595, 1386, 1292, 1197, 1174, 1145, 1072, 918, 891, 864, 808, 731, 700, 657, 557, 547 cm^{-1}. MS (FAB): *m/z* (%) 473 (13, [M$^+$+H]+2), 471 (13, [M$^+$+H]), 391 (3), 317 (36), 315 (36). Anal. Calcd for C$_{20}$H$_{14}$BrF$_3$O$_3$S: C, 50.97; H, 2.99. Found: C, 50.98; H, 3.10.
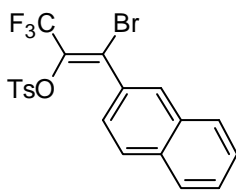
(*Z*)-1-Bromo-3,3,3-trifluoro-1-(3-fluorophenyl)-2-tosyloxypropene [(*Z*)-5h]. Purified by silica gel column chromatography (hexane/AcOEt 8:1). Yield: 77%, a colorless solid. Mp: 61.6–63.2 °C. R_f 0.32 (hexane/AcOEt 8:1). ^{1}H NMR (400 MHz, CDCl$_3$): δ 2.48 (s, 3H), 7.08–7.15 (m, 2H), 7.16 (d, *J* = 8.0 Hz, 1H), 7.35–7.40 (m, 3H), 7.93 (d, *J* = 8.4 Hz, 2H); ^{13}C NMR (100 MHz, CDCl$_3$): δ 21.9, 115.6 (d, *J* = 24.4 Hz), 117.3 (d, *J* = 20.6 Hz), 119.0 (q, *J* = 274.5 Hz), 124.2 (d, *J* = 1.6 Hz), 127.5 (q, *J* = 3.1 Hz), 128.3, 129.7, 130.0 (d, *J* = 8.4 Hz), 133.1, 134.9 (q, *J* = 37.3 Hz), 136.3 (d, *J* = 7.6 Hz), 146.0, 161.8 (d, *J* = 246.2 Hz); ^{19}F NMR (282 MHz, CDCl$_3$): δ –60.7 (s, 3F), –112.2 (td, *J* = 9.0, 4.5 Hz, 1F). IR (KBr): ν 3060, 1647, 1587, 1384, 1303, 1267, 1195, 1180, 1149, 1080, 839, 792, 734, 692, 663, 543 cm^{-1}. MS (FAB): *m/z* (%) 441 (11, [M$^+$+H]+2), 439 (11, [M$^+$+H]), 359 (3), 285 (27), 283 (27). Anal. Calcd for C$_{16}$H$_{11}$BrF$_4$O$_3$S: C, 43.75; H, 2.52. Found: C, 43.74; H, 2.60.
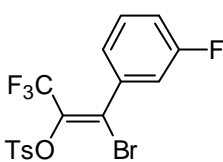
(*E*)-1-Bromo-3,3,3-trifluoro-1-(3-fluorophenyl)-2-tosyloxypropene [(*E*)-5h]. Purified by silica gel column chromatography (hexane/AcOEt 8:1) followed by recrystallization from hexane. Yield: 10%, colorless prisms. Mp: 76.2–76.6 °C. R_f 0.24 (hexane/AcOEt 8:1). ^{1}H NMR (400 MHz, CDCl$_3$): δ 2.41 (s, 3H), 6.85 (dt, *J* = 9.0, 2.4 Hz, 1H), 6.95 (tdd, *J* = 2.4, 1.2, 0.8 Hz, 1H), 7.09 (t, *J* = 1.2 Hz, 1H), 7.12 (d, *J* = 8.4 Hz, 2H), 7.19 (td, *J* = 8.0, 5.6 Hz, 1H), 7.44 (d, *J* = 8.4 Hz, 2H); ^{13}C NMR (100 MHz, CDCl$_3$): δ 21.7, 116.3 (d, *J* = 23.6 Hz), 116.8 (d, *J* = 21.4 Hz), 119.6 (q, *J* = 273.7 Hz), 124.8, 128.0, 129.5, 129.6, 129.4 (q, *J* = 2.0 Hz), 131.8, 138.3 (q, *J* = 37.0 Hz), 145.8, 148.4, 161.8 (d, *J* = 245.5 Hz; ^{19}F NMR (282 MHz, CDCl$_3$): δ –62.8 (s, 3F), –112.5 (td, *J* = 9.0, 4.5 Hz, 1F). IR (KBr): ν 3074, 2920, 1625, 1587, 1388, 1296, 1201, 1180, 1143, 1074, 871, 798, 788, 705, 694, 682, 557, 543 cm^{-1}. MS (FAB): *m/z* (%) 439 (18, [M$^+$+H]+2), 437 (18, [M$^+$+H]). Anal. Calcd for C$_{16}$H$_{11}$BrF$_4$O$_3$S: C, 43.75; H, 2.52. Found: C, 43.77; H, 2.68.

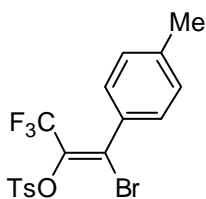**(*Z*)-1-Bromo-3,3,3-trifluoro-1-(3-thienyl)-2-tosyloxypropene [(*Z*)-5i].** Purified by silica gel column chromatography (hexane/AcOEt 8:1). Yield: 72%, a colorless solid. Mp: 82.5–83.0 °C. R_f 0.20 (hexane/AcOEt 8:1). ^{1}H NMR (400 MHz, CDCl$_3$): δ 2.51 (s, 3H), 7.15 (dd, *J* = 4.8, 1.2 Hz, 1H), 7.35 (dd, *J* = 4.8, 2.8 Hz, 1H), 7.38 (d, *J* = 8.4 Hz, 2H), 7.51 (dd, *J* = 2.8, 1.2 Hz, 1H), 7.93 (d, *J* = 8.4 Hz, 2H); ^{13}C NMR (100 MHz, CDCl$_3$): δ 21.9, 119.2 (q, *J* = 274.5 Hz), 123.9 (q, *J* = 3.5 Hz), 126.2, 127.5 (d, *J* = 2.3 Hz), 127.7, 128.3, 129.7, 133.1, 133.7, 134.1 (d, *J* = 37.4 Hz), 145.9; ^{19}F NMR (282 MHz, CDCl$_3$): δ –60.3. IR (KBr): ν 3105, 1595, 1394, 1290, 1197, 1182, 1145, 1078, 846, 810, 790, 763, 688, 671, 657, 611, 549 cm^{-1}. MS (FAB): *m/z* (%) 429 (50, [M$^+$+H]+2), 427 (50, [M$^+$+H]), 347 (8), 273 (75), 271 (75). Anal. Calcd for C$_{14}$H$_{10}$BrF$_3$O$_3$S$_2$: C, 39.36; H, 2.36. Found: C, 39.26; H, 2.19.
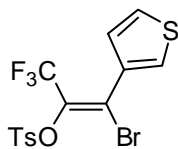
(*E*)-1-Bromo-3,3,3-trifluoro-1-(3-thienyl)-2-tosyloxypropene [(*E*)-5i]. Purified by silica gel column chromatography (hexane/AcOEt 8:1) followed by recrystallization from hexane. Yield: 8%, colorless prisms. Mp: 77.3–78.5 °C. R_f 0.13 (hexane/AcOEt 8:1). ^{1}H NMR (400 MHz, CDCl$_3$): δ 2.41 (s, 3H), 7.10–7.16 (m, 4H), 7.46 (dd, *J* = 2.8, 1.2 Hz, 1H), 7.55 (d, *J* = 8.4 Hz, 2H); ^{13}C NMR (100 MHz, CDCl$_3$): δ 21.8, 120.0 (q, *J* = 273.7 Hz), 120.3 (q, *J* = 2.0 Hz), 125.3, 127.9, 128.1, 129.43, 129.44 (q, *J* = 53.0 Hz), 129.6, 131.8, 134.9, 145.6; ^{19}F NMR (282 MHz, CDCl$_3$): δ –61.9. IR (KBr): ν 3136, 1618, 1593, 1386, 1288, 1203, 1176, 1136, 1072, 802, 790, 707, 698, 675, 650, 632, 561, 542 cm^{-1}. MS (FAB): *m/z* (%) 429 (8, [M$^+$+H]+2), 427 (8, [M$^+$+H]), 273 (8), 271 (8). Anal. Calcd for C$_{14}$H$_{10}$BrF$_3$O$_3$S$_2$: C, 39.36; H, 2.36. Found: C, 39.21; H, 2.51.
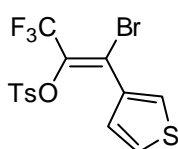
General procedure for cross-coupling reaction of 2 with tributyl(aryl)stannanes.

A Schlenk tube (20 mL) equipped with a magnetic stirring bar was charged with Pd$_2$(dba)$_3$ (11 mg, 13 μmol), P(2-furyl)$_3$ (24 mg, 0.1 mmol), and **2** (0.21 g, 0.50 mmol). The tube was then capped with a rubber septum, evacuated for 5 min and purged with argon. The evacuation-purge operation was repeated twice. Toluene (5 mL) was added to the mixture at room temperature. The solution was stirred at room temperature for 5 min and degassed by three freeze-thaw cycles before treatment with arylstannane (0.53 mmol). The resulting mixture was heated at 90 °C for 24 h. The reaction was monitored by TLC. After the mixture was allowed to cool to room temperature, 1 M aq. KF (5 mL) was added, and then the resulting mixture was stirred for 1 h. The organic layer was extracted with AcOEt (15 mL × 3 times) and washed with 1M aq. KF (15 mL) and sat. aq. NaCl (15 mL), dried over anhydrous MgSO$_4$, and then concentrated *in vacuo*. The residue was purified by column chromatography on silica gel containing 5 wt% finely ground KF[20] followed by recrystallization.

(*Z*)-1-Bromo-1-(4-(*N,N*-dimethylamino)phenyl)-3,3,3-trifluoro-2-tosyloxypropene [(*Z*)-5j]. Purified by silica gel column chromatography (hexane/AcOEt 8:1) followed by recrystallization from hexane. Yield: 68%, pale yellow prisms. Mp: 125.6–126.6 °C. R_f 0.35 (hexane/AcOEt 4:1). ^{1}H NMR (400 MHz, CDCl$_3$): δ 2.42 (s, 3H), 2.96 (s, 6H), 6.60 (d, *J* = 8.4 Hz, 2H), 7.22 (d, *J* = 8.4 Hz, 2H), 7.32
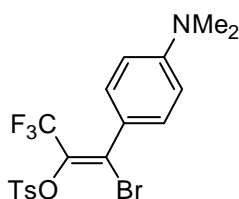
(d, J = 8.0 Hz, 2H), 7.89 (d, J = 8.0 Hz, 2H); ^{13}C NMR (100 MHz, CDCl$_3$): δ 21.8, 40.1, 110.8, 119.4 (q, J = 273.7 Hz), 121.0, 128.4, 129.6, 130.1, 131.5 (q, J = 3.0 Hz), 131.8 (q, J = 33.6 Hz), 133.3, 145.6, 151.3; ^{19}F NMR (282 MHz, CDCl$_3$): δ −60.2.   IR (KBr): ν 2912, 1604, 1525, 1375, 1292, 1247, 1199, 1172, 1074, 916, 819, 800, 763, 732, 665, 561 cm^{-1}.   MS (FAB): m/z (%) 466 (33, [M$^+$+H]+2), 465 (13, M$^+$+2), 464 (33, [M$^+$+H]), 463 (33, M$^+$), 310 (100), 308 (100).   Anal. Calcd for C$_{18}$H$_{17}$BrF$_3$NO$_3$S: C, 46.56; H, 3.69.   Found: C, 46.65; H, 3.67.

(*E*)-1-Bromo-1-(4-(*N*,*N*-dimethylamino)phenyl)-3,3,3-trifluoro-2-tosyloxypropene
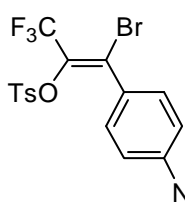
[(*E*)-5j].   Purified by silica gel column chromatography (hexane/AcOEt 8:1) followed by recrystallization from hexane.   Yield: 8%, pale yellow prisms.   Mp: 141.5–142.3 °C.   R$_f$ 0.11 (hexane/AcOEt 4:1). ^{1}H NMR (400 MHz, CDCl$_3$): δ 2.36 (s, 3H), 2.99 (s, 6H), 6.38 (d, J = 8.8 Hz, 2H), 7.03 (d, J = 8.8 Hz, 2H), 7.14 (d, J = 8.8 Hz, 2H), 7.43 (d, J = 8.8 Hz, 2H); ^{13}C NMR (100 MHz, CDCl$_3$): δ 21.7, 40.0, 110.5, 120.2 (q, J = 272.9 Hz), 121.7, 128.1, 129.1, 130.0 (q, J = 32.3 Hz), 130.5 (q, J = 3.0 Hz), 130.7, 132.4, 144.6, 150.9; ^{19}F NMR (282 MHz, CDCl$_3$): δ −61.7.   IR (KBr): ν 2976, 1602, 1525, 1377, 1307, 1280, 1190, 1178, 1151, 1062, 910, 846, 812, 711, 655, 542 cm^{-1}.   MS (FAB): m/z (%) 466 (35, [M$^+$+H]+2), 465 (15, M$^+$+2), 464 (35, [M$^+$+H]), 463 (35, M$^+$), 310 (100), 308 (100).   Anal. Calcd for C$_{18}$H$_{17}$BrF$_3$NO$_3$S: C, 46.56; H, 3.69.   Found: C, 46.79; H, 3.73.

(*Z*)-1-Bromo-3,3,3-trifluoro-1-(4-formylpheyl)-2-tosyloxypropene   [(*Z*)-5k].
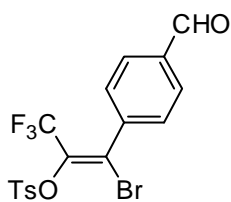
Purified by silica gel column chromatography (hexane/AcOEt 8:1) followed by recrystallization from hexane.   Yield: 82%, colorless prisms.   Mp: 79.1–80.0 °C.   R$_f$ 0.37 (hexane/AcOEt 4:1). ^{1}H NMR (300 MHz, CDCl$_3$): δ 2.48 (s, 3H), 7.40 (d, J = 8.4 Hz, 2H), 7.55 (d, J = 8.1 Hz, 2H), 7.91–7.95 (m, 4H), 10.05 (s, 1H); ^{13}C NMR (100 MHz, CDCl$_3$): δ 21.8, 118.9 (q, J = 274.5 Hz), 127.3 (q, J = 3.0 Hz), 128.3, 129.1, 129.4, 129.7, 133.0, 135.1 (q, J = 38.2 Hz), 137.0, 140.1, 146.1, 190.8; ^{19}F NMR (282 MHz, CDCl$_3$): δ −60.6.   IR (KBr): ν 3061, 1708, 1649, 1593, 1419, 1388, 1303, 1232, 1197, 1141, 1103, 1080, 923, 827, 815, 800, 723, 707, 678, 665, 632, 559, 542 cm^{-1}.   MS (FAB): m/z (%) 451 (37, [M$^+$+H]+2), 450 (6, M$^+$+2), 449 (37, [M$^+$+H]), 448 (6, M$^+$), 293 (12), 155 (100).   Anal. Calcd for C$_{17}$H$_{12}$BrF$_3$O$_4$S: C, 45.45; H, 2.69.   Found: C, 45.42; H, 2.58.

(*E*)-1-Bromo-3,3,3-trifluoro-1-(4-formylphenyl)-2-tosyloxypropene   [(*E*)-5k].
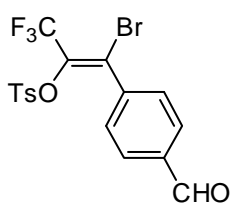
Purified by silica gel column chromatography (hexane/AcOEt 8:1) followed by recrystallization from hexane.   Yield: 11%, colorless prisms.   Mp: 91.0–91.6 °C.   R$_f$ 0.28 (hexane/AcOEt 4:1). ^{1}H NMR (300 MHz, CDCl$_3$): δ 2.37 (s, 3H), 7.09 (d, J = 8.1 Hz, 2H), 7.43–7.48 (m, 4H), 7.72 (d, J = 8.1 Hz, 2H), 10.00 (s, 1H); ^{13}C NMR (100 MHz, CDCl$_3$): δ 21.7, 119.5 (q, J = 273.7 Hz), 124.0 (q, J = 2.3 Hz), 127.9, 129.0, 129.6, 129.7, 132.1, 134.5 (q, J = 37.3 Hz), 136.7, 140.6, 145.9, 190.7; ^{19}F NMR (282 MHz, CDCl$_3$): δ −63.0.   IR (KBr): ν 3057, 1703, 1604, 1597, 1494, 1386, 1307, 1234, 1186, 1145, 1074, 920, 823, 813, 806, 732, 704, 692, 659,

642, 551, 522 cm^{-1}.   MS (FAB): m/z (%) 451 (100, [M$^+$+H]+2), 450 (21, M$^+$+2), 449 (100, [M$^+$+H]), 448 (21, M$^+$), 294 (26), 155 (49).   Anal. Calcd for C$_{17}$H$_{12}$BrF$_3$O$_4$S: C, 45.45; H, 2.69.   Found: C, 45.42; H, 2.64.

(Z)-1-Bromo-3,3,3-trifluoro-1-(2-furyl)-2-tosyloxypropene [(Z)-5l].   Purified by silica gel column chromatography (hexane/AcOEt 8:1).   Yield: 73%, a brown oil.   R$_f$ 0.51 (hexane/AcOEt 4:1). ^{1}H NMR (300 MHz, CDCl$_3$): δ 2.47 (s, 3H), 6.49 (dd, J = 3.6, 1.5 Hz, 1H), 6.84 (d, J = 3.3 Hz, 1H), 7.38 (d, J = 8.1 Hz, 2H), 7.57 (bs, 1H), 7.91 (d, J = 8.1 Hz, 2H); ^{13}C NMR (100 MHz, CDCl$_3$): δ 21.7, 112.1, 116.83, 116.86, 117.4 (q, J = 2.2 Hz), 119.3 (q, J = 274.3 Hz), 128.6, 129.8, 133.1, 145.1 (q, J = 35.0 Hz), 145.7, 146.2; ^{19}F NMR (282 MHz, CDCl$_3$): δ −61.44.   IR (neat): ν 2928, 1797, 1597, 1469, 1392, 1298, 1195, 1180, 1147, 1084, 862, 813, 754, 707, 690, 561 cm^{-1}.   MS (FAB): m/z (%) 413 (13, [M$^+$+H]+2), 412 (3, M$^+$+2), 411 (13, [M$^+$+H]), 410 (3, M$^+$), 257 (53), 255 (53), 155 (100).   Anal. Calcd for C$_{14}$H$_{10}$BrF$_3$O$_4$S: C, 40.89; H, 2.45.   Found: C, 40.89; H, 2.60.
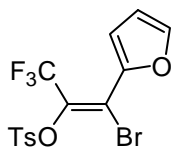
(E)-1-Bromo-3,3,3-trifluoro-1-(2-furyl)-2-tosyloxypropene [(E)-5l].   Purified by silica gel column chromatography (hexane/AcOEt 8:1).   Yield: 14%, a brown oil.   R$_f$ 0.39 (hexane/AcOEt 4:1). ^{1}H NMR (400 MHz, CDCl$_3$): δ 2.44 (s, 3H), 6.41 (dd, J = 3.6, 2.0 Hz, 1H), 6.93 (d, J = 3.6 Hz, 4H), 7.28 (d, J = 8.4 Hz, 2H), 7.40 (bs, 1H), 7.73 (d, J = 8.4 Hz, 2H); ^{13}C NMR (100 MHz, CDCl$_3$): δ 21.8, 107.4, 113.9 (q, J = 2.2 Hz), 117.5, 120.0 (q, J = 273.0 Hz), 128.3, 129.5, 132.4, 145.1, 145.7, 145.9 (q, J = 32.0 Hz), 146.0; ^{19}F NMR (282 MHz, CDCl$_3$): δ −61.43.   IR (neat): ν 2926, 1610, 1597, 1465, 1390, 1296, 1195, 1180, 1143, 1074, 883, 813, 754, 705, 686, 559 cm^{-1}.   MS (FAB): m/z (%) 413 (8, [M$^+$+H]+2), 412 (3, M$^+$+2), 411 (8, [M$^+$+H]), 410 (3, M$^+$), 257 (27), 255 (27), 155 (100).   Anal. Calcd for C$_{14}$H$_{10}$BrF$_3$O$_4$S: C, 40.89; H, 2.45.   Found: C, 40.96; H, 2.71.
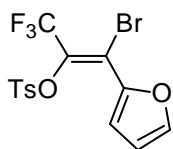
(Z)-1-Bromo-3,3,3-trifluoro-1-(2-benzofuryl)-2-tosyloxypropene   [(Z)-5m].   Purified by silica gel column chromatography (hexane/AcOEt 8:1) followed by recrystallization from hexane.   Yield: 62%, colorless prisms.   Mp: 109.3–110.0 °C.   R$_f$ 0.43 (hexane/AcOEt 4:1). ^{1}H NMR (400 MHz, CDCl$_3$): δ 2.45 (s, 3H), 7.14 (s, 1H), 7.22–7.28 (m, 1H), 7.35–7.39 (m, 3H), 7.48 (d, J = 8.8 Hz, 1H), 7.59 (d, J = 7.6 Hz, 1H), 7.91 (d, J = 8.4 Hz, 2H); ^{13}C NMR (100 MHz, CDCl$_3$): δ 21.9, 111.7, 112.51, 112.53, 117.5 (q, J = 3.1 Hz), 119.1 (q, J = 274.5 Hz), 121.9, 123.6, 126.7, 127.2, 128.4, 129.8, 132.9, 135.7 (q, J = 38.9 Hz), 146.15, 146.19, 155.5; ^{19}F NMR (282 MHz, CDCl$_3$): δ −61.0.   IR (KBr): ν 3136, 1595, 1560, 1446, 1381, 1301, 1193, 1180, 1153, 1078, 979, 871, 817, 810, 750, 704, 688, 559, 538 cm^{-1}.   MS (FAB): m/z (%) 463 (13, [M$^+$+H]+2), 462 (3, M$^+$+2), 461 (13, [M$^+$+H]), 460 (3, M$^+$), 307 (100), 305 (100), 155 (46).   Anal. Calcd for C$_{18}$H$_{12}$BrF$_3$O$_4$S: C, 46.87; H, 2.62.   Found: C, 46.85; H, 2.64.
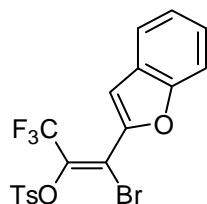
(Z)-1-Bromo-3,3,3-trifluoro-1-(2-thienyl)-2-tosyloxypropene [(Z)-5n].   Purified by silica gel column chromatography (hexane/AcOEt 8:1) followed by recrystallization from hexane.   Yield: 81%, colorless plates.   Mp: 78.2–79.1 °C. R_f 0.43 (hexane/AcOEt 4:1). ^{1}H NMR (300 MHz, CDCl$_3$): δ 2.47 (s, 3H), 7.01 (dd, J = 5.1, 3.6 Hz, 1H), 7.26–7.28 (m, 1H), 7.38 (d, J = 8.1 Hz, 2H), 7.56 (dd, J = 5.1, 1.2 Hz, 1H), 7.93 (d, J = 8.1 Hz, 2H); ^{13}C NMR (100 MHz, CDCl$_3$): δ 21.9, 119.2 (q, J = 274.5 Hz), 121.9 (q, J = 3.1 Hz), 126.9, 128.4, 129.7, 130.5, 130.6, 132.9, 134.4 (q, J = 37.4 Hz), 135.4, 146.0; ^{19}F NMR (282 MHz, CDCl$_3$): δ –60.3.   IR (KBr): ν 3093, 1620, 1595, 1512, 1491, 1417, 1396, 1377, 1288, 1240, 1199, 1182, 1145, 1101, 1076, 1045, 873, 839, 812, 723, 705, 686, 661, 619, 584, 547, 516 cm^{-1}.   MS (FAB): m/z (%) 429 (25, [M$^+$+H]+2), 428 (6, M$^+$+2), 427 (25, [M$^+$+H]), 426 (6, M$^+$), 273 (100), 271 (100), 155 (83).   Anal. Calcd for C$_{14}$H$_{10}$BrF$_3$O$_3$S$_2$: C, 39.36; H, 2.36.   Found: C, 39.32; H, 2.49.

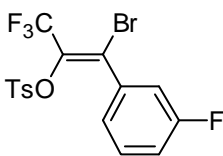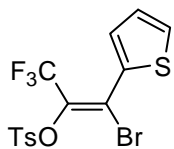**(E)-1-Bromo-3,3,3-trifluoro-1-(2-thienyl)-2-tosyloxypropene [(E)-5n].**   Purified by silica gel column chromatography (hexane/AcOEt 8:1) followed by recrystallization from hexane.   Yield: 6%, colorless prisms.   Mp: 69.7–70.1 °C. R_f 0.31 (hexane/AcOEt 4:1). ^{1}H NMR (300 MHz, CDCl$_3$): δ 2.41 (s, 3H), 6.92 (dd, J = 5.2, 4.0 Hz, 1H), 7.19 (d, J = 8.4 Hz, 2H), 7.38 (dd, J = 4.0, 1.6 Hz, 1H), 7.42 (dd, J = 5.2, 1.6 Hz, 1H), 7.64 (d, J = 8.4 Hz, 2H); ^{13}C NMR (100 MHz, CDCl$_3$): δ 21.8, 118.8 (q, J = 2.0 Hz), 120.1 (q, J = 265.3 Hz), 126.9, 128.3, 129.4, 130.1, 131.8, 132.1 (q, J = 31.0 Hz), 132.7, 136.3, 145.8; ^{19}F NMR (282 MHz, CDCl$_3$): δ –61.3.   IR (KBr): ν 3099, 1606, 1597, 1415, 1383, 1356, 1288, 1246, 1213, 1192, 1182, 1136, 1095, 1066, 1045, 920, 895, 839, 812, 727, 715, 682, 661, 613, 578, 549, 518 cm^{-1}.   MS (FAB): m/z 429 (35, [M$^+$+H]+2), 428 (6, M$^+$+2), 427 (35, [M$^+$+H]), 426 (6, M$^+$), 273 (57), 271 (57), 155 (100).   Anal. Calcd for C$_{14}$H$_{10}$BrF$_3$O$_3$S$_2$: C, 39.36; H, 2.36.   Found: C, 39.36; H, 2.51.
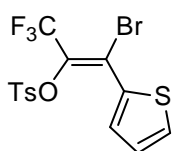
Preparation of 1,1-dibromopropanone.   Prepared according to the procedure reported in the literature.[21]   Purified by distillation (70 °C/53 Torr).   Yield: 87%, a colorless liquid. R_f 0.44 (hexane/AcOEt 8:1). ^{1}H NMR (400 MHz, CDCl$_3$): δ 2.57 (s, 3H), 5.75 (s, 1H); ^{13}C NMR (100 MHz, CDCl$_3$): δ 22.3, 42.9, 194.1.   IR (neat): ν 3016, 2927, 1732, 1703, 1421, 1359, 1245, 1213, 1147, 721, 677, 553 cm^{-1}.   MS (EI): m/z (%) 218 (27, M$^+$+4), 216 (58, M$^+$+2), 214 (27, M$^+$), 175 (48), 173 (100), 171 (48).   Anal. Calcd for C$_3$H$_4$Br$_2$O: C, 16.69; H, 1.87.   Found: C, 16.94; H, 1.93.

Preparation of 1,1-dibromo-2-tosyloxypropene (7a).   To a solution of 1,1-dibromopropanone (0.65 g, 3.0 mmol) in THF (10 mL) was added LHMDS (1.6 M in THF solution, 2.0 mL) dropwise at –78 °C over a period of 10 min.   The solution was stirred at –78 °C for 20 min before treatment with Ts$_2$O (1.1 g, 3.3 mmol). The resulting mixture was stirred at –78 °C for 30 min, then at –50 ~ –40 °C for 1h, and warmed to 0 °C over a period of 30 min before quenching with sat. aq. NH$_4$Cl.   The aqueous layer was extracted with Et$_2$O (10 mL × 3 times).   The combined organic layer was washed with sat. aq. NaCl, dried over anhydrous MgSO$_4$, and concentrated *in vacuo*.   Purification of the residue product by silica gel column chromatography (hexane/AcOEt 8:1) followed by recrystallization from hexane gave **7a** (0.34 g, 31% yield) as colorless prisms.   Mp:
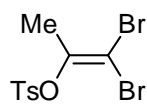
53.2–53.9 °C. R_f 0.34 (hexane/AcOEt 8:1). ^{1}H NMR (400 MHz, CDCl$_3$): δ 2.23 (s, 3H), 2.48 (s, 3H), 7.38 (d, J = 8.0 Hz, 2H), 7.87 (d, J = 8.0 Hz, 2H); ^{13}C NMR (100 MHz, CDCl$_3$): δ 20.2, 21.9, 87.0, 128.2, 129.7, 133.0, 145.6, 146.3.   IR (KBr): ν 3091, 3070, 1595, 1433, 1371, 1197, 1184, 1168, 1087, 925, 837, 813, 731, 702, 655, 611, 553, 540, 513, 480 cm^{-1}.   MS (EI): m/z (%) 372 (3, M$^+$+4), 370 (6, M$^+$+2), 368 (3, M$^+$). Anal. Calcd for C$_{10}$H$_{10}$Br$_2$O$_3$S: C, 32.46; H, 2.72.   Found: C, 32.54; H, 2.80.

Ethyl 3,3-dibromo-2-tosyloxyacrylate (7b).   Purified by silica gel column chromatography (hexane/AcOEt 8:1).   Yield: 66%, a colorless solid. Mp: 44.6–45.2 °C. R_f 0.22 (hexane/AcOEt 8:1). ^{1}H NMR (400 MHz, CDCl$_3$): δ 1.31 (t, J = 7.2 Hz, 3H), 2.48 (s, 3H), 4.25 (q, J = 6.8 Hz, 2H), 7.37 (d, J = 8.4 Hz, 2H), 7.85 (d, J = 8.4 Hz, 2H); ^{13}C NMR (100 MHz, CDCl$_3$): δ 13.9, 21.9, 62.7, 100.1, 128.4, 129.7, 132.7, 138.7, 145.9, 159.7.   IR (KBr): ν 2985, 2962, 1735, 1595, 1444, 1384, 1272, 1195, 1174, 1130, 1109, 1085, 1016, 931, 881, 815, 729, 680, 655, 590, 549, 515 cm^{-1}.   MS (EI): m/z (%) 431 (29, [M$^+$+H]+4), 429 (82, [M$^+$+H]+2), 427 (29, [M$^+$+H]), 385 (10), 383 (16), 381 (11).   Anal. Calcd for C$_{12}$H$_{12}$Br$_2$O$_5$S: C, 33.67; H, 2.83.   Found: C, 33.67; H, 2.80.
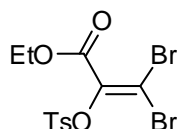
Preparation of 1,1-dibromo-4-phenyl-2-(trifluoromethyl)butene (7c).   A two-necked round-bottomed flask (500 mL) equipped with a magnetic stirring bar and a dropping funnel was charged with CBr$_4$ (9.9 g, 30 mmol), PPh$_3$ (16 g, 60 mmol), and hexane (200 mL) under an argon atmosphere at 0 °C.   To the mixture was added 1,1,1-trifluoro-4-phenylbutan-2-one (2.0 g, 10.0 mmol) dropwise at 0 °C.   The resulting mixture was warmed to room temperature and stirred for 22 h.   The reaction mixture was rinsed with hexane, and the combined organic layer was washed with sat. aq. NaCl (100 mL × 3 times), dried over anhydrous MgSO$_4$, and concentrated under reduced pressure.   The residue was purified by column chromatography on silica gel and then GPC to give **7c** (1.2 g, 32% yield) as a colorless oil. R_f 0.68 (hexane/AcOEt 8:1). ^{1}H NMR (400 MHz, CDCl$_3$): δ 2.70–2.75 (m, 2H), 2.78–2.83 (m, 2H), 7.20–7.25 (m, 3H), 7.29–7.33 (m, 2H); ^{13}C NMR (100 MHz, CDCl$_3$): δ 33.4, 36.8, 98.9 (q, J = 3.6 Hz), 122.5 (q, J = 274.4 Hz), 126.4, 128.2, 128.4, 135.4 (q, J = 29.8 Hz), 139.6; ^{19}F NMR (282 MHz, CDCl$_3$): δ –60.5.   IR (neat): ν 3064, 3028, 2949, 2869, 1600, 1585, 1496, 1456, 1301, 1271, 1163, 1136, 1087, 1070, 819, 808, 796, 748, 698, 640 cm^{-1}.   MS (EI): m/z (%) 360 (1, M$^+$+4), 358 (2, M$^+$+2), 356 (1, M$^+$), 279 (20), 277 (20), 91 (100).   Anal. Calcd for C$_{11}$H$_9$Br$_2$F$_3$: C, 36.91; H, 2.53. Found: C, 37.21; H, 2.65.
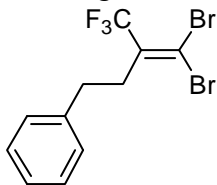
(Z)-1-Bromo-1-phenyl-2-tosyloxypropene [(Z)-8a].   Purified by preparative TLC (hexane/AcOEt 8:1) followed by HPLC and recrystallization from hexane.   Yield: 48%, colorless prisms.   Mp: 55.2–56.0 °C. R_f 0.15 (hexane/AcOEt 8:1). ^{1}H NMR (400 MHz, CDCl$_3$): δ 2.08 (s, 3H), 2.47 (s, 3H), 7.27–7.38 (m, 7H), 7.92 (d, J = 8.8 Hz, 2H); ^{13}C NMR (100 MHz, CDCl$_3$): δ 19.1, 21.8, 113.1, 128.2, 128.3, 128.8, 129.2, 129.5, 133.5, 136.9, 144.1, 145.2.   IR (KBr): ν 3085, 3064, 1658, 1444, 1350, 1197, 1174, 1151, 1089, 927, 866, 819, 761, 742, 692, 650, 597, 542, 522 cm^{-1}.   MS (FAB): m/z (%) 369 (10, [M$^+$+H]+2), 367 (10, [M$^+$+H]), 213 (10), 211 (10), 197 (7), 195 (7).
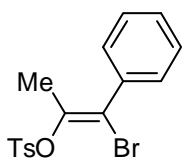
Anal. Calcd for $C_{16}H_{15}BrO_3S$: C, 52.33; H, 4.12.　　Found: C, 52.20; H, 4.04.

(*E*)-1-Bromo-1-phenyl-2-tosyloxypropene [(*E*)-8a].　　Purified by preparative TLC (hexane/AcOEt 8:1) followed by HPLC.　　Yield: 22%, a colorless oil. R_f 0.15 (hexane/AcOEt 8:1).　　^{1}H NMR (400 MHz, CDCl$_3$): δ 2.37 (s, 3H), 2.44 (s, 3H), 7.02 (d, *J* = 8.4 Hz, 2H), 7.10–7.17 (m, 5H), 7.29 (d, *J* = 8.4 Hz, 2H); ^{13}C NMR (100 MHz, CDCl$_3$): δ 21.4, 21.7, 117.7, 127.5, 127.7, 128.1, 129.23, 129.26, 129.5, 135.9, 142.6, 144.5.　　IR (neat): ν 2920, 2850, 1371, 1195, 1180, 1157, 1091, 929, 906, 761, 692, 667 cm^{-1}.　　MS (FAB): *m/z* (%) 369 (24, [M$^+$+H]+2), 367 (24, [M$^+$+H]), 197 (39), 195 (39).　　Anal. Calcd for $C_{16}H_{15}BrO_3S$: C, 52.33; H, 4.12.　　Found: C, 52.24; H, 4.03.
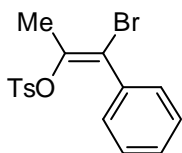
(*Z*)-Ethyl 3-bromo-3-phenyl-2-tosyloxyacrylate [(*Z*)-8b].　　Purified by preparative TLC (hexane/AcOEt 8:1) followed by HPLC and recrystallization from hexane.　　Yield: 55%, colorless prisms.　　Mp: 73.0–73.9 °C. R_f 0.16 (hexane/AcOEt 8:1).　　^{1}H NMR (400 MHz, CDCl$_3$): δ 0.95 (t, *J* = 7.2 Hz, 3H), 2.48 (s, 3H), 3.98 (q, *J* = 7.2 Hz, 2H), 7.27–7.29 (m, 2H), 7.33–7.39 (m, 5H), 7.93 (d, *J* = 8.4 Hz, 2H); ^{13}C NMR (100 MHz, CDCl$_3$): δ 13.5, 21.9, 62.0, 128.0, 128.3, 128.5, 129.5, 129.6, 129.9, 133.2, 136.5, 136.8, 145.5, 160.4.　　IR (KBr): ν 2981, 1730, 1633, 1390, 1284, 1195, 1182, 1130, 1083, 927, 813, 738, 696, 663, 599, 547, 534 cm^{-1}.　　MS (FAB): *m/z* (%) 427 (97, [M$^+$+H]+2), 425 (83, [M$^+$+H]), 381 (75), 379 (62).　　Anal. Calcd for $C_{18}H_{17}BrO_5S$: C, 50.83; H, 4.03.　　Found: C, 50.63; H, 3.96.
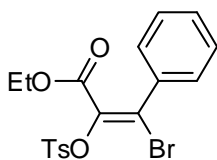
(*E*)-Ethyl 3-bromo-3-phenyl-2-tosyloxyacrylate [(*E*)-8b].　　Purified by preparative TLC (hexane/AcOEt 8:1) followed by HPLC.　　Yield: 2%, a colorless oil.　　R_f 0.16 (hexane/AcOEt 8:1).　　^{1}H NMR (400 MHz, CDCl$_3$): δ 1.40 (t, *J* = 7.2 Hz, 3H), 2.39 (s, 3H), 4.36 (q, *J* = 7.2 Hz, 2H), 7.05 (d, *J* = 8.0 Hz, 2H), 7.13–7.15 (m, 5H), 7.41 (d, *J* = 8.0 Hz, 2H); ^{13}C NMR (100 MHz, CDCl$_3$): δ 14.1, 21.7, 62.4, 127.6, 127.9, 128.8, 129.2, 129.3, 131.8, 133.6, 134.6, 135.5, 144.9, 161.3.　　IR (neat): ν 2981, 2925, 1732, 1596, 1444, 1382, 1259, 1193, 1178, 1105, 1083, 939, 752, 692, 667 cm^{-1}.　　MS (FAB): *m/z* (%) 427 (70, [M$^+$+H]+2), 425 (66, [M$^+$+H]), 381 (14), 379 (14).　　Anal. Calcd for $C_{18}H_{17}BrO_5S$: C, 50.83; H, 4.03.　　Found: C, 50.81; H, 4.07.
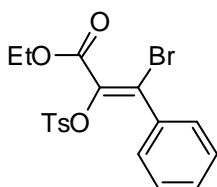
Ethyl 3,3-diphenyl-2-tosyloxyacrylate (9b).　　Purified by preparative TLC (hexane/AcOEt 8:1) followed by HPLC.　　Yield: 16%, a colorless solid.　　Mp: 103.4–104.4 °C.　　R_f 0.16 (hexane/AcOEt 8:1).　　^{1}H NMR (400 MHz, CDCl$_3$): δ 1.02 (t, *J* = 7.2 Hz, 3H), 2.38 (s, 3H), 4.04 (q, *J* = 7.2 Hz, 2H), 7.04 (d, *J* = 8.4 Hz, 2H), 7.09–7.19 (m, 7H), 7.31–7.33 (m, 3H), 7.55 (d, *J* = 8.4 Hz, 2H); ^{13}C NMR (100 MHz, CDCl$_3$): δ 13.6, 21.7, 61.5, 100.8, 127.6, 127.7, 127.9, 128.3, 128.4, 129.1, 129.6, 133.1, 133.5, 136.9, 137.9, 144.5, 144.6, 162.5.　　IR (KBr): ν 3032, 2976, 1730, 1595, 1371, 1253, 1191, 1174, 1076, 941, 779, 756, 696, 680, 551 cm^{-1}.　　MS (FAB): *m/z* (%) 423 (40, [M$^+$+H]), 422 (8, M$^+$), 378 (27), 377 (100).　　Anal. Calcd for $C_{24}H_{22}O_5S$: C, 68.23; H, 5.25.　　Found: C, 68.28; H, 5.19.
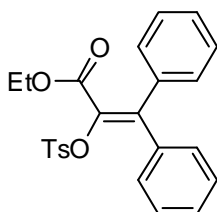
(Z)-1-Bromo-1,4-diphenyl-2-(trifluoromethyl)but-1-ene   [(Z)-8c].   Purified by preparative TLC (hexane) followed by HPLC and recrystallization from hexane.   Yield: 12%, colorless prisms. Mp: 62.8–63.4 °C. R_f 0.37 (hexane). ^{1}H NMR (400 MHz, CDCl$_3$): δ 2.42 (t, J = 6.8 Hz, 2H), 2.70 (t, J = 6.8 Hz, 2H), 6.90–6.92 (m, 2H), 7.03–7.05 (m, 2H), 7.16–7.22 (m, 3H), 7.31–7.34 (m, 3H); ^{13}C NMR (100 MHz, CDCl$_3$): δ 33.5, 35.0, 123.2 (q, J = 273.7 Hz), 126.1, 127.0 (q, J = 3.9 Hz), 127.3, 128.3, 128.4, 128.8, 131.5 (q, J = 28.2 Hz), 139.5, 139.8; ^{19}F NMR (282 MHz, CDCl$_3$): δ –61.0.   IR (KBr): ν 3022, 2937, 2866, 1629, 1602, 1488, 1454, 1444, 1313, 1303, 1271, 1232, 1164, 1136, 1088, 1064, 1021, 871, 761, 752, 700, 586, 488 cm^{-1}.   MS (EI): m/z (%) 356 (10, M$^+$+2), 354 (10, M$^+$), 275 (71), 265 (36), 263 (36).   Anal. Calcd for C$_{17}$H$_{14}$BrF$_3$: C, 57.48; H, 3.98.   Found: C, 57.63; H, 4.08.
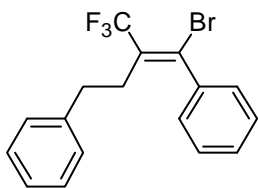
(E)-1-Bromo-1,4-diphenyl-2-(trifluoromethyl)but-1-ene   [(E)-8c].   Purified by preparative TLC (hexane) followed by HPLC.   Yield: 3%, a colorless oil. R_f 0.37 (hexane). ^{1}H NMR (400 MHz, CDCl$_3$): δ 2.84–2.89 (m, 2H), 2.92–2.97 (m, 2H), 7.27–7.51 (m, 10H); ^{13}C NMR (100 MHz, CDCl$_3$): δ 33.8, 35.8, 122.7 (q, J = 274.5 Hz), 126.2, 127.70, 127.72, 127.9, 128.3 (d, J = 2.3 Hz), 128.9, 130.5 (q, J = 28.2 Hz), 133.5 (q, J = 4.6 Hz), 139.4, 140.4; ^{19}F NMR (282 MHz, CDCl$_3$): δ –57.8.   IR (neat): ν 3062, 3028, 1641, 1496, 1456, 1444, 1319, 1271, 1224, 1161, 1122, 1089, 1029, 881, 808, 754, 696, 661, 634, 559 cm^{-1}.   MS (EI): m/z (%) 356 (4, M$^+$+2), 354 (4, M$^+$), 275 (31), 265 (13), 263 (13).   Anal. Calcd for C$_{17}$H$_{14}$BrF$_3$: C, 57.48; H, 3.98.   Found: C, 57.64; H, 4.09.
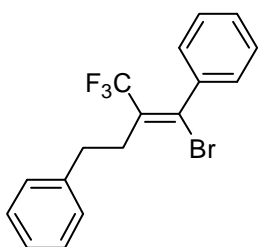
1,1,4-Triphenyl-2-(trifluoromethyl)but-1-ene (9c).   Purified by preparative TLC (hexane/AcOEt 8:1) followed by GPC.   Yield: 47%, a colorless solid.   Mp: 71.9–72.4 °C. R_f 0.31 (hexane). ^{1}H NMR (400 MHz, CDCl$_3$): δ 2.57–2.61 (m, 2H), 2.79–2.83 (m, 2H), 6.97–7.02 (m, 4H), 7.17–7.32 (m, 11H); ^{13}C NMR (100 MHz, CDCl$_3$): δ 31.9, 35.3, 124.5 (q, J = 274.5 Hz), 125.8, 127.32, 127.39, 127.6, 127.72, 127.76, 128.1, 128.2, 128.3, 140.5, 140.6, 140.8, 149.4 (q, J = 3.8 Hz); ^{19}F NMR (282 MHz, CDCl$_3$): δ –56.4.   IR (KBr): ν 3057, 3028, 2939, 1635, 1595, 1488, 1444, 1326, 1263, 1191, 1168, 1134, 1110, 1060, 1006, 763, 744, 727, 696, 619, 567 cm^{-1}.   MS (EI): m/z (%) 352 (9, M$^+$), 261 (100), 241 (96), 221 (54).   Anal. Calcd for C$_{23}$H$_{19}$F$_3$: C, 78.39; H, 5.43. Found: C, 78.17; H, 5.48.
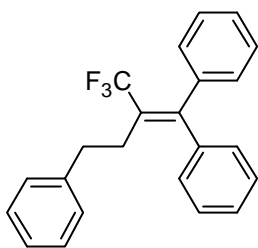
Preparation of oxidative adduct of 2 [*trans*-(*E*)-11].   A vial tube (5 mL) equipped with a magnetic stirring bar was charged with Pd(PPh$_3$)$_4$ (0.23 g, 0.20 mmol) and **2** (0.20 mmol) under an argon atmosphere.   Toluene (2 mL) was added to the mixture at room temperature.   The resulting solution was heated on a hot plate at 80 °C for 12 h.   Upon completion of the reaction, the reaction mixture was allowed to cool down to room temperature, diluted wit hexane (3 mL), and filtered.   Recrystallization of the concentrated filtrate from CH$_2$Cl$_2$/EtOH gave *trans*-(*E*)-**11** as colorless prisms
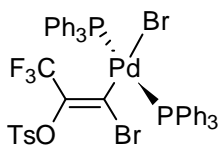
(0.14 g, 68%).   Mp: 225.1–225.9 °C (dec.) ^{1}H NMR (400 MHz, CDCl$_3$): δ 2.40 (s, 3H), 7.19 (d, J = 8.4 Hz, 2H), 7.35–7.42 (m, 18H), 7.53 (d, J = 8.4 Hz, 2H), 7.64–7.69 (m, 12H); ^{13}C NMR (100 MHz, CDCl$_3$): δ 21.7, 119.6 (q, J = 272.2 Hz), 127.6, 128.0 (t, J = 5.3 Hz), 128.8, 130.2, 130.3 (t, J = 24.4 Hz), 131.2 (q, J = 29.7 Hz), 134.3, 134.8 (t, J = 6.1 Hz), 144.2, 146.5 (q, J = 6.8 Hz); ^{19}F NMR (282 MHz, CDCl$_3$): δ –61.5 (t, J = 5.6 Hz); ^{31}P NMR (121 MHz, CDCl$_3$): δ 22.6 (q, J = 5.6 Hz).   IR (KBr): ν 3055, 1596, 1573, 1481, 1434, 1363, 1280, 1195, 1170, 1128, 1095, 1041, 889, 744, 692, 655, 563, 520, 495 cm^{-1}.   MS (FAB): m/z (%) 976 (15, [M$^+$–Br+H]+2), 975 (20, [M$^+$–Br]+2), 974 (15, [M$^+$–Br+H]), 973 (20, [M$^+$–Br]), 449 (100).   Anal. Calcd for C$_{46}$H$_{37}$Br$_2$F$_3$P$_2$PdS: C, 52.37; H, 3.53.   Found: C, 52.21; H, 3.64.

General procedure for cross-coupling reaction of (Z)-5 with arylboronic acids.

In a vial tube (5 mL) equipped with a magnetic stirring bar were placed Pd(PPh$_3$)$_4$ (11 mg, 10 μmol), (Z)-**5** (0.20 mmol), and arylboronic acid (0.24 mmol).   The vial tube was then capped with a rubber septum, evacuated for 5 min and charged with argon. The evacuation–purge operation was repeated twice.   Toluene (2 mL) and 5 M aq. Cs$_2$CO$_3$ (80 μL, 0.40 mmol) were added to the mixture at room temperature under an argon atmosphere.   The solution was stirred at room temperature for 5 min and heated on a hot plate at 100 °C for 24 h.   Upon completion of the reaction, the reaction mixture was allowed to cool down to room temperature, diluted with AcOEt (3 mL), and filtered through a Florisil pad.   To the filtrate was added water (5 mL), and the aqueous layer was extracted with AcOEt (3 mL × 3 times).   The combined organic layer was washed with sat. aq. NaCl (10 mL), dried over anhydrous MgSO$_4$, and evaporated under reduced pressure.   The residue was purified by preparative TLC.

3,3,3-Trifluoro-1,1-diphenyl-2-tosyloxypropene (6aa).   Purified by preparative TLC (hexane/AcOEt 8:1).   Yield: 97%, a colorless solid.   Mp: 124.0–125.2 °C.   R$_f$ 0.39 (hexane/AcOEt 4:1). ^{1}H NMR (400 MHz, CDCl$_3$): δ 2.37 (s, 3H), 7.00 (d, J = 8.4 Hz, 2H), 7.08 (d, J = 8.6 Hz, 2H), 7.13–7.26 (m, 5H), 7.32–7.38 (m, 3H), 7.44 (d, J = 8.4 Hz, 2H); ^{13}C NMR (100 MHz, CDCl$_3$): δ 21.7, 120.2 (q, J = 273.7 Hz), 127.8, 127.9, 128.0, 128.6, 128.9, 129.1, 129.1, 129.3, 129.6, 132.1, 136.3 (q, J = 76.3 Hz), 144.0 (q, J = 2.5 Hz), 144.9; ^{19}F NMR (282 MHz, CDCl$_3$): δ –59.7.   IR (KBr): ν 3055, 3037, 1633, 1595, 1446, 1367, 1305, 1278, 1195, 1176, 1126, 1056, 777, 769, 738, 729, 717, 702, 655, 617, 559 cm^{-1}.   MS (FAB): m/z (%) 419 (41, [M$^+$+H]), 418 (4, M$^+$), 399 (8), 264 (23), 263 (100).   Anal. Calcd for C$_{22}$H$_{17}$F$_3$O$_3$S: C, 63.15; H, 4.10.   Found: C, 63.21; H, 4.07.
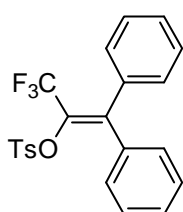
(Z)-3,3,3-Trifluoro-1-(4-methoxyphenyl)-1-phenyl-2-tosyloxypropene   (6ab). Purified by preparative TLC (hexane/AcOEt 8:1).   Yield: 88%, a colorless solid.   Mp: 116.6–117.8 °C.   R$_f$ 0.36 (hexane/AcOEt 4:1). ^{1}H NMR (300 MHz, CDCl$_3$): δ 2.37 (s, 3H), 3.78 (s, 3H), 6.64 (d, J = 6.6 Hz, 2H), 6.94 (d, J = 6.9 Hz, 2H), 7.09 (d, J = 7.5 Hz, 2H), 7.15–7.18 (m, 2H), 7.32–7.36 (m, 3H), 7.49 (d, J = 8.7 Hz, 2H); ^{13}C NMR (100 MHz, CDCl$_3$): δ 21.7, 55.2, 113.1, 120.4 (q, J = 273.0 Hz), 127.9, 128.9, 129.1, 129.22, 129.24, 130.1 (q, J = 35.8

114
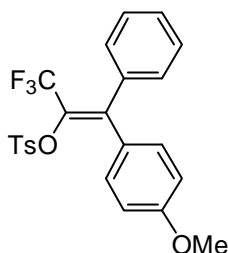
Hz), 131.3, 132.4, 136.1, 143.5 (q, J = 1.9 Hz), 144.8, 159.8; ^{19}F NMR (282 MHz, CDCl$_3$): δ −59.4.   IR (KBr): ν 3066, 3008, 2960, 1600, 1510, 1382, 1325, 1305, 1255, 1176, 1163, 1126, 1066, 943, 831, 752, 729, 702, 677, 549 cm^{-1}.   MS (FAB): m/z (%) 449 (61, [M$^+$+H]), 448 (8, M$^+$), 294 (55), 293 (100).   Anal. Calcd for C$_{23}$H$_{19}$F$_3$O$_4$S: C, 61.60; H, 4.27.   Found: C, 61.68; H, 4.32.

(Z)-3,3,3-Trifluoro-1-phenyl-2-tosyloxy-1-(4-trifluoromethylphenyl)propene   (6ad).
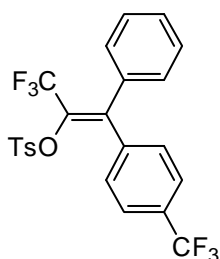
Purified by preparative TLC (hexane/AcOEt 8:1).   Yield: 83%, a colorless solid.   Mp: 110.2–116.5 °C.   R$_f$ 0.35 (hexane/AcOEt 8:1).   ^{1}H NMR (400 MHz, CDCl$_3$): δ 2.37 (s, 3H), 7.07 (d, J = 8.4 Hz, 2H), 7.13 (d, J = 8.0 Hz, 2H), 7.19 (dd, J = 7.6, 1.6 Hz, 2H), 7.35–7.42 (m, 7H); ^{13}C NMR (100 MHz, CDCl$_3$): δ 21.6, 119.9 (q, J = 273.7 Hz), 123.5 (q, J = 269.9 Hz), 124.7 (q, J = 3.8 Hz), 127.7, 128.3, 129.0 (d, J = 1.4 Hz), 129.3, 129.4, 129.9, 130.3 (q, J = 32.8 Hz), 132.2 (q, J = 37.0 Hz), 132.2, 135.0, 140.2, 142.3 (q, J = 1.4 Hz), 145.4; ^{19}F NMR (282 MHz, CDCl$_3$): δ −60.2, −63.3.   IR (KBr): ν 3049, 3031, 1595, 1409, 1377, 1325, 1193, 1176, 1147, 1112, 1058, 1016, 939, 842, 813, 729, 715, 702, 650, 561 cm^{-1}.   MS (FAB): m/z (%) 487 (35, [M$^+$+H]), 486 (3, M$^+$), 467 (29), 331 (100).   Anal. Calcd for C$_{23}$H$_{16}$F$_6$O$_3$S: C, 56.79; H, 3.32.   Found: C, 56.84; H, 3.30.

(Z)-3,3,3-Trifluoro-1-phenyl-1-(3-thienyl)-2-tosyloxypropene   (6ai).
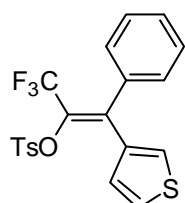
Purified by preparative TLC (hexane/AcOEt 8:1).   Yield: 60%, a colorless solid. Mp: 112.6–113.3 °C.   R$_f$ 0.17 (hexane/AcOEt 8:1).   ^{1}H NMR (400 MHz, CDCl$_3$): δ 2.38 (s, 3H), 6.93 (dd, J = 3.2 Hz, 1.2 Hz, 1H), 6.97 (dd, J = 5.2, 1.2 Hz, 1H), 7.12 (dd, J = 5.2, 3.2 Hz, 1H), 7.15–7.19 (m, 4H), 7.33–7.39 (m, 3H), 7.63 (d, J = 8.4 Hz, 2H); ^{13}C NMR (100 MHz, CDCl$_3$): δ 21.7, 120.3 (q, J = 273.7 Hz), 124.7, 127.9, 128.2, 128.5, 128.9, 129.0, 129.1, 129.3, 130.4 (q, J = 35.8 Hz), 131.8, 135.5, 137.1, 138.2 (q, J = 2.9 Hz), 145.3; ^{19}F NMR (282 MHz, CDCl$_3$): δ −58.9.   IR (KBr): ν 3114, 1633, 1596, 1369, 1307, 1265, 1193, 1178, 1157, 1128, 1056, 956, 916, 804, 763, 723, 702, 648, 561 cm^{-1}.   MS (FAB): m/z (%) 425 (44, [M$^+$+H]), 424 (2, M$^+$), 270 (23), 269 (100).   Anal. Calcd for C$_{20}$H$_{15}$F$_3$O$_3$S$_2$: C, 56.59; H, 3.56.   Found: C, 56.52; H, 3.58.

(E)-3,3,3-Trifluoro-1-(4-methoxyphenyl)-1-phenyl-2-tosyloxypropene   (6ba).
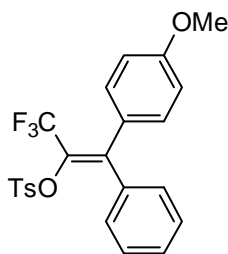
Purified by preparative TLC (hexane/AcOEt 8:1).   Yield: 82%, a colorless solid.   Mp: 90.2–92.4 °C.   R$_f$ 0.12 (hexane/AcOEt 8:1).   ^{1}H NMR (400 MHz, CDCl$_3$): δ 2.37 (s, 3H), 3.82 (s, 3H), 6.86 (d, J = 8.4 Hz, 2H), 6.99 (d, J = 7.2 Hz, 2H), 7.08–7.17 (m, 6H), 7.20–7.25 (m, 1H), 7.42 (d, J = 8.4 Hz, 2H); ^{13}C NMR (100 MHz, CDCl$_3$): δ 21.7, 55.2, 120.4 (q, J = 273.0 Hz), 127.7, 127.9, 128.2, 128.6, 129.2, 129.8, 130.1 (q, J = 36.0 Hz), 130.7, 132.1, 137.0, 144.0 (q, J = 1.8 Hz), 144.9, 160.1; ^{19}F NMR (282 MHz, CDCl$_3$): δ −59.6.   IR (KBr): ν 3055, 3035, 2976, 1606, 1510, 1363, 1294, 1274, 1247, 1195, 1168, 1122, 1055, 1029, 941, 829, 815, 771, 744, 717, 624, 543 cm^{-1}.   MS (FAB): m/z (%) 449 (72, [M$^+$+H]), 448 (8, M$^+$), 429 (8), 294 (52), 293 (100).   Anal. Calcd for C$_{23}$H$_{19}$F$_3$O$_4$S: C, 61.60; H, 4.27.   Found: C, 61.38; H, 4.40.

(*E*)-3,3,3-Trifluoro-1-(4-methoxyphenyl)-2-tosyloxy-1-(4-trifluoromethylphenyl)-propene (6bd).
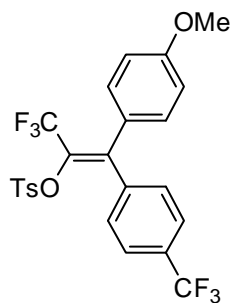
Purified by preparative TLC (hexane/AcOEt 8:1). Yield: 70%, a colorless solid. Mp: 87.4–89.2 °C. R_f 0.09 (hexane/AcOEt 8:1). ^{1}H NMR (400 MHz, CDCl$_3$): δ 2.38 (s, 3H), 3.79 (s, 3H), 6.64 (d, *J* = 6.8 Hz, 2H), 6.93 (d, *J* = 6.8 Hz, 2H), 7.09 (d, *J* = 8.4 Hz, 2H), 7.17 (d, *J* = 7.6 Hz, 2H), 7.35 (d, *J* = 7.6 Hz, 2H), 7.49 (d, *J* = 8.4 Hz, 2H); ^{13}C NMR (100 MHz, CDCl$_3$): δ 21.6, 55.3, 113.7, 120.1 (q, *J* = 272.9 Hz), 123.6 (q, *J* = 270.2 Hz), 124.6 (q, *J* = 3.8 Hz), 127.2, 127.7, 129.4, 130.1, 130.3 (q, *J* = 32.3 Hz), 130.7, 131.4 (q, *J* = 38.5 Hz), 132.3, 140.6, 142.3 (q, *J* = 2.7 Hz), 145.3, 160.3; ^{19}F NMR (282 MHz, CDCl$_3$): δ −60.1, −63.3. IR (KBr): ν 3024, 2977, 2939, 1606, 1595, 1512, 1407, 1373, 1326, 1298, 1253, 1197, 1168, 1130, 1110, 1058, 1029, 844, 829, 813, 744, 715, 655, 561 cm^{-1}. MS (FAB): *m/z* (%) 517 (60, [M$^+$+H]), 516 (8, M$^+$), 497 (14), 362 (69), 361 (100). Anal. Calcd for C$_{24}$H$_{18}$F$_6$O$_4$S: C, 55.81; H, 3.51. Found: C, 56.05; H, 3.69.

(*E*)-3,3,3-Trifluoro-1-phenyl-2-tosyloxy-1-(4-trifluoromethylphenyl)propene (6da).
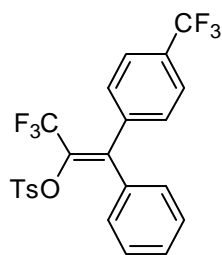
Purified by preparative TLC (hexane/AcOEt 8:1). Yield: 97%, a colorless solid. Mp: 110.0–111.0 °C. R_f 0.23 (hexane/AcOEt 8:1). ^{1}H NMR (400 MHz, CDCl$_3$): δ 2.38 (s, 3H), 7.00 (d, *J* = 7.2 Hz, 2H), 7.10 (d, *J* = 8.4 Hz, 2H), 7.18 (t, *J* = 7.2 Hz, 2H), 7.23–7.25 (m, 1H), 7.32 (d, *J* = 8.0 Hz, 2H), 7.44 (d, *J* = 8.4 Hz, 2H), 7.61 (d, *J* = 8.4 Hz, 2H); ^{13}C NMR (100 MHz, CDCl$_3$): δ 21.7, 120.0 (q, *J* = 273.8 Hz), 123.6 (q, *J* = 270.0 Hz), 125.1 (q, *J* = 3.8 Hz), 127.9, 128.1, 129.0, 129.3, 129.5 (d, *J* = 2.2 Hz), 129.5, 131.0 (q, *J* = 32.0 Hz), 131.7 (q, *J* = 36.6 Hz), 132.1, 136.0, 139.6, 142.5 (q, *J* = 3.0 Hz), 145.2; ^{19}F NMR (282 MHz, CDCl$_3$): δ −59.9, −63.3. IR (KBr): ν 3043, 1645, 1618, 1595, 1409, 1371, 1325, 1180, 1136, 1118, 1062, 945, 833, 773, 731, 719, 673, 563 cm^{-1}. MS (FAB): *m/z* (%) 487 (42, [M$^+$+H]), 467 (15), 332 (28), 331 (100). Anal. Calcd for C$_{23}$H$_{16}$F$_6$O$_3$S: C, 56.79; H, 3.32. Found: C, 57.07; H, 3.62.

(*E*)-3,3,3-Trifluoro-1-(3-fluorophenyl)-1-(4-methoxyphenyl)-2-tosyloxypropene
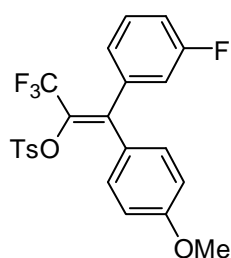
(6hb). Purified by preparative TLC (hexane/AcOEt 8:1). Yield: 90%, a colorless solid. Mp: 136.0–136.6 °C. R_f 0.10 (hexane/AcOEt 8:1). ^{1}H NMR (400 MHz, CDCl$_3$): δ 2.38 (s, 3H), 3.79 (s, 3H), 6.65 (d, *J* = 8.8 Hz, 2H), 6.87 (dt, *J* = 9.2, 2.4 Hz, 1H), 6.94 (d, *J* = 8.8 Hz, 2H), 6.99 (d, *J* = 8.0 Hz, 1H), 7.05–7.08 (m, 1H), 7.10 (d, *J* = 8.4 Hz, 2H), 7.30–7.35 (m, 1H), 7.48 (d, *J* = 8.4 Hz, 2H); ^{13}C NMR (100 MHz, CDCl$_3$): δ 21.7, 55.2, 113.3, 116.0 (d, *J* = 21.4 Hz), 116.3 (d, *J* = 22.1 Hz), 120.2 (q, *J* = 272.9 Hz), 125.1, 128.3, 128.6 (d, *J* = 122.8 Hz), 129.6 (d, *J* = 8.4 Hz), 130.6 (d, *J* = 35.9 Hz), 131.3, 132.4, 138.1 (d, *J* = 7.6 Hz), 142.2 (q, *J* = 1.9 Hz), 144.9, 160.0, 160.8, 163.2; ^{19}F NMR (282 MHz, CDCl$_3$): δ −59.7 (s, 3F), −113.1 (m, 1F). IR (KBr): ν 3070, 2964, 1600, 1585, 1510, 1487, 1380, 1280, 1255, 1193, 1178, 1132, 1068, 829, 732, 673, 555, 522 cm^{-1}. MS (FAB): *m/z* (%) 467 (35, [M$^+$+H]), 466 (5, M$^+$), 423 (17), 422 (54), 312 (20), 311 (100). Anal. Calcd for C$_{23}$H$_{18}$F$_4$O$_4$S: C, 59.22; H, 3.89. Found: C, 59.18; H, 3.97.

116

(*E*)-3,3,3-Trifluoro-1-(2-naphthyl)-1-(3-thienyl)-2-tosyloxypropene (6ig). Purified by preparative TLC (hexane/AcOEt 8:1). Yield: 88%, a colorless solid. Mp: 124.0–125.3 °C. R_f 0.13 (hexane/AcOEt 8:1). ^{1}H NMR (400 MHz, CDCl$_3$): δ 2.08 (s, 3H), 6.63 (d, *J* = 8.0 Hz, 2H), 6.81 (d, *J* = 4.8 Hz, 1H), 7.17 (d, *J* = 8.4 Hz, 1H), 7.24 (d, *J* = 9.6 Hz, 2H), 7.28–7.29 (m, 2H), 7.40–7.61 (m, 5H), 7.76 (d, *J* = 8.4 Hz, 1H); ^{13}C NMR (100 MHz, CDCl$_3$): δ 21.5, 120.4 (q, *J* = 272.9 Hz), 125.7, 126.1, 126.5, 126.9, 127.30, 127.34, 127.5, 128.1, 128.41, 128.42, 128.8, 129.6, 130.8 (q, *J* = 42.8 Hz), 132.1, 132.4, 132.9, 133.4, 135.3, 138.5 (q, *J* = 2.1 Hz), 144.8; ^{19}F NMR (282 MHz, CDCl$_3$): δ –59.8. IR (KBr): ν 3120, 3055, 1620, 1595, 1415, 1384, 1299, 1265, 1191, 1178, 1149, 1122, 1064, 850, 812, 775, 740, 721, 705, 663, 551 cm^{-1}. MS (FAB): *m/z* (%) 475 (31, [M$^+$+H]), 474 (8, M$^+$), 423 (31), 422 (85), 320 (28), 319 (100). Anal. Calcd for C$_{24}$H$_{17}$F$_3$O$_3$S$_2$: C, 60.75; H, 3.61. Found: C, 60.52; H, 3.64.
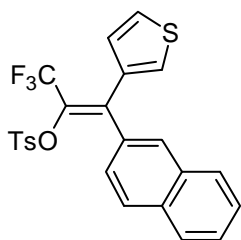
General procedure for cross-coupling reaction of 6 with arylboronic acids.

In a vial (5 mL) equipped with a magnetic stirring bar were placed Pd(OAc)$_2$ (0.50 mg, 2.0 μmol), Xphos (2.5 mg, 5.0 μmol), **6** (0.10 mmol), and arylboronic acid (0.20 mmol). The vial was then capped with a rubber septum, evacuated for 5 min and purged with argon. The evacuation–purge operation was repeated twice. THF (0.5 mL) and 2 M aq. K$_3$PO$_4$ (0.15 mL, 0.30 mmol) were added to the mixture under an argon atmosphere. The mixture was stirred at room temperature for 5 min and heated on a hot plate at 80 °C for 2 h. Upon completion of the reaction, the resulting mixture was allowed to cool down to room temperature, diluted with Et$_2$O (5 mL), and filtered through a Florisil pad. The filtrate was treated with water (10 mL). The aqueous layer was separated and extracted with Et$_2$O (5 mL × 3 times). The combined organic layer was washed with sat. aq. NaCl (15 mL), dried over MgSO$_4$ and evaporated under reduced pressure. The residue was purified by preparative TLC (hexane/AcOEt 8:1) followed by recrystallization from hexane.

(*E*)-3,3,3-Trifluoro-1-(4-methoxyphenyl)-1,2-diphenylpropene (13aba).[3f] Yield: 95%.

(*E*)-3,3,3-Trifluoro-1-(4-methoxyphenyl)-1-phenyl-2-(4-trifluoromethylphenyl)-propene (13abd). Yield: 96%, colorless prisms. Mp: 104.7–105.3 °C. R_f 0.42 (hexane/AcOEt 8:1). ^{1}H NMR (400 MHz, CDCl$_3$): δ 3.69 (s, 3H), 6.57 (d, *J* = 9.2 Hz, 2H), 6.78 (d, *J* = 9.2 Hz, 2H), 7.28 (dd, *J* = 8.0, 5.6 Hz, 2H), 7.35–7.39 (m, 5H), 7.50 (d, *J* = 8.0 Hz, 2H); ^{13}C NMR (100 MHz, CDCl$_3$): δ 55.1, 109.6, 113.1, 123.2 (q, *J* = 272.4 Hz), 123.8 (q, *J* = 269.9 Hz), 124.8 (q, *J* = 3.8 Hz), 127.8, 127.9, 128.4, 129.6 (q, *J* = 32.0 Hz), 131.2, 131.8, 132.4, 139.1, 140.1, 151.0 (q, *J* = 3.0 Hz), 158.8; ^{19}F NMR (282 MHz, CDCl$_3$): δ –55.7, –63.1. IR (KBr): ν 3058, 3006, 2993, 1602, 1510, 1467, 1444, 1326, 1307, 1261, 1224, 1184, 1166, 1136, 1109, 1068, 1033, 1022, 983, 827, 790, 700, 677, 567 cm^{-1}. MS (FAB): *m/z* (%) 423 (65, [M$^+$+H]), 422 (100, M$^+$), 403 (18). Anal. Calcd for C$_{23}$H$_{16}$F$_6$O: C, 65.40; H, 3.82. Found: C, 65.38; H, 3.86.

117
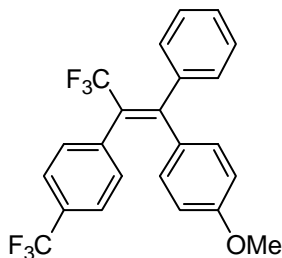
(*E*)-3,3,3-Trifluoro-2-(4-methoxyphenyl)-1-phenyl-1-(4-trifluoromethylphenyl)-propene (13adb). Yield: 96%, colorless prisms. Mp: 71.7–72.4 °C. R_f 0.44 (hexane/AcOEt 8:1). ^{1}H NMR (400 MHz, CDCl$_3$): δ 3.77 (s, 3H), 6.75 (d, J = 8.8 Hz, 2H), 7.04 (d, J = 8.8 Hz, 2H), 7.14 (d, J = 8.8 Hz, 2H), 7.28 (dd, J = 8.0, 1.6 Hz, 2H), 7.32 (d, J = 8.0 Hz, 2H), 7.34–7.40 (m, 3H); ^{13}C NMR (100 MHz, CDCl$_3$): δ 55.1, 113.5, 123.2 (q, J = 271.7 Hz), 123.7 (q, J = 269.9 Hz), 124.6 (q, J = 3.9 Hz), 126.2, 128.00, 128.04, 128.3 (d, J = 2.2 Hz), 128.9 (q, J = 32.8 Hz), 129.8, 130.1 (q, J = 27.7 Hz), 132.3, 139.6, 144.6, 148.3 (q, J = 3.7 Hz), 159.1; ^{19}F NMR (282 MHz, CDCl$_3$): δ −56.8, −63.2. IR (KBr): ν 2962, 2935, 1614, 1514, 1323, 1294, 1255, 1226, 1168, 1143, 1109, 1064, 1018, 813, 736, 700, 648, 534 cm^{-1}. MS (FAB): *m/z* (%) 423 (39, [M$^+$+H]), 422 (100, M$^+$), 403 (10), 353 (4), 345 (4). Anal. Calcd for C$_{23}$H$_{16}$F$_6$O: C, 65.40; H, 3.82. Found: C, 65.18; H, 3.99.
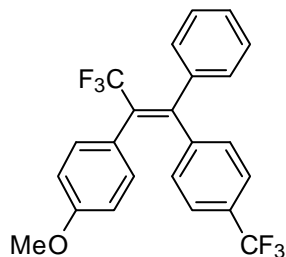
(*Z*)-3,3,3-Trifluoro-1-(4-methoxyphenyl)-1-phenyl-2-(4-trifluoromethylphenyl)propene (13bad). Yield: 95%, colorless prisms. Mp: 125.5–126.7 °C. R_f 0.33 (hexane/AcOEt 8:1). ^{1}H NMR (400 MHz, CDCl$_3$): δ 3.84 (s, 3H), 6.87–6.91 (m, 4H), 7.05–7.07 (m, 3H), 7.22 (d, J = 8.8 Hz, 2H), 7.35 (d, J = 8.0 Hz, 2H), 7.45 (d, J = 8.0 Hz, 2H); ^{13}C NMR (100 MHz, CDCl$_3$): δ 55.2, 113.3, 123.2 (q, J = 276.0 Hz), 123.7 (q, J = 269.9 Hz), 124.7 (q, J = 3.8 Hz), 127.6, 127.7, 129.5, 129.6 (q, J = 32.8 Hz), 129.8, 129.9, 131.8, 132.1, 138.9, 140.6, 151.4 (q, J = 2.6 Hz), 159.3; ^{19}F NMR (282 MHz, CDCl$_3$): δ −56.2, −63.4. IR (KBr): ν 3003, 2979, 1604, 1573, 1508, 1469, 1325, 1290, 1249, 1178, 1143, 1118, 1066, 1033, 1020, 821, 761, 696, 624, 570 cm^{-1}. MS (FAB): *m/z* (%) 423 (32, [M$^+$+H]), 422 (100, M$^+$), 403 (5). Anal. Calcd for C$_{23}$H$_{16}$F$_6$O: C, 65.40; H, 3.82. Found: C, 65.21; H, 4.07.
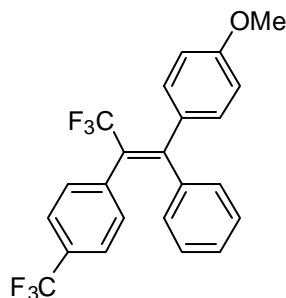
(*Z*)-3,3,3-Trifluoro-2-(4-methoxyphenyl)-1-(2-naphthyl)-1-(3-thienyl)propene (13igb). Yield: 95%, colorless prisms. Mp: 137.0–137.9 °C. R_f 0.25 (hexane/AcOEt 8:1). ^{1}H NMR (400 MHz, CDCl$_3$): δ 3.70 (s, 3H), 6.68 (d, J = 8.8 Hz, 2H), 6.96 (dd, J = 4.8, 0.8 Hz, 1H), 7.03 (dd, J = 8.4, 1.6 Hz, 1H), 7.17 (d, J = 9.2 Hz, 2H), 7.28 (dd, J = 4.8 Hz, 2.8 Hz, 1H), 7.36–7.40 (m, 4H), 7.51 (d, J = 8.4 Hz, 1H), 7.60 (d, J = 8.0 Hz, 1H), 7.67 (d, J = 8.0 Hz, 1H); ^{13}C NMR (100 MHz, CDCl$_3$): δ 55.1, 113.3, 123.6 (q, J = 273.7 Hz), 124.80, 124.83, 125.8, 126.2, 127.00, 127.04, 127.2, 127.3, 128.0, 128.6 (d, J = 1.5 Hz), 129.26 (q, J = 28.9 Hz), 129.28, 132.1, 132.5, 132.6, 138.3, 140.0, 144.6 (q, J = 3.1 Hz), 158.8; ^{19}F NMR (282 MHz, CDCl$_3$): δ −56.6. IR (KBr): ν 3112, 3007, 1606, 1510, 1465, 1319, 1288, 1249, 1157, 1103, 1028, 1002, 840, 827, 815, 759, 690, 540 cm^{-1}. MS (FAB): *m/z* (%) 411 (21, [M$^+$+H]), 410 (53, M$^+$). Anal. Calcd for C$_{24}$H$_{17}$F$_3$OS: C, 70.23; H, 4.17. Found: C, 70.42; H, 4.14.
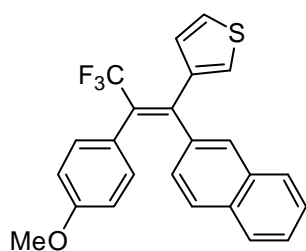
118

(E)-3,3,3-Trifluoro-1-phenyl-1,2-bis(3-thienyl)propene (13aii). Yield: 91%, colorless plates. Mp: 52.3–53.0 °C. R_f 0.50 (hexane/AcOEt 8:1). ^{1}H NMR (400 MHz, CDCl$_3$): δ 6.37 (dd, J = 5.2, 1.2 Hz, 1H), 6.67 (dd, J = 3.2, 1.2 Hz, 1H), 6.96–6.99 (m, 2H), 7.24–7.28 (m, 3H), 7.32–7.37 (m, 4H); ^{13}C NMR (100 MHz, CDCl$_3$): δ 119.6, 120.5 (q, J = 272.2 Hz), 124.2, 125.2, 126.0 (q, J = 28.2 Hz), 126.4, 127.7, 127.8, 127.9, 128.3, 128.4, 129.8, 134.8 (q, J = 1.6 Hz), 140.1, 141.5; ^{19}F NMR (282 MHz, CDCl$_3$): δ –56.5. IR (KBr): ν 3105, 3093, 1618, 1558, 1442, 1301, 1257, 1222, 1184, 1157, 1112, 1072, 1004, 839, 794, 771, 732, 704, 686, 650, 594 cm^{-1}. MS (FAB): m/z (%) 337 (21, [M$^+$+H]), 336 (69, M$^+$). Anal. Calcd for C$_{17}$H$_{11}$F$_3$S$_2$: C, 60.70; H, 3.30. Found: C, 60.93; H, 3.34.
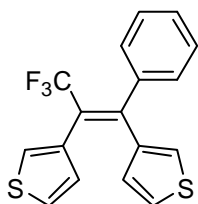
(Z)-3,3,3-Trifluoro-1-(3-fluorophenyl)-1-(4-methoxyphenyl)-2-(2-naphthyl)propene (13hbg). Yield: 90%, colorless prisms. Mp: 120.6–121.7 °C. R_f 0.30 (hexane/AcOEt 8:1). ^{1}H NMR (400 MHz, CDCl$_3$): δ 3.62 (s, 3H), 6.51 (d, J = 8.8 Hz, 2H), 6.85 (d, J = 8.8 Hz, 2H), 7.03–7.08 (m, 2H), 7.14 (d, J = 7.6 Hz, 1H), 7.31–7.39 (m, 2H), 7.43–7.49 (m, 2H), 7.71 (d, J = 8.4 Hz, 1H), 7.74–7.79 (m, 3H); ^{13}C NMR (100 MHz, CDCl$_3$): δ 55.0, 109.6, 113.1, 114.7 (d, J = 20.6 Hz), 115.7 (d, J = 23.6 Hz), 123.5 (q, J = 273.8 Hz), 124.3, 126.1 (d, J = 33.5 Hz), 127.4 (d, J = 7.6 Hz), 128.0, 128.5 (q, J = 28.2 Hz), 128.9, 129.3 (d, J = 8.4 Hz), 130.5, 131.2, 132.2, 132.3, 132.4, 132.7, 142.7 (d, J = 7.6 Hz), 148.4-148.6 (m), 158.6, 160.9, 163.3; ^{19}F NMR (282 MHz, CDCl$_3$): δ –55.8 (s, 3F), –113.8 (q, J = 9.6 Hz, 1F). IR (KBr): ν 3058, 3006, 2956, 2837, 1606, 1583, 1510, 1461, 1433, 1319, 1303, 1249, 1166, 1155, 1105, 1029, 831, 817, 794, 765, 750, 522 cm^{-1}. MS (FAB): m/z (%) 423 (50, [M$^+$+H]), 422 (100, M$^+$), 403 (4), 353 (5). Anal. Calcd for C$_{26}$H$_{18}$F$_4$O: C, 73.93; H, 4.30. Found: C, 74.05; H, 4.30.
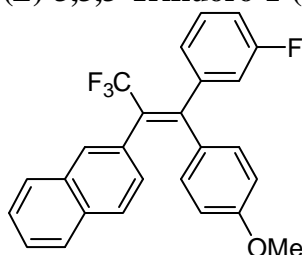
4,4'-Bis(3,3,3-trifluoro-1,1-diphenylpropen-2-yl)biphenyl (13aah). Yield: 45%, colorless prisms. Mp: 248.2–251.0 °C. R_f 0.35 (hexane/AcOEt 8:1). ^{1}H NMR (400 MHz, CDCl$_3$): δ 6.93–6.95 (m, 4H), 7.04–7.05 (m, 6H), 7.27–7.41 (m, 18H); ^{13}C NMR (100 MHz, CDCl$_3$): δ 123.4 (q, J = 273.0 Hz), 126.2, 127.3, 127.6, 127.7, 127.8, 128.3 (d, J = 2.3 Hz), 128.7 (q, J = 28.7 Hz), 129.5, 131.6, 134.0, 139.3, 140.2, 140.7, 150.2 (q, J = 2.9 Hz); ^{19}F NMR (282 MHz, CDCl$_3$): δ –56.1. IR (KBr): ν 3055, 1610, 1597, 1496, 1444, 1330, 1276, 1222, 1166, 1141, 1120, 1107, 1074, 1033, 983, 813, 765, 758, 734, 696, 636, 588 cm^{-1}. MS (FAB): m/z (%) 646 (100, M$^+$), 627 (4), 569 (6). Anal. Calcd for C$_{42}$H$_{28}$F$_6$: C, 78.01; H, 4.36. Found: C, 77.89; H, 4.61.
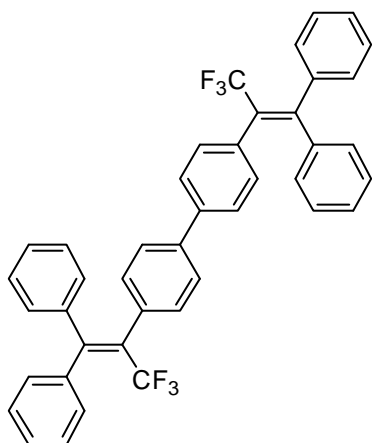
One-pot synthesis of 13aba. In a vial (5 mL) equipped with a magnetic stirring bar were placed PdCl$_2$(PPh$_3$)$_2$ (7.0 mg, 10 μmol), P(*m*-tolyl)$_3$ (3.0 mg, 10 μmol), **2** (85 mg, 0.20 mmol), and phenylboronic acid (28 mg, 0.22 mmol). The tube was then capped with a rubber septum, evacuated for 5 min and purged with argon. The evacuation–purge operation was repeated twice. Toluene (2 mL) and 5 M aq. Cs$_2$CO$_3$ (80 μL, 0.40 mmol) was added to the mixture at room temperature under an argon atmosphere. The mixture was stirred at room temperature for 5 min and heated on a hot plate at 80 °C for 24 h. Upon completion of the reaction, the mixture was allowed to cool down to room temperature. To the mixture *p*-methoxyphenylboronic acid (36 mg, 0.24 mmol) and 5 M aq. Cs$_2$CO$_3$ (80 μL, 0.40 mmol) were added under an argon atmosphere. The resulting mixture was heated again on a hot plate at 100 °C. After 24 h, the reaction mixture was allowed to cool down to room temperature. To the vial were added Pd(OAc)$_2$ (2.5 mg, 10 μmol), Xphos (10 mg, 20 μmol), phenylboronic acid (27 mg, 0.40 mmol), THF (1 mL), and 2 M aq. K$_3$PO$_4$ (0.30 mL, 0.60 mmol) under an argon atmosphere. The solution was stirred for 5 min at room temperature and heated on a hot plate at 80 °C for 12 h. Upon completion of the reaction, the reaction mixture was diluted with AcOEt (5 mL) and filtered through a Florisil pad. The filtrate was treated with water (10 mL), and the aqueous layer was separated and extracted with AcOEt (5 mL × 3 times). The combined organic layer was washed with sat. aq. NaCl (15 mL), dried over MgSO$_4$, and evaporated under reduced pressure. The residue was purified by preparative TLC and recrystallization from hexane, giving rise to **13aba** (49 mg, 69% yield).

General procedure for cross-coupling reaction of (*Z*)-5 with terminal alkynes.

A vial (5 mL) equipped with a magnetic stirring bar was charged with Pd(PPh$_3$)$_4$ (5.7 mg, 5.0 μmol) and (*Z*)-**5** (0.10 mmol). The vial was then capped with a rubber septum, evacuated for 5 min and purged with argon. The evacuation–purge operation was repeated twice, and then NEt$_3$ (2 mL) and terminal alkyne (0.20 mmol) were added to the mixture under an argon atmosphere. The mixture was stirred at room temperature for 5 min and then heated on a hot plate at 100 °C for 3 h. Upon completion of the reaction, the resulting mixture was allowed to cool to room temperature, diluted with AcOEt (5 mL), and filtered through a Florisil pad. To the filtrate was added water (10 mL), and the aqueous layer was extracted with AcOEt (5 mL × 3 times). The combined organic layer was washed with sat. aq. NaCl (15 mL), dried over MgSO$_4$, and evaporated under reduced pressure. The residue was purified by preparative TLC followed by HPLC or recrystallization.

(*Z*)-1,1,1-Trifluoro-3,5-diphenyl-2-tosyloxypent-2-en-4-yne (15aa). Purified by silica gel chromatography (hexane/AcOEt 20:1) followed by recrystallization from hexane. Yield: 80%, colorless prisms. Mp: 97.0–97.7 °C. R$_f$ 0.35 (hexane/AcOEt 4:1). ^{1}H NMR (400 MHz, CDCl$_3$): δ 2.34 (s, 3H), 7.25 (d, *J* = 8.4 Hz, 2H), 7.30–7.36 (m, 3H), 7.40–7.43 (m, 5H), 7.45–7.49 (m, 2H), 7.96 (d, *J* = 8.4 Hz, 2H); ^{13}C NMR (100 MHz, CDCl$_3$): δ 21.6, 84.8, 102.3, 119.8 (q, *J* = 273.0 Hz), 121.5, 127.3 (q, *J* =3.0 Hz), 128.0, 128.1, 128.22, 128.28 (d, *J* =1.6 Hz), 129.2, 129.4, 129.6, 131.8, 132.7, 133.3, 137.2 (q, *J* = 36.6 Hz), 145.5; ^{19}F NMR (282 MHz, CDCl$_3$): δ –60.5. IR (KBr): ν 3066, 2204, 1612,
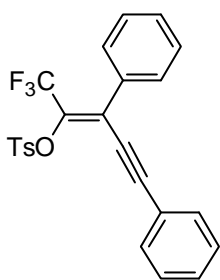
1595, 1575, 1489, 1444, 1383, 1332, 1298, 1199, 1192, 1178, 1141, 1109, 1085, 1008, 993, 906, 808, 781, 756, 723, 704, 667, 644, 607, 590, 559, 540, 511 cm^{-1}.　MS (FAB): m/z (%) 443 (6, [M$^+$+H]), 423 (1), 287 (100), 155 (42).　Anal. Calcd for C$_{24}$H$_{17}$F$_3$O$_3$S: C, 65.15; H, 3.87.　Found: C, 65.13; H, 4.15.

(Z)-1,1,1-Trifluoro-5-(4-methoxyphenyl)-3-phenyl-2-tosyloxypent-2-en-yne (15ab). Purified by silica gel chromatography (hexane/AcOEt 30:1). Yield: 99%, a pale yellow oil. R$_f$ 0.19 (hexane/AcOEt 4:1). ^{1}H NMR (400 MHz, CDCl$_3$): δ 2.37 (s, 3H), 3.83 (s, 3H), 6.83 (d, J = 8.8 Hz, 2H), 7.26 (d, J = 8.4 Hz, 2H), 7.34 (d, J = 8.8 Hz, 2H), 7.39–7.45 (m, 5H), 7.93 (d, J = 8.4 Hz, 2H); ^{13}C NMR (100 MHz, CDCl$_3$): δ 21.8, 55.3, 84.1, 103.0, 113.8, 119.9 (q, J = 276.4 Hz), 127.7 (q, J = 3.0 Hz), 128.20, 128.27, 128.35, 128.36, 129.1, 129.6, 133.0, 133.4, 133.7, 136.5 (q, J = 36.6 Hz), 145.4, 160.4; ^{19}F NMR (282 MHz, CDCl$_3$): δ −60.4.　IR (neat): ν 2937, 2198, 1599, 1508, 1386, 1300, 1251, 1195, 1184, 1136, 1087, 1033, 908, 833, 769, 698, 665, 561 cm^{-1}.　MS (FAB): m/z (%) 473 (5, [M$^+$+H]), 472 (3, M$^+$), 453 (3), 318 (48), 317 (100), 155 (5).　Anal. Calcd for C$_{25}$H$_{19}$F$_3$O$_4$S: C, 63.55; H, 4.05.　Found: C, 63.55; H, 4.21.
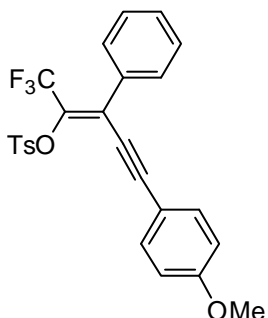
(Z)-1,1,1-Trifluoro-3-phenyl-2-tosyloxy-5-(4-trifluoromethylphenyl)pent-2-en-4-yne (15ac). Purified by silica gel chromatography (hexane/AcOEt 30:1) followed by recrystallization from hexane. Yield: 87%, colorless prisms. Mp: 82.3–83.1 °C. R$_f$ 0.45 (hexane/AcOEt 4:1). ^{1}H NMR (400 MHz, CDCl$_3$): δ 2.38 (s, 3H), 7.28 (d, J = 8.4 Hz, 2H), 7.41–7.46 (m, 5H), 7.55 (d, J = 8.4 Hz, 2H), 7.58 (d, J = 8.4 Hz, 2H), 7.92 (d, J = 8.4 Hz, 2H); ^{13}C NMR (100 MHz, CDCl$_3$): δ 21.7, 86.7, 100.1, 119.6 (q, J = 273.0 Hz), 123.5 (q, J = 269.9 Hz), 125.0 (q, J = 3.8 Hz), 125.4, 126.9 (q, J = 2.8 Hz), 128.1, 128.33, 128.36, 129.4, 129.6, 130.9 (q, J = 32.0 Hz), 132.21, 132.28, 133.4, 138.1 (q, J = 37.3 Hz), 145.6; ^{19}F NMR (282 MHz, CDCl$_3$): δ −61.0, −63.5.　IR (KBr): ν 3066, 2208, 1614, 1595, 1377, 1323, 1296, 1195, 1178, 1147, 1124, 1105, 1064, 1006, 906, 846, 812, 769, 721, 705, 698, 669, 646, 536 cm^{-1}.　MS (FAB): m/z (%) 511 (5, [M$^+$+H]), 491 (5), 356 (26), 355 (100), 155 (33).　Anal. Calcd for C$_{25}$H$_{16}$F$_6$O$_3$S: C, 58.82; H, 3.16.　Found: C, 58.82; H, 3.40.
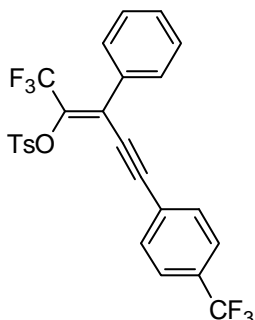
(Z)-1,1,1-Trifluoro-3-phenyl-2-tosyloxy-5-(trimethylsilyl)pent-2-en-4-yne (15ad). Purified by silica gel chromatography (hexane/AcOEt 20:1) followed by HPLC (hexane). Yield: 88%, a pale yellow oil. R$_f$ 0.52 (hexane/AcOEt 4:1). ^{1}H NMR (300 MHz, CDCl$_3$): δ 0.20 (s, 9H), 2.46 (s, 3H), 7.35–7.37 (m, 7H), 7.92 (d, J = 8.1 Hz, 2H); ^{13}C NMR (100 MHz, CDCl$_3$): δ −0.3, 21.9, 98.9, 109.9, 119.7 (q, J = 273.0 Hz), 127.4 (q, J = 3.0 Hz), 128.1, 128.33, 128.37, 128.39, 129.2, 129.6, 132.7, 133.3, 137.9 (q, J = 36.6 Hz), 154.4; ^{19}F NMR (282 MHz, CDCl$_3$): δ −60.7.　IR (neat): ν 2962, 2142, 1599, 1492, 1446, 1390, 1323, 1251, 1195, 1180, 1141, 1132, 1091, 1039, 1020, 908, 848, 771, 754, 698, 669, 597, 559,
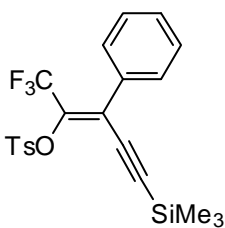
543, 530 cm^{-1}.   MS (FAB): m/z (%) 439 (81, [M$^+$+H]), 438 (8, M$^+$), 423 (9), 283 (100), 155 (98).   Anal. Calcd for C$_{21}$H$_{21}$F$_3$O$_3$SSi: C, 57.52; H, 4.83.   Found: C, 57.54; H, 4.55.

(Z)-5-(Dimethylphenylsilyl)-1,1,1-trifluoro-3-phenyl-2-tosyloxypent-2-en-4-yne
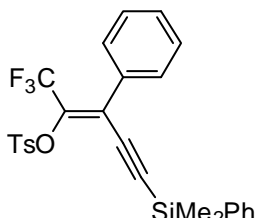
(15ae).   Purified by silica gel chromatography (hexane/AcOEt 20:1) followed by HPLC (hexane).   Yield: 75%, a pale yellow oil.   R$_f$ 0.54 (hexane/AcOEt 4:1). ^{1}H NMR (300 MHz, CDCl$_3$): δ 0.44 (s, 6H), 2.39 (s, 3H), 7.25 (d, J = 8.1 Hz, 2H), 7.37–7.40 (m, 8H), 7.58–7.62 (m, 2H), 7.88 (d, J = 8.1 Hz, 2H); ^{13}C NMR (100 MHz, CDCl$_3$): δ −1.1, 21.8, 100.4, 107.6, 119.7 (q, J = 273.8 Hz), 127.2 (q, J = 2.3 Hz), 127.8, 128.2, 128.3, 128.4, 129.3, 129.5, 129.6, 132.5, 133.0, 133.6, 135.6, 138.2 (q, J = 36.6 Hz), 145.5; ^{19}F NMR (282 MHz, CDCl$_3$): δ −60.6.   IR (neat): ν 3068, 2962, 2142, 1597, 1492, 1446, 1429, 1390, 1323, 1249, 1197, 1180, 1141, 1130, 1039, 1020, 908, 840, 817, 783, 771, 754, 738, 719, 698, 667, 613, 559, 543 cm^{-1}.   MS (FAB): m/z (%) 501 (35, [M$^+$+H]), 500 (5, M$^+$), 485 (11), 423 (42), 155 (61), 135 (100).   Anal. Calcd for C$_{26}$H$_{23}$F$_3$O$_3$SSi: C, 62.38; H, 4.63. Found: C, 62.52; H, 4.60.

(Z)-1,1,1-Trifluoro-5-phenyl-3-(*p*-tolyl)-2-tosyloxypent-2-en-4-yne (15ca).
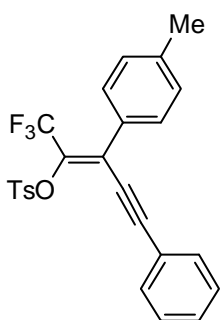
Purified by silica gel chromatography (hexane/AcOEt 30:1) followed by recrystallization from hexane.   Yield: 83%, colorless prisms.   Mp: 95.9–96.8 °C.   R$_f$ 0.55 (hexane/AcOEt 4:1). ^{1}H NMR (400 MHz, CDCl$_3$): δ 2.36 (s, 3H), 2.41 (s, 3H), 7.21–7.27 (m, 4H), 7.30–7.41 (m, 7H), 7.94 (d, J = 8.4 Hz, 2H); ^{13}C NMR (100 MHz, CDCl$_3$): δ 21.4, 21.7, 85.0, 102.0, 119.9 (q, J = 272.2 Hz), 121.7, 127.5 (q, J = 2.4 Hz), 128.1, 128.2, 128.3, 128.9, 129.3, 129.6, 129.9, 131.9, 133.4, 136.9 (q, J = 36.6 Hz), 139.4, 145.4; ^{19}F NMR (282 MHz, CDCl$_3$): δ −60.4.   IR (KBr): ν 3064, 2204, 1612, 1595, 1386, 1298, 1199, 1192, 1084, 904, 758, 707, 694, 613, 561, 540 cm^{-1}.   MS (FAB): m/z (%) 457 (8, [M$^+$+H]), 437 (2), 302 (31), 301 (100), 155 (16).   Anal. Calcd for C$_{25}$H$_{19}$F$_3$O$_3$S: C, 65.78; H, 4.20.   Found: C, 65.73; H, 4.32.

(Z)-1,1,1-Trifluoro-3-(4-formylphenyl)-5-phenyl-2-tosyloxypent-2-en-4-yne (15ka).
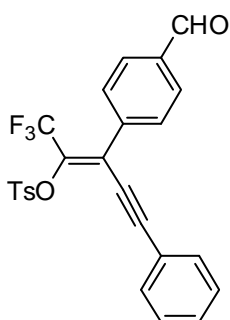
Purified by preparative TLC (hexane/AcOEt 4:1).   Yield: 72%, a yellow oil.   R$_f$ 0.20 (hexane/AcOEt 4:1). ^{1}H NMR (400 MHz, CDCl$_3$): δ 2.37 (s, 3H), 7.28–7.41 (m, 7H), 7.61 (d, J = 8.0 Hz, 2H), 7.93 (d, J = 8.4 Hz, 4H), 10.0 (s, 1H); ^{13}C NMR (100 MHz, CDCl$_3$): δ 21.8, 84.1, 103.3, 119.6 (q, J = 272.9 Hz), 121.3, 126.1 (q, J = 3.1 Hz), 128.2, 129.10, 129.13, 129.5, 129.71, 129.72, 131.9, 133.3, 136.5, 138.0 (q, J = 37.4 Hz), 138.7, 145.7, 191.1; ^{19}F NMR (282 MHz, CDCl$_3$): δ −60.8.   IR (KBr): ν 2848, 2204, 1705, 1606, 1597, 1491, 1442, 1384, 1336, 1301, 1195, 1180, 1139, 1116, 1087, 1008, 910, 831, 742, 673, 561 cm^{-1}.   MS (FAB): m/z (%) 471 (78, [M$^+$+H]), 370 (9), 316 (68), 315 (100), 289 (45), 155 (52).   Anal. Calcd for C$_{25}$H$_{17}$F$_3$O$_4$S: C, 63.82; H, 3.64. Found: C, 63.95; H, 3.75.

(*E*)-1,1,1-Trifluoro-5-phenyl-3-(2-thienyl)-2-tosyloxypent-2-en-4-yne (15na).
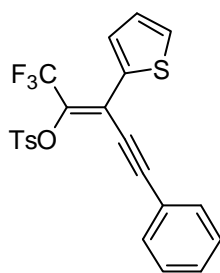
Purified by silica gel chromatography (hexane/AcOEt 30:1) followed by recrystallization from hexane. Yield: 62%, colorless plates. Mp: 76.5–77.4 °C. R_f 0.31 (hexane/AcOEt 4:1). ^{1}H NMR (400 MHz, CDCl$_3$): δ 2.33 (s, 3H), 7.05 (dd, *J* = 5.2, 3.6 Hz, 1H), 7.23 (d, *J* = 8.4 Hz, 2H), 7.31–7.42 (m, 6H), 7.49 (dd, *J* = 5.2, 1.2 Hz, 1H), 7.91 (d, *J* = 8.4 Hz, 2H); ^{13}C NMR (100 MHz, CDCl$_3$): δ 21.7, 84.5, 101.3, 120.0 (q, *J* = 272.7 Hz), 120.5 (q, *J* = 2.8 Hz), 121.4, 127.3, 128.1, 128.3, 129.2, 129.5, 129.6, 129.7, 131.9, 133.2, 133.7, 136.2 (q, *J* = 37.4 Hz), 145.6; ^{19}F NMR (282 MHz, CDCl$_3$): δ −60.8. IR (KBr): ν 3093, 2206, 1595, 1523, 1489, 1442, 1423, 1384, 1363, 1298, 1199, 1190, 1174, 1141, 1109, 1084, 1049, 987, 979, 883, 875, 846, 808, 756, 713, 702, 692, 650, 613, 559, 542, 534, 515 cm^{-1}. MS (FAB): *m/z*: 449 (6, [M$^+$+H]), 294 (33), 293 (100), 155 (8). Anal. Calcd for C$_{22}$H$_{15}$F$_3$O$_3$S$_2$: C, 58.92; H, 3.37. Found: C, 59.00; H, 3.49.

(*Z*)-1,1,1-Trifluoro-2-tosyloxy-3-(4-trifluoromethylphenyl)-5-(trimethylsilyl)pent-2-en-4-yne (15dd).
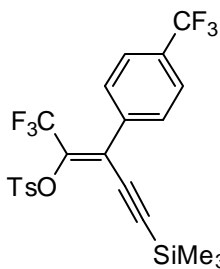
Purified by silica gel chromatography (hexane/AcOEt 30:1) followed by recrystallization from hexane. Yield: 81%, colorless prisms. Mp: 106.1–106.8 °C. R_f 0.35 (hexane/AcOEt 8:1). ^{1}H NMR (400 MHz, CDCl$_3$): δ 0.22 (s, 9H), 2.48 (s, 3H), 7.37 (d, *J* = 8.4 Hz, 2H), 7.50 (d, *J* = 8.4 Hz, 2H), 7.64 (d, *J* = 8.4 Hz, 2H), 7.91 (d, *J* = 8.4 Hz, 2H); ^{13}C NMR (100 MHz, CDCl$_3$): δ −0.4, 21.9, 98.1, 111.1, 119.5 (q, *J* =273.8 Hz), 123.6 (q, *J* = 269.9 Hz), 125.2 (q, *J* = 38.0 Hz), 125.9 (q, *J* = 1.9 Hz), 128.2, 128.8 (d, *J* = 2.3 Hz), 129.7, 131.2 (q, *J* = 32.0 Hz), 133.2, 136.3, 138.5 (q, *J* = 37.4 Hz), 145.6; ^{19}F NMR (282 MHz, CDCl$_3$): δ −60.9, −63.3. IR (KBr): ν 2970, 1624, 1597, 1379, 1323, 1193, 1180, 1165, 1147, 1132, 1066, 1030, 1014, 910, 848, 717, 678, 534 cm^{-1}. MS (FAB): *m/z* (%) 507 (14, [M$^+$+H]), 487 (26), 332 (19), 155 (100). Anal. Calcd for C$_{22}$H$_{20}$F$_6$O$_3$SSi: C, 52.17; H, 3.98. Found: C, 52.05; H, 4.06.

1,4-Bis[(*E*)-5,5,5-trifluoro-3-phenyl-4-tosyloxypent-3-en-1-ynyl]benzene (15af).
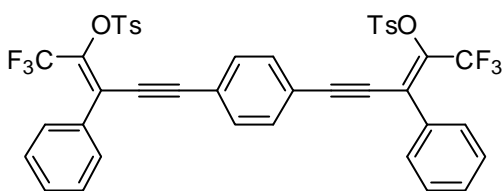
Purified by silica gel chromatography (hexane/AcOEt 8:1) followed by recrystallization from hexane. Yield: 54%, pale yellow needles. Mp: 182.4–183.3 °C. R_f 0.32 (hexane/AcOEt 4:1). ^{1}H NMR (300 MHz, CDCl$_3$): δ 2.37 (s, 6H), 7.27 (d, *J* = 8.4 Hz, 4H), 7.36 (s, 4H), 7.38–7.44 (m, 10H), 7.91 (d, *J* = 8.4 Hz, 4H); ^{13}C NMR (100 MHz, CDCl$_3$): δ 21.8, 87.0, 101.3, 119.7 (q, *J* = 272.9 Hz), 122.7, 127.1 (q, *J* = 3.0 Hz), 128.1, 128.3 (2C), 129.3, 129.6, 131.7, 132.4, 133.3, 137.7 (q, *J* = 36.6 Hz), 145.6; ^{19}F NMR (282 MHz, CDCl$_3$): δ −60.8. IR (KBr): ν 3039, 2200, 1614, 1597, 1384, 1332, 1301, 1192, 1139, 1116, 1087, 1006, 908, 842, 775, 742, 715, 698, 667, 559, 543 cm^{-1}. MS (FAB): *m/z* (%) 807 (3, [M$^+$+H]), 652 (28), 651 (70), 498 (28), 497 (100), 496 (78), 155 (33). Anal. Calcd for C$_{42}$H$_{28}$F$_6$O$_6$S$_2$: C, 62.53; H, 3.50. Found: C, 62.49; H, 3.71.

1,3-Bis[(*E*)-5,5,5-trifluoro-3-phenyl-4-tosyloxypent-3-en-1-ynyl]benzene (15ag).
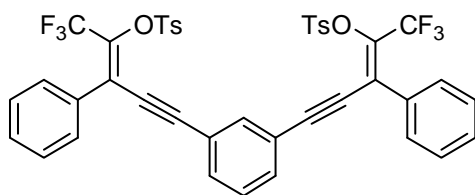
Purified by silica gel chromatography (hexane/AcOEt 8:1) followed by recrystallization from hexane. Yield: 44%, pale yellow needles. Mp: 60.0–61.0 °C. R_f 0.32 (hexane/AcOEt 4:1). ^{1}H NMR (300 MHz, CDCl$_3$): δ 2.32 (s, 6H), 7.24 (d, *J* = 8.4 Hz, 4H), 7.42 (s, 14H), 7.92 (d, *J* = 8.4 Hz, 4H); ^{13}C NMR (100 MHz, CDCl$_3$): δ 21.7, 85.5, 100.6, 119.7 (q, *J* = 272.2 Hz), 122.0, 126.9 (q, *J* = 3.3 Hz), 128.2, 128.3, 129.4, 129.7, 130.7, 132.5, 132.8, 133.4, 135.0, 135.4, 137.8 (q, *J* = 36.6 Hz), 145.7; ^{19}F NMR (282 MHz, CDCl$_3$): δ –60.7. IR (KBr): ν 3059, 2204, 1614, 1159, 1386, 1329, 1307, 1195, 1138, 1112, 1087, 1022, 925, 904, 813, 798, 742, 715, 698, 667, 563, 540 cm^{-1}. MS (FAB): *m/z* (%) 807 (3, [M$^+$+H]), 651 (45), 497 (100), 496 (46), 155 (72). Anal. Calcd for C$_{42}$H$_{28}$F$_6$O$_6$S$_2$: C, 62.53; H, 3.50. Found: C, 62.32; H, 3.48.

Transformation of 15aa into 3,5-diphenyl-2-(trifluoromethyl)furan (16).
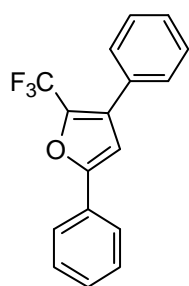
In a vial (5 mL) equipped with a magnetic stirring bar placed added CuI (1.0 mg, 5.0 μmol), Cs$_2$CO$_3$ (65 mg, 0.40 mmol), and **15aa** (44 mg, 0.10 mmol). The vial was then capped with a rubber septum, evacuated for 5 min and purged with argon. The evacuation–purge operation was repeated twice, and then THF (0.20 mL) was added to the mixture under an argon atmosphere. The mixture was stirred at room temperature for 5 min and heated on a hot plate at 80 °C for 18 h. Upon completion of the reaction, the resulting mixture was allowed to cool to room temperature, diluted with Et$_2$O (3 mL), and filtered through a Florisil pad. The filtrate was treated with water (5 mL). The aqueous layer was separated and extracted with Et$_2$O (5 mL × 3 times). The combined organic layer was washed with sat. aq. NaCl (15 mL), dried over MgSO$_4$, and evaporated under reduced pressure. The crude product was purified by preparative TLC (hexane/AcOEt 4:1), giving **16** (20 mg, 69%) as a colorless oil. R_f 0.78 (hexane/AcOEt 4:1). ^{1}H NMR (400 MHz, CDCl$_3$): δ 6.81 (s, 1H), 7.37–7.49 (m, 8H), 7.75 (d, *J* = 6.8 Hz, 2H); ^{13}C NMR (100 MHz, CDCl$_3$): δ 107.9, 119.8 (q, *J* = 266.1 Hz), 124.3, 128.2, 128.3, 128.4 (d, *J* = 1.5 Hz), 128.72, 128.75, 128.9, 130.1 (q, *J* = 3.0 Hz), 130.5, 135.1 (q, *J* = 41.2 Hz), 154.6 (d, *J* = 1.5 Hz); ^{19}F NMR (282 MHz, CDCl$_3$): δ –60.6. IR (neat): ν 3061, 1626, 1599, 1583, 1556, 1485, 1452, 1398, 1315, 1294, 1168, 1120, 1085, 1057, 966, 931, 817, 759, 696, 673, 538 cm^{-1}. MS (EI): *m/z* (%) 289 (100, [M$^+$+H]), 288 (100, M$^+$), 269 (62), 219 (36), 191 (100), 165 (70), 95 (63). Anal. Calcd for C$_{17}$H$_{11}$F$_3$O: C, 70.83; H, 3.85. Found: C, 70.81; H, 4.13.

124

Data of X-ray crystallographic analysis.

Table 10.   Crystal data and structure refinement for (*Z*)-**5a** (CCDC-657359).
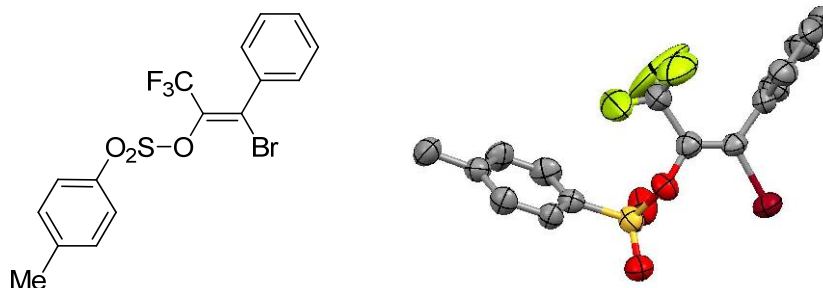
Empirical formula	$C_{16}H_{12}BrF_3O_3S$
Formula weight	421.23
Temperature	300(2) K
Wavelength	0.71073 Å
Crystal system	Monoclinic
Space group	P2(1)/c
Unit cell dimensions	$a = 9.9162(17)$ Å, $\alpha = 90°$
	$b = 8.3917(15)$ Å, $\beta = 102.742(3)°$
	$c = 20.928(4)$ Å, $\gamma = 90°$
Volume	1698.6(5) Å^3
Z	4
Density (calculated)	1.647 Mg/m^3
Absorption coefficient	2.585 mm^{-1}
F(000)	840
Crystal size	$0.50 \times 0.50 \times 0.50$ mm^3
Theta range for data collection	2.00 to 25.50°
Index ranges	$-11<=h<=12, -7<=k<=10, -25<=l<=24$
Reflections collected	8909
Independent reflections	3158 [R(int) = 0.0584]
Completeness to theta = 25.50°	99.9 %
Absorption correction	Empirical
Max. and min. transmission	0.3581 and 0.3581
Refinement method	Full-matrix least-squares on F^2
Data / restraints / parameters	3158 / 0 / 218
Goodness-of-fit on F^2	1.123
Final R indices [I>2sigma(I)]	$R_1 = 0.0504$, $wR_2 = 0.1553$
R indices (all data)	$R_1 = 0.0627$, $wR_2 = 0.1608$
Largest diff. peak and hole	0.728 and -0.583 e.Å^{-3}

Table 11. Crystal data and structure refinement for (*Z*)-**5c**.
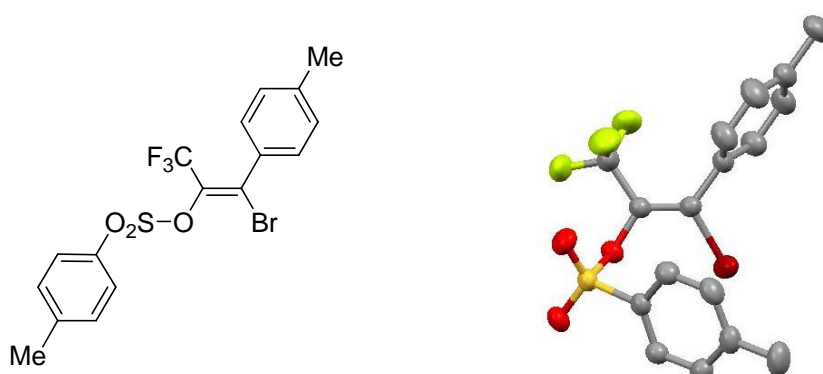
Empirical formula	$C_{17}H_{14}BrF_3O_3S$
Formula weight	435.25
Temperature	293(2) K
Wavelength	0.71073 Å
Unit cell dimensions	a = 6.2991(5) Å, α = 82.7260(10)°
	b = 8.1775(7) Å, β = 80.803(2)°
	c = 17.5809(14) Å, γ = 85.9680(10)°
Volume	885.61(13) Å^3
Z	2
Density (calculated)	1.632 Mg/m^3
Absorption coefficient	2.482 mm^{-1}
F(000)	436
Crystal size	0.50 × 0.50 × 0.30 mm^3
Theta range for data collection	2.36 to 27.05°
Index ranges	–8<=h<=5, –10<=k<=9, –20<=l<=22
Reflections collected	5426
Independent reflections	3744 [R(int) = 0.0155]
Completeness to theta = 25.50°	96.4 %
Max. and min. transmission	0.5231 and 0.3701
Refinement method	Full-matrix least-squares on F^2
Data / restraints / parameters	3744 / 0 / 228
Goodness-of-fit on F^2	1.066
Final R indices [I>2sigma(I)]	R_1 = 0.0337, wR_2 = 0.0930
R indices (all data)	R_1 = 0.0393, wR_2 = 0.0959
Largest diff. peak and hole	0.496 and –0.435 e.Å^{-3}

Table 12. Crystal data and structure refinement for (*Z*)-**5n**.
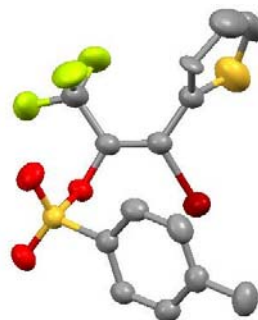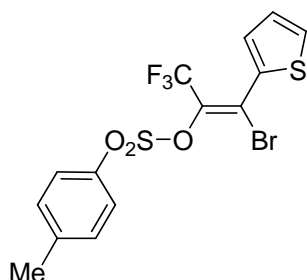
Empirical formula	$C_{14}H_{10}BrF_3O_3S_2$
Formula weight	427.25
Temperature	300(2) K
Wavelength	0.71073 Å
Crystal system	Triclinic
Space group	P-1
Unit cell dimensions	a = 6.1927(5) Å, α = 96.1500(10)°
	b = 8.2035(6) Å, β = 98.2450(10)°
	c = 16.2084(12) Å, γ = 93.2960(10)°
Volume	807.99(11) Å^3
Z	2
Density (calculated)	1.756Mg/m^3
Absorption coefficient	2.842 mm^{-1}
F(000)	424
Crystal size	0.50 × 0.50 × 0.50 mm^3
Theta range for data collection	2.50 to 25.50°
Index ranges	–6<=h<=7, –9<=k<=8, –19<=l<=17
Reflections collected	4430
Independent reflections	2956 [R(int) = 0.0192]
Completeness to theta = 25.50°	98.4 %
Absorption correction	None
Refinement method	Full-matrix least-squares on F^2
Data / restraints / parameters	2956 / 0 / 210
Goodness-of-fit on F^2	1.102
Final R indices [I>2sigma(I)]	R_1 = 0.0532, wR_2 = 0.1812
R indices (all data)	R_1 = 0.0572, wR_2 = 0.1851
Largest diff. peak and hole	1.390 and –1.036 e.Å^{-3}

Table 13. Crystal data and structure refinement for (*Z*)-**8a** (CCDC-657361).
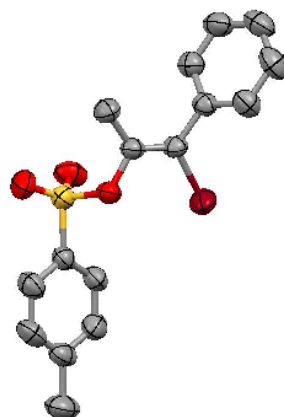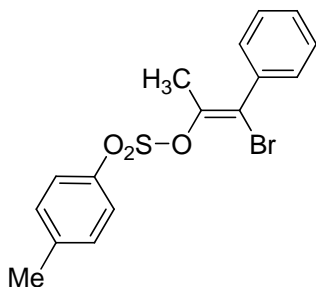
Empirical formula	$C_{16}H_{15}BrF_3O_3S$
Formula weight	367.25
Temperature	300(2) K
Wavelength	0.71073 Å
Crystal system	Monoclinic
Space group	P2(1)/c
Unit cell dimensions	a = 14.5715(18) Å, α = 90°
	b = 9.2194(11) Å, β = 93.513(2)°
	c = 12.0161(15) Å, γ = 90°
Volume	1611.2(3) Å^3
Z	4
Density (calculated)	1.514 Mg/m^3
Absorption coefficient	2.687 mm^{-1}
F(000)	744
Crystal size	$0.50 \times 0.50 \times 0.50 \text{ mm}^3$
Theta range for data collection	2.62 to 25.50°
Index ranges	−17<=h<=17, −10<=k<=11, −14<=l<=10
Reflections collected	8541
Independent reflections	2998 [R(int) = 0.0230]
Completeness to theta = 25.50°	100.0 %
Absorption correction	SADABS
Max. and min. transmission	0.3468 and 0.3468
Refinement method	Full-matrix least-squares on F^2
Data / restraints / parameters	2998 / 0 / 193
Goodness-of-fit on F^2	1.052
Final R indices [I>2sigma(I)]	R_1 = 0.0354, wR_2 = 0.0940
R indices (all data)	R_1 = 0.0431, wR_2 = 0.0980
Largest diff. peak and hole	0.811 and −0.757 e.Å^{-3}

Table 14. Crystal data and structure refinement for (*Z*)-**8b** (CCDC-657362).
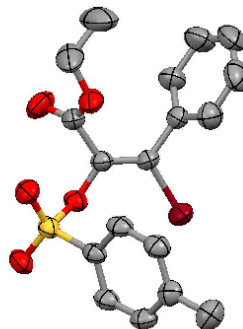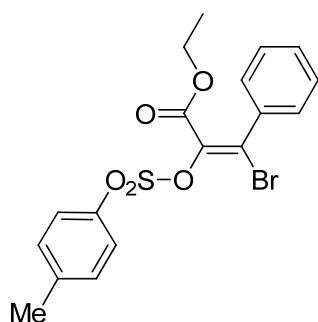
Empirical formula	$C_{18}H_{17}BrO_5S$
Formula weight	425.29
Temperature	300(2) K
Wavelength	0.71073 Å
Crystal system	Monoclinic
Space group	P2(1)/c
Unit cell dimensions	a = 6.1892(9) Å, α = 90°
	b = 8.2107(11) Å, β = 93.212(2)°
	c = 36.297(5) Å, γ = 90°
Volume	1841.6(4) Å^3
Z	4
Density (calculated)	1.534 Mg/m^3
Absorption coefficient	2.370 mm^{-1}
F(000)	864
Crystal size	0.50 × 0.50 × 0.50 mm^3
Theta range for data collection	2.25 to 25.50°
Index ranges	–6<=h<=7, –9<=k<=9, –35<=l<=43
Reflections collected	9712
Independent reflections	3428 [R(int) = 0.0564]
Completeness to theta = 25.50°	99.9 %
Absorption correction	None
Max. and min. transmission	0.3837 and 0.3837
Refinement method	Full-matrix least-squares on F^2
Data / restraints / parameters	3428 / 0 / 229
Goodness-of-fit on F^2	0.992
Final R indices [I>2sigma(I)]	R_1 = 0.0358, wR_2 = 0.0955
R indices (all data)	R_1 = 0.0435, wR_2 = 0.0983
Largest diff. peak and hole	0.422 and –0.425 e.Å^{-3}

Table 15. Crystal data and structure refinement for (*Z*)-**8b** (CCDC-657363).
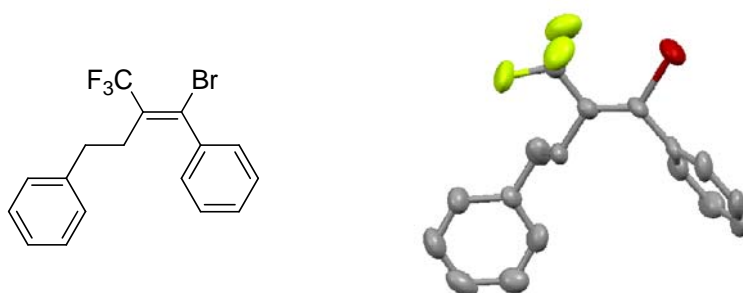
Empirical formula	$C_{17}H_{14}BrF_3$
Formula weight	355.19
Temperature	300(2) K
Wavelength	0.71073 Å
Crystal system	Monoclinic
Space group	P2(1)/n
Unit cell dimensions	a = 10.354(5) Å, α = 90°
	b = 14.496(7) Å, β = 114.662(8)°
	c = 10.894(5) Å, γ = 90°
Volume	1485.9(13) Å^3
Z	4
Density (calculated)	1.588 Mg/m^3
Absorption coefficient	2.789 mm^{-1}
F(000)	712
Crystal size	0.50 × 0.50 × 0.30 mm^3
Theta range for data collection	2.28 to 25.50°
Index ranges	–12<=h<=11, –17<=k<=17, –13<=l<=12
Reflections collected	7420
Independent reflections	2748 [R(int) = 0.0698]
Completeness to theta = 25.50°	99.4 %
Absorption correction	Empirical
Max. and min. transmission	0.4884 and 0.3361
Refinement method	Full-matrix least-squares on F^2
Data / restraints / parameters	2748 / 0 / 190
Goodness-of-fit on F^2	1.047
Final R indices [I>2sigma(I)]	R_1 = 0.1004, wR_2 = 0.2375
R indices (all data)	R_1 = 0.1558, wR_2 = 0.2608
Largest diff. peak and hole	2.337 and –1.086 e.Å^{-3}

Table 16. Crystal data and structure refinement for *trans*-(*E*)-**11** (see Figure 1).

Empirical formula	$C_{46}H_{37}Br_2F_3O_3P_2PdS$
Formula weight	1054.98
Temperature	300(2) K
Wavelength	0.71073 Å
Crystal system	Triclinic
Space group	P-1
Unit cell dimensions	a = 12.0557(9) Å, α = 91.4180(10)°
	b = 14.0130(11) Å, β = 103.2290(10)°
	c = 14.4863(11) Å, γ = 113.0460(10)°
Volume	2174.3(3) Å^3
Z	2
Density (calculated)	1.611 Mg/m^3
Absorption coefficient	2.439 mm^{-1}
F(000)	1052
Theta range for data collection	1.46 to 25.50°
Index ranges	−14<=h<=11, −16<=k<=16, −17<=l<=17
Reflections collected	11897
Independent reflections	7941 [R(int) = 0.0179]
Completeness to theta = 25.50°	97.9 %
Absorption correction	Empirical
Max. and min. transmission	0.4884 and 0.3361
Refinement method	Full-matrix least-squares on F^2
Data / restraints / parameters	7941 / 0 / 615
Goodness-of-fit on F^2	1.014
Final R indices [I>2sigma(I)]	R_1 = 0.0328, wR_2 = 0.0844
R indices (all data)	R_1 = 0.0402, wR_2 = 0.0870
Largest diff. peak and hole	0.953 and −0.379 e.Å^{-3}

Table 17. Crystal data and structure refinement for **6aba** (CCDC-657360).
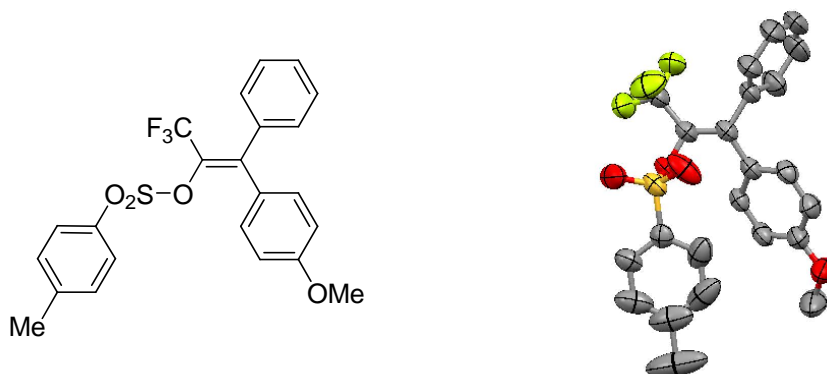
Empirical formula	$C_{23}H_{19}F_3O_4S$
Formula weight	448.44
Temperature	300(2) K
Wavelength	0.71073 Å
Crystal system	Triclinic
Space group	P-1
Unit cell dimensions	a = 10.2200(18) Å, α = 75.867(3)°
	b = 11.1353(19) Å, β = 70.324(3)°
	c = 11.260(2) Å, γ = 65.320(3)°
Volume	1088.3(3) Å^3
Z	2
Density (calculated)	1.368 Mg/m^3
Absorption coefficient	0.201 mm^{-1}
F(000)	464
Crystal size	0.50 × 0.50 × 0.50 mm^3
Theta range for data collection	1.94 to 25.98°
Index ranges	−12<=h<=11, −13<=k<=6, −13<=l<=13
Reflections collected	6194
Independent reflections	4182 [R(int) = 0.0146]
Completeness to theta = 25.50°	97.8 %
Absorption correction	Empirical
Max. and min. transmission	0.9062 and 0.9062
Refinement method	Full-matrix least-squares on F^2
Data / restraints / parameters	4182 / 48 / 282
Goodness-of-fit on F^2	1.051
Final R indices [I>2sigma(I)]	R_1 = 0.0508, wR_2 = 0.1448
R indices (all data)	R_1 = 0.0600, wR_2 = 0.1527
Largest diff. peak and hole	0.245 and −0.301 e.Å^{-3}

References

(1) (a) Borvendeg, J. *Drugs Future* **1985**, *10*, 395. (b) Borvendeg, J.; Anheuer, Z. *Exp. Clin. Endocrinol.* **1985**, *86*, 368. (c) Borvendeg, J.; Hermann, I.; Csuka, O. *Acta Physiol. Hung.* **1996**, *84*, 405. (d) Erdelyi-Toth, V.; Gyergyay, F.; Szamel, I.; Pap, E.; Kralovanszky, J.; Bojti, E.; Csorgo, M.; Drabant, S.; Klebovich, I. *Anti-Cancer Drugs* **1997**, *8*, 603. (e) Monostory, K.; Jemnitz, K.; Vereczkey, L.; Czira, G. *Drug Metab. Dispos.* **1997**, *25*, 1370.

(2) Reviews on antiestrogens: (a) Magarian, R. A.; Overacre, L. B.; Singh, S.; Meyer, K. L. *Curr. Med. Chem.* **1994**, *1*, 61. (b) Jordan, V. C. *J. Med. Chem.* **2003**, *46*, 883. (c) Jordan, V. C. *J. Med. Chem.* **2003**, *46*, 1081.

(3) (a) Middleton, W. J.; Metzger, D.; Snyder, J. A. *J. Med. Chem.* **1971**, *14*, 1193. (b) Németh, G.; Kapiller-Dezsofi, R.; Lax, G.; Simig, G. *Tetrahedron* **1996**, *52*, 12821. (c) Shimizu, M.; Fujimoto, T.; Minezaki, H.; Hata, T.; Hiyama, T. *J. Am. Chem. Soc.* **2001**, *123*, 6947. (d) Shimizu, M.; Fujimoto, T.; Liu, X.; Minezaki, H.; Hata, T.; Hiyama, T. *Tetrahedron* **2003**, *59*, 9811. (e) Li, Y.; Lu, L.; Zhao, X. *Org. Lett.* **2004**, *6*, 4467. (f) Liu, X.; Shimizu, M.; Hiyama, T. *Angew. Chem. Int. Ed.* **2004**, *43*, 879. (g) Konno, T.; Daitoh, T.; Noiri, A.; Chae, J.; Ishihara, T.; Yamanaka, H. *Org. Lett.* **2004**, *6*, 933. (h) Kim, M. S.; Jeong, I. H. *Tetrahedron Lett.* **2005**, *46*, 3545. (i) Konno, T.; Daitoh, T.; Noiri, A.; Chae, J.; Ishihara, T.; Yamanaka, H. *Tetrahedron* **2005**, *61*, 9391. (j) Zhang, J.; Zhao, X.; Li, Y.; Lu, L. *Tetrahedron Lett.* **2006**, *47*, 4737. (k) Zhang, J.; Zhao, X.; Lu, L. *Tetrahedron Lett.* **2007**, *48*, 1911.

(4) General reviews on cross-coupling reaction: (a) *Metal-catalyzed Cross-coupling Reactions*; 1st ed.; Diederich, F., Stang, P. J., Eds.; Wiley-VCH: Weinheim, 1998. (b) *Top. Curr. Chem.* **2002**, *219*. (c) *Special Issue on 30 Years of the Cross-coupling Reaction*; Tamao, K., Hiyama, T., Negishi, E., Eds., 2002; *J. Organomet. Chem.* **2002**, *653*, 1–303. (d) *Handbook of Organopalladium Chemistry for Organic Synthesis*; Negishi, E., de Meijere, A., Eds.; Wiley-VCH: Weinheim, 2004. (e) *Metal-catalyzed cross-coupling reactions*; 2nd ed.; Diederich, F., de Meijere, A., Eds.; Wiley-VCH: Weinheim, 2004. (f) Tsuji, J. *Palladium Reagents and Catalysts: New Perspectives for the 21st Century*; Wiley: Chichester, 2004. (g) Nicolaou, K. C.; Bulger, P. G.; Sarlah, D. *Angew. Chem., Int. Ed.* **2005**, *44*, 4442. (h) Nolan, S. P.; Navarro, O. *Comprehensive Organometallic Chemistry III*; Crabtree, R., Mingos, D. M. P., Eds.; Elsevier: Oxford, 2007; Vol. 11, p 1.

(5) Palladium-catalyzed reactions of RR′C=CBr$_2$ leading to unsymmetrical tri- and tetrasubsituted alkenes were reported. Hydrogenolysis: (a) Uenishi, J.; Kawahama, R.; Yonemitsu, O.; Tsuji, J. *J. Org. Chem.* **1998**, *63*, 8965. Intramolecular bis(carbopalladation): (b) Ma, S.; Xu, B.; Ni, B. *J. Org. Chem.* **2000**, *65*, 8532. Cross-coupling reaction with organostannanes: (c) Sorg, A.; Siegel, K.; Brückner, R. *Synlett* **2004**, 321. See also, (d) Larock, R. C.; Doty, M. J.; Han, X. *J. Org. Chem.* **1999**, *64*, 8770. Sequential synthesis of tetra-arylated ethenes starting from vinyl sulfide was reported. (e) Itami, K.; Mineno, M.; Muraoka, N.; Yoshida, J.-i. *J. Am. Chem. Soc.* **2004**, *126*, 11778.

(6) Bromine–lithium and –zinc exchange of 2-substituted 1,1-dibromo-3,3,3-trifluoropropenes R(CF$_3$)C=CBr$_2$ (R: carbonaceous group) were reported to take place stereoselectively. (a) Morken, A.; Bachand, P. C.;

Swenson, D. C.; Burton, D. J. *J. Am. Chem. Soc.* **1993**, *115*, 5430. (b) Uno, H.; Nibu, N.; Misobe, N. *Bull. Chem. Soc. Jpn.* **1999**, *72*, 1365. (c) Li, Y.; Lu, L.; Zhao, X. *Org. Lett.* **2004**, *6*, 4467.

(7) A wide variety of two-fold cross-coupling reaction of 1,1-dihalo-1-alkenes (RHC=CX$_2$) with organometallic reagents constitute an efficient method for the stereoselective synthesis of trisubstituted olefins. (a) Minato, A.; Suzuki, K.; Tamao, K. *J. Am. Chem. Soc.* **1987**, *109*, 1257. (b) Roush, W. R.; Moriarty, K. J.; Brown, B. B. *Tetrahedron Lett.* **1990**, *31*, 6509. (c) Shen, W.; Wang, L. *J. Org. Chem.* **1999**, *64*, 8873. (d) Sugihara, T. In *Handbook of Organopalladium Chemistry for Organic Synthesis*; Negishi, E., Ed; John Wiley & Sons, Inc.: New York, 2002, Vol. 1, p 649. (e) Zeng, X.; Qian, M.; Hu, Q.; Negishi, E. *Angew. Chem. Int. Ed.* **2004**, *43*, 2259. (f) Molander, G. A.; Yokoyama, Y. *J. Org. Chem.* **2006**, *71*, 2493. (g) Tan, Z.; Negishi, E. *Angew. Chem. Int. Ed.* **2006**, *45*, 762. (h) Wang, J.-R.; Manabe, K. *Synthesis* **2009**, 1405.

(8) Eliel, E. L.; Wilen, S. H.; Mander, L. N. *Stereochemistry of Organic Compounds*; John Wiley & Sons, Inc.: New York, 1994.

(9) Miyaura, N. In *Metal-Catalyzed Cross-Coupling Reactions*; 2nd ed.; de Meijere, A.; Diederich, F., Eds; Wiley-VCH: Weinheim, 2004, Vol. 1, Chapter 2, p 80.

(10) Clément, S.; Guyard, L.; Knorr, M.; Villafañe, F.; Strohmann, C.; Kubicki, M. M. *Eur. J. Inorg. Chem.* **2007**, 5052.

(11) Emsley, J. *The Elements,* 3rd ed.; Oxford University Press: Oxford, 2000.

(12) Bondi, A. *J. Phys. Chem.* **1964**, *68*, 441.

(13) Bartolome, C.; Espinet, P.; Villafane, F.; Giesa, S.; Martin, A.; Orpen, A. G. *Organometallics* **1996**, *15*, 2019.

(14) Pereira, R.; Furst, A.; Iglesias, B.; Germain, P.; Gronemeyer, H.; de Lera, A. R. *Org. Biomol. Chem.* **2006**, *4*, 4514.

(15) Oxidative adduct with *cis*-configuration has been isolated in only one case so far. Urata, H.; Tanaka, M.; Fuchikami, T. *Chem. Lett.* **1987**, *16*, 751.

(16) Nguyen, H. N.; Huang, X.; Buchwald, S. L. *J. Am. Chem. Soc.* **2003**, *125*, 11818.

(17) Legros, J.; Crousse, B.; Bonnet-Delpon, D.; Bégué, J.-P. *J. Fluorine Chem.* **2001**, *107*, 121.

(18) Gore, M. P.; Nanjappan, P.; Hoops, G. C.; Woodard, R. W. *J. Org. Chem.* **1990**, *55,* 758.

(19) Creary, X. *J. Org. Chem.* **1987**, *52,* 5026. Compound data were identical to those reported in the literature: Singh, R. P.; Cao, G.; Kirchmeier, R. L.; Shreeve, J. M. *J. Org. Chem.* **1999**, *64,* 2873.

(20) Harrowven, D. C.; Guy, I. L. *Chem. Commun.* **2004**, 1968.

(21) Barluenga, J.; Llavona, L.; Concellón, J. M.; Yus, M. *J. Chem. Soc., Perkin Trans. 1* **1991**, 297.

Chapter 5

Synthesis, Structure, and Photophysical Properties of Dimethoxybis(3,3,3-trifluoropropenyl)benzenes

A series of dimethoxybis(3,3,3-trifluoropropenyl)benzenes were synthesized by reduction of the corresponding dimethoxybis(3,3,3-trifluoropropynyl)benzenes and found to exhibit visible light from violet to blue in solution and in the solid states such as powder and spin-coated thin film.

1. Introduction

Motivated by the progress in such optoelectronic devices as organic light-emitting diodes (OLED),[1] semiconductor lasers,[2] and fluorescent sensors,[3] much interest has been paid to π-conjugated systems that emit visible light in the solid state.[4] However, the development of organic molecules exhibiting highly efficient solid-state luminescence is an extremely challenging task because the molecular aggregation of chromophores, inherently in the solid, mostly results in the concentration quenching of luminescence. Therefore, examples of organic solids that exhibit intense emission with high absolute quantum yield are quite limited.[5] Two highly emissive organic solid materials are shown in Figure 1.[5i,k] The common structural feature of emissive organic solids reported so far is that they contain multiple aromatic rings and/or polycyclic aromatic hydrocarbon skeletons. Such polycyclic structure often causes problem in solubility, which is one of the undesirable factors in the easy purification and processing of organic materials. Meanwhile, emission colors of π-conjugated molecules are closely related to their conjugation lengths, and organic materials with good solubility have the potential of being applicable to solution processing, which is a fascinating method for the easy and low-cost fabrication of large area optoelectronic devices. Therefore, it is intriguing to raise the question of how small can we minimize the aromatic component of highly emissive organic solids from both fundamental and practical viewpoints.[6]

λ_{em} = 469 nm
Φ_{PL} = 0.80 (crystal)

λ_{em} = 552 nm
Φ_{PL} = 0.85 (neat film)
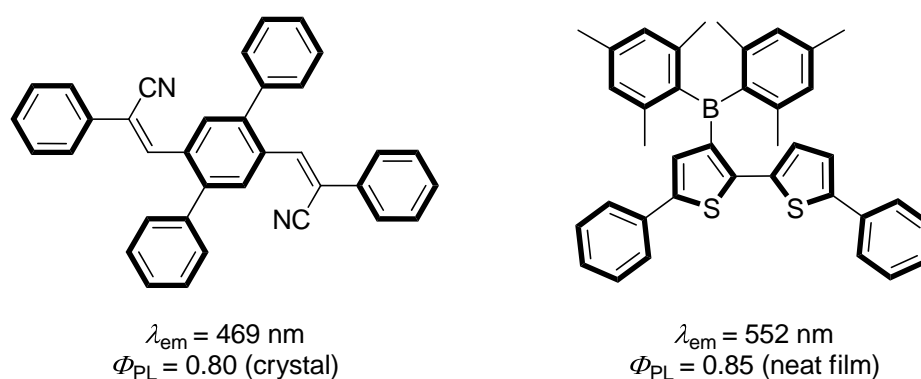
Figure 1. Examples of emitting organic solids.

In the course of the synthetic study on CF_3-containing π-conjugated systems, the author found by chance that 1,2-dimethoxy-4,5-bis[(Z)-3,3,3-trifluoropropenyl]-benzene [(Z,Z)-**1**] emitted violet light weakly in cyclohexane and even in powder form

136

upon irradiation with UV light. This observation prompted the author to explore the molecular/electronic structures of dimethoxybis(3,3,3-trifluoropropenyl)benzenes as a minimal chromophore of emissive organic solids. Described in this Chapter are synthesis, structure, photopysical properties, and theoretical calculations of dimethoxybis(3,3,3-trifluoropropenyl)benzenes **1–3** (Figure 2).
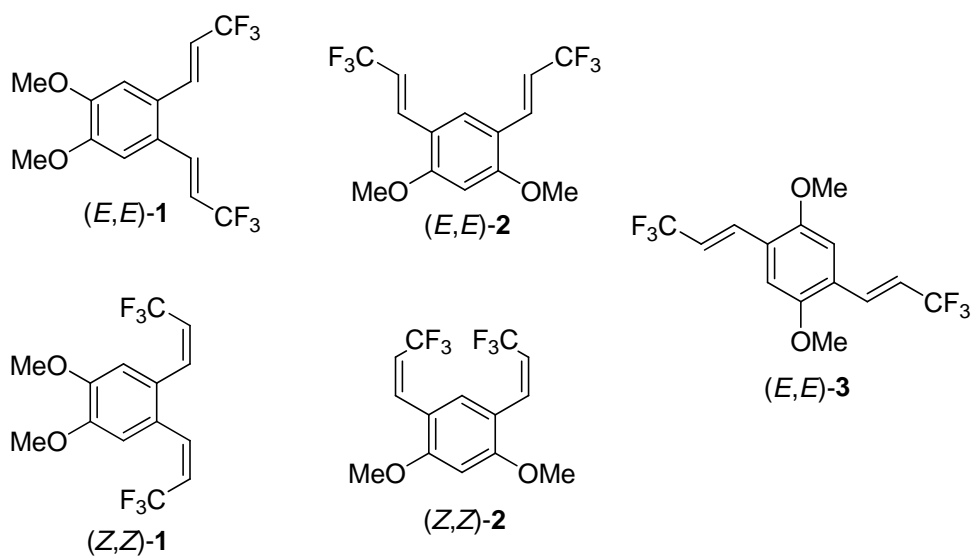
Figure 2. Dimethoxybis(3,3,3-trifluoropropenyl)benzenes **1–3**.

2. Results and Discussion

2-1. Synthesis of dimethoxybis(3,3,3-trifluoropropenyl)benzenes 1–3

Dimethoxybenzene (*E,E*)-**1** was prepared by stereoselective reduction of 1,2-dimethoxy-4,5-bis(3,3,3-trifluoropropynyl)benzene (**5**) with LiAlH$_4$,[7] while (*Z,Z*)-**1** was prepared by hydrogenation of **5** using the Lindlar catalyst (Scheme 1).[8] Bis(trifluoropropynyl)benzene **5** was prepared by Pd-catalyzed cross-coupling reaction of 1,2-diiodo-4,5-dimethoxybenzene (**4**) with 3,3,3-trifluropropynylzinc chloride prepared in situ from 3,3,3-trifluoropropynyllithium with ZnCl$_2$•TMEDA.[9] It should be noted that addition of stoichiometric amount of Ag$_2$O is indispensable for obtaining **5** in good yields (Table, entry 3).
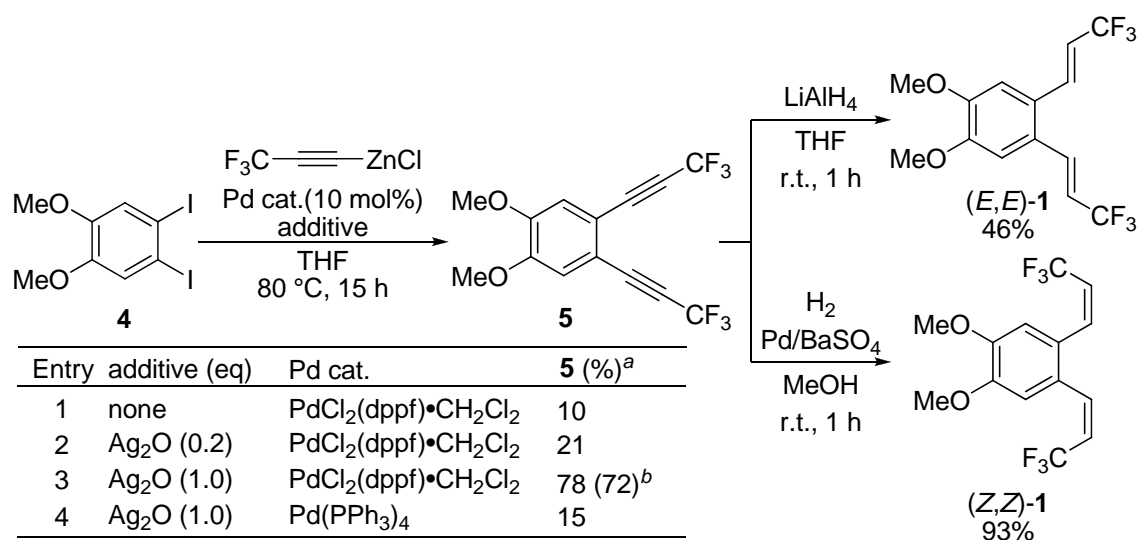
Scheme 1. Synthesis of 1,2-dimethoxy-4,5-bis(3,3,3-trifluoropropenyl)benzenes (**1**).

Entry	additive (eq)	Pd cat.	5 (%)[a]
1	none	PdCl$_2$(dppf)•CH$_2$Cl$_2$	10
2	Ag$_2$O (0.2)	PdCl$_2$(dppf)•CH$_2$Cl$_2$	21
3	Ag$_2$O (1.0)	PdCl$_2$(dppf)•CH$_2$Cl$_2$	78 (72)[b]
4	Ag$_2$O (1.0)	Pd(PPh$_3$)$_4$	15

[a] ^{19}F NMR yield. [b] Isolated yield.

In a similar manner, both (*E,E*)-**2** and (*Z,Z*)-**2** were prepared starting with 1,5-diiodo-2,4-dimethoxybenzene (**6**) (Scheme 2).

Entry	additive (eq)	Pd cat.	7 (%)[a]
1	Ag$_2$O (1.0)	PdCl$_2$(dppf)•CH$_2$Cl$_2$	51
2	none	Pd(PPh$_3$)$_4$	63 (69)[b]
3	Ag$_2$O (1.0)	Pd(PPh$_3$)$_4$	70
4	18-Cr-6 (1.0)	Pd(PPh$_3$)$_4$	61

[a] ^{19}F NMR yield. [b] Isolated yield.
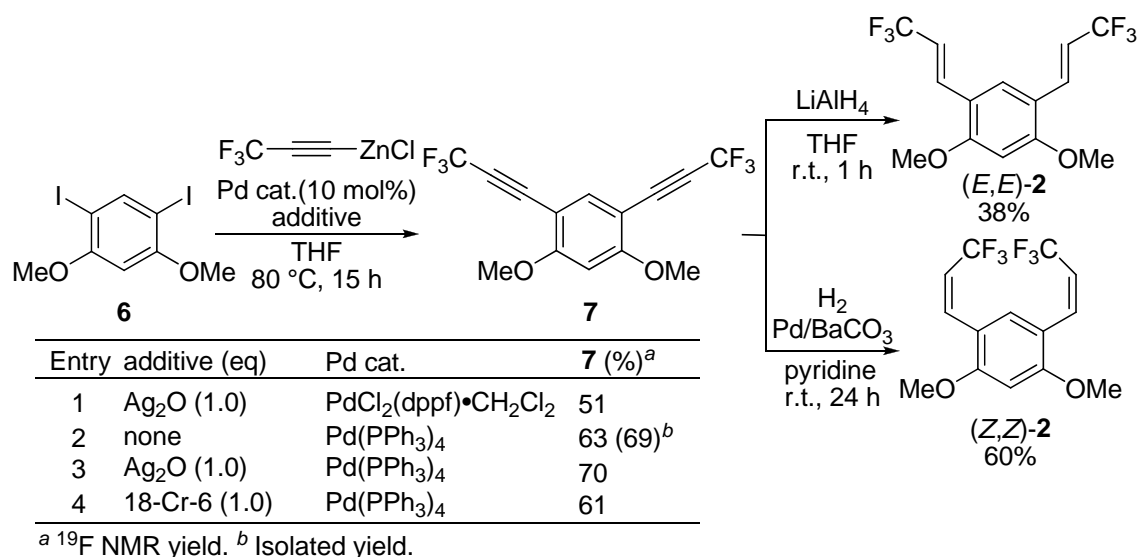
Scheme 2. Synthesis of 1,5-dimethoxy-2,4-bis(3,3,3-trifluoropropenyl)benzenes (**2**).

When LiAlH$_4$ reduction of diethynylbenzene **9** was attempted, the reaction resulted in the production of a complex mixture (Scheme 3). On the other hand, hydrogenation of **9** with the Lindlar catalyst gave desired (*Z,Z*)-**3** quantitatively. Configuration of the two C=C bonds was confirmed based on the coupling constant between vicinal two olefinic hydrogens in the crude products (J = 12.4 Hz by ^{1}H NMR). However, (*Z,Z*)-**3** easily isomerized during purification on silica gel column chromatography to give a mixture of (*Z,Z*)-**3** and (*E,E*)-**3** with a ratio of 2:1. Then, the

138

mixture was irradiated with a UV lamp in the presence of a catalytic amount of I_2, and (*E,E*)-**3** was isolated as a single stereoisomer in 77% yield.
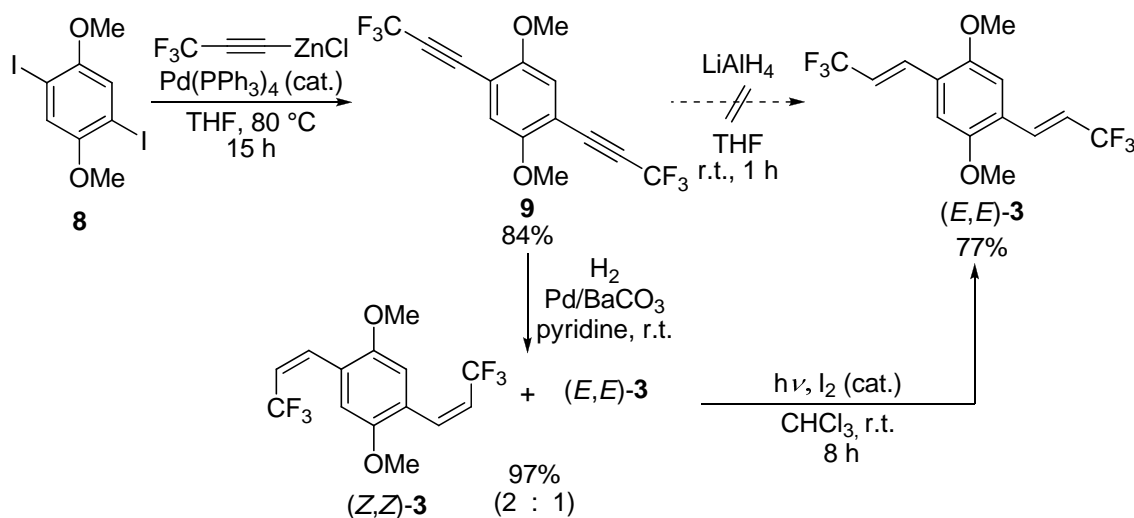
Scheme 3. Preparation of 1,4-dimethoxy-2,5-bis[(*E*)-trifluoropropenyl]benzene **3**.

2-2. X-ray crystallography

Molecular and packing structures of (*E,E*)-**2** and (*E,E*)-**3** were unambiguously clarified by X-ray crystallographic analysis of their single crystals obtained by recrystallization from CH_2Cl_2/hexane in both cases. The molecular structure of (*E,E*)-**2** is shown in Figure 3. Two trifluoropropenyl and two MeO groups were positioned on the plane of the benzene ring, in other words, all carbon and oxygen atoms were on the same plane as shown in Figure 3b.
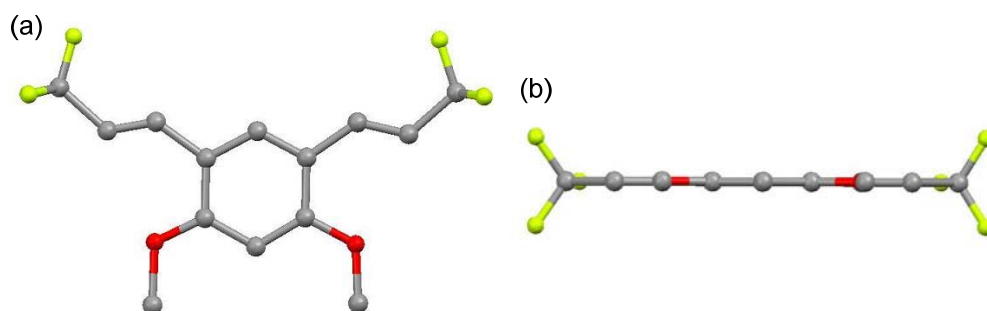
Figure 3. Molecular structure of (*E,E*)-**2**: (a) top view and (b) side view.

Packing diagram of (*E,E*)-**2** revealed that the molecules were closely packed with an interplanar distance being 3.56 Å (Figure 4a) and the closest contact between adjacent benzene centers being 3.73 Å (Figure 4b), suggesting the presence of strong π–π electronic interactions between the molecules.
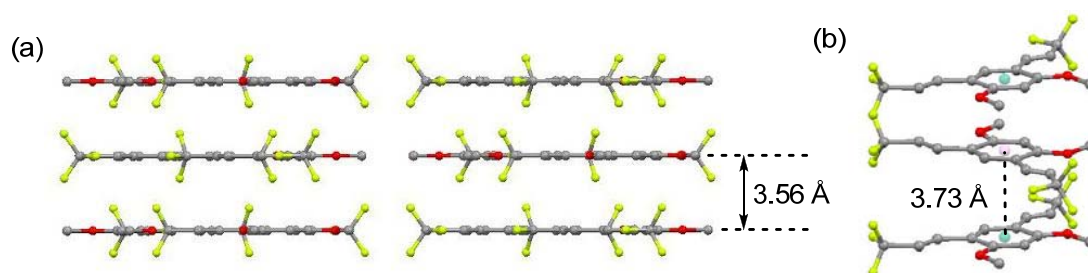
Figure 4. Packing diagram of (*E,E*)-**2**: (a) viewed along the *c*-axis; (b) viewed from oblique direction to *bc* plane.

On the other hand, (*E,E*)-**3** adopted slightly twisted conformation with the dihedral angle being 12° and 2° for C(1)–C(2)–C(3)–C(4) and C(6)–O(1)–C(5)–C(2), respectively (Figure 5).
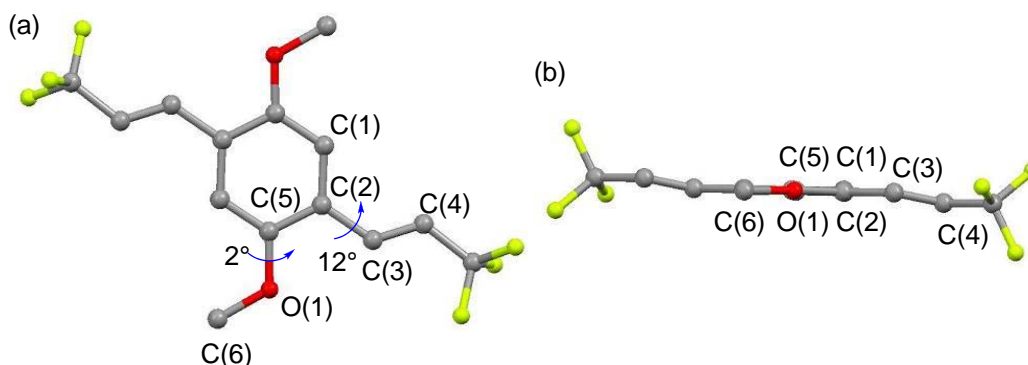
Figure 5. Molecular structure of (*E,E*)-**3**: (a) top view and (b) side view.

Packing diagram of (*E,E*)-**3** is shown in Figure 6. Whereas the interplanar distance (3.58 Å) was close to that of crystal (*E,E*)-**2** (Figure 6a), adjacent two molecules were far apart from each other (Figure 6b). In other words, the benzene rings of adjacent molecules were largely slipped. These results suggest that (*E,E*)-**3** may be more emissive than (*E,E*)-**2** in the solid state.
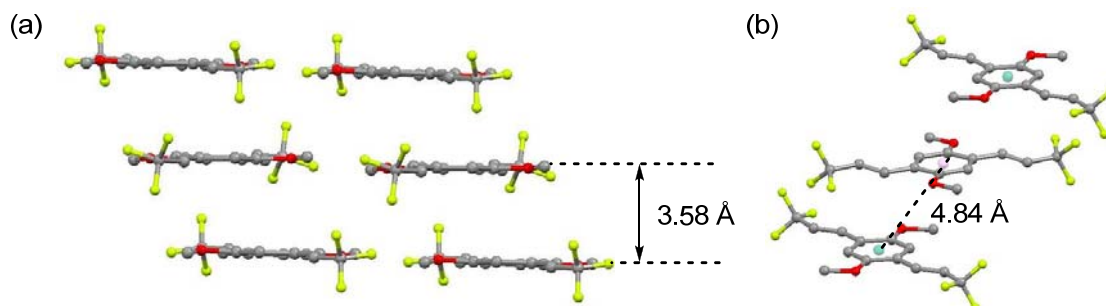
Figure 6. Packing diagram of (*E,E*)-**3**: (a) viewed along the *b*-axis; (b) viewed from oblique direction to *ab* plane.

2-3. Photophysical properties

Absorption and fluorescence properties of dimethoxybenzenes **1–3** in cyclohexane, powder, neat-film, and PMMA film are summarized in Table 1.

Table 1. Photophysical data of **1–3**.

Compound		Absorption		Fluorescence		Stokes shift
		λ_{abs} [nm]	ε [M^{-1} cm^{-1}]	λ_{em} [nm]	$\Phi_{PL}{}^a$	$\Delta\lambda$ [nm]
(*E,E*)-**1**	c-C$_6$H$_{12}{}^b$	304	10500	362	0.22	58
	powder	—	—	380	0.05	—
	neat film^c	—	—	388	0.09	—
	PMMA-film^d	—	—	410	0.12	—
(*Z,Z*)-**1**	c-C$_6$H$_{12}{}^b$	301	9000	373	0.10	72
	powder	—	—	386	0.10	—
	neat film^c	—	—	389	0.14	—
	PMMA-film^d	—	—	381	0.18	—
(*E,E*)-**2**	c-C$_6$H$_{12}{}^b$	324	5800	366	0.44	42
	powder	—	—	397	0.12	—
	neat film^c	—	—	400	0.13	—
	PMMA-film^d	—	—	405	0.25	—
(*Z,Z*)-**2**	c-C$_6$H$_{12}{}^b$	312	5600	364	0.15	52
	powder	—	—	388	0.10	—
	neat film^c	—	—	388	0.06	—
	PMMA-film^d	—	—	412	0.19	—
(*E,E*)-**3**	c-C$_6$H$_{12}{}^b$	360	9900	407	0.34	47
	powder	—	—	441	0.31	—
	neat film^c	—	—	434	0.37	—
	PMMA-film^d	—	—	428	0.49	—

^{a} Absolute quantum yields determined with a calibrated integrating sphere system.
^{b} Measured in 1 × 10^{-5} M in cyclohexane. ^{c} Spin-coated thin film prepared from a CH$_2$Cl$_2$ solution. ^{d} Dispersed in PMMA film.

Absorption spectra of **1–3** in cyclohexane measured at a concentration of 1 × 10^{-5} M are shown in Figure 7. The spectra of **1** and **2** were similar in shape, and absorption maxima (λ_{abs}) ranged from 301 to 324 nm. Considering that λ_{abs} of *E,E* and *Z,Z* compounds were almost the same, configuration around the C=C bond of trifluoropropenyl moieties does not seem likely to affect the electronic structures of **1** and **2** so much. Meanwhile, (*E,E*)-**3** showed an absorption around 360 nm.
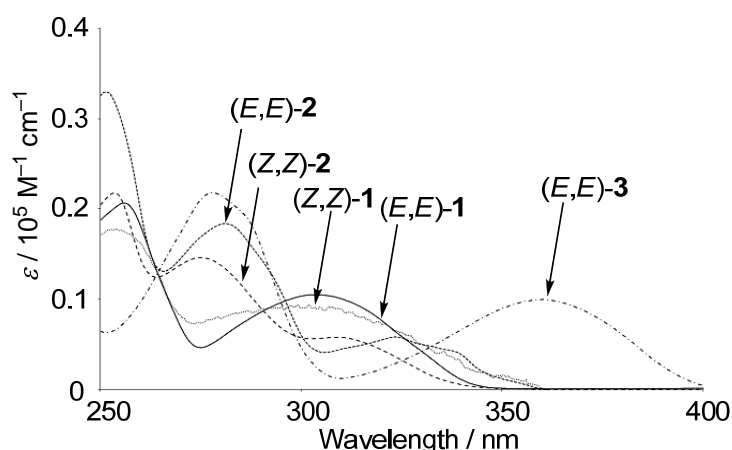
Figure 7. UV-vis spectra of **1–3** in cyclohexane (1×10^{-5} M).

Normalized fluorescence spectra of **1–3** in cyclohexane under irradiation of UV light (λ_{ex} = 265 nm) are shown in Figure 8a.   Both **1** and **2** exhibited violet emission with emission maxima (λ_{em}) ranging from 362 to 373 nm, while (*E,E*)-**3** emitted violet-blue light (λ_{em} = 403 nm, Figure 8b).   Absolute quantum yields (Φ_{PL}) decreased in the following order: (*E,E*)-**2** (0.44) > (*E,E*)-**3** (0.34) > (*E,E*)-**1** (0.22) > (*Z,Z*)-**2** (0.15) > (*Z,Z*)-**1** (0.10), indicating that the molecular design including *E,E*-configuration is more favorable for efficient emission in cyclohexane.
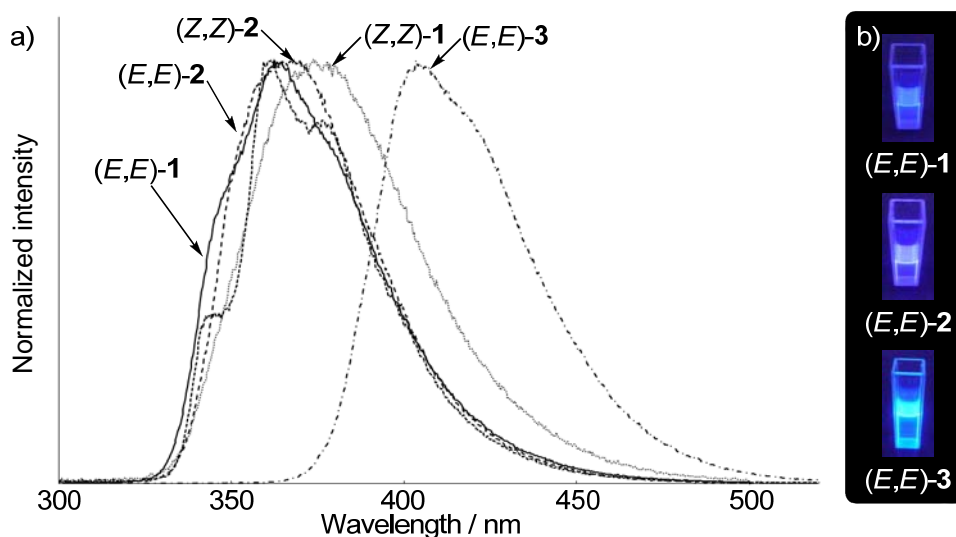
Figure 8.   (a) Normalized fluorescence spectra of **1–3** in cyclohexane (λ_{ex} = 265 nm). (b) Photographs of (*E,E*)-**1–3** in cyclohexane taken under UV light (λ = 265 nm).

Fluorescence spectra of powders of **1–3** (Figure 9) showed that λ_{em} of **1–3** moderately red-shifted (13–34 nm) compared with those in cyclohexane.   In addition, powders of **1–3** exhibited lower Φ_{PL} than those of the solution, except for powder

(Z,Z)-**1** showing Φ_{PL} similar to that in cyclohexane. These results imply stronger electronic interactions such as π–π staking are operating in powders than in their dilute solutions.
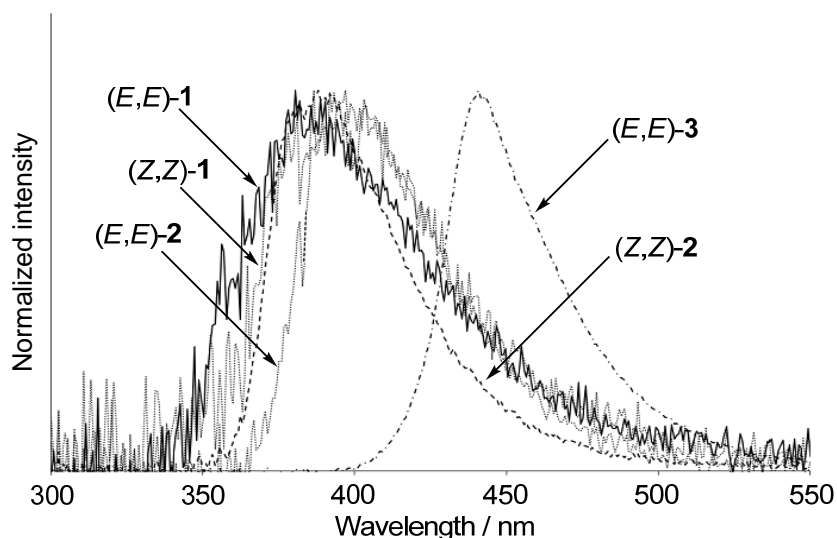
Figure 9. Normalized fluorescence spectra of **1**–**3** in powder form ($\lambda_{ex} = 265$ nm).

Spin-coated thin films of **1**–**3** fabricated on a quartz plate showed almost the same λ_{em} as those in powder (Table 1). Quantum yields of the films **1**–**3**, except for (Z,Z)-**2**, were enhanced compared to those in powder. The differences in Φ_{PL} between the neat films and powders indicate that photophysical properties of **1**–**3** in the solid states depend on their morphologies.

Investigation on fluorescence properties of **1**–**3** dispersed in PMMA film revealed that Φ_{PL} of **1**–**3** in PMMA were higher than those in powder or neat film. It should be noted that polymer films of (Z,Z)-**1** and (E,E)-**3** exhibited higher Φ_{PL} than those in solutions. In particular, (E,E)-**3** showed moderate quantum yield of 0.49. In polymer films, each molecule would be separated by each other like in a dilute solution, at the same time, their intramolecular rotations would be suppressed to some extent by the polymer chain. As a result, the quantum yield increased by diminishing the non-radiative decay process.

To gain further insights into electronic structures of **1**–**3**, solvent effect on the photophysical properties of **1**–**3** was investigated, and the results are summarized in Table 2.

143

Table 2. Solvent effect on absorption and fluorescence characteristics of **1–3**.[a]

Compound	Solvent (ε_r[b])	Absorption		Fluorescence	
		λ_{abs} [nm]	ε [M^{-1} cm^{-1}]	λ_{em} [nm]	Φ_{PL}[c]
(*E,E*)-**1**	*c*-C$_6$H$_{12}$ (2.0)	304	10500	362	0.22
	dioxane (2.2)	302	13300	376	0.25
	Et$_2$O (4.3)	302	11600	370	0.24
	CH$_2$Cl$_2$ (9.1)	303	11000	379	0.22
	CH$_3$CN (37)	302	13400	389	0.15
	DMSO (47)	308	13400	392	0.21
(*Z,Z*)-**1**	*c*-C$_6$H$_{12}$ (2.0)	301	9000	373	0.10
	dioxane (2.2)	312	9000	377	0.07
	Et$_2$O (4.3)	305	8000	370	0.12
	CH$_2$Cl$_2$ (9.1)	307	7900	378	0.12
	CH$_3$CN (37)	305	8200	389	0.11
	DMSO (47)	311	10400	400	0.03
(*E,E*)-**2**	*c*-C$_6$H$_{12}$ (2.0)	324	5800	366	0.44
	dioxane (2.2)	325	6100	370	0.37
	Et$_2$O (4.3)	324	6300	370	0.40
	CH$_2$Cl$_2$ (9.1)	325	6300	374	0.37
	CH$_3$CN (37)	325	6400	379	0.23
	DMSO (47)	328	6400	383	0.33
(*Z,Z*)-**2**	*c*-C$_6$H$_{12}$ (2.0)	312	5600	364	0.15
	dioxane (2.2)	313	6800	370	0.05
	Et$_2$O (4.3)	312	6300	370	0.09
	CH$_2$Cl$_2$ (9.1)	311	7100	370	0.05
	CH$_3$CN (37)	314	6700	379	0.04
	DMSO (47)	316	7200	379	0.04
(*E,E*)-**3**	*c*-C$_6$H$_{12}$ (2.0)	360	9900	407	0.34
	dioxane (2.2)	365	8900	425	0.29
	Et$_2$O (4.3)	363	9700	420	0.33
	CH$_2$Cl$_2$ (9.1)	364	9000	425	0.27
	CH$_3$CN (37)	364	9400	431	0.18
	DMSO (47)	371	8700	438	0.28

[a] Measured in 1 × 10^{-5} M in cyclohexane. [b] Dielectric constant. [c] Absolute quantum yields determined with a calibrated integrating sphere system.

As a representative example, absorption and fluorescence spectra of (*E,E*)-**3** in 1,4-dioxane, Et$_2$O, CH$_2$Cl$_2$, CH$_3$CN, and DMSO along with the spectra measured in cyclohexane are shown in Figure 10 and 11, respectively. Absorption spectra were almost the same as that in cyclohexane, except for slight red-shift of λ_{abs}, indicating that the changes in geometrical and electronic structures in their ground states can be negligible. Absorption spectra of the other compounds were also nearly the same as

those in cyclohexane.
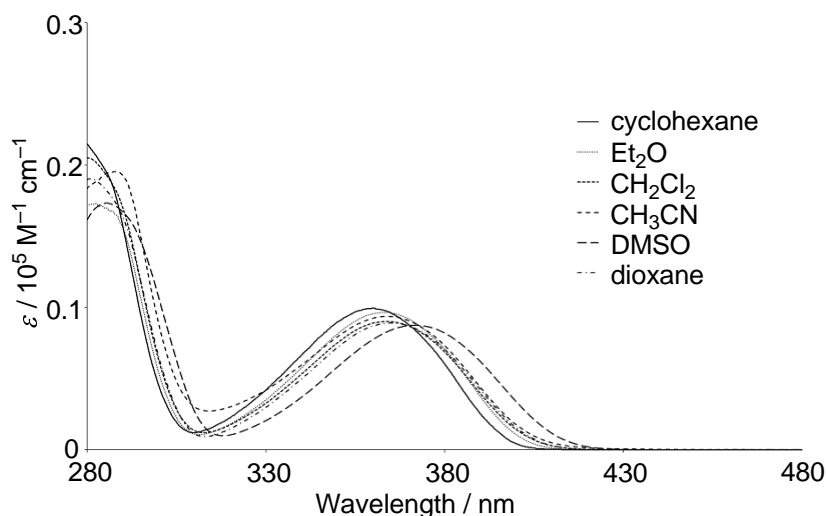
Figure 10. UV-vis spectra of (*E*,*E*)-**3** in various solvents.

In contrast, the fluorescence spectra exhibited significant red-shift of λ_{em} according to increase in solvent polarity from cyclohexane ($\varepsilon_{\text{r}} = 2.0$) to DMSO ($\varepsilon_{\text{r}} = 47$). Considering that absorption spectra were independent of solvent polarity, the excited states of (*E*,*E*)-**3** should be more polar than the ground states, probably due to the charge separation in the excited states via intramolecular charge-transfer (ICT) from the donor (OMe) to the acceptor (CF$_3$CHC=C). As for quantum yield, polar solvents like CH$_3$CN and DMSO gave much lower Φ_{PL} than cyclohexane, medium polar solvents did not show any drastic changes in Φ_{PL} in comparison with the cyclohexane solution. For the other compounds, similar behaviors in fluorescence spectra were observed (Table 2).
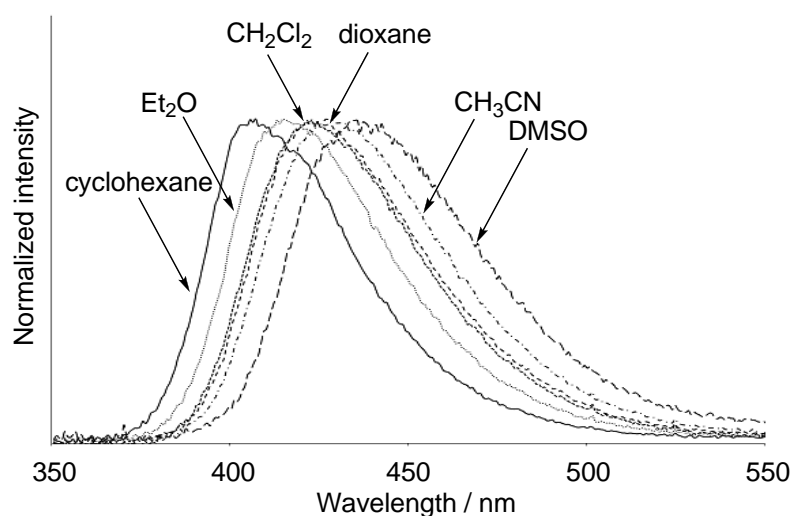
Figure 11. Normalized fluorescence spectra of (*E*,*E*)-**3** in various solvents.

145

2-4. Theoretical studies

To gain further insights into the electronic structures of the unique fluorophores, theoretical calculations of (*E,E*)-**2** and (*E,E*)-**3** were carried out by DFT methods using the Gaussian 03 package.[10] To examine the geometrical effect on the electronic structures, geometry optimization of (*E,E*)-**2** was carried out at B3LYP/6-31G(d) level with the six conformers (rotamers **A**–**F** shown in Figure 12) as an initial structure for the calculation.
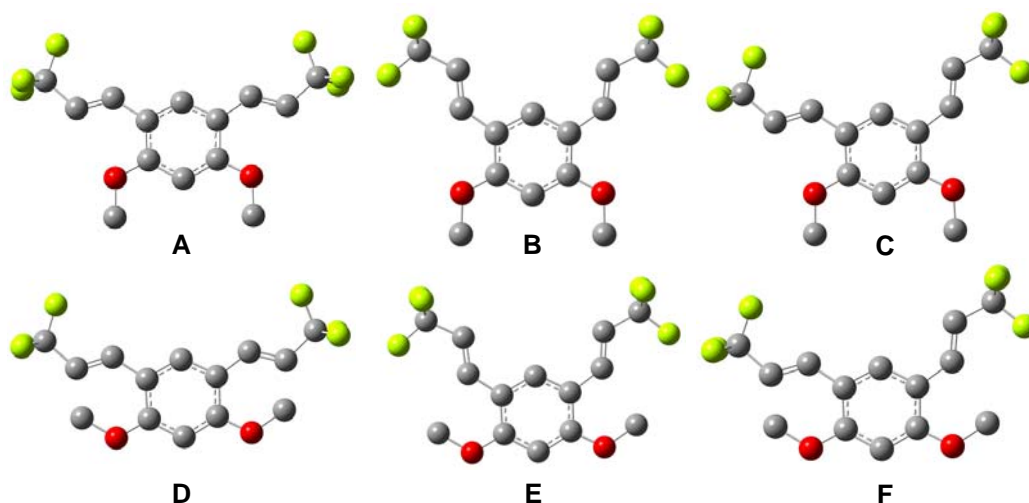
Figure 12. Molecular structures of rotamers **A**–**F**.

As a result of the calculations, three optimized structures **G**, **H**, and **I** were observed (Figure 13). In the rotamers **G** and **H**, two trifluoropropenyl and MeO groups were found coplanar to the benzene core, while two trifluoropropenyl groups of **I** slightly twisted from the benzene plane with the dihedral angles being 10° and 13°. Among the three rotamers, the most stable rotamer was found **G** adopting nearly the same geometry as the structure obtained by X-ray crystallography, though small relative energy differences among the rotamers indicate the conformational interconversion is quite easy (0 kcal/mol for **G**, 0.097 kcal/mol for **H**, and 0.19 kcal/mol for **I**).
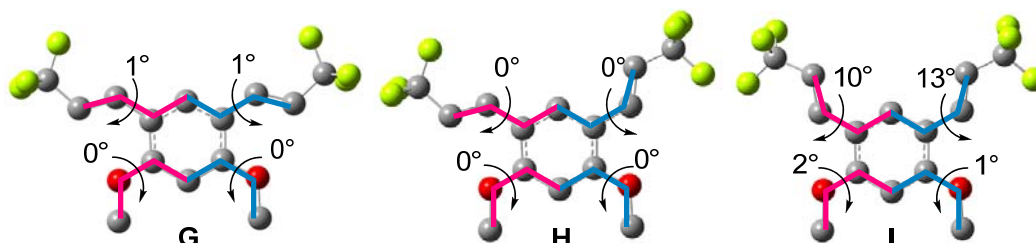
Figure 13. The three optimized geometries of (*E,E*)-**2**. Blue and pink lines represent the dihedral angles measured.

Geometries of (*E,E*)-**3** and their fluorine-free counterparts (*E,E*)-**10** and (*E,E*)-**11** for comparison (Figure 14) were also optimized. Since the optimized geometry of (*E,E*)-**2** was almost the same as that obtained by X-ray crystallography, the initial structure of (*E,E*)-**3** was set based on the geometry obtained by X-ray crystallography. The initial geometries for (*E,E*)-**10** and -**11** were determined by substitution of CF$_3$ in the initial structures of (*E,E*)-**2** and -**3** with CH$_3$, respectively.
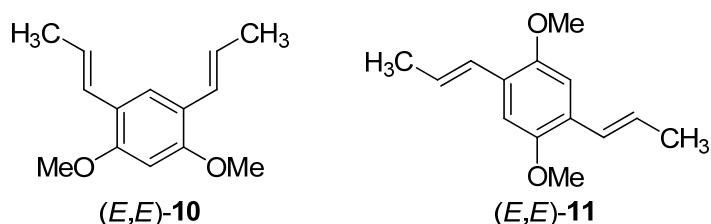
Figure 14. Fluorine-free analogs of (*E,E*)-**2** and (*E,E*)-**3**.

The calculations led to almost the same geometry of (*E,E*)-**10** to (*E,E*)-**2**, and both of (*E,E*)-**3** and (*E,E*)-**11** adopted a geometry similar to that of crystalline (*E,E*)-**3**, though the propenyl moiety in (*E,E*)-**11** was more twisted than (*E,E*)-**3** (Figure 15). Frontier orbitals of (*E,E*)-**2**, -**3**, -**10**, and -**11** calculated at B3LYP/6-31G(d) level are illustrated in center and right of Figure 15. HOMO of (*E,E*)-**2** delocalized on two oxygen atoms, the benzene ring, and ethenyl moieties, while LUMO exhibited localization of isosurface of functional waves as π* synmetry on the benzene core and extended to trifluoropropenyl moiety including two C–F σ* bonds of each CF$_3$ group, indicating π–σ* conjugation (negative hyperconjugation) should be operative in the system. Fluorine-free (*E,E*)-**10** showed similar distribution of frontier orbitals with smaller π–σ* conjugation. On the other hand, HOMOs of (*E,E*)-**3** and -**11** also delocalized on the π-electron system. Notably, LUMOs of (*E,E*)-**3** and -**11** clearly localized on CX$_3$C=CC$_6$H$_4$C=CCX$_3$ (X = F, H) skelton, indicating the HOMO–LUMO transition might be assigned to charge-transfer (CT) from the donor (OMe) to the acceptor (CX$_3$C=C).

147
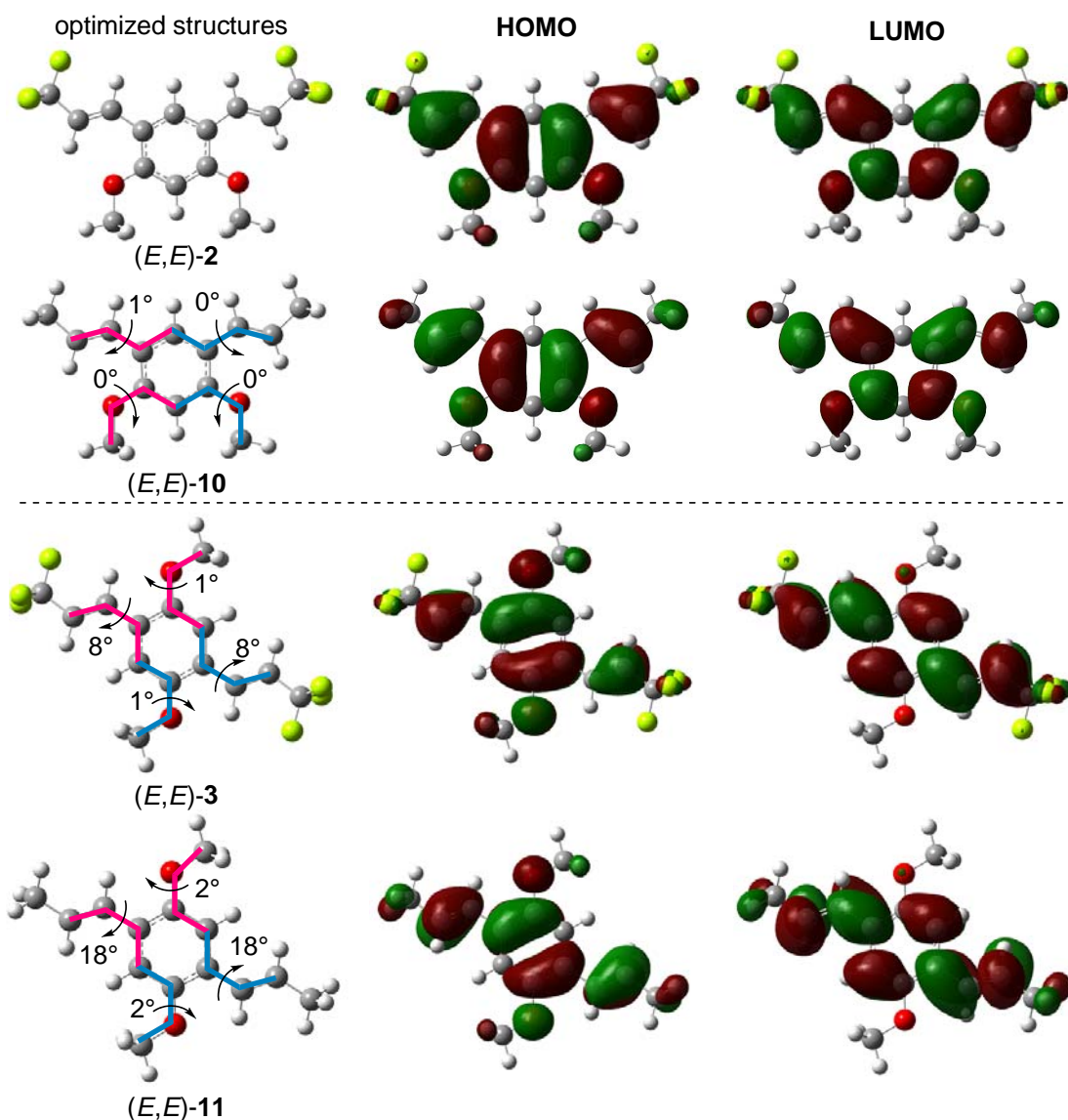
Figure 15. Optimized geometries (left) and HOMOs (center) and LUMOs (right) of (*E,E*)-**2**, -**3**, -**10**, and -**11**. Blue and pink lines represent the dihedral angles measured.

Energy levels of the frontier orbitals in **2**, **3**, **10**, and **11**, and each HOMO–LUMO energy gap are listed in Table 3. Substitution of CH_3 in (*E,E*)-**10** and (*E,E*)-**11** with CF_3 lowered the both of HOMO and LUMO energy. It should be noted that the degree of decrease in LUMO energy by CF_3 substitution was larger than that in HOMO: HOMO of (*E,E*)-**2** decreased by 0.97 eV, while LUMO decreased by 1.02 eV; HOMO and LUMO of (*E,E*)-**11** decreased by 0.90 eV and 1.17 eV, respectively. Therefore, the HOMO–LUMO gaps of (*E,E*)-**2** and (*E,E*)-**3** became smaller than (*E,E*)-**10** and (*E,E*)-**11** by 0.06 eV and 0.27 eV, respectively. These results indicate π–σ* conjugation effectively worked. The HOMO–LUMO gap in (*E,E*)-**3** was smaller than that in

(*E,E*)-**2** by 0.76 eV, which is consistent with the fact that absorption edge of (*E,E*)-**3** was observed in longer-wavelength region relative to that of (*E,E*)-**2**.

Table 3. Calculated energy levels of HOMOs and LUMOs.

	(*E,E*)-**2**	(*E,E*)-**10**	(*E,E*)-**3**	(*E,E*)-**11**
E_{LUMO} (eV)	−1.39	−0.37	−2.10	−0.93
E_{HOMO} (eV)	−5.88	−4.91	−5.82	−4.92
$\mathit{\Delta}E$ (eV)	4.48	4.54	3.72	3.99

3. Conclusions

In summary, the author demonstrated that dimethoxybis(3,3,3-trifluoropropenyl)-benzenes serve as minimal fluorophores that exhibit visible light from violet-blue to blue in solution and in the solid states. In addition, molecular orbital calculations disclosed that CF_3 groups should play an important role in extending conjugation of the π-electron systems.

149

4. Experimental Section

Dichloro(*N,N,N',N'*-tetramethylethylenediamine)zinc (ZnCl₂•TMEDA) was purchased from Aldrich, recrystallized from THF, and then dried at 50 °C under vacuum for 24 h. 1,2-Diiodo-4,5-dimethoxybenzene was prepared from 1,2-dimethoxybenzene by the reported procedure,[11] and the preparation of 1,5-diiodo-2,4-dimethoxybenzene[12] and 1,4-diiodo-2,5-dimethoxybenzene[13] was effected by applying the same procedure to 1,3-dimethoxy- and 1,4-dimethoxybenzenes, respectively. Spectroscopic-grade solvents for UV–vis absorption and fluorescence measurements were purchased from Kanto Chemical Co., Inc. and degassed by bubbling with argon before use. Thin films, PMMA, and polystyrene films were fabricated by spin-coating method with a MIKASA MS-A-100 spin coater. UV–vis absorption spectra were measured with a Shimadzu UV-2550 spectrometer. Fluorescence spectra were recorded by Hamamatsu Photonics C9920–02 Absolute PL Quantum Yield Measurement System, and absolute quantum yields were determined using a calibrated integrating sphere system. The absolute quantum yields Φ_{PL} were obtained by averaging values of three to five measurement with different lots of samples.

Preparation of 1,2-dimethoxy-4,5-bis(3,3,3-trifluoropropynyl)benzene (5): A typical procedure for Pd-catalyzed cross-coupling reaction of 3,3,3-trifluoropropynylzinc chloride with diiodobenzene. To a THF (5.1 mL) solution of 1,1-dichloro-3,3,3-tri-fluoro-2-tosyloxypropene (0.34 g, 1.0 mmol) was added BuLi (1.4 mL, 2.2 mmol, 1.6 M in hexane) at −78 °C (see Chapter 2). The solution was stirred at −78 °C for 30 min before addition of ZnCl₂•TMEDA (0.28 g, 1.1 mmol) in one portion. The resulting solution was stirred at −78 °C for 30 min and at room temperature for additional 30 min. The mixture was added to a THF (3.0 mL) solution of 1,2-diiodo-4,5-dimethoxybenzene (4) (0.10 g, 0.26 mmol), PdCl₂(dppf)•CH₂Cl₂ (21 mg, 26 μmol), and Ag₂O (59 mg, 0.26 mmol), and the resulting mixture was then heated at 80 °C for 15 h before cooling down to room temperature. Silica gel (1.0 g) and AcOEt (30 mL) were added to the reaction mixture; the slurry was concentrated *in vacuo*. The residue was all absorbed on the silica gel and then silica gel column chromatography (hexane/AcOEt 5:1) was performed, giving rise to **5** (59 mg, 72 %) as a colorless solid. Mp: 99.0–99.6 °C. T_d (5 wt%): 122.9 °C. R_f 0.42 (hexane/AcOEt 4:1). ¹H NMR (400 MHz, CDCl₃): δ 3.93 (s, 6H), 7.02 (s, 2H); ¹³C NMR (100 MHz, CDCl₃): δ 56.2, 79.0 (q, *J* = 52.9 Hz), 83.6 (q, *J* = 6.9 Hz), 114.5, 114.7 (q, *J* = 256.8 Hz), 115.5, 151.0; ¹⁹F NMR (282 MHz, CDCl₃): δ −50.6. IR (KBr): ν 2247, 1518, 1400, 1283, 1254, 1132, 999, 868, 718, 569 cm⁻¹. MS (EI): *m/z* (%) 322 (100, M⁺), 300 (20). Anal. Calcd for C₁₄H₈F₆O₂: C, 52.19; H, 2.50. Found: C, 52.00; H, 2.75.
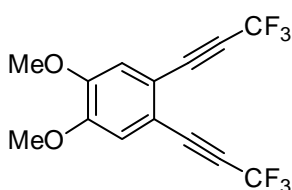
1,5-Dimethoxy-2,4-bis(3,3,3-trifluoropropynyl)benzene (7). A typical procedure using Pd(PPh₃)₄ (30 mg, 26 μmol) instead of PdCl₂(dppf)•CH₂Cl₂ and without Ag₂O gave **7** in 69% yield (57 mg) as a colorless solid. Purified by silica gel column chromatography (hexane/AcOEt 4:1). Mp: 169.5–170.2 °C. T_d (5 wt%): 130.0 °C. R_f 0.17 (hexane/AcOEt 4:1). ¹H NMR (400 MHz, CDCl₃): δ 3.96 (s, 6H), 6.41 (s, 1H), 7.63
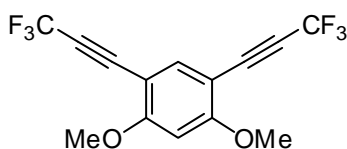
(s, 1H); ^{13}C NMR (100 MHz, CDCl$_3$): δ 56.2, 79.0 (q, J = 52.1 Hz), 82.1 (q, J = 6.4 Hz), 94.6, 100.6, 114.8 (q, J = 255.9 Hz), 139.6, 164.4; ^{19}F NMR (282 MHz, CDCl$_3$): δ –49.9.   IR (KBr): ν 2247, 1609, 1506, 1290, 1175, 1111, 1020, 824, 552 cm^{-1}.   MS (EI): m/z (%) 322 (100, M$^+$), 303 (15), 253 (11).   Anal. Calcd for C$_{14}$H$_8$F$_6$O$_2$: C, 52.19; H, 2.50.   Found: C, 52.06; H, 2.60.

1,4-Dimethoxy-2,5-bis(3,3,3-trifluoropropynyl)benzene (9).   A typical procedure using Pd(PPh$_3$)$_4$ (30 mg, 26 µmol) instead of PdCl$_2$(dppf)•CH$_2$Cl$_2$ and without Ag$_2$O gave **9** in 84% yield (69 mg) as a colorless solid.   Mp: 116.8–117.6 °C.   T$_d$ (5 wt%): 129.6 °C.   R$_f$ 0.69 (hexane/AcOEt 4:1). ^{1}H NMR (400 MHz, CDCl$_3$): δ 3.87 (s, 6H), 7.02 (s, 2H); ^{13}C NMR (100 MHz, CDCl$_3$): δ 56.5, 81.2 (q, J = 52.9 Hz), 82.2 (q, J = 6.1 Hz), 111.3, 114.7 (q, J = 257.1 Hz), 116.2, 154.9; ^{19}F NMR (282 MHz, CDCl$_3$): δ –50.5.   IR (KBr): ν 2259, 1506, 1402, 1288, 1134, 1030, 868, 667 cm^{-1}.   MS (EI): m/z (%) 322 (100, M$^+$), 307 (45).   Anal. Calcd for C$_{14}$H$_8$F$_6$O$_2$: C, 52.19; H, 2.50.   Found: C, 51.90; H, 2.56.
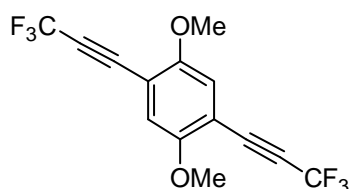
1,2-Dimethoxy-4,5-bis[(*E*)-3,3,3-trifluoropropenyl]benzene [(*E*,*E*)-1].   To a THF (0.28 mL) solution of **5** (29 mg, 91 µmol) was added LiAlH$_4$ (8.7 mg, 0.23 mmol) at room temperature.   The solution was stirred at room temperature for 1 h.   The reaction mixture was quenched with sat. aq. NH$_4$Cl (10 mL) and extracted with AcOEt (10 mL × 3 times).   The combined organic phase was dried over anhydrous MgSO$_4$ and concentrated *in vacuo*.   The residue was purified by column chromatography on silica gel (hexane/AcOEt 8:1) to give (*E*,*E*)-**1** (13 mg, 46%) as a colorless solid.   Mp: 124.2–125.2 °C.   T$_d$ (5 wt%): 119.4 °C.   R$_f$ 0.47 (hexane/AcOEt 4:1). ^{1}H NMR (400 MHz, CDCl$_3$): δ 3.95 (s, 6H), 6.05 (dq, J = 16.0, 6.6 Hz, 2H), 6.94 (s, 2H), 7.39 (dq, J = 16.0, 2.1 Hz, 2H); ^{13}C NMR (100 MHz, CDCl$_3$): δ 56.2, 109.0, 117.6 (q, J = 33.6 Hz), 123.1 (q, J = 267.9 Hz), 125.8, 133.7 (q, J = 6.9 Hz), 150.3; ^{19}F NMR (282 MHz, CDCl$_3$): δ –63.8 (d, J = 6.6 Hz).   IR (KBr): ν 1601, 1516, 1319, 1283, 1097, 966, 665, 544 cm^{-1}.   MS (EI): m/z (%) 326 (45, M$^+$), 307 (12), 257 (100).   Anal. Calcd for C$_{14}$H$_{12}$F$_6$O$_2$: C, 51.54; H, 3.71.   Found: C, 51.63; H, 4.00.
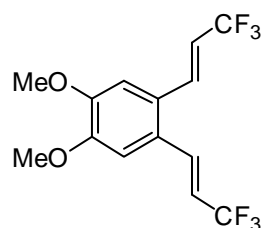
1,2-Dimethoxy-4,5-bis[(*Z*)-3,3,3-trifluoropropenyl]benzene [(*Z*,*Z*)-1].   A drop of quinoline and Pd/BaSO$_4$ (4.0 mg, 5 wt%) were added to methanol (2.5 mL) at room temperature, and the mixture was stirred for 10 min before **6** (80 mg, 0.25 mmol) was added.   The reaction mixture was stirred for another 10 min filled with H$_2$ gas (1 atm) and further stirred at room temperature for 1 h before filtration through a Celite-Florisil pad.   The filtrate was concentrated *in vacuo*.   The residue was purified by GPC to give (*Z*,*Z*)-**1** (75 mg, 93%) as a colorless solid.   Mp: 57.4–58.1°C.   T$_d$ (5 wt%): 109.7 °C.   R$_f$ 0.45 (hexane/AcOEt 4:1). ^{1}H NMR (400 MHz, CDCl$_3$): δ 3.89 (s, 6H), 5.82 (dq, J = 12.4, 12.7 Hz, 2H), 6.90 (s, 2H), 6.92 (d, J = 12.4 Hz, 2H); ^{13}C NMR (100 MHz, CDCl$_3$): δ 56.2, 113.4, 119.1 (q, J = 33.9 Hz), 122.4 (q, J =
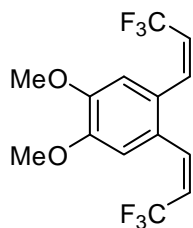
270.0 Hz), 125.4, 137.2 (q, J = 5.7 Hz), 148.7; ^{19}F NMR (282 MHz, CDCl$_3$): δ −58.2 (d, J = 12.7 Hz).   IR (KBr): ν 3011, 1717, 1508, 1279, 1134, 718, 419 cm^{-1}.   MS (EI): m/z (%) 326 (78, M$^+$), 307 (19), 257 (100), 242 (14), 188 (12).   Anal. Calcd for C$_{14}$H$_{12}$F$_6$O$_2$: C, 51.54; H, 3.71.   Found: C, 51.40; H, 3.80.

1,5-Dimethoxy-2,4-bis[(E)-3,3,3-trifluoropropenyl]benzene   [(E,E)-2].   The procedure for synthesis of (E,E)-**1** was applied to **7** to give (E,E)-**2** (16 mg, 38%).   Purified by silica gel column chromatography (hexane/AcOEt 9:1).   Yield: 38%, a colorless solid.   Mp: 108.8–109.9 °C.   T$_d$ (5 wt%): 130.8 °C.   R$_f$ 0.36 (hexane/AcOEt 4:1). ^{1}H NMR (400 MHz, CDCl$_3$): δ 3.94 (s, 6H), 6.26 (dq, J = 15.6, 5.4 Hz, 2H), 7.30 (dq, J = 15.6, 2.2 Hz, 2H), 7.46 (s, 2H); ^{13}C NMR (100 MHz, CDCl$_3$): δ 55.7, 94.8, 114.9 (q, J = 33.5 Hz), 115.1, 123.9 (q, J = 268.3 Hz), 129.1, 131.9 (q, J = 7.2 Hz), 160.2; ^{19}F NMR (282 MHz, CDCl$_3$): δ −63.4 (d, J = 5.4 Hz).   IR (KBr): ν 2949, 1651, 1614, 1471, 1304, 1269, 1117, 1028, 827, 519 cm^{-1}.   MS (EI): m/z (%) 326 (100, M$^+$), 307 (10).   Anal. Calcd for C$_{14}$H$_{12}$F$_6$O$_2$: C, 51.54; H, 3.71.   Found: C, 51.80; H, 3.68.
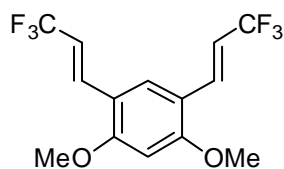
1,5-Dimethoxy-2,4-bis[(Z)-3,3,3-trifluoropropenyl]benzene [(Z,Z)-2].   To pyridine (3.2 mL) was added Pd/BaCO$_3$ (5.0 mg, 5 wt%) at room temperature, and the mixture was stirred for 10 min before **7** (0.10 g, 0.31 mmol) was added.   After additional 10 min of stirring, the flask was filled with H$_2$ gas (1 atm), and the mixture was vigorously agitated at room temperature for 24 h.   The mixture was filtered through a Celite-Florisil pad, and then the filtrate was concentrated *in vacuo*.   The residue was purified by GPC to give (Z,Z)-**2** (62 mg, 60%) as a colorless solid.   Mp: 89.7–91.2 °C.   T$_d$ (5 wt%): 127.0 °C.   R$_f$ 0.34 (hexane/AcOEt 4:1). ^{1}H NMR (400 MHz, CDCl$_3$): δ 3.89 (s, 6H), 5.64–5.76 (m, 2H), 6.41 (s, 1H), 7.00 (d, J = 12.8 Hz, 2H), 7.47 (s, 1H); ^{13}C NMR (100 MHz, CDCl$_3$): δ 55.7, 93.7, 115.0, 116.8 (q, J = 34.8 Hz), 122.9 (q, J = 269.9 Hz), 131.1–131.3 (m), 133.9–134.0 (m), 159.1; ^{19}F NMR (282 MHz, CDCl$_3$): δ −58.8 (d, J = 7.6 Hz).   IR (KBr): ν 2982, 1612, 1497, 1319, 1209, 1115, 1026, 924, 822, 745, 559 cm^{-1}.   MS (EI): m/z (%) 326 (100, M$^+$), 307 (12).   Anal. Calcd for C$_{14}$H$_{12}$F$_6$O$_2$: C, 51.54; H, 3.71.   Found: C, 51.66; H, 3.75.

1,4-dimethoxy-2,5-bis[(E)-3,3,3-trifluoropropenyl]benzene [(E,E)-3].   To pyridine (3.5 mL) was added Pd/BaCO$_3$ (5.0 mg, 5 wt%) at room temperature, and then the mixture was stirred for 10 min before **9** (0.10 g, 0.31 mmol) was added.   After another 10 min of stirring, the flask was filled with H$_2$ gas, and the whole mixture was stirred at room temperature for 2 h before filtration through a Celite-Florisil pad.   The filtrate was concentrated *in vacuo*.   The residue was purified by silica gel column chromatography (hexane/AcOEt 4:1), giving a mixture of (Z,Z)-**3** and (E,E)-**3** (ZZ:EE = 2 : 1, 99 mg, 97 %) as a colorless solid.   To a CHCl$_3$ (10 mL) solution of (Z,Z)-**3** and (E,E)-**3** (29 mg, 89 μmol) was added I$_2$ (2.0 mg, 7.9 μmol).   The reaction mixture was stirred under irradiation of UV light (UVA-100HA Riko) at room temperature for 8 h, quenched with sat. aq. Na$_2$S$_2$O$_3$ (10 mL), and then extracted with AcOEt (10 mL × 3 times).
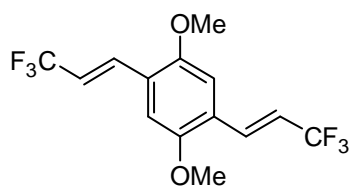
The combined organic layers were dried over anhydrous MgSO$_4$ and concentrated *in vacuo*. The residue was purified by silica gel column chromatography (hexane/AcOEt 6:1) to give (*E,E*)-**3** (22 mg, 77%) as a colorless solid. Mp: 159.5–160.2 °C. T$_d$ (5 wt%): 147.4 °C. R$_f$ 0.63 (hexane/AcOEt 4:1). ^{1}H NMR (400 MHz, CDCl$_3$): δ 3.88 (s, 6H), 6.36 (dq, *J* = 16.4, 7.9 Hz, 2H), 6.94 (s, 2H), 7.39 (dq, *J* = 16.4, 2.4 Hz, 2H), 7.47 (s, 1H); ^{13}C NMR (100 MHz, CDCl$_3$): δ 56.1, 111.0, 117.5 (q, *J* = 33.5 Hz), 123.6 (q, *J* = 268.4 Hz), 124.3, 132.3 (q, *J* = 6.7 Hz), 151.9; ^{19}F NMR (282 MHz, CDCl$_3$): δ −63.7 (d, *J* = 7.9 Hz). IR (KBr): ν 3017, 1661, 1499, 1414, 1310, 1281, 1215, 1111, 1040, 970, 905, 654 cm^{-1}. MS (EI): *m/z* (%) 326 (100, M$^+$), 311 (11), 242 (10). Anal. Calcd for C$_{14}$H$_{12}$F$_6$O$_2$: C, 51.54; H, 3.71. Found: C, 50.99; H, 3.99.

Crystallographic data for (*E,E*)-3

Table 4. Crystal data and structure refinement for (*E,E*)-**3** (see Figure 5).

Empirical formula	C$_{14}$ H$_{12}$ F$_6$ O$_2$
Formula weight	326.24
Temperature	293(2) K
Wavelength	0.71073 Å
Crystal system	Triclinic
Space group	P–1
Unit cell dimensions	a = 9.2332(19) Å, α = 63.033(3)°
	b = 9.244(2) Å, β = 79.160(4)°
	c = 9.675(2) Å, γ = 75.059(3)°
Volume	708.7(3) Å^3
Z	2
Density (calculated)	1.529 Mg/m^3
Absorption coefficient	0.153 mm^{-1}
F(000)	332
Crystal size	0.40 × 0.40 × 0.20 mm^3
Theta range for data collection	2.29 to 25.50°
Index ranges	–11<=h<=11, –10<=k<=11, –8<=l<=11
Reflections collected	3825
Independent reflections	2572 [R(int) = 0.0123]
Completeness to theta = 25.50°	97.8 %
Absorption correction	Empirical
Max. and min. transmission	0.9461 and 0.9461
Refinement method	Full-matrix least-squares on F^2
Data / restraints / parameters	2572 / 0 / 201
Goodness-of-fit on F^2	1.069
Final R indices [I>2sigma(I)]	R$_1$ = 0.0660, wR$_2$ = 0.1941
R indices (all data)	R$_1$ = 0.0809, wR$_2$ = 0.2070
Largest diff. peak and hole	0.415 and –0.306 e.Å^{-3}

UV–vis and fluorescence spectra of 1–3 in cyclohexane.

UV–vis and fluorescence spectra of **1**–**3** in cyclohexane were measured with 1 × 10^{-5} M solution prepared from degassed spectroscopic-grade cyclohexane.

A typical procedure for preparation of spin-coated films 1–3.

In a glass tube, solid sample of (*E,E*)-**2** (2.0 mg) was dissolved in CH_2Cl_2 (0.50 mL). The resulting solution was dropped onto a quartz plate (10 mm × 10 mm) and spin-coated at 100 rpm over a period of 300 sec. The deposited film was dried under reduced pressure at room temperature for 2 h.

A typical procedure for preparation of PMMA films doped with 1–3.

In a glass tube, 5.0 mg of solid sample (*E,E*)-**3** was dissolved in a 15 wt% PMMA chlorobenzene solution (1.00 mL). The resulting solution was dropped onto a quartz plate (10 mm × 10 mm) and spin-coated at 300 rpm for 20 sec followed by further spin-coat at 100 rpm over a period of 280 sec. The deposited film was dried under reduced pressure at room temperature for 1.5 h.

Molecular orbital calculations.

Molecular structures were optimized by DFT methods at the B3LYP/6-31G(d) level using Gaussian 03 package.[7] Cartesian coordinates for geometry optimization study for rotamer **A** of (*E,E*)-**2** and (*E,E*)-**3** were obtained from X-ray crystallographic analysis (Tables 5 and 11) and the coordinates for the other rotamers **B**–**F** are listed in Tables 6–10. Energy levels of molecular orbitals were calculated at the B3LYP/6-31G(d) level. Absolute energies (in hartree) of calculated compounds are as follows: −1290.172984 [(*E,E*)-**2** calculated from rotamer **A**], −1290.172687 [(*E,E*)-**2** calculated from rotamer **B**], −1290.172843 [(*E,E*)-**2** calculated from rotamer **C**], −1290.172991 [(*E,E*)-**2** calculated from rotamer **D**], −1290.172663 [(*E,E*)-**2** calculated from rotamer **E**], −1290.172779 [(*E,E*)-**2** calculated from rotamer **F**], −1290.169840 [(*E,E*)-**3**], −694.728268 [(*E,E*)-**10**], and −694.728678 [(*E,E*)-**11**].

Table 5. Cartesian coordinates of the initial structure of (*E,E*)-**2** (rotamer **A**).

F	−4.791398	1.655800	0.608987	H	−2.604015	1.100334	0.035313	C	3.030803	0.178405	−2.204411
F	−4.930727	1.571873	2.782573	C	1.124196	−0.093083	−0.545296	H	3.731858	−0.483001	−1.714874
F	2.658453	1.644834	−4.039713	O	2.968768	−1.375265	0.195270	C	3.541637	0.802537	−3.458293
C	−0.982919	−0.087427	0.773162	C	1.797101	0.422648	−1.736796	F	3.862727	−0.139062	−4.381298
C	−0.375150	−0.970728	1.699934	H	1.180991	1.105079	−2.318926	C	3.594164	−2.253271	1.122826
O	−1.129376	−1.365321	2.757957	C	−4.651644	0.837722	1.676290	H	3.065042	−3.212205	1.184718
C	0.942100	−1.402524	1.512468	C	−0.574408	−2.248594	3.724370	H	3.656524	−1.801519	2.120513
H	1.388850	−2.075813	2.229068	H	−0.293328	−3.208288	3.273438	H	4.601142	−2.420225	0.737924
C	1.688494	−0.976080	0.408910	H	−1.361988	−2.412227	4.461222	F	−5.626566	−0.102174	1.589064
C	−0.196038	0.313670	−0.313987	H	0.298399	−1.803333	4.217674	F	4.676404	1.509707	−3.227583
H	−0.645741	0.991756	−1.035398	C	−3.302270	0.210529	1.771021				
C	−2.346983	0.432930	0.855421	H	−3.165986	−0.432844	2.629062				

Table 6. Cartesian coordinates of the initial structure of (*E,E*)-**2** (rotamer **B**).

F	−3.809765	−3.028074	−1.412648	C	−2.110612	−0.978487	−0.746783	C	−1.681993	−2.248705	−0.690288
F	−2.679284	−4.271099	−0.024185	H	−3.137827	−0.824838	−1.071271	H	−0.683190	−2.526693	−0.383936
F	4.710949	0.938255	1.620062	C	0.735917	1.265688	0.325010	C	2.747159	−0.184459	0.884922
C	−1.408041	0.266346	−0.438574	O	0.925212	3.613467	0.541749	H	2.288887	−1.140086	0.671976
C	−1.954051	1.570997	−0.529517	C	2.105891	0.986832	0.753803	C	4.166079	−0.265702	1.335229
O	−3.244211	1.669712	−0.941482	H	2.673396	1.883400	0.995225	F	4.949616	−0.845463	0.390988
C	−1.180414	2.690231	−0.204650	C	−2.559284	−3.397695	−1.055442	C	0.393126	4.928728	0.445073
H	−1.613344	3.676812	−0.279811	C	−3.847704	2.952194	−1.056166	H	−0.464191	5.063415	1.116059
C	0.145636	2.549723	0.218017	H	−3.876671	3.467898	−0.088401	H	0.096316	5.164671	−0.584288
C	−0.076554	0.175979	−0.013214	H	−4.867019	2.769033	−1.398888	H	1.199845	5.596375	0.750819
H	0.359449	−0.817336	0.062254	H	−3.323537	3.575918	−1.790752	F	−2.040422	−4.103599	−2.091765

154

F	4.284534	−1.031858	2.448776

Table 7. Cartesian coordinates of the initial structure of (*E,E*)-**2** (rotamer **C**).

F	−2.436934	−4.023956	−0.519758	H	−1.173588	−2.067896	−0.528190	C	1.570650	1.325660	−2.532458
F	−3.983962	−3.787691	0.997416	C	0.854057	1.302682	−0.093712	H	1.072741	0.413046	−2.828775
F	2.949864	3.133242	−3.230891	O	1.567086	3.057889	1.322521	C	2.314384	2.008562	−3.629371
C	−0.569959	−0.518246	0.819906	C	1.526962	1.818414	−1.285211	F	1.483754	2.357320	−4.644294
C	−0.526902	0.118073	2.085511	H	2.065830	2.747153	−1.108449	C	1.610021	3.712248	2.584402
O	−1.200653	−0.484071	3.099145	C	−2.641943	−3.810289	0.799422	H	2.075558	3.077331	3.348280
C	0.183365	1.310708	2.258372	C	−1.197977	0.107768	4.392140	H	0.607054	4.010296	2.913912
H	0.205167	1.781429	3.230156	H	−0.181580	0.172167	4.799753	H	2.220837	4.603452	2.433782
C	0.867445	1.901500	1.190758	H	−1.798150	−0.552253	5.019973	F	−2.179959	−4.903562	1.457307
C	0.127830	0.111478	−0.218598	H	−1.652379	1.106084	4.375283	F	3.251475	1.190098	−4.170659
H	0.105710	−0.362320	−1.197115	C	−2.000633	−2.563033	1.305612				
C	−1.272530	−1.763079	0.511698	H	−2.169503	−2.365988	2.355084				

Table 8. Cartesian coordinates of the initial structure of (*E,E*)-**2** (rotamer **D**).

F	−2.329363	−3.630605	2.530660	H	−1.073813	−1.924287	1.564036	C	2.736683	2.539582	−0.216831
F	−3.134871	−4.840215	0.906181	C	0.778536	0.935420	−0.448870	H	2.607069	3.049390	−1.161224
F	4.039439	2.366390	1.765649	O	0.914326	2.261694	−2.402695	C	3.880625	3.034493	0.601199
C	−1.022168	−0.764551	−0.234712	C	1.938117	1.545391	0.200560	F	3.732484	4.347416	0.910926
C	−1.496923	−0.385479	−1.515111	H	2.166680	1.111192	1.171854	C	2.049372	2.887262	−1.817283
O	−2.588115	−1.042975	−1.985186	C	−3.114617	−3.589200	1.430851	H	2.855903	2.165471	−1.638729
C	−0.854681	0.622167	−2.242375	C	−3.191366	−2.057450	−1.192063	H	1.788395	3.388563	−0.877103
H	−1.230656	0.897905	−3.216558	H	−2.493429	−2.881505	−0.999253	H	2.383370	3.630405	−2.542687
C	0.266689	1.279160	−1.724989	H	−4.034488	−2.427174	−1.777264	F	−4.379006	−3.334395	1.852609
C	0.104039	−0.080475	0.240318	H	−3.558260	−1.654635	−0.239946	F	5.050098	2.935214	−0.079601
H	0.482758	−0.358236	1.221078	C	−2.668993	−2.587349	0.420470				
C	−1.603676	−1.796924	0.622179	H	−3.274568	−2.553039	−0.474426				

Table 9. Cartesian coordinates of the initial structure of (*E,E*)-**2** (rotamer **E**).

F	−4.657260	−0.000700	1.884642	H	−2.604847	−1.095120	1.994809	C	1.778401	1.232575	−1.778623
F	−4.860926	0.789115	−0.136655	C	1.495626	−0.636542	−0.079224	H	0.777645	1.634765	−1.705729
F	3.901874	1.413285	−2.834843	O	3.330978	−2.059801	0.368760	C	2.663941	1.948309	−2.741045
C	−0.658959	−0.991258	1.108311	C	2.204365	0.179984	−1.063819	F	2.817114	3.251159	−2.393533
C	−0.072515	−2.085536	1.791794	H	3.234972	−0.131798	−1.221368	C	4.066863	−1.296829	−0.579248
O	−0.859415	−2.750288	2.676592	C	−4.092901	0.831627	0.980957	H	4.152232	−0.248210	−0.268659
C	1.257332	−2.445513	1.549588	C	−2.203493	−2.329846	2.873567	H	3.610594	−1.350333	−1.575393
H	1.687461	−3.282398	2.079710	H	−2.248683	−1.302181	3.254644	H	5.060369	−1.746163	−0.612002
C	2.037608	−1.738019	0.629033	H	−2.619336	−3.010138	3.618072	F	−4.207842	2.091321	1.472330
C	0.161553	−0.312349	0.198478	H	−2.785390	−2.405277	1.946688	F	2.132824	1.948917	−3.989616
H	−0.271422	0.530424	−0.335128	C	−2.672612	0.498511	0.672787				
C	−2.033035	−0.518239	1.270717	H	−2.210208	1.142538	−0.062161				

Table 10. Cartesian coordinates of the initial structure of (*E,E*)-**2** (rotamer **F**).

F	0.107421	−2.293406	4.026749	H	−0.032231	−1.008583	2.089737	C	−1.222295	2.873428	−0.475004
F	1.894626	−3.529280	3.855149	C	−0.038171	0.829823	−1.414709	H	−1.307053	2.524258	0.544545
F	−1.697247	4.636534	−1.999231	O	0.536107	0.797270	−3.709054	C	−1.791249	4.230739	−0.713144
C	0.520294	−1.118385	0.024354	C	−0.649620	2.157594	−1.454781	F	−1.167954	5.165991	0.047416
C	1.092359	−1.755757	−1.104809	H	−0.620703	2.616356	−2.441128	C	−0.044720	2.091941	−3.803072
O	1.620443	−2.991653	−0.910746	C	0.701095	−3.247402	3.274843	H	0.477520	2.811925	−3.161011
C	1.100956	−1.121341	−2.351478	C	1.577362	−3.577361	0.384324	H	−1.110263	2.071324	−3.543183
H	1.541229	−1.622391	−3.200906	H	2.132144	−2.974595	1.113876	H	0.067285	2.390315	−4.846363
C	0.545697	0.152254	−2.514083	H	2.055330	−4.552710	0.283074	F	−0.050952	−4.371155	3.389251
C	−0.021002	0.156124	−0.186782	H	0.544158	−3.712483	0.727297	F	−3.103964	4.279216	−0.373374
H	−0.464097	0.660735	0.668498	C	0.874511	−2.855411	1.846759				
C	0.447659	−1.674071	1.374963	H	1.364570	−3.599041	1.233902				

Table 11. Cartesian coordinates of the initial structure of (*E,E*)-**3**.

O	0.126747	0.085229	−2.763632	H	1.923900	1.079661	−3.142802	F	−4.425588	0.007216	−3.474868
C	0.103225	0.048948	−1.398834	H	1.151012	0.200171	−4.491197	O	−0.126757	−0.085197	2.763648
C	1.247218	0.063028	−0.604195	H	2.004884	−0.708605	−3.213676	C	−0.103234	−0.048918	1.398848
H	2.223057	0.096441	−1.071703	C	−3.633220	−0.235041	−1.252005	C	−1.247228	−0.062998	0.604210
C	−2.368475	−0.033765	−1.647887	F	−3.917675	−0.429261	−0.222027	H	−2.223068	−0.096409	1.071717
H	−2.184832	0.128128	−2.704366	F	−5.692824	0.726091	−1.853567	C	2.368470	0.033784	1.647899
C	−1.177270	−0.018203	−0.796672	F	−5.450777	−1.407356	−2.171819	H	2.184828	−0.128092	2.704380
C	1.379878	0.168771	−3.424771	C	−4.788088	−0.224601	−2.195971	C	1.177261	0.018230	0.796688

C	−1.379888	−0.168735	3.424785	C	3.633218	0.235026	1.252005	C	4.788096	0.224573	2.195961
H	−1.923914	−1.079622	3.142817	H	3.917669	0.429221	0.222024	F	4.425609	−0.007216	3.474864
H	−1.151023	−0.200134	4.491211	F	5.692805	−0.726145	1.853557				
H	−2.004891	0.708644	3.213691	F	5.450812	1.407312	2.171782				

Table 12. Cartesian coordinates of the initial structure of (*E,E*)-**10**.

C	−1.325814	0.419839	0.222363	C	1.454206	0.929915	−2.287595	C	3.251268	−1.746005	0.572027
C	−0.718045	−0.463462	1.149135	H	0.838095	1.612346	−2.869725	H	2.722147	−2.704939	0.633919
O	−1.472272	−0.858055	2.207158	C	−4.994539	1.344988	1.125491	H	3.313629	−1.294253	1.569715
C	0.599204	−0.895258	0.961669	C	−0.917303	−1.741328	3.173571	H	4.258246	−1.912959	0.187125
H	1.045954	−1.568547	1.678270	H	−0.636224	−2.701021	2.722640	H	2.499700	1.976483	−4.469287
C	1.345599	−0.468814	−0.141889	H	−1.704884	−1.904960	3.910423	H	4.093616	1.867476	−3.827154
C	−0.538933	0.820936	−0.864786	H	−0.044496	−1.296067	3.666875	H	3.451909	0.567388	−4.736845
H	−0.988636	1.499023	−1.586197	C	−3.645166	0.717795	1.220223	H	−5.105143	1.992429	0.280809
C	−2.689878	0.940196	0.304623	H	−3.508882	0.074422	2.078264	H	−5.214641	1.923983	1.997971
H	−2.946910	1.607600	−0.515486	C	2.687908	0.685672	−2.755209				
C	0.781301	0.414183	−1.096095	H	3.388963	0.024266	−2.265672				
O	2.625873	−0.867999	−0.355528	C	3.198741	1.309804	−4.009091				

Table 13. Cartesian coordinates of the initial structure of (*E,E*)-**11**.

O	0.126750	0.085221	−2.763637	H	−3.917671	−0.429269	−0.222032	H	−2.004887	0.708636	3.213685
C	0.103228	0.048940	−1.398838	C	−4.788084	−0.224609	−2.195976	C	3.633221	0.235018	1.252001
C	1.247221	0.063020	−0.604200	O	−0.126754	−0.085205	2.763642	H	3.917672	0.429213	0.222018
H	2.223060	0.096433	−1.071708	C	−0.103231	−0.048926	1.398844	C	4.788099	0.224565	2.195956
C	−2.368472	−0.033773	−1.647892	C	−1.247225	−0.063006	0.604205	H	−4.500630	−0.040783	−3.210115
H	−2.184829	0.128120	−2.704372	H	−2.223064	−0.096417	1.071712	H	−5.501830	0.525392	−1.925854
C	−1.177267	−0.018211	−0.796677	C	2.368470	0.033776	1.647894	H	−5.311014	−1.157925	−2.176917
C	1.379881	0.168763	−3.424775	H	2.184830	−0.128100	2.704376	H	4.500653	0.040760	3.210103
H	1.923903	1.079653	−3.142808	C	1.177264	0.018222	0.796682	H	5.311052	1.157869	2.176876
H	1.151015	0.200161	−4.491201	C	−1.379885	−0.168743	3.424781	H	5.501824	−0.525456	1.925834
H	2.004887	−0.708614	−3.213681	H	−1.923911	−1.079630	3.142812				
C	−3.633217	−0.235049	−1.252009	H	−1.151020	−0.200142	4.491206				

Table 14. Cartesian coordinates of the optimized structure of (*E,E*)-**2** from rotamer **A**.

F	−4.791398	1.655800	0.608987	H	−2.604015	1.100334	0.035313	C	3.030803	0.178405	−2.204411
F	−4.930727	1.571873	2.782573	C	1.124196	−0.093083	−0.545296	H	3.731858	−0.483002	−1.714874
F	2.658454	1.644834	−4.039712	O	2.968768	−1.375265	0.195270	C	3.541638	0.802537	−3.458293
C	−0.982919	−0.087427	0.773162	C	1.797101	0.422648	−1.736796	F	3.862727	−0.139062	−4.381299
C	−0.375150	−0.970728	1.699934	H	1.180991	1.105079	−2.318926	C	3.594164	−2.253271	1.122826
O	−1.129376	−1.365321	2.757957	C	−4.651644	0.837722	1.676290	H	3.065042	−3.212206	1.184718
C	0.942100	−1.402524	1.512468	C	−0.574407	−2.248595	3.724370	H	3.656525	−1.801519	2.120513
H	1.388850	−2.075814	2.229068	H	−0.293328	−3.208288	3.273438	H	4.601142	−2.420225	0.737924
C	1.688494	−0.976080	0.408910	H	−1.361988	−2.412227	4.461223	F	−5.626566	−0.102174	1.589064
C	−0.196038	0.313670	−0.313987	H	0.298400	−1.803334	4.217674	F	4.676404	1.509707	−3.227583
H	−0.645741	0.991757	−1.035398	C	−3.302270	0.210529	1.771021				
C	−2.346983	0.432929	0.855421	H	−3.165986	−0.432844	2.629062				

Table 15. Cartesian coordinates of the optimized structure of (*E,E*)-**2** from rotamer **B**.

F	−4.014166	−2.979675	−1.287483	H	−3.252719	−0.772818	−0.886644	C	2.888933	−0.075108	0.827278
F	−2.747809	−4.305603	−0.109064	C	0.760922	1.163715	0.359014	H	2.552063	−1.022489	0.416669
F	4.688521	1.066974	1.869256	O	0.993804	3.503093	0.513512	C	4.276094	−0.118973	1.371520
C	−1.367124	0.171525	−0.399988	C	2.136872	1.034107	0.843113	F	5.168961	−0.487913	0.419582
C	−1.900774	1.477682	−0.537669	H	2.577787	1.940406	1.244455	C	0.483000	4.825087	0.413614
O	−3.184409	1.556239	−0.977040	C	−2.738799	−3.385629	−1.106070	H	-0.374190	4.975034	1.082004
C	−1.129171	2.603703	−0.234186	C	−3.799778	2.829914	−1.109372	H	0.191346	5.063807	−0.616881
H	−1.549720	3.592268	−0.348633	H	−3.838425	3.357915	−0.148269	H	1.299516	5.480979	0.718895
C	0.188470	2.451898	0.208199	H	−4.815396	2.632608	−1.455336	F	−2.363833	−4.047153	−2.229266
C	−0.049076	0.065690	0.054763	H	−3.278611	3.451021	−1.848722	F	4.384396	−1.032788	2.368339
H	0.359897	−0.927570	0.207934	C	−1.804316	−2.264904	−0.801487				
C	−2.204643	−0.989064	−0.709337	H	−0.774249	−2.582673	−0.668957				

Table 16. Cartesian coordinates of the optimized structure of (*E,E*)-**2** from rotamer **C**.

F	−2.486793	−4.076861	−0.477103	O	−1.203234	−0.500582	3.083934	H	0.055018	−0.444740	−1.223717
F	−4.018541	−3.816300	1.050736	C	0.176432	1.282371	2.213502	C	−1.304030	−1.808751	0.515961
F	2.976048	3.230293	−3.161867	H	0.209262	1.765506	3.178924	H	−1.217492	−2.127037	−0.521051
C	−0.593417	−0.562154	0.799507	C	0.847997	1.854574	1.127503	C	0.819577	1.238826	−0.147252
C	−0.536601	0.090155	2.059112	C	0.093975	0.048505	−0.256845	O	1.555266	3.010945	1.221788

C	1.533216	1.855012	−1.267070	C	−2.027096	−2.596454	1.326688	H	2.109464	3.063601	3.234370
H	2.049770	2.779611	−1.033315	H	−2.184438	−2.386628	2.375389	H	0.635981	3.995995	2.817267
C	−2.678411	−3.846834	0.841165	C	1.610747	1.397048	−2.524458	H	2.240905	4.572118	2.289004
C	−1.188975	0.104161	4.371042	H	1.132631	0.482907	−2.863831	F	−2.214689	−4.934202	1.507413
H	−0.169444	0.169440	4.770574	C	2.370406	2.103305	−3.594951	F	3.333599	1.306399	−4.121689
H	−1.786582	−0.547806	5.009669	F	1.561476	2.453299	−4.626327				
H	−1.640383	1.103698	4.347765	C	1.629603	3.686718	2.469197				

Table 17. Cartesian coordinates of the optimized structure of (*E,E*)-**2** from rotamer **D**.

F	−2.455778	−3.449272	2.854410	H	−1.137035	−1.816473	1.844551	C	2.732684	2.571467	0.002039
F	−2.938561	−4.891918	1.294487	C	0.839881	0.894159	−0.254720	H	2.685832	2.982667	−0.996637
F	3.843392	2.624797	2.104481	O	1.128556	2.039303	−2.304080	C	3.784417	3.173777	0.870515
C	−0.926382	−0.842964	−0.050700	C	1.916668	1.600006	0.438825	F	3.584986	4.505825	1.035526
C	−1.282671	−0.602778	−1.401267	H	2.058443	1.268963	1.465701	C	0.782894	2.289090	−3.660693
O	−2.302742	−1.341920	−1.908592	C	−3.077955	−3.593384	1.662948	H	0.920430	1.393629	−4.279258
C	−0.601024	0.357120	−2.156706	C	−2.710281	−1.143915	−3.256607	H	1.464199	3.070787	−3.999506
H	−0.886701	0.527038	−3.184237	H	−1.895937	−1.366545	−3.957079	H	−0.251269	2.643858	−3.750683
C	0.445623	1.099863	−1.600421	H	−3.067158	−0.119502	−3.419606	F	−4.403622	−3.400735	1.878346
C	0.127811	−0.076167	0.461892	H	−3.530995	−1.843208	−3.422268	F	5.014798	3.040713	0.314140
H	0.415874	−0.247676	1.496364	C	−2.563319	−2.672590	0.609201				
C	−1.560851	−1.811643	0.842310	H	−3.061297	−2.760386	−0.346291				

Table 18. Cartesian coordinates of the optimized structure of (*E,E*)-**2** from rotamer **E**.

F	−4.717520	0.128014	2.088748	H	−2.656652	−1.025923	1.961112	C	1.744053	1.310464	−2.069287
F	−4.951374	1.183586	0.196094	C	1.322174	−0.445779	−0.327080	H	0.812040	1.846248	−1.915169
F	3.775049	1.255439	−3.295745	O	3.172410	−1.854399	0.056778	C	2.600806	1.903409	−3.135250
C	−0.743344	−0.718567	0.995675	C	2.097963	0.219566	−1.318075	F	2.890821	3.201238	−2.868438
C	−0.131711	−1.793998	1.687939	H	3.059875	−0.230019	−1.597004	C	3.807476	−2.942295	0.713492
O	−0.886618	−2.395278	2.644617	C	−4.166904	1.074400	1.297659	H	3.905890	−2.757368	1.790588
C	1.175283	−2.189204	1.387618	C	−0.357002	−3.505121	3.356391	H	4.800399	−3.017249	0.267871
H	1.628860	−3.006457	1.929516	H	0.108762	−4.332945	2.680300	H	3.263225	−3.881022	0.550450
C	1.898414	−1.522592	0.393464	H	−1.145813	−3.820382	4.040843	F	−4.268233	2.256556	1.954342
C	0.010950	−0.088145	0.001917	H	0.532709	−3.222906	3.933298	F	1.970217	1.894730	−4.336452
H	−0.458225	0.710426	−0.563239	C	−2.752740	0.779187	0.929706				
C	−2.117130	−0.332710	1.324650	H	−2.291345	1.549679	0.318955				

Table 19. Cartesian coordinates of the optimized structure of (*E,E*)-**2** from rotamer **F**.

F	0.241014	−2.202889	4.252798	H	0.000665	−0.920473	2.328418	C	−1.043282	3.116055	−0.330522
F	2.000495	−3.452099	3.949463	C	−0.228573	0.898659	−1.172380	H	−0.892267	2.894520	0.721962
F	−1.778637	4.743857	−1.892020	O	0.101606	0.836142	−3.504649	C	−1.599444	4.476319	−0.580323
C	0.363175	−1.060255	0.223382	C	−0.756014	2.256574	−1.318075	F	−0.788015	5.441766	−0.080959
C	0.790061	−1.735940	−0.950077	H	−0.919070	2.584546	−2.339140	C	0.500135	0.177907	−4.698931
O	1.271341	−2.994985	−0.790312	C	0.763893	−3.170845	3.466898	H	0.319160	0.891710	−5.503797
C	0.705772	−1.115452	−2.200191	C	1.705772	−3.728508	−1.928502	H	−0.094180	−0.727511	−4.875312
H	1.034358	−1.643709	−3.083203	H	2.039280	−4.694652	−1.547209	H	1.566141	−0.081209	−4.676328
C	0.202483	0.184858	−2.316291	H	2.542187	−3.227392	−2.431208	F	0.018393	−4.288125	3.659161
C	−0.133787	0.238728	0.056571	H	0.886099	−3.881805	−2.641230	F	−2.800298	4.636445	0.030294
H	−0.478026	0.756647	0.947106	C	0.817798	−2.798934	2.023850				
C	0.390908	−1.606889	1.579656	H	1.226783	−3.563169	1.377887				

Table 20. Cartesian coordinates of the optimized structure of (*E,E*)-**3**.

O	0.126747	0.085229	−2.763633	H	−3.917674	−0.429261	−0.222028	C	−1.379889	−0.168734	3.424785
C	0.103225	0.048948	−1.398834	F	−5.692823	0.726091	−1.853568	H	−1.923915	−1.079622	3.142817
C	1.247218	0.063028	−0.604195	F	−5.450777	−1.407356	−2.171820	H	−1.151024	−0.200133	4.491211
H	2.223057	0.096441	−1.071703	C	−4.788086	−0.224601	−2.195972	H	−2.004891	0.708644	3.213690
C	−2.368475	−0.033761	−1.647888	F	−4.425589	0.007216	−3.474868	C	3.633224	0.235026	1.252006
H	−2.184832	0.128128	−2.704367	O	−0.126757	−0.085197	2.763647	H	3.917669	0.429221	0.222024
C	−1.177270	−0.018203	−0.796673	C	−0.103234	−0.048918	1.398848	F	5.692804	−0.726145	1.853558
C	1.379878	0.168771	−3.424771	C	−1.247228	−0.062998	0.604209	F	5.450811	1.407312	2.171782
H	1.923900	1.079661	−3.142803	H	−2.223068	−0.096409	1.071716	C	4.788095	0.224573	2.195961
H	1.151012	0.200169	−4.491197	C	2.368470	0.033784	1.647899	F	4.425609	−0.007215	3.474864
H	2.004884	−0.708605	−3.213676	H	2.184828	−0.128092	2.704381				
C	−3.633220	−0.235041	−1.252005	C	1.177261	0.018230	0.796688				

Table 21. Cartesian coordinates of the optimized structure of (*E,E*)-**10**.

C	−1.329221	0.408036	0.225053	O	−1.471138	−0.869942	2.218174	H	1.047202	−1.570700	1.680836
C	−0.718409	−0.470018	1.150615	C	0.599653	−0.899391	0.962498	C	1.347679	−0.474658	−0.140770

C	−0.537471	0.802597	−0.862803	H	−0.620689	−2.710085	2.719331	H	3.302896	−1.304061	1.585069
H	−0.988770	1.477326	−1.587131	H	−1.685018	−1.924217	3.917367	H	4.257024	−1.929110	0.212206
C	−2.698195	0.933198	0.301806	H	−0.029105	−1.308179	3.663735	H	2.463115	1.979585	−4.506497
H	−2.945599	1.583320	−0.539911	C	−3.661138	0.744099	1.220186	H	4.106639	1.949945	−3.837045
C	0.785798	0.402697	−1.097552	H	−3.475882	0.110057	2.080108	H	3.517058	0.574729	−4.762886
O	2.636385	−0.878158	−0.347674	C	2.695340	0.710975	−2.770363	H	−5.123418	1.996193	0.234550
C	1.455953	0.923360	−2.295748	H	3.377136	0.058184	−2.236827	H	−5.226897	2.006967	2.006445
H	0.816419	1.590072	−2.877882	C	3.214284	1.338151	−4.032048	H	−5.813937	0.613333	1.107072
C	−5.021043	1.374480	1.131105	C	3.246049	−1.753868	0.584994				
C	−0.905602	−1.751462	3.172777	H	2.713696	−2.712131	0.648444				

Table 22. Cartesian coordinates of the optimized structure of (*E*,*E*)-**11**.

O	0.133321	0.066690	−2.766453	H	−3.816574	−0.658490	−0.273559	H	−1.992665	0.778143	3.200685
C	0.103647	0.042093	−1.394463	C	−4.820522	−0.237948	−2.190953	C	3.625507	0.299634	1.285560
C	1.247853	0.017100	−0.599661	O	−0.133322	−0.066687	2.766454	H	3.816580	0.658471	0.273556
H	2.226195	−0.001549	−1.063644	C	−0.103646	−0.042090	1.394462	C	4.820523	0.237939	2.190955
C	−2.378453	0.038145	−1.650771	C	−1.247853	−0.017097	0.599662	H	−4.547576	0.110479	−3.192776
H	−2.209120	0.347018	−2.679500	H	−2.226195	0.001552	1.063643	H	−5.589018	0.440775	−1.794129
C	−1.180264	0.017897	−0.802361	C	2.378451	−0.038143	1.650771	H	−5.298102	−1.222808	−2.291060
C	1.390821	0.115737	−3.414207	H	2.209117	−0.347008	2.679503	H	4.547573	−0.110479	3.192779
H	1.962130	1.008972	−3.126497	C	1.180264	−0.017895	0.802361	H	5.298106	1.222797	2.291055
H	1.175540	0.155321	−4.484013	C	−1.390821	−0.115732	3.414205	H	5.589016	−0.440790	1.794135
H	1.992665	−0.778136	−3.200686	H	−1.962132	−1.008966	3.126499				
C	−3.625504	−0.299642	−1.285560	H	−1.175541	−0.155316	4.484011				

References

(1) (a) *Highly Efficient OLEDs with Phosphorescent Materials*; Yersin, H., Ed.; Wiley–VCH, Weinheim, 2008. (b) *Organic Light-Emitting Devices. Synthesis, Properties and Applications*; Müllen, K., Scherf, U., Eds.; Wiley-VCH, Weinheim, 2006. (c) Friend, R. H.; Gymer, R. W.; Holmes, A. B.; Burroughes, J. H.; Marks, R. N.; Taliani, C.; Bradley, D. D. C.; Dos Santos, D. A.; Brédas, J. L.; Lögdlund, M.; Salaneck, W. R. *Nature* **1999**, *397*, 121.

(2) (a) Samuel, I. D. W.; Turnbull, G. A. *Chem. Rev.* **2007**, *107*, 1272. (b) Samuel, I. D. W.; Turnbull, G. A. *Mater. Today* **2004**, *7*, 28. (c) Scherf, U.; Riechel, S.; Lemmer, U.; Mahrt, R. F. *Curr. Opin. Solid State Mater. Sci.* **2001**, *5*, 143. (d) McGehee, M. D.; Heeger, A. J. *Adv. Mater.* **2000**, *12*, 1655. (e) Kranzelbinder, G.; Leising, G. *Rep. Prog. Phys.* **2000**, *63*, 729. (f) Tessler, N. *Adv. Mater.* **1999**, *11*, 363. (g) Kozlov, V. G.; Forrest, S. R. *Curr. Opin. Solid State Mater. Sci.* **1999**, *4*, 203.

(3) Reviews on fluorescent sensors: (a) Thomas III, S. W.; Joly, G. D.; Swager, T. M. *Chem. Rev.* **2007**, *107*, 1339. (b) Basabe-Desmonts, L.; Reinhoudt, D. N.; Crego-Calama, M. *Chem. Soc. Rev.* **2007**, *36*, 993. (c) Wolfbeis, O. S. *J. Mater. Chem.* **2005**, *15*, 2657. (d) Callan, J. F.; de Silva, A. P.; Magri, D. C. *Tetrahedron* **2005**, *61*, 8551. (e) Martinez-Manez, R.; Sancenon, F. *Chem. Rev.* **2003**, *103*, 4419. (f) de Silva, A. P.; Gunaratne, H. Q. N.; Gunnlaugsson, T.; Huxley, A. J. M.; McCoy, C. P.; Rademacher, J. T.; Rice, T. E. *Chem. Rev.* **1997**, *97*, 1515. Selected examples of solid-state fluorescent sensors: (g) Sreejith, S.; Divya, K. P.; Ajayaghosh, A. *Chem. Commun.* **2008**, 2903. (h) Dale, T. J.; Rebek, J. *J. Am. Chem. Soc.* **2006**, *128*, 4500. (i) Zhang, S. W.; Swager, T. M. *J. Am. Chem. Soc.* **2003**, *125*, 3420. (j) Yang, J. S.; Swager, T. M. *J. Am. Chem. Soc.* **1998**, *120*, 11864. (k) Yang, J. S.; Swager, T. M. *J. Am. Chem. Soc.* **1998**, *120*, 5321.

(4) (a) Saragi, T. P. I.; Spehr, T.; Siebert, A.; Fuhrmann-Lieker, T.; Salbeck, J. *Chem. Rev.* **2007**, *107*, 1011. (b) Burn, P. L.; Lo, S. C.; Samuel, I. D. W. *Adv. Mater.* **2007**, *19*, 1675. (c) Perepichka, I. F.; Perepichka, D. F.; Meng, H.; Wudl, F. *Adv. Mater.* **2005**, *17*, 2281. (d) Akcelrud, L. *Prog. Polym. Sci.* **2003**, *28*, 875. (e) Mitschke, U.; Bäuerle, P. *J. Mater. Chem.* **2000**, *10*, 1471. (f) Kim, D. Y.; Cho, H. N.; Kim, C. Y. *Prog. Polym. Sci.* **2000**, *25*, 1089. (g) Kraft, A.; Grimsdale, A. C.; Holmes, A. B. *Angew. Chem. Int. Ed.* **1998**, *37*, 402.

(5) (a) Lai, W. Y.; Xia, R.; He, Q. Y.; Levermore, P. A.; Huang, W.; Bradley, D. D. C. *Adv. Mater.* **2009**, *21*, 355. (b) Shimizu, M.; Mochida, K.; Hiyama, T. *Angew. Chem. Int. Ed.* **2008**, *47*, 9760. (c) Huang, J.; Qiao, X.; Xia, Y.; Zhu, X.; Ma, D.; Cao, Y.; Roncali, J. *Adv. Mater.* **2008**, *20*, 4172. (d) Lai, M. Y.; Chen, C. H.; Huang, W. S.; Lin, J. T.; Ke, T. H.; Chen, L. Y.; Tsai, M. H.; Wu, C. C. *Angew. Chem. Int. Ed.* **2008**, *47*, 581. (e) Ishow, E.; Brosseau, A.; Clavier, G.; Nakatani, K.; Tauc, P.; Fiorini-Debuisschert, C.; Neveu, S.; Sandre, O.; Léaustic, A. *Chem. Mater.* **2008**, *20*, 6597. (f) Lee, Y. T.; Chiang, C. L.; Chen, C. T. *Chem. Commun.* **2008**, 217. (g) Kitamura, C.; Matsumoto, C.; Kawatsuki, N.; Yoneda, A.; Asada, K.; Kobayashi, T.; Naito, H. *Bull. Chem. Soc. Jpn.* **2008**, *81*, 754. (h) Chen, Z.; Bouffard, J.; Kooi, S. E.; Swager, T. M. *Macromolecules* **2008**, *41*, 6672. (i) Wakamiya, A.; Mori, K.; Yamaguchi, S. *Angew. Chem. Int. Ed.* **2007**, *46*, 4273. (j) Luo, J.; Zhou, Y.; Niu, Z. Q.; Zhou, Q. F.; Ma, Y.; Pei, J. *J. Am. Chem. Soc.* **2007**, *129*, 11314. (k) Xie, Z.; Wang, H.; Li, F.; Xie, W.; Liu, L.; Yang, B.; Ye, L. Ma, Y. *Cryst. Growth Des.* **2007**, *7*, 2512. (l) Li, Y.; Li, F.; Zhang, H.; Xie, Z.;

Xie, W.; Xu, H.; Li, B.; Shen, F.; Ye, L.; Hanif, M.; Ma, D.; Ma, Y. *Chem. Commun.* **2007**, 231. (m) Zhao, C. H.; Wakamiya, A.; Inukai, Y.; Yamaguchi, S. *J. Am. Chem. Soc.* **2006**, *128*, 15934. (n) Hayer, A.; de Halleux, V.; Köhler, A.; El-Garoughy, A.; Meijer, E. W.; Barbera, J.; Tant, J.; Levin, J.; Lehmann, M.; Gierschner, J.; Cornil, J.; Geerts, Y. H. *J. Phys. Chem. B* **2006**, *110*, 7653. (o) Kim, Y.; Bouffard, J.; Kooi, S. E.; Swager, T. M. *J. Am. Chem. Soc.* **2005**, *127*, 13726. (p) Lee, S. H.; Jang, B. B.; Kafafi, Z. H. *J. Am. Chem. Soc.* **2005**, *127*, 9071. (q) Chan, K. L.; McKiernan, M. J.; Towns, C. R.; Holmes, A. B. *J. Am. Chem. Soc.* **2005**, *127*, 7662. (r) Yui, G.; Yin, S.; Liu, Y.; Chen, J.; Xu, X.; Sun, X.; Ma, D.; Zhan, X.; Peng, Q.; Shuai, Z.; Tang, B.; Zhu, D.; Fang, W.; Luo, Y. *J. Am. Chem. Soc.* **2005**, *127*, 6335. (s) Chao, T. C.; Lin, Y. T.; Yang, C. Y.; Hung, T. S.; Chou, H. C.; Wu, C. C.; Wong, K. T. *Adv. Mater.* **2005**, *17*, 992. (t) Wong, K. T.; Chien, Y. Y.; Chen, R. T.; Wang, C. F.; Lin, Y. T.; Chiang, H. H.; Hsieh, P. Y.; Wu, C. C.; Chou, C. H.; Su, Y. O.; Lee, G. H.; Peng, S. M. *J. Am. Chem. Soc.* **2002**, *124*, 11576. (u) Ariu, M.; Lidzey, D. G.; Sims, M.; Cadby, A. J.; Lane, P. A.; Bradley, D. D. C. *J. Phys.: Condens. Matter* **2002**, *14*, 9975.

 (6) Pyromellitic diimides were recently reported to act as minimal cores for n-channel transistor materials with high mobility. Zheng, Q.; Huang, J.; Sarjeant, A.; Katz, H. E. *J. Am. Chem. Soc.* **2008**, *130*, 14410.

 (7) Borden, W. T. *J. Am. Chem. Soc.* **1970**, *92*, 4898.

 (8) Rylander, P. N. In *Hydrogenation Methods*; Academic Press: New York, 1985, pp. 54–65.

 (9) Konno, T.; Chae, J.; Kanda, M.; Nagai, G.; Tamura, K.; Ishihara, T.; Yamanaka, H. *Tetrahedron*, **2003**, *59*, 7571.

(10) Frisch, M. J.; Trucks, G. W.; Schlegel, H. B.; Scuseria, G. E.; Robb, M. A.; Cheeseman, J. R.; Montgomery, J. A., Jr.; Vreven, T.; Kudin, K. N.; Burant, J. C.; Millam, J. M.; Iyengar, S. S.; Tomasi, J.; Barone, V.; Mennucci, B.; Cossi, M.; Scalmani, G.; Rega, N.; Petersson, G. A.; Nakatsuji, H.; Hada, M.; Ehara, M.; Toyota, K.; Fukuda, R.; Hasegawa, J.; Ishida, M.; Nakajima, T.; Honda, Y.; Kitao, O.; Nakai, H.; Klene, M.; Li, X.; Knox, J. E.; Hratchian, H. P.; Cross, J. B.; Bakken, V.; Adamo, C.; Jaramillo, J.; Gomperts, R.; Stratmann, R. E.; Yazyev, O.; Austin, A. J.; Cammi, R.; Pomelli, C.; Ochterski, J. W.; Ayala, P. Y.; Morokuma, K.; Voth, G. A.; Salvador, P.; Dannenberg, J. J.; Zakrzewski, V. G.; Dapprich, S.; Daniels, A. D.; Strain, M. C.; Farkas, O.; Malick, D. K.; Rabuck, A. D.; Raghavachari, K.; Foresman, J. B.; Ortiz, J. V.; Cui, Q.; Baboul, A. G.; Clifford, S.; Cioslowski, J.; Stefanov, B. B.; Liu, G.; Liashenko, A.; Piskorz, P.; Komaromi, I.; Martin, R. L.; Fox, D. J.; Keith, T.; Al-Laham, M. A.; Peng, C. Y.; Nanayakkara, A.; Challacombe, M.; Gill, P. M. W.; Johnson, B.; Chen, W.; Wong, M. W.; Gonzalez, C.; Pople, J. A. *Gaussian 03*, revision C.02; Gaussian, Inc.: Wallingford, CT, 2004.

(11) Kovalenko, S. V.; Peabody, S.; Manoharan, M.; Clark, R. J.; Alabugin, I. V. *Org. Lett.* **2004**, *6*, 2457.

(12) Kajigaeshi, S.; Kakinami, T.; Moriwaki, M.; Watanabe, M.; Fujisaki, S.; Okamoto, T. *Chem. Lett.* **1988**, *17*, 795.

(13) Waybright, S. M.; Singleton, C. P.; Wachter, K.; Murphy, C. J.; Bunz, U. H. F. *J. Am. Chem. Soc.* **2001**, *123*, 1828.

Chapter 6

Synthesis, Structure, and Photophysical Properties of Diaminobis(3,3,3-trifluoropropenyl)benzenes: Minimal Fluorophores Exhibiting Highly Efficient Solid-state Emission

A series of diaminobis(3,3,3-trifluoropropenyl)benzenes were prepared by Pd-catalyzed amination reaction of the corresponding dibromobis(3,3,3-trifluoropropenyl)benzenes. The diaminobenzenes emitted visible light ranging from violet-blue to green-yellow in solution as well as in the solid states such as microcrystal, powder, and spin-coated thin film. In particular, 1,4-dipiperidino-2,5-bis(3,3,3-trifluoropropenyl)benzene was found to exhibit extremely high absolute quantum yield in solid. Furthermore, the molecular design of 1,4-bis(alkenyl)-2,5-dipiperidinobenzene was extended to the realization of multi-color emissive organic solids with high absolute quantum yields.

1. Introduction

As described in Chapter 5, the author disclosed that dimethoxybis(3,3,3-trifluoropropenyl)benzenes serve as minimal fluorophores in solution as well as in the solid states.   However, the absolute quantum yield Φ_{PL} in the solid state was at most 0.37, which is not high enough.   With the aim at improving Φ_{PL} and tuning emission colors in the solid state, the author planned the replacement of two MeO groups with more electron-donating amino groups of the bis(trifluoropropenyl)benzenes.   Described in this Chapter are synthesis, structure, photophysical properties, and theoretical calculations of diaminobis(3,3,3-trifluoropropenyl)benzenes **1** and **2** (Figure 1).   Extensive application of the molecular design to multi-color emissive organic solids **3–6** is also demonstrated.

1a: R^1, R^2 = –(CH$_2$)$_5$–   **2a**: R^1, R^2 = –(CH$_2$)$_5$–   **3**: $R^3 = R^4$ = Me
1b: R^1, R^2 = –(CH$_2$)$_4$–   **2b**: R^1, R^2 = –(CH$_2$)$_4$–   **4**: $R^3 = R^4$ = H
1c: R^1, R^2 = Me   **2c**: R^1, R^2 = Me   **5**: R^3 = CO$_2$Et, R^4 = H
1d: R^1 = Me, R^2 = H   **6**: $R^3 = R^4$ = C(O)Me
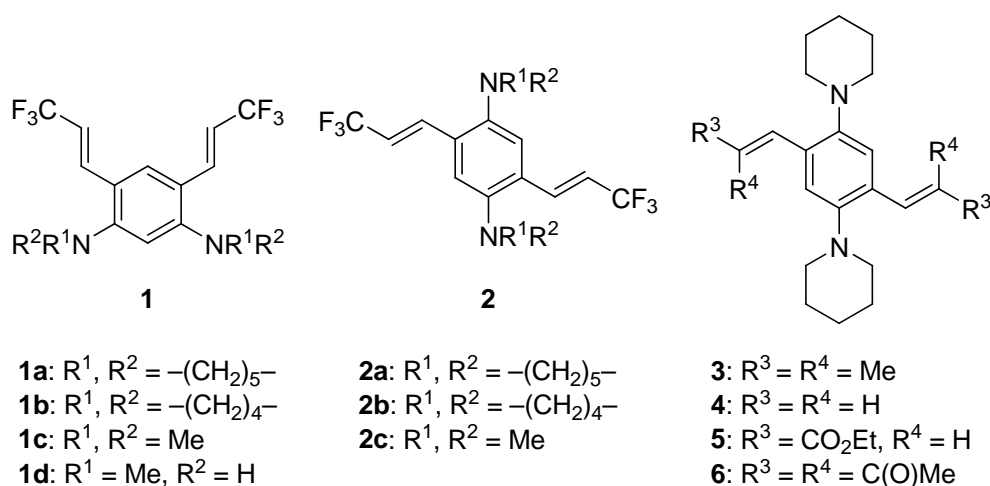
Figure 1. Emissive diaminobenzenes **1–6**.

2. Results and Discussion

2-1. Synthesis of diaminobis(3,3,3-trifluoropropenyl)benzenes 1 and 2

At first, 1,5-dibromo-2,4-bis[(*E*)-3,3,3-trifluoropropenyl]benzene (**8**) was prepared by the Wittig-type reaction of 4,6-dibromoisophthalaldehyde (**7**) with (2,2,2-trifluoroethyl)diphenylphosphine oxide.[1]   Since **8** was produced as a mixture of stereoisomers (*EE/EZ/ZZ* = 78:13:9), the mixture was photo-isomerized followed by recrystallization from CH$_2$Cl$_2$, giving (*E,E*)-**8** as a single stereoisomer. Diaminobenzenes **1** were synthesized by Pd-catalyzed amination of **8** using the corresponding amines in 59–94% yields (Scheme 1).[2]
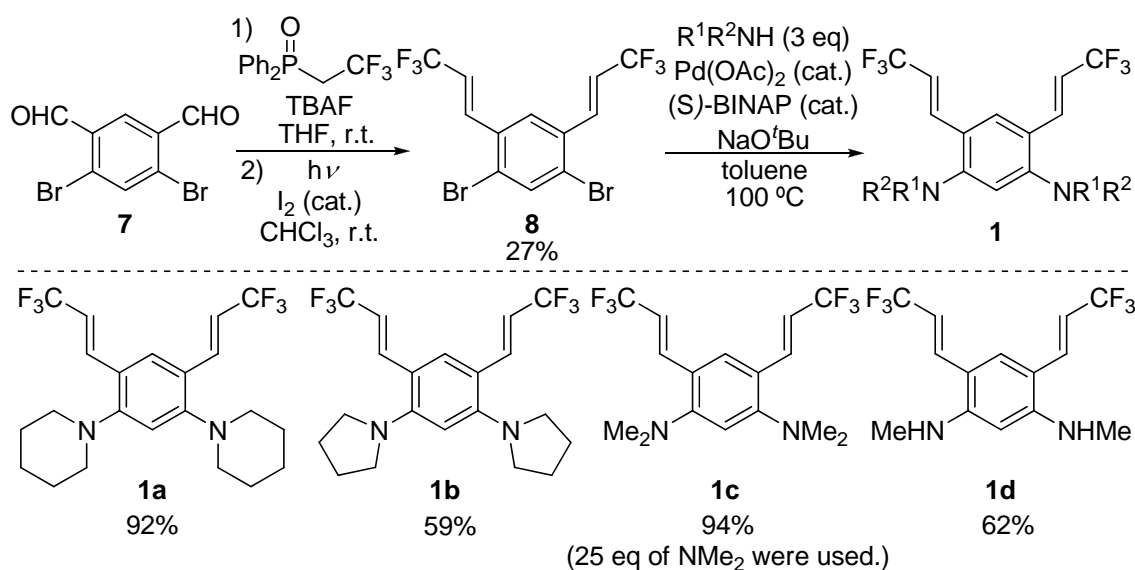
Scheme 1. Synthesis of 1,5-diamino-2,4-bis[(*E*)-3,3,3-trifluoropropenyl]benzenes **1**.

Preparation of 1,4-diamino-2,5-bis(trifluoropropenyl)benzenes **2a–c** were prepared in a similar manner to **1** in high yields (Scheme 2).   The amination of **10** with *N*-methylamine failed due presumably to the instability of the product under the reaction conditions.
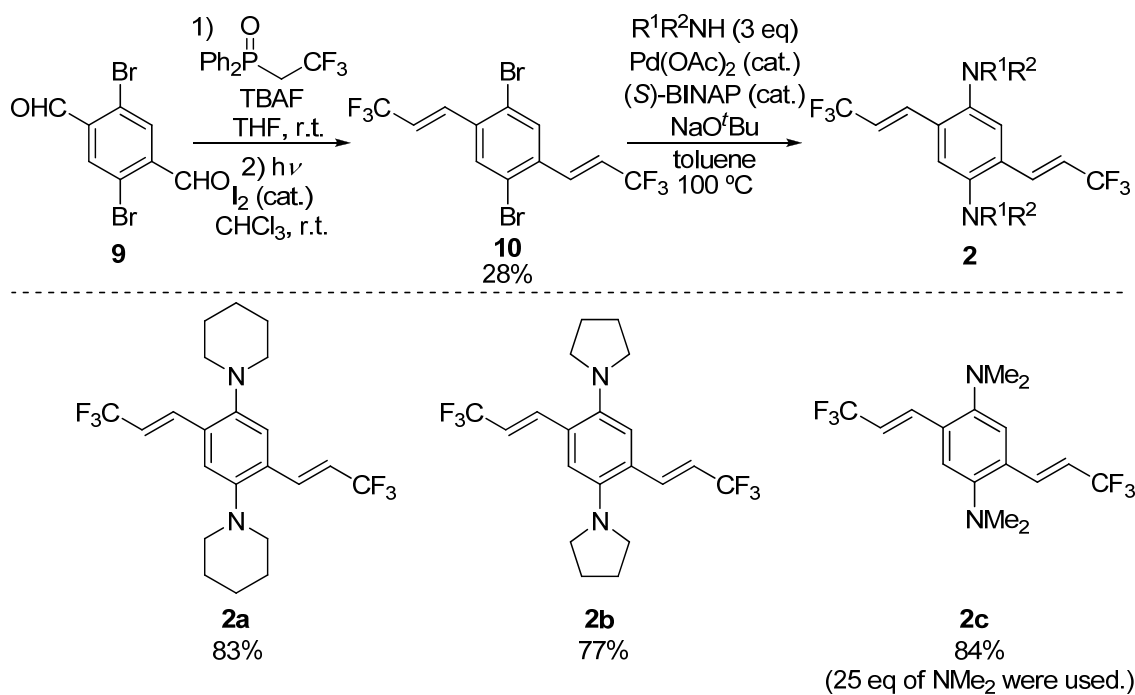
Scheme 2. Synthesis of 1,4-diamino-2,5-bis[(*E*)-3,3,3-trifluoropropenyl]benzenes **2**.

2–2. X-ray crystallography

Single crystals of **1a**, **1c**, and **2a** were obtained by recrystallization from CH$_2$Cl$_2$/MeOH, hexane, and THF/EtOH, respectively. The X-ray crystallographic analysis of their single crystals revealed that two trifluoropropenyl and amino groups deviated from the benzene plane by 19–36° and 32–72°, respectively, and the adjacent two molecules were far apart from each other with distances over 5 Å, which are much larger than those observed in the dimethoxy-substituted counterparts (Figures 2–7).
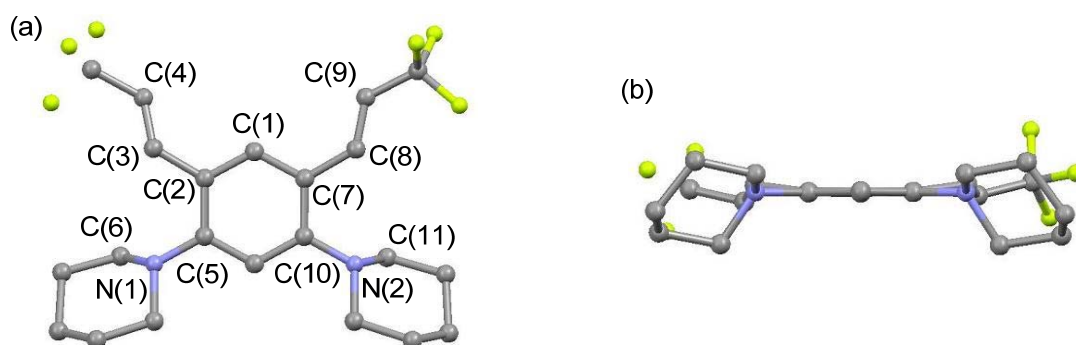
Figure 2. Molecular structure of **1a**: (a) top view and (b) side view.
Selected dihedral angles (°): C(1)–C(2)–C(3)–C(4) 30.1(4); C(1)–C(7)–C(8)–C(9) 23.4(2); C(2)–C(5)–N(1)–C(6) 64.9(4); C(7)–C(10)–N(2)–C(11) 66.2(6).
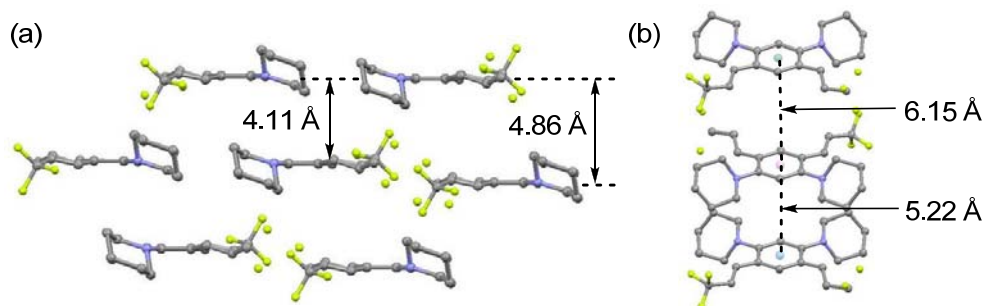
Figure 3. Packing diagram of **1a**: (a) viewed from oblique direction to *bc* plane; (b) viewed along *a*-axis.
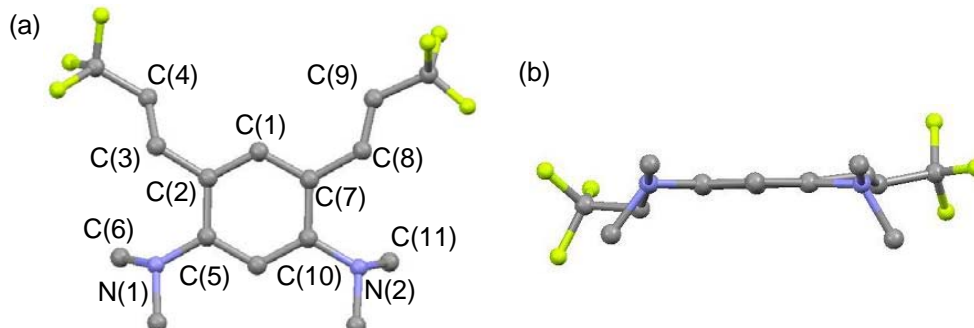
Figure 4. Molecular structure of **1c**: (a) top view and (b) side view.
Selected dihedral angles (°): C(1)–C(2)–C(3)–C(4) 36.2(5); C(1)–C(7)–C(8)–C(9) 19.1(7); C(2)–C(5)–N(1)–C(6) 62.3(9); C(7)–C(10)–N(2)–C(11) 68.5(7).

164
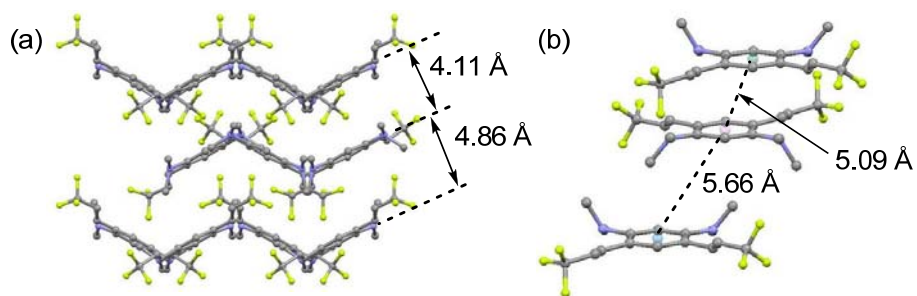
Figure 5. Packing diagram of **1c**: (a) viewed along the *c*-axis; (b) viewed from oblique direction to *bc* plane.
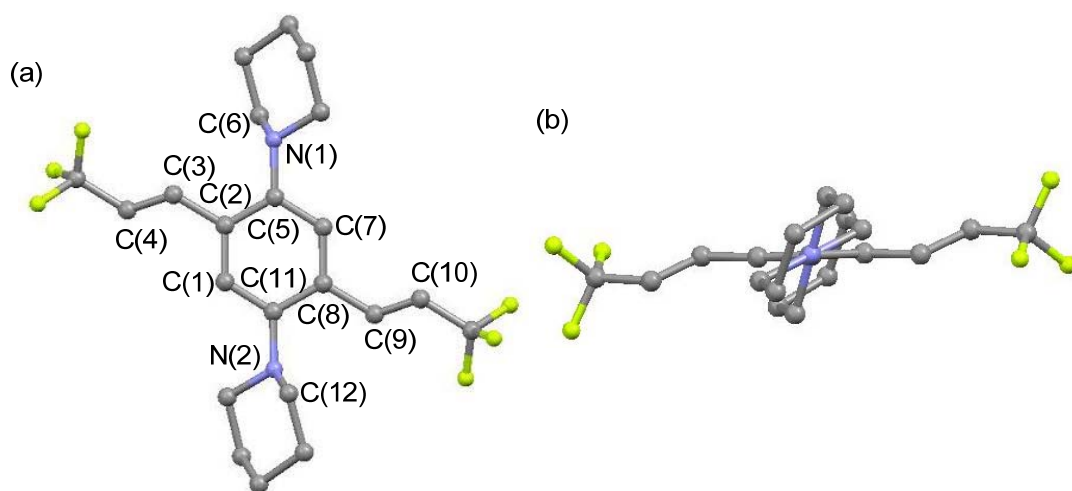
Figure 6. Molecular structure of **2a**: (a) top view and (b) side view.
Selected dihedral angles (°): C(1)–C(2)–C(3)–C(4) 32.7(1); C(2)–C(5)–N(1)–C(6) 72.6(3); C(7)–C(8)–C(9)–C(10) 32.7(1); C(8)–C(11)–N(2)–C(12) 72.6(3).
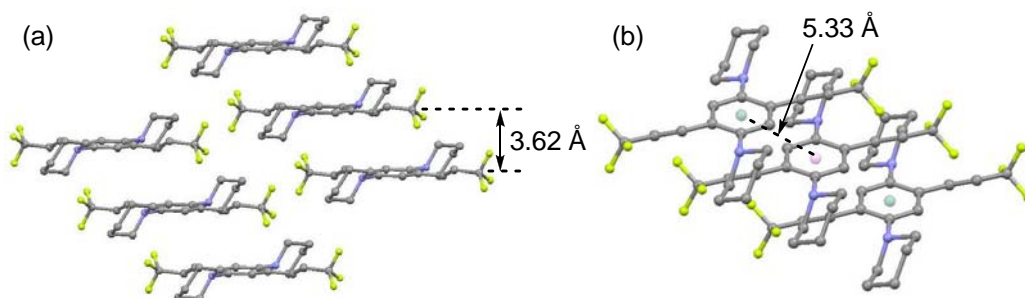
Figure 7. Packing diagram of **2a**: (a) viewed along the *b*-axis; (b) viewed from oblique direction to *ac* plane.

2–3. Photophysical properties of 1 and 2

Absorption and fluorescence properties of **1** and **2** are summarized in Table 1.

Table 1. Absorption and fluorescence data of **1** and **2**.

Compound		Absorption		Fluorescence		Stokes shift
		λ_{abs} [nm]	ε [M^{-1} cm^{-1}]	λ_{em} [nm]	$\Phi_f{}^a$	$\Delta\lambda$ [nm]
1a	cyclohexane[b]	319	16900	425	0.17	106
	solid (powder)	—	—	441	0.21	—
	film (spin-coated)[c]	—	—	434	0.15	—
	film (PMMA)[d]	—	—	430	0.14	—
1b	cyclohexane[b]	331	20200	429	0.08	98
	solid (powder)	—	—	454	0.12	—
	film (spin-coated)[c]	—	—	442	0.06	—
	film (PMMA)[d]	—	—	440	0.10	—
1c	cyclohexane[b]	319	16700	424	0.14	105
	solid (crystal)	—	—	435	0.18	—
	solid (powder)	—	—	430	0.23	—
	film (spin-coated)[c]	—	—	421	0.22	—
	film (PMMA)[d]	—	—	435	0.11	—
1d	cyclohexane[b]	330	18100	417	0.16	87
	solid (powder)	—	—	—	0.00	—
	film (spin-coated)[c]	—	—	471	0.01	—
	film (PMMA)[d]	—	—	432	0.05	—
2a	cyclohexane[b]	380	3500	523	0.49	143
	solid (crystal)	—	—	523	0.98	—
	solid (powder)	—	—	527	0.88	—
	film (spin-coated)[c]	—	—	526	1.00	—
	film (PMMA)[d]	—	—	542	0.94	—
2b	cyclohexane[b]	403	4100	542	0.57	139
	solid (powder)	—	—	558	0.38	—
	film (spin-coated)[c]	—	—	550	0.24	—
	film (PMMA)[d]	—	—	573	0.21	—
2c	cyclohexane[b]	383	4300	521	0.57	138
	solid (crystal)	—	—	537	0.91	—
	solid (powder)	—	—	540	0.86	—
	film (spin-coated)[c]	—	—	536	0.80	—
	film (PMMA)[d]	—	—	555	0.75	—

[a] Absolute quantum yield determined with a calibrated integrating sphere system. [b] Measured at 1×10^{-5} M in cyclohexane. [c] Spin-coated film prepared from a CH_2Cl_2 solution. [d] Dispersed in poly(methyl methacrylate) film.

Absorption spectra of **1** in cyclohexane measured at a concentration of 1×10^{-5} M are shown in Figure 8.   Absorption maxima (λ_{abs}) of **1a** and **1c** were observed at 319 nm, while the λ_{abs} of **1b** and **1d** red-shifted relative to those of **1a** and **1c**.
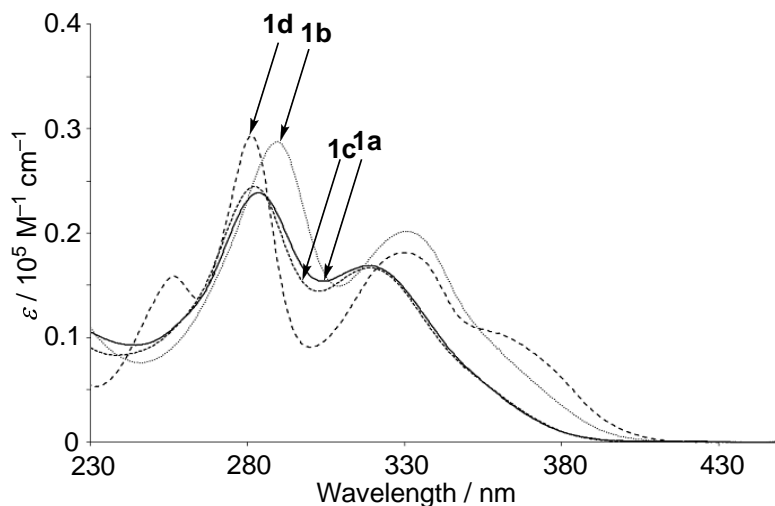
Figure 8.   UV-vis spectra of cyclohexane solutions **1** (1×10^{-5} M).

UV-vis spectra of **2** in cyclohexane showed weak absorption around 390 nm, which more red-shifted compared to those of **1** and the corresponding dimethoxybenzenes discussed in Chapter 5.   This observation means that **2** have the lowest HOMO–LUMO gaps among the series of tested bis(trifluoropropenyl)benzenes.
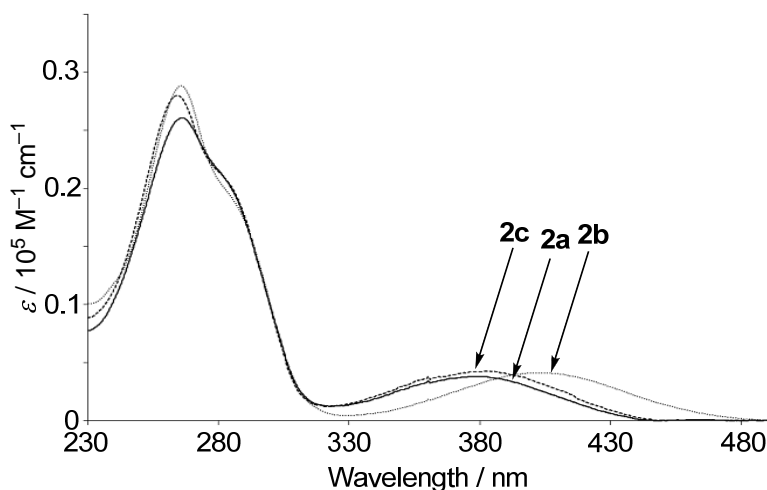
Figure 9.   UV-vis spectra of cyclohexane solutions **2** (1×10^{-5} M).

Upon UV irradiation, cyclohexane solutions **1** emitted violet-blue to blue light (λ_{em} = 417–429 nm) as shown in Figure 10b.   Compared to the corresponding dimethoxybenzenes, **1** showed red-shift of λ_{em} by approximately 60 nm.   As for Φ_{PL},

they ranged from 0.08 to 0.17, lower than those of the dimethoxybenzenes.
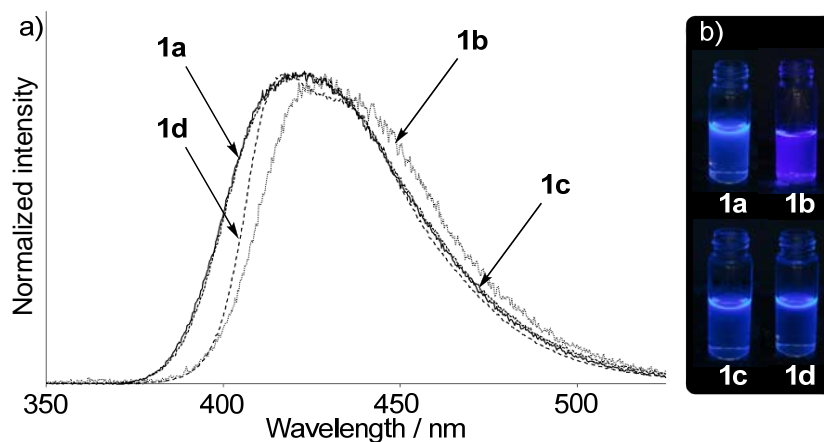
Figure 10. (a) Normalized fluorescence spectra of **1** in cyclohexane (λ_{ex} = 300 nm). (b) Photographs of **1** in cyclohexane taken under UV light (λ = 365 nm).

Cyclohexane solutions **2** emitted bright green to green-yellow light with moderate Φ_{PL} (0.49–0.57) as shown in Figure 11b. Remarkably large Stokes shift (138–142 nm) was observed, indicating drastic changes in the geometries and/or electronic distributions between the excited states and the ground states.
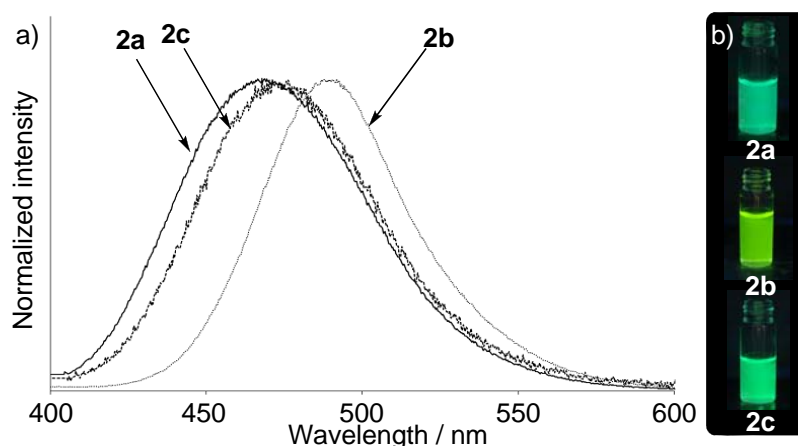
Figure 11. (a) Fluorescence spectra of **2** in cyclohexane (λ_{ex} = 400 nm). (b) Photographs of **2** in cyclohexane taken under UV light (λ = 365 nm).

Solid-fluorescence spectra of **1** in crystal and powder (Figure 12) showed that λ_{em} slightly red-shifted (6–25 nm) compared with those in cyclohexane. Quantum yields of **1a–c** were almost the same or slightly higher than those in cyclohexane. On the other hand, **1d** was completely non-fluorescent in powder form. The fact that the λ_{em} and Φ_{PL} in the solid states and in cyclohexane were almost the same suggests the emission from powders **1a–c** could be ascribed to emission from the monomeric

molecules as well as in the dilute solutions.
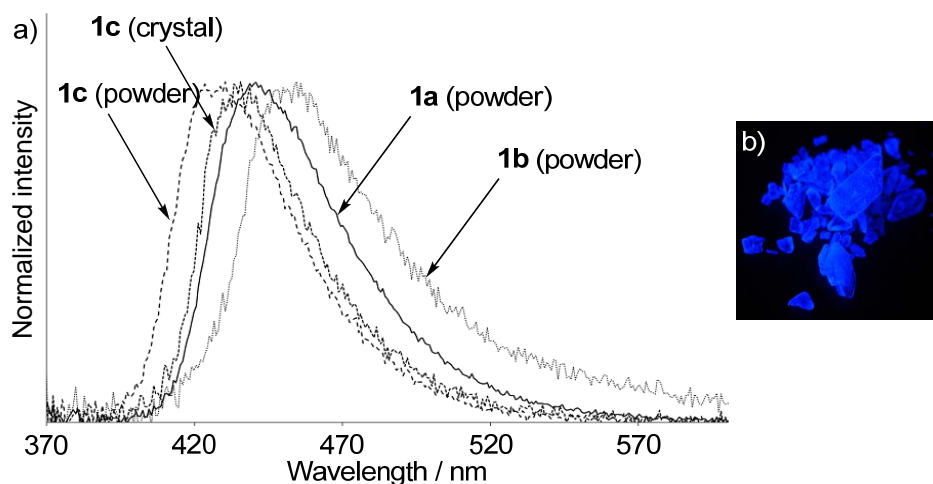
Figure 12. (a) Normalized fluorescence spectra of **1a–c** in crystal and powder forms (λ_{ex} = 360 nm). (b) A photograph of crystal **1c** taken under UV light (λ = 365 nm).

Emission maxima of crystals and powders **2** slightly red-shifted (4–19 nm) compared to those in cyclohexane (Figure 13a), indicating that intermolecular interactions in the crystal and powder forms were weak as well as **1**. Remarkably, crystals **2a** and **2c** emitted green to green-yellow light with excellent Φ_{PL} of 0.98 and 0.91, respectively (Figure 13b), much higher values than those in cyclohexane. On the other hand, Φ_{PL} of **2b** in powder was lower than that in cyclohexane. In view that fluorophores that exhibit high Φ_{PL} over 0.90 are quite rare and that the precedents generally contain multiple aromatic rings, it is noteworthy that bis(alkenyl)*benzenes* **2a** and **2c** can serve as highly emissive organic solids.
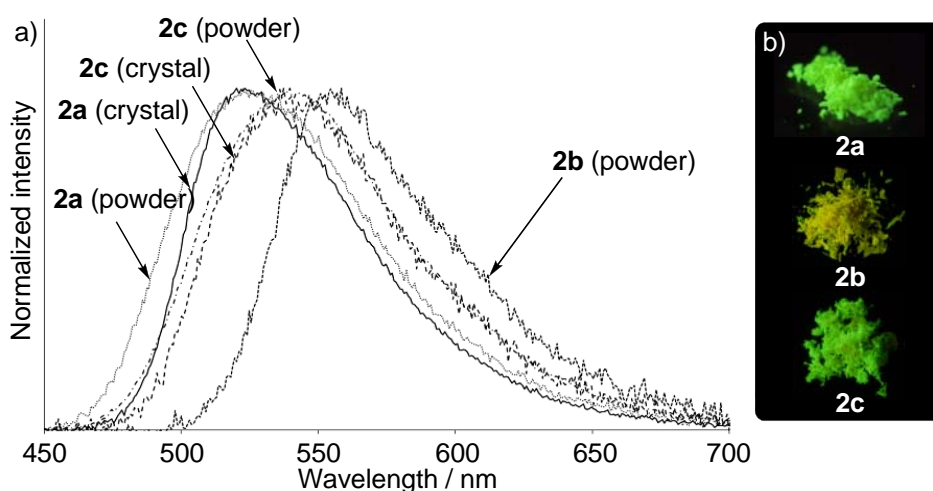
Figure 13. (a) Normalized fluorescence spectra of crystals and powders **2** (λ_{ex} = 360 nm). (b) Photographs of powders **2** taken under UV light (λ = 365 nm).

169

Spin-coated neat films on quarts plate **1** and **2** showed almost the same spectra as those in cyclohexane. Quantum yields of films **1** were lower than those in powder. On the other hand, notably, films **2a** and **2c** showed excellently high Φ_{PL} (1.00 for **2a**, and 0.86 for **2c**) as well as the crystals and powders. PMMA films doped with **1a–d** exhibited almost the same Φ_{PL} as those in the solutions, implying that each molecule is separated from one another by the polymer chains. It should be noted that polymer films **2a** and **2c** exhibited high Φ_{PL} (0.94 for **2a** and 0.75 for **2c**) as well as in the solid state, implying the possibility in the application of these unique fluorophores as dopant materials.

In order to gain further insights into emission properties, fluorescence spectra of **1a** and **2a** in a CH_3CN/H_2O mixed solvent were measured and shown in Figures 14 and 15, respectively. As the fraction of H_2O increased, an emission peak around 450 nm became broader and then split into two with λ_{em} at 440 and 530 nm (Figure 14). Since **1a** is insoluble to H_2O, increase in water fraction should induce aggregation of molecules. Therefore, the dual emission at high water fraction might be ascribed to formation of excimer or exciplex of **1a** induced by molecular aggregation.
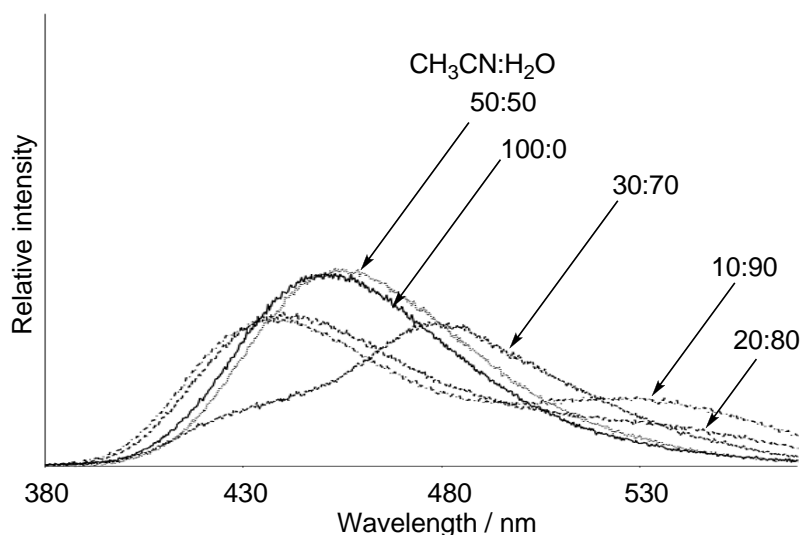
Figure 14. Fluorescence spectra of **1a** in a CH_3CN/H_2O mixture ($\lambda_{ex} = 300$ nm).

In contrast, emission peak of **2a** in CH_3CN/H_2O blue-shifted from 550 to 520 nm without any splitting of the peak as H_2O fraction increased (Figure 15). Moreover, relative emission intensity was markedly enhanced afterwards the fraction of water

surpasses 0.70. These results indicate aggregation of molecules induced the dramatic enhancement of emission intensity, probably due to the restriction of intramolecular rotation.
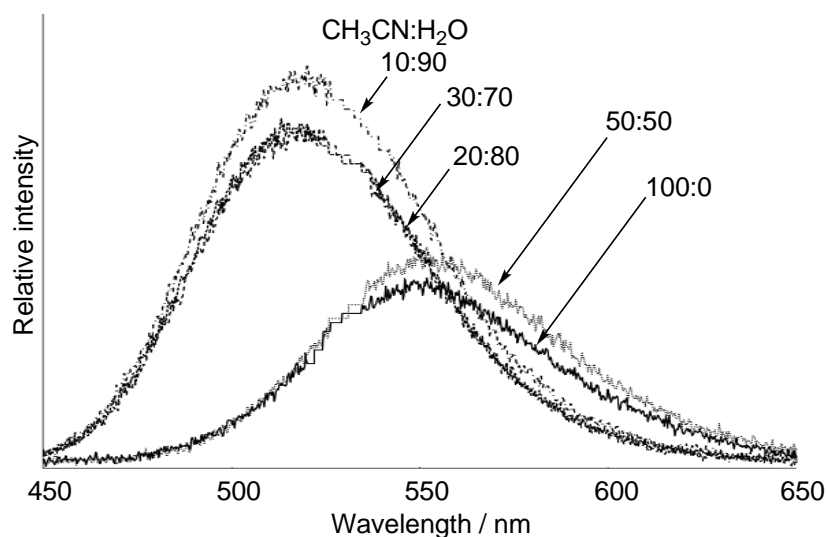
Figure 15. Fluorescence spectra of **2a** in a CH_3CN/H_2O mixture ($\lambda_{ex} = 400$ nm).

For further consideration on electronic structure of the diaminobenzenes, solvent effect on the photophysical properties of **1a** and **2a** in various solvents were measured, and the results are summarized in Table 2.

Table 2. Solvent effect on absorption and fluorescence properties of **1a** and **2a**.[a]

Compound	Solvent (ε_r[b])	Absorption		Fluorescence	
		λ_{abs} [nm]	ε [M^{-1} cm^{-1}]	λ_{em}[c] [nm]	Φ_{PL}[d]
1a	c-C_6H_{12} (2.0)	319	16900	425	0.17
	dioxane (2.2)	336	5900	434	0.15
	Et_2O (4.3)	325	14900	426	0.13
	CH_2Cl_2 (9.1)	326	16300	441	0.12
	CH_3CN (37)	324	16800	452	0.12
	DMSO (47)	327	17600	457	0.16
2a	c-C_6H_{12} (2.0)	380	3500	523	0.49
	dioxane (2.2)	388	3600	559	0.62
	Et_2O (4.3)	381	4100	541	0.55
	CH_2Cl_2 (9.1)	388	4100	563	0.57
	CH_3CN (37)	391	4100	567	0.57
	DMSO (47)	386	4200	582	0.51

[a] Measured in 1×10^{-5} M. [b] Dielectric constant. [c] Emission maxima upon irradiation with UV light ($\lambda_{ex} = 360$ nm). [d] Absolute quantum yields determined with a calibrated integrating sphere system.

In UV-vis spectra, no significant changes in shapes or λ_{abs} were observed in both cases, although the polarity of the solvents examined varies with wide range. This indicates non-polar nature of the ground state of **1a** and **2a**. In contrast to absorption spectra, fluorescence spectra were strongly affected by the solvent polarity as shown in Figure 16a. According to increase in solvent polarity, λ_{em} markedly red-shifted from 523 to 582 nm. Notably, the fluorescence and absorption spectra of cyclohexane solution **2a** rarely overlapped, in other words, significant Stokes shift (143 nm) was observed. The large Stokes shift and remarkable fluorescence solvatochromism indicate drastic changes in geometry upon excitation, and stabilization of the intramolecular charge-transfer (ICT) states by polar solvents. Quantum yields showed moderate values (0.49–0.62) independent of the solvent polarity. These characteristic behaviors of were also observed with **1a** (Table 2).
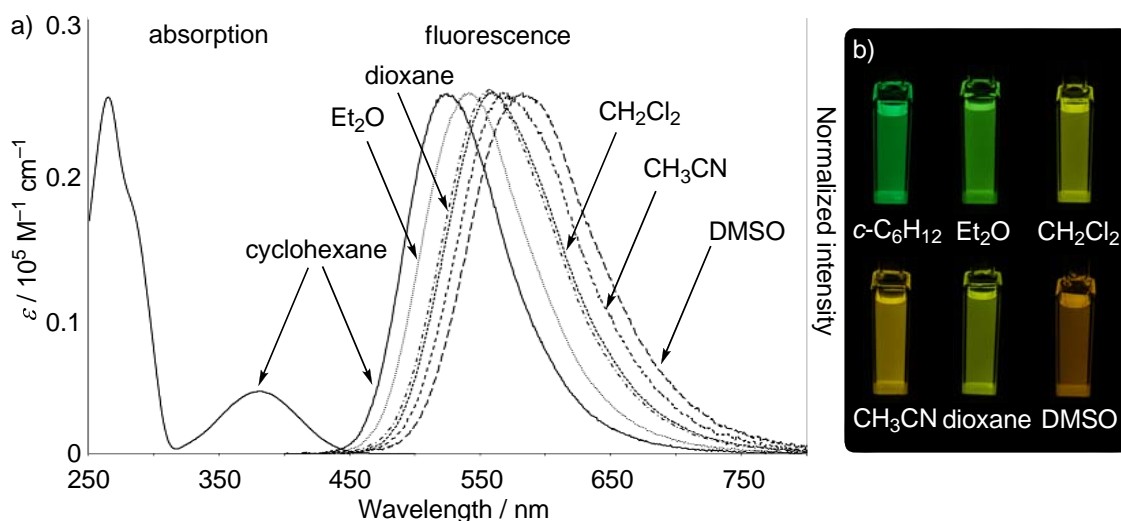
Figure 16. (a) Normalized fluorescence spectra of **2a** in various solvents ($\lambda_{ex} = 360$ nm). (b) Photographs of **2a** in each solvent taken under UV lamp ($\lambda = 365$ nm).

2–4. Theoretical calculations

To gain deeper insights into the electronic structures of the diaminobenzenes, molecular orbital calculations of **1** and **2** were performed by the DFT methods at B3LYP/6-31G(d)//B3LYP/6-31G(d) level using the Gaussian 03 package.[3] For geometry optimization study, the initial structures were set based on the data obtained by X-ray crystallography of **1a**, **1c**, and **2a**. The optimized structures of **1** and **2** are shown in Figures 17. The optimized geometries of **1a** and **1c** were found quite similar to those observed by X-ray analysis. Namely, the two trifluoropropenyl and amino

groups were largely deviated from the benzene plane by approximately 30° and 66°, respectively.   In the optimized structure **1b**, the torsion angles of two pyrrolidinyl groups from benzene planar were much smaller (32.0° and 38.5°) than those observed for **1a** and **1c**.   In the case of **1d**, NMeH group were found on the benzene plane, presumably due to smaller steric repulsion between NMeH and adjacent trifluoropropenyl group.   Optimized structure of **2a** was found to adopt almost the same geometry as that observed by X-ray analysis with large twist of two trifluoropropenyl groups with dihedral angle being 71° and with moderate twist of two piperidyl groups with dihedral angle of 29°.   Diaminobenzenes **2b** and **2c** also adopted similar structures to that of **2a**.
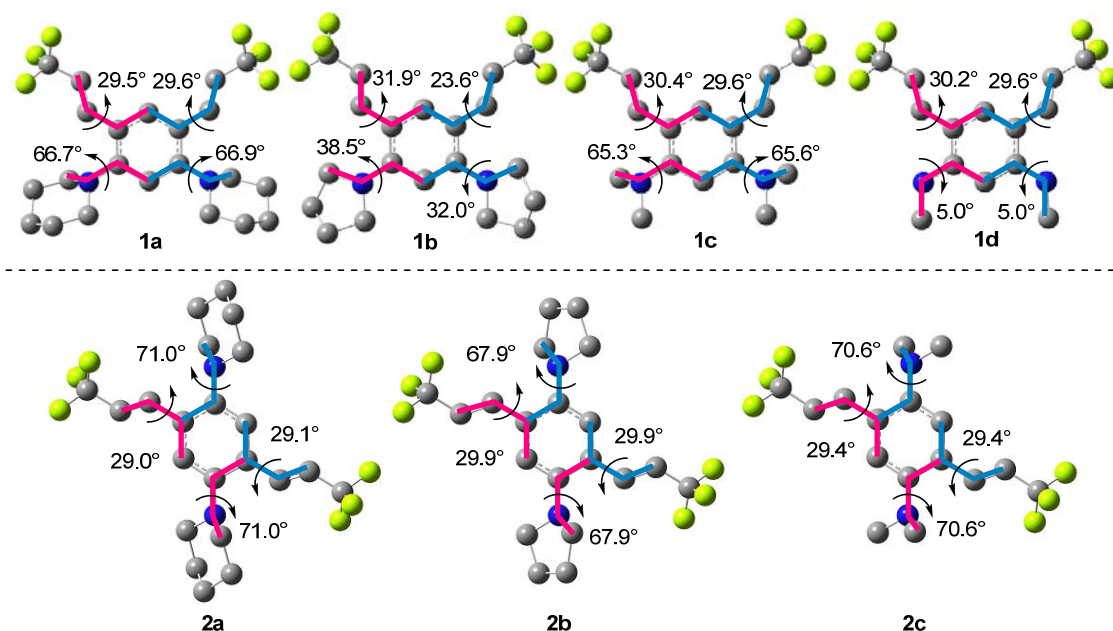
Figure 17.   Optimized structures of **1** and **2** at B3LYP/6-31G(d) level. Blue and pink lines represent the dihedral angles measured.

The energy diagram of frontier orbitals of **1** and **2** are shown in Figures 18 and 19, respectively.   In the case of **1**, energy levels of HOMOs and LUMOs increased in the following order: **1c** < **1a** < **1d** < **1b**.   Due probably to the effective conjugation of two lone-pairs on NHMe and pyrrolidinyl group with π and π^* orbitals of benzene core, the energy levels of **1b** and **1d** should increase.   The HOMO–LUMO gaps decreased as follows: **1a**, **1c** (4.21 eV) > **1d** (4.15 eV) > **1b** (4.12 eV).   This result agrees well with the experimental observation that **1b** and **1d** showed absorptions in long-wavelength side relative to those of **1a** and **1c**.
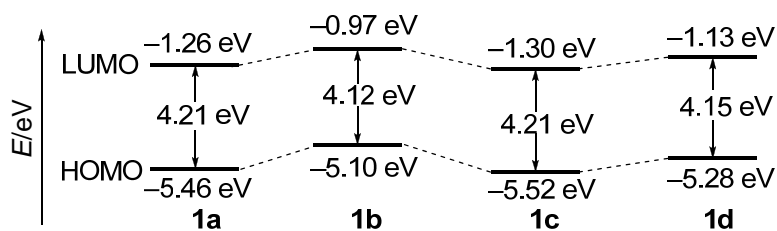
Figure 18. Energy diagram of the frontier orbitals of **1**.

The energy diagram of **2** is shown in Figure 19. Bis(pyrrolidino)benzene **2b** showed the highest frontier orbital energy levels and the smallest HOMO–LUMO gap relative to those of **2a** and **2c**.
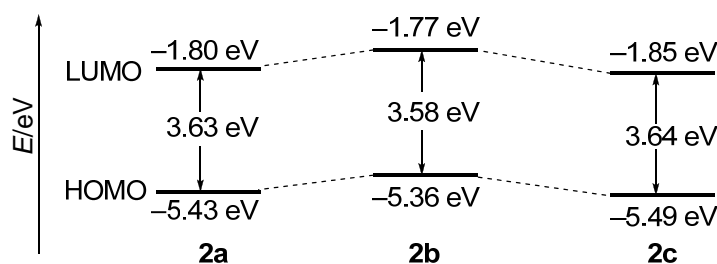
Figure 19. Energy diagram of the frontier orbitals of **2**.

The molecular orbital drawings of HOMOs and LUMOs of **1** and **2** are shown in Figures 20. HOMOs of **1** and **2** delocalized on the benzene ring, two nitrogen atoms, and two ethenyl moieties. Whereas LUMO of **1a** and **1c** delocalized on the benzene ring and two trifluoropropenyl groups including two C–F σ* bonds, LUMO of **1b** and **1d** were distinctively different from those of **1a** and **1c** in the symmetry of the wave function distribution. Furthermore, the extremely poor lobe density on amino groups is notable feature for **1b** and **1d**, indicating the charge-transfer (CT) from the donor (–NR$_2$) in the HOMO to the acceptor (CF$_3$C=C–) in the LUMO. Similarly, LUMOs of **2** distinctively delocalized on CF$_3$C=C–C$_6$H$_4$–C=CCF$_3$ framework, indicating that charge-transfer (CT) nature in the HOMO–LUMO transition as well as **1b** and **1d**. The time-dependent DFT (TD–DFT) calculations of **2a** supported that the absorption band at 380 nm can be assigned to intermolecular charge-transfer (ICT) from the HOMO to the LUMO. This result is consistent with the observed large Stokes shift and the fluorescence solvatochromism.
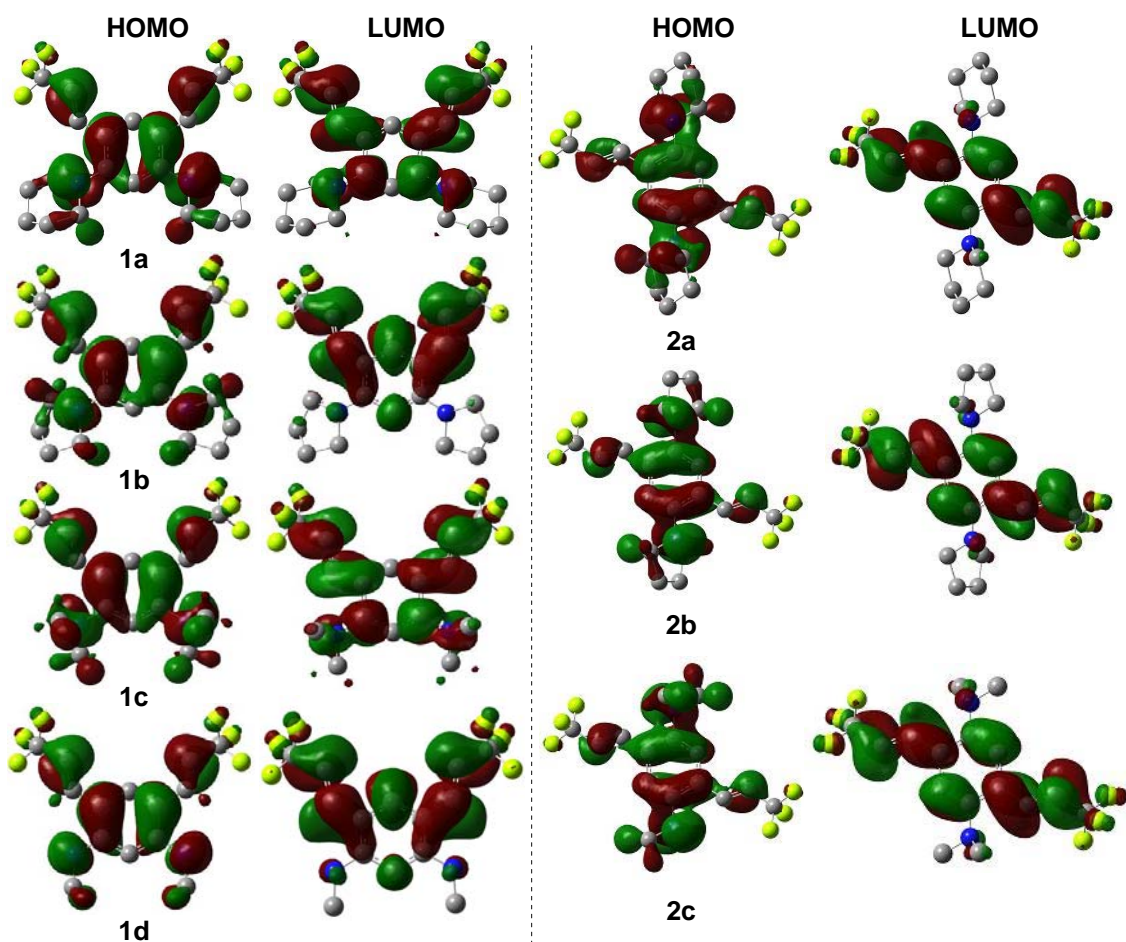
Figure 20. Molecular orbital drawings of the HOMO and LUMO of **1** and **2** calculated at B3LYP/6-31G(d) level.

2–6. The molecular design for highly emissive organic solids

As described above, 1,4-diamino-2,5-bis(3,3,3-trifluoropropenyl)benzenes, in particular, **2a** exhibited extremely high Φ_{PL} in the solid states. Large Stokes shifts should lead to suppression of energy transfer via Förster mechanism.[4] Furthermore, the characteristic packing structure in which adjacent molecules are far apart each other with the distances over 5Å probably prevent electronic interactions such as π–π interactions, leading to suppression of energy transfer by way of Dexter mechanism.[4] The reason why **2a** showed large Stokes shift would be rationalized by assuming that the twisted conformation in the ground state changed into a planar conformation in the excited state.[4,5] In addition, such long intermolecular distances might be ascribed to the twisted molecular structure in the solid state, which would prevent concentration quenching.[6] Based on these considerations, molecular design for highly emissive

175

organic solids can be proposed as follows (Figure 21): (1) alkenyl groups terminated by electron-withdrawing groups (EWG) are arranged in 1,4-positions onto a benzene. (2) bulky electron-donating groups (EDG) are introduced at 2,5-positions.
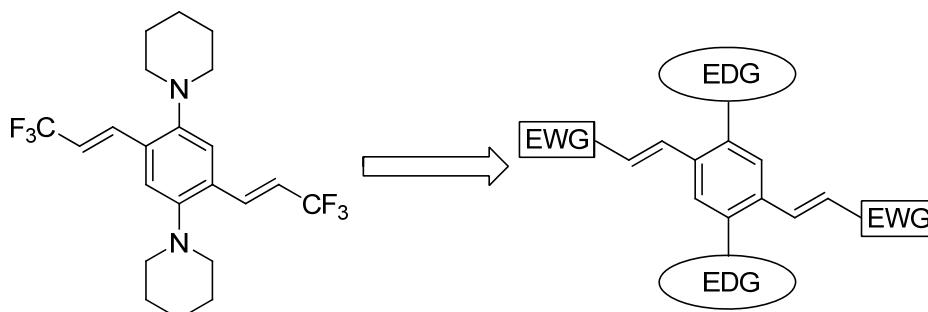
Figure 21. Proposed molecular design for highly emissive organic solids.

2–7. Application to the multi-color emissive organic solids

To examine the validity of the proposed molecular design in Figure 21, the author prepared 1,4-bis(alkenyl)-2,5-dipiperidinobenzenes **3**, **4**, **5**, and **6** in which the terminal carbons of the alkenyl moieties were substituted by Me, H, EtO_2C, and Ac groups, respectively, in place of CF_3 groups (the details of the preparation are described in Experimental Section).   Their photophysical properties of **3–6** along with those of **2** for comparison are summarized in Table 3.

Table 3. Photophysical properties of **2a–6**.

Compound	Absorption λ_{abs} [nm]^a (ε)^b	Fluorescence λ_{em} (Φ_f)^{c,d}			
		solution^a	crystals^e	thin film^f	PS film^g
3	331 (4600)	439 (0.31)	441 (0.73)	439 (0.65)	439 (0.68)
4	351 (4900)	469 (0.53)	486 (0.94)	480 (0.89)	487 (1.00)
2a	380 (3500)	523 (0.49)	523 (0.98)	526 (1.00)	543 (1.00)
5	410 (6300)	566 (0.66)	596 (0.89)	591 (0.80)	595 (1.00)
6	425 (4400)	656 (0.09)	638 (0.43)	641 (0.34)	659 (0.15)

^{a} 1 x 10^{-5} M in cyclohexane. ^{b}: M^{-1} cm^{-1} . ^{c} Emission maxima upon irradiation with UV light (λ_{em} = 310 nm for **3**, 320 nm for **4**, 360 nm for **2a** and **5**, 365 nm for **6**). ^{d} Absolute quantum yield determined by a calibrated integrating sphere system. ^{e} Prepared by recrystallization from mixed solvents: **3** from toluene/hexane; **4** from Et_2O/hexane; **2a**, **5**, and **6** from CH_2Cl_2/hexane. ^{f} Prepared by spin-coating from a solution of THF for **3** and **4**, and of toluene for **2a**, **5**, and **6**. ^{g} Dispersed in a polystyrene (PS) film.

Absorption spectra of **2a** and **3–6** in cyclohexane showed two characteristic absorptions in all case: one with larger ε (>15000) which were assigned to π–π* transition; the other one with smaller ε (<6300), which could be ascribed to ICT

176

transition.   Absorption edges red-shifted in the order of **3** < **4** < **2a** < **5** < **6**. Normalized emission spectra of **2a** and **3**–**6** in cyclohexane are shown in Figure 22a. Emission maxima red-shifted in the same order as observed in absorption spectra. Emission colors of **3**, **4**, **2a**, **5**, and **6** are blue, blue-green, green, yellow, and red, respectively as shown in Figure 22b, and Φ_{PL} of the solutions ranged from 0.09 to 0.66.
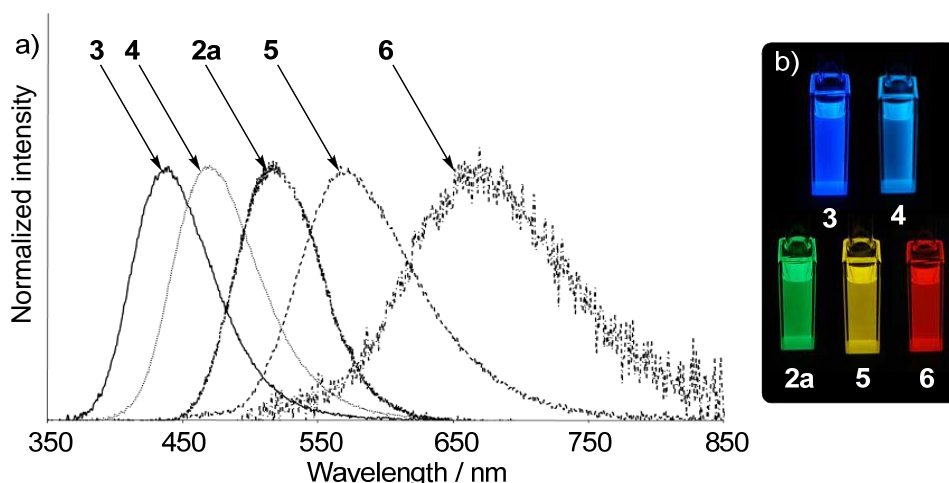
Figure 22.   (a) Normalized fluorescence spectra of **2a** and **3**–**6** in cyclohexane. (b) Photographs of **2a** and **3**–**6** in cyclohexane taken under UV light ($\lambda = 365$ nm).

Fluorescence properties of microcrystals, spin-coated neat films of **2a** and **3**–**6** were then investigated (Table 3).   Bis(2-methylpropenyl) and divinyl derivatives **3** and **4** in both crystal and thin film emitted blue and greenish blue light (Figure 23a), respectively, with high to excellent Φ_{PL} ranging from 0.65 to 0.94.   Crystals and a thin film of **5** showed intense orange fluorescence (λ_{em} = 596 and 591 nm) with excellent Φ_{PL} of 0.89 and 0.80, respectively.   Moreover, diacetyl derivative **6** exhibited red fluorescence in crystals and a thin film with emission maxima at 638 and 641 nm and Φ_{PL} of 0.43 and 0.34, respectively.   Since red fluorophores normally have a tendency to aggregate in the solid state and result in concentration quenching of fluorescence, the quantum yields of solid **6** are rather high as Φ_{PL} of red emitters.[7]   Furthermore, solids **2a** and **3**–**5** dispersed in a PS film also showed strong fluorescence in colors similar to those of crystals and thin films with excellent Φ_{PL} of 0.68 and 1.00 (Figure 23b).   This behavior is quite attractive in view that the benzenes have a potential of dopant emitters in host materials.   It should also be noted that Φ_{PL} of **2a** and **3**–**6** in cyclohexane were much lower than those in solid states.   Thus, aggregation-induced enhanced emission

177

(AIEE) is operative in all cases probably due to the restriction of intramolecular rotation.[8]   These results demonstrate that 1,4-bis(alkenyl)-2,5-dipiperidinobenzenes are unique and promising solid fluorophores in multi-colors.
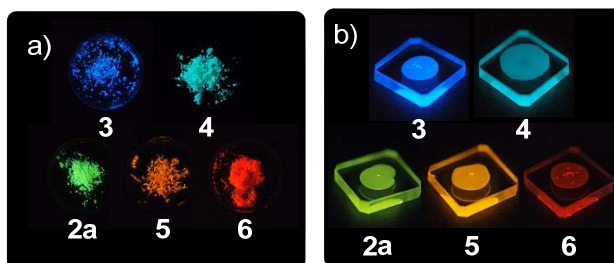
Figure 23.   (a) Photographs of microcrystals **2a** and **3**–**6** and (b) PS films doped with **2a** and **3**–**6** taken under UV light (λ = 365 nm).

Moreover, a mixture of blue-emitter **3** and orange-emitter **5** with the ratio of 16:1 dispersed in PS film emitted bright white light as shown in Figure 24b.   Fluorescence spectra covers all visible-light region from 350 nm to 850 nm, which can be regarded as the sum of each spectra of PS films **3** and **5** (Figure 24a).   It should be noted that the CIE coordinates of the film was found to be (0.337, 0.345) close to pure white emission (0.330, 0.330).   Quantum yield of the film exhibited good value of 0.61.
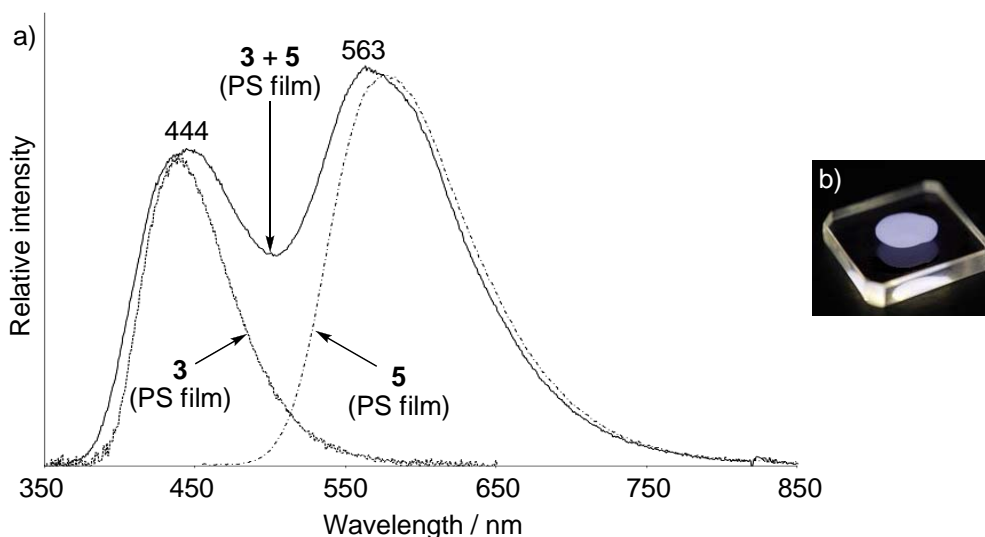
Figure 24.   (a) Fluorescence spectra of PS film doped with a mixture of **3** and **5** (λ_{ex} = 310 nm).   (b) A photograph of the PS film taken under UV light (λ = 365 nm).

Solvent effect on photophysical properties of **3–6** were summarized in Table 4.

Table 4.   Solvent effect on photophysical properties of **3–6**.[a]

Compound	Solvent (ε_r[b])	Absorption		Fluorescence	
		λ_{abs} [nm]	ε [M^{-1} cm^{-1}]	λ_{em}[c] [nm]	Φ_{PL}[d]
3	c-C$_6$H$_{12}$ (2.0)	331	4600	439	0.31
	dioxane (2.2)	334	5300	448	0.35
	Et$_2$O (4.3)	330	5100	439	0.29
	CH$_2$Cl$_2$ (9.1)	325	4300	442	0.07
	CH$_3$CN (37)	—[e]	—	—	—
	DMSO (47)	340	2600	447	0.07
4	c-C$_6$H$_{12}$ (2.0)	351	4900	469	0.53
	dioxane (2.2)	356	4200	488	0.42
	Et$_2$O (4.3)	350	4400	474	0.45
	CH$_2$Cl$_2$ (9.1)	360	4600	497	0.54
	CH$_3$CN (37)	—[e]	—	—	—
	DMSO (47)	359	4100	500	0.29
5	c-C$_6$H$_{12}$ (2.0)	410	6300	566	0.66
	dioxane (2.2)	418	6100	612	0.44
	Et$_2$O (4.3)	410	6700	591	0.61
	CH$_2$Cl$_2$ (9.1)	420	6400	628	0.58
	CH$_3$CN (37)	417	6200	649	0.25
	DMSO (47)	424	6800	653	0.20
6	c-C$_6$H$_{12}$ (2.0)	425	4400	656	0.09
	dioxane (2.2)	431	6200	697	0.02
	Et$_2$O (4.3)	423	6400	698	0.03
	CH$_2$Cl$_2$ (9.1)	434	5700	—	0.00
	CH$_3$CN (37)	432	6200	—	0.00
	DMSO (47)	434	6000	—	0.00

[a] Measured in 1×10^{-5} M solution. [b] Dielectric constant. [c] Emission maxima upon irradiation with UV light ($\lambda_{em} = 310$ nm for **3**, 320 nm for **4**, 360 nm for **5**, 365 nm for **6**). [d] Absolute quantum yields determined with a calibrated integrating sphere system. [e] Insoluble in CH$_3$CN.

Absorption spectra of **3–6** in cyclohexane, 1,4-dioxane, Et$_2$O, CH$_2$Cl$_2$, CH$_3$CN, and DMSO did not show any significant change of the spectra shape and λ_{abs} as well as **1a** and **2a**.   Fluorescence spectra of the solutions **5** are shown in Figures 25 as a representative example.   Remarkable fluorescence solvatochromism was recognized with ester-substituted benzene **5** in which λ_{em} ranged from 566 nm to 653 nm (Figure 25a).   Dramatic change in emission color was evident as shown in the Figure 25b. Meanwhile, Φ_{PL} gradually decreased as the solvent polarity increased.   As well as **5**, the other compounds also exhibited fluorescence solvatochromism, indicating the intramolecular CT nature upon the excitation.
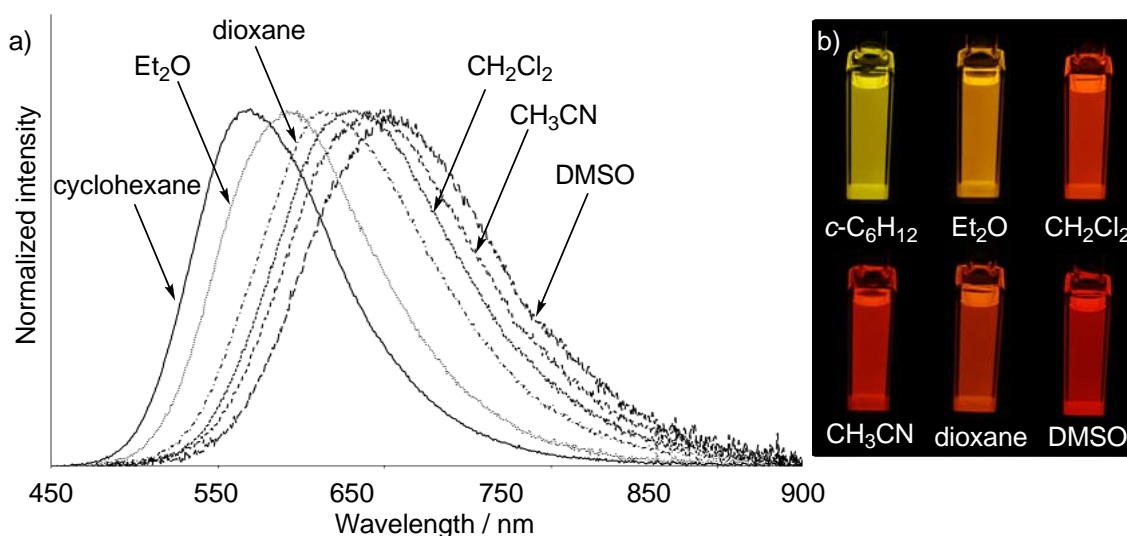
Figure 25. (a) Normalized fluorescence spectra of **5** in various solvents (λ_{ex} = 360 nm). b) Photographs of **5** in each solvent taken under UV lamp (λ = 365 nm).

To gain further insights into electronic structures of **3**–**6**, molecular orbital calculations of **3**–**6** using DFT method at B3LYP/6-31G(d) level were carried out. Geometry optimization study revealed the all compounds adopted similar conformation to that of **2a** with dihedral angles of piperidyl group to the benzene core being approximately 70° as shown in Figure 26.
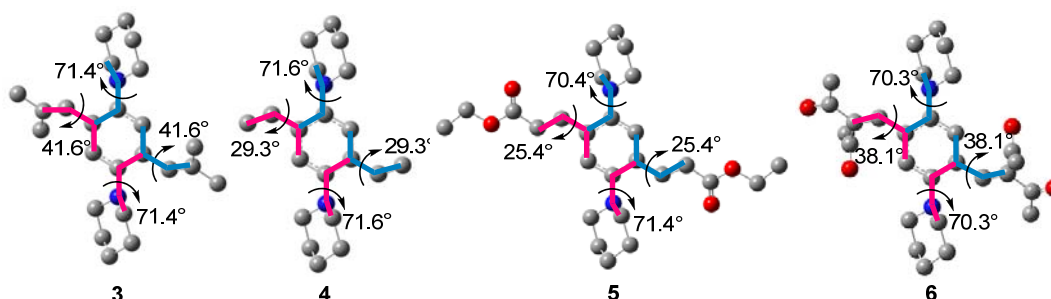
Figure 26. The optimized structures of **2a** and **3**–**6** at B3LYP/6-31G(d) level. Blue and pink lines represent the dihedral angles measured.

Molecular drawings of the HOMOs and LUMOs shown in Figure 27 clearly showed the delocalization of the HOMO orbitals on the benzene core and nitrogen atoms, and localization of the LUMO orbitals on two trifluoropropenyl and a benzene core in all cases. According to time-dependent DFT calculations at B3LYP/6-31G(d) level, the first transitions can be assigned to the transition from the HOMO to the LUMO in all cases (detail results are listed in Table 31 in Experimental Section),

supporting the ICT transition upon excitation as well as **2a**, consistent with the observation of large Stokes shift and fluorescence solvatochromism.
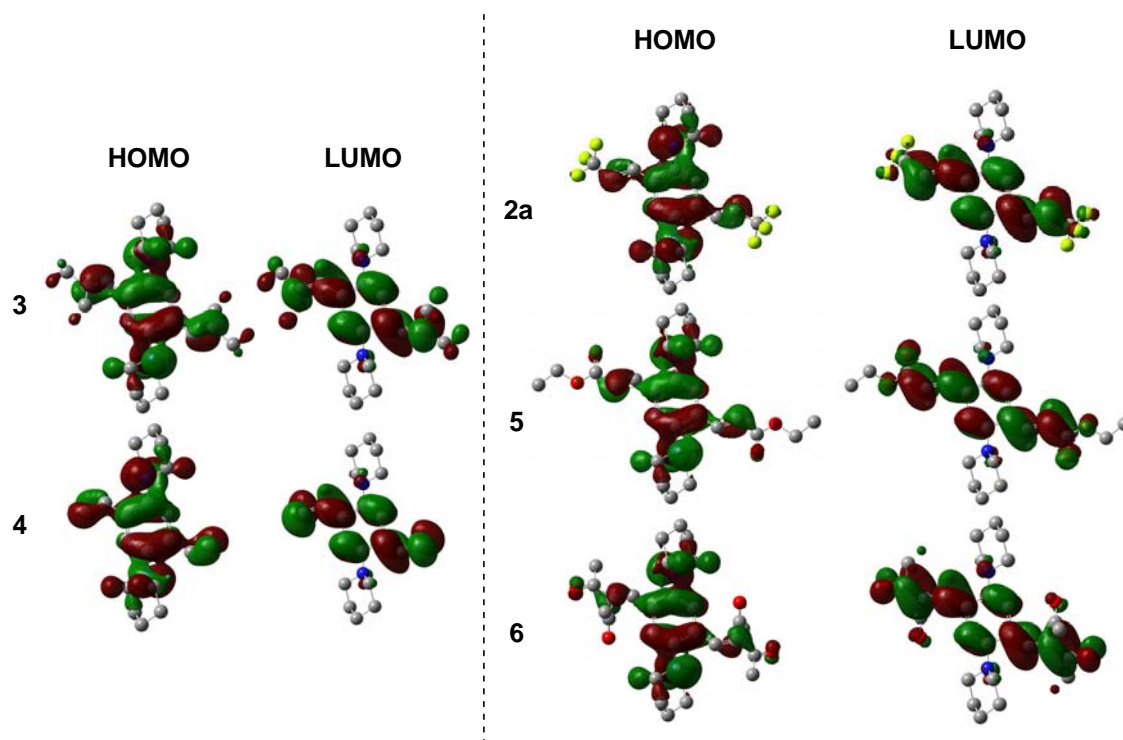
Figure 27.   Molecular orbital drawings of the HOMO (left) and LUMO (right).

Energy diagram of the frontier orbitals of **2a** and **3**–**6** is illustrated in Figure 28. HOMOs and LUMOs decreased as the electronegativity of substituents increased, except for the HOMO of **2a** being lower than those of **5** and **6**, probably due to the strong inductive effect of a CF_3 group.   The HOMO–LUMO gaps became narrower in the order of **3** > **4** > **2a** > **5** > **6**, which showed good agreement with the observation that λ_{abs} of the diaminobenzenes red-shifted in this order.
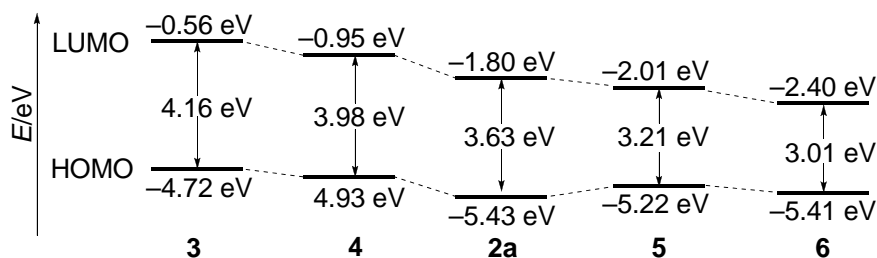
Figure 28.   Energy levels of frontier orbitals of **2a** and **3**–**6**.

To elucidate the electrochemical properties of the dipiperidinobenzenes, cyclic voltammetry (CV) of **2a** and **3**–**6** were investigated.   Reversible waves were observed only at oxidation side (Figure 29).   Cyclic voltammogram of **3** exhibited reversible two

oxidation waves at $E^1_{1/2,ox}$ = +0.465 V and at $E^2_{1/2,ox}$ = +0.679 V, indicating reversible formation of radical cation and cation, respectively.   The other compounds showed one reversible oxidation wave.
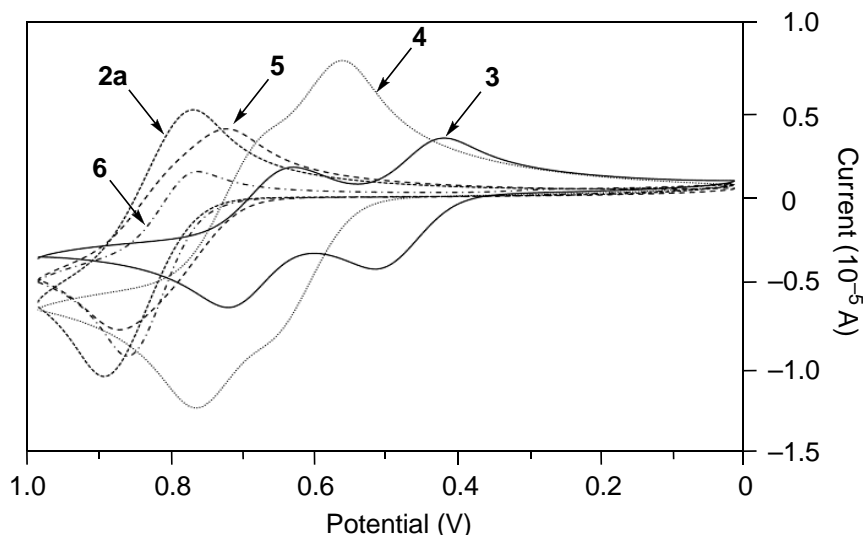
Figure 30.   Cyclic voltammograms of **2a–6** in CH_2Cl_2 with 0.1 M Bu_4ClO_4 at a scan rate of 0.1 Vs^{-1}.   Determined potential was relative to Ag/AgCl reference electrode.

Oxidation potentials relative to Ag/AgCl reference are shown in Table 6 along with the calculated HOMO energies in comparison.   The first oxidation potential $E^1_{1/2,\,ox}$ increased in the following order: **3 < 4 < 5 < 6 < 2a**.   Since high oxidation potential means low HOMO energy, the $E^1_{1/2,\,ox}$ is inversely proportional to the HOMO level.   In fact, the HOMO energies decreased in the same order.

Table 5.   Oxidation potential of **2a** and **3–6** vs Ag/AgCl.

Compound	$E^1_{1/2,\,ox}$ (V)	$E^2_{1/2,\,ox}$ (V)	calc. HOMO (eV)
3	0.465	0.679	−4.72
4	0.667	—	−4.93
2a	0.840	—	−5.43
5	0.806	—	−5.22
6	0.821	—	−5.41

3. Conclusion

In summary, the author has studied preparation and photophysical properties of diaminobis(3,3,3-trifluoropropenyl)benzenes as minimal fluorophores and has found that 1,4-diamino-2,5-bis(3,3,3-trifluoropropenyl)benzenes exhibit brilliant green emission in the solid states.   Furthermore, the molecular design has been extended to the creation of multi-color emissive organic solids.

4. Experimental Section

Bis(dibenzylideneacetone)palladium(0) [Pd$_2$(dba)$_3$], (carbethoxy-methylene)triphenylphophorane, 2-dicyclohexylphosphino-2',6'-diisopropoxybiphenyl (Ruphos), and piperidine were purchased from Sigma-Aldrich Co., Inc. 2,5-Dibromoterephthalaldehyde,[9] isopropyltriphenylphosphonium bromide,[10] 1,4-dibromo-2,5-divinylbenzene,[11] 2,2,2-trifluoroethyldiphenyl phosphine oxide,[12] and diethyl 2,5-dibromoterephthalate[13] were prepared according to the procedures reported in the literatures.

Preparation of 1,5-dibromo-2,4-bis[(*E*)-3,3,3-trifluoropropenyl]benzene (8). To a THF solution of TBAF (0.895 M, 11.2 mL, 10 mmol) was added molecular sieves 4 Å (powder, 7.7 g) activated by heating at 300 °C under vacuum for 12 h, and the mixture was stirred at room temperature for 12 h. To the mixture was added dropwise a THF (20 mL) solution of dialdehyde **7** (0.58 g, 2.0 mmol) and 2,2,2-trifluoroethyldiphenylphosphine oxide (2.27 g, 8.0 mmol) at 0 °C over 30 min. After the mixture was stirred at room temperature for 2 h, silica gel (1.0 g) was added to the flask and the resulting solution was stirred for 10 min. The mixture was filtered through a Celite pad and the residue was washed with Et$_2$O (20 mL). The filtrate was washed with H$_2$O (50 mL), and then the aqueous layer was extracted with AcOEt (50 mL × 3 times). The combined organic layer was washed with brine (50 mL × 3 times), dried over anhydrous MgSO$_4$, and concentrated *in vacuo*. The residue was dissolved in CHCl$_3$ (200 mL), and I$_2$ (38 mg, 0.15 mmol) was added to the solution. The solution was stirred upon irradiation by UV light (UVA-100HA Riko) at room temperature for 12 h. The resulting solution was concentrated under reduced pressure to give a solid residue, which was purified by recrystallization from CH$_2$Cl$_2$ (5 mL),

giving rise to give **8** (227 mg, 27%) as colorless plates. Mp: 102.5–102.9 °C. T$_d$ (5 w%): 119.5 °C. R$_f$ 0.70 (hexane/AcOEt 4:1). ^{1}H NMR (400 MHz, CDCl$_3$): δ 6.24 (dq, *J* = 16.0, 6.5 Hz, 2H), 7.44 (dq, *J* = 16.0, 2.0 Hz, 2H), 7.62 (s, 1H), 7.91 (s, 1H); ^{13}C NMR (100 MHz, CDCl$_3$): δ 120.1 (q, *J* = 34.3 Hz), 122.6 (q, *J* = 267.7 Hz), 125.7, 125.8, 133.4, 135.1 (q, *J* = 6.8 Hz), 137.1; ^{19}F NMR (282 MHz, CDCl$_3$): δ −64.4 (d, *J* = 6.5 Hz). IR (KBr): ν 1666, 1458, 1323, 1279, 1128, 968 cm^{-1}. MS (EI): *m/z* 426 (50, M$^+$+4), 424 (100, M$^+$+2), 422 (52, M$^+$), 345 (7), 343 (7), 326 (8), 325 (8), 324 (8), 264 (22), 195 (18). Anal. Calcd for C$_{12}$H$_6$Br$_2$F$_6$: C, 33.99; H, 1.43. Found: C, 34.17: H, 1.47.
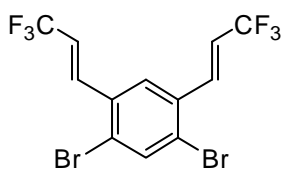
1,4-Dibromo-2,5-bis[(*E*)-3,3,3-trifluoropropenyl]benzene (10). According to the

procedure for preparation of **8** using 2,5-dibromoterephthalaldehyde (**9**) in place of **7**, **10** was obtained as a colorless solid in 28%. Purified by silica gel column chromatography (hexane/AcOEt 20:1). Mp: 127.0–127.8 °C. T$_d$ (5 w%): 127.2 °C. R$_f$ 0.70 (hexane/AcOEt 4:1). ^{1}H NMR (400 MHz, CDCl$_3$): δ 6.23 (dq, *J* = 16.0, 6.2 Hz, 2H), 7.43 (dq, *J* = 16.0, 2.0 Hz, 2H), 7.77 (s, 2H); ^{13}C NMR (67.8 MHz, CDCl$_3$): δ 120.4 (q, *J* = 34.4 Hz), 122.5 (q, *J* = 267.6 Hz), 123.5, 131.7, 134.5 (q, *J* = 6.9 Hz), 135.9; ^{19}F NMR (282 MHz, CDCl$_3$): δ −64.4 (d, *J* = 6.2 Hz). IR (KBr): ν = 1665, 1470, 1331, 1315, 1286, 1126, 966 cm^{-1}. EI-MS *m/z*: 426 (50, M$^+$+4),
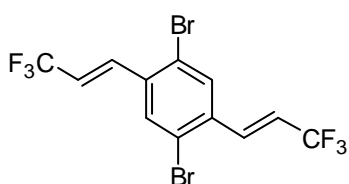
424 (100, M$^+$+2), 422 (52, M$^+$), 345 (8), 343 (9), 326 (8), 325 (9), 324 (8), 323 (7), 264 (25), 195 (17).   Anal. Calcd for C$_{12}$H$_6$Br$_2$F$_6$: C, 33.99; H, 1.43.   Found: C, 34.02: H, 1.63.

Synthesis of 1,5-dipiperidino-2,4-bis[(*E*)-3,3,3-trifluoropropenyl]benzene (1a): A representative procedure for Pd-catalyzed amination of dibromobenzenes.   To a toluene (1 mL) solution of Pd(OAc)$_2$ (3.2 mg, 14 μmol) and (*S*)-BINAP (13 mg, 21 μmol) in was added **8** (30 mg, 71 μmol), piperidine (32 μL, 0.21 mmol) and NaO*t*-Bu (21 mg, 0.21 mmol) at room temperature.   After stirred at 100 °C for 17 h, the reaction mixture was allowed to cool to room temperature, filtered through a Florisil pad, and then concentrated *in vacuo*.   The residue was purified by column chromatography on Florisil (hexane/AcOEt 9:1) followed by recrystallization from CH$_2$Cl$_2$/MeOH to give **1a** (28 mg, 92%) as colorless prisms.   Mp: 149.2–149.9 °C. T$_d$ (5 w%): 174.1 °C.   R$_f$ 0.50 (hexane/AcOEt 4:1). ^{1}H NMR (400 MHz, CDCl$_3$): δ 1.59–1.65 (m, 4H), 1.73–1.78 (m, 8H), 2.92–2.95 (m, 8H), 6.16 (dq, *J* = 16.4, 6.7 Hz, 2H), 6.63 (s, 1H), 7.37 (dq, *J* = 16.4, 2.2 Hz, 2H), 7.50 (s, 1H); ^{13}C NMR (100 MHz, CDCl$_3$): δ 24.4, 26.3, 53.9, 108.7, 113.5 (q, *J* = 33.3 Hz), 121.3, 123.9 (q, *J* = 267.7 Hz), 127.0, 134.8 (q, *J* = 4.6 Hz), 155.3; ^{19}F NMR (282 MHz, CDCl$_3$): δ –63.2 (d, *J* = 6.7 Hz).   IR (KBr): ν 2951, 2808, 1655, 1599, 1497, 1319, 1267, 1126, 991, 860, 600 cm^{-1}.   MS (EI): *m/z* 432 (38, M$^+$), 349 (100), 265 (19).   Anal. Calcd for C$_{22}$H$_{26}$F$_6$N$_2$: C, 61.10; H, 6.06.   Found: C, 60.98; H, 6.10.
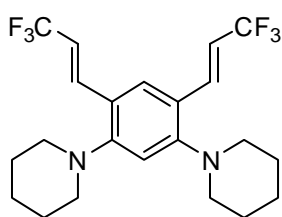
1,5-Dipyrrolidino-2,4-bis[(*E*)-3,3,3-trifluoropropenyl]benzene (1b).   Purified by Florisil column chromatography (hexane/AcOEt 9:1).   Yield: 59%, a colorless solid.   Mp: 128.2–129.1 °C.   Td (5 w%): 176.4 °C.   R$_f$ 0.48 (hexane/AcOEt 4:1). ^{1}H NMR (400 MHz, CDCl$_3$): δ 1.93–1.99 (m, 8H), 3.28–3.31 (m, 8H), 5.91 (dq, *J* = 16.0, 6.6 Hz, 2H), 6.23 (s, 1H), 7.30 (s, 1H), 7.34 (dq, *J* = 16.0, 2.0 Hz, 2H); ^{13}C NMR (100 MHz, CDCl$_3$): δ 25.6, 52.1, 100.9, 111.4 (q, *J* = 33.3 Hz), 114.5, 124.0 (q, *J* = 267.5 Hz), 129.9, 137.0 (q, *J* = 6.9 Hz), 150.8; ^{19}F NMR (282 MHz, CDCl$_3$): δ –62.8 (d, *J* = 6.6 Hz).   IR (KBr): ν 2971, 2872, 1647, 1595, 1508, 1317, 1271, 1119, 986, 866, 611, 419 cm^{-1}.   MS (EI): *m/z* 404 (61, M$^+$), 385 (20), 321 (100), 293 (32).   HRMS Calcd for C$_{20}$H$_{22}$F$_6$N$_2$: M$^+$ 404.1687. Found: 404.1690.
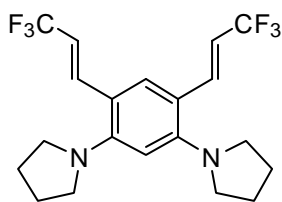
1,5-Bis(*N*,*N*-dimethylamino)-2,4-bis[(*E*)-3,3,3-trifluoropropenyl]benzene (1c).   The same procedure as the representative one using 50% aq. HNMe$_2$ (25 eq) in place of piperidine at 100 °C for 16 h gave **1c** as colorless prisms in 94% yield.   Purified by column chromatography on Florisil (hexane/AcOEt 9:1) followed by recrystallization from hexane.   Mp: 92.0–92.5°C.   T$_d$ (5 w%): 120.2 °C.   R$_f$ 0.52 (hexane/AcOEt 4:1). ^{1}H NMR (400 MHz, CDCl$_3$): δ 2.80 (s, 12H), 6.13 (dq, *J* = 16.4, 6.6 Hz, 2H), 6.61 (s, 1H), 7.37 (dq, *J* = 16.4, 2.1 Hz, 2H), 7.45 (s, 1H); ^{13}C NMR (100 MHz, CDCl$_3$): δ 44.4, 107.2, 113.4 (q, *J* = 33.3 Hz), 120.2, 123.9 (q, *J* = 267.5 Hz), 128.1, 135.2 (q, *J* = 6.8 Hz), 154.9; ^{19}F NMR
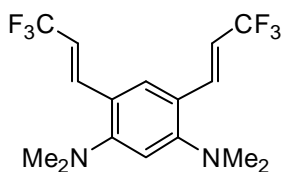
(282 MHz, CDCl$_3$): δ −63.2 (d, J = 6.6 Hz).   IR (KBr): ν 1655, 1599, 1506, 1456, 1319, 1269, 1105, 982, 870, 652 cm^{-1}.   MS (EI): m/z 352 (100, M$^+$), 333 (71), 269 (100). Anal. Calcd for C$_{16}$H$_{18}$F$_6$N$_2$: C, 54.54; H, 5.15.   Found: C, 54.70; H, 5.17.

1,5-Bis(*N*-methylamino)-2,4-bis[(*E*)-3,3,3-trifluoropropenyl]benzene (1d).   Purified by Florisil column chromatography (hexane/AcOEt 9:1). Yield: 62%, a colorless solid.   Mp: 112.3–112.7 °C.   T$_d$ (5 w%): 144.2 °C.   R$_f$ 0.53 (hexane/AcOEt 4:1). ^{1}H NMR (400 MHz, CDCl$_3$): δ 2.95 (d, J = 4.4 Hz, 6H), 4.16–4.17 (m, 2H), 5.83 (s, 1H), 5.97 (dq, J = 16.0, 6.6 Hz, 2H), 7.09 (dq, J = 16.0, 2.0 Hz, 2H), 7.25 (s, 1H); ^{13}C NMR (100 MHz, CDCl$_3$): δ 30.6, 91.7, 108.8, 112.8 (q, J = 33.2 Hz), 124.0 (q, J = 267.6 Hz), 128.4, 132.3 (q, J = 6.6 Hz), 149.8; ^{19}F NMR (282 MHz, CDCl$_3$): δ −62.8 (d, J = 6.6 Hz).   IR (KBr): ν 2941, 1616, 1533, 1261, 1121, 964, 818, 700, 468 cm^{-1}. MS (EI): m/z 324 (66, M$^+$), 241 (100).   HRMS Calcd for C$_{14}$H$_{14}$F$_6$N$_2$: M$^+$ 324.1061.   Found: 324.1055.
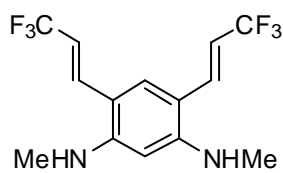
1,4-Dipiperidino-2,5-bis[(*E*)-3,3,3-trifluoropropenyl]benzene (2a).   Purified by Florisil column chromatography (hexane/AcOEt 15:1) followed by recrystallization from THF/EtOH.   Yield: 83%, yellow prisms.   Mp: 187.0–187.5 °C.   T$_d$ (5 w%): 169.8 °C.   R$_f$ 0.84 (hexane/AcOEt 4:1). ^{1}H NMR (400 MHz, CDCl$_3$): δ 1.54–1.64 (m, 4H), 1.70–1.80 (m, 8H), 2.84–2.86 (m, 8H), 6.23 (dq, J = 16.0, 6.6 Hz, 2H), 7.12 (s, 1H), 7.52–7.56 (m, 2H), 7.50 (s, 1H); ^{13}C NMR (100 MHz, CDCl$_3$): δ 24.3, 26.5, 54.4, 115.6 (q, J = 33.3 Hz), 117.9, 123.7 (q, J = 267.9 Hz), 129.8, 134.6 (q, J = 6.8 Hz), 148.4; ^{19}F NMR (282 MHz, CDCl$_3$): δ −63.5 (d, J = 6.6 Hz).   IR (KBr): ν 2947, 2806, 1661, 1495, 1418, 1275, 1111, 982, 951, 891, 660, 490 cm^{-1}.   MS (EI): m/z: 432 (100, M$^+$), 349 (16), 265 (19).   Anal. Calcd for C$_{22}$H$_{26}$F$_6$N$_2$: C, 61.10; H, 6.06.   Found: C, 60.81; H, 5.99.
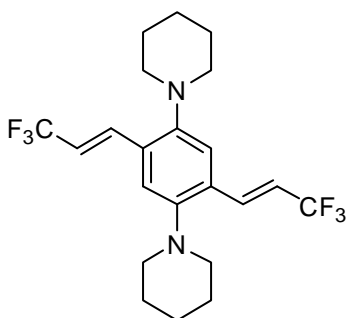
1,4-Dipyrrolidino-2,5-bis[(*E*)-3,3,3-trifluoropropenyl]benzene (2b).   Purified by Florisil column chromatography (hexane/AcOEt 9:1). Yield: 77%, a yellow solid.   Mp: 167.1–167.6 °C.   T$_d$ (5 w%): 158.4 °C.   R$_f$ 0.77 (hexane/AcOEt 4:1). ^{1}H NMR (300 MHz, CDCl$_3$): δ 1.93–1.97 (m, 8H), 3.06–3.16 (m, 8H), 6.12 (dq, J = 16.2, 6.6 Hz, 2H), 6.98 (s, 2H). 7.45 (dq, J = 16.2, 1.5 Hz, 2H); ^{13}C NMR (100 MHz, CDCl$_3$): δ 25.1, 52.7, 115.0 (q, J = 34.1 Hz), 115.9, 123.7 (q, J = 267.2 Hz), 127.3, 136.3 (q, J = 8.3 Hz), 143.6; ^{19}F NMR (282 MHz, CDCl$_3$): δ −63.4 (d, J = 6.6 Hz).   IR (KBr): ν 2986, 2811, 1717, 1653, 1506, 1418, 1279, 1128, 1097, 989, 891, 664, 419 cm^{-1}.   MS (EI): m/z 404 (100, M$^+$), 385 (12), 333 (18), 321 (25), 293 (21).   HRMS Calcd for C$_{20}$H$_{22}$F$_6$N$_2$: M$^+$ 404.1687.   Found: 404.1692.

185
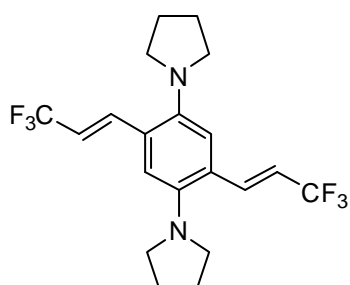
2,5-Bis(3,3,3-trifluoropropynyl)-1,4-bis(*N*,*N*-dimethylamino)benzene (2c). The similar procedure to the representative one using 50% aq. HNMe$_2$ (25 eq) in place of piperidine at 120 °C for 17 h gave **2c** as a yellow solid in 84% yield. Purified by column chromatography on Florisil (hexane/AcOEt 15:1). Mp: 155.1–155.7 °C. T_d (5 w%): 121.1 °C. R_f 0.86 (hexane/AcOEt 4:1). ^{1}H NMR (400 MHz, CDCl$_3$): δ 2.70 (s, 12H), 6.22 (dq, *J* = 16.2, 6.7 Hz, 2H), 7.12 (s, 2H), 7.53 (dq, *J* = 16.2, 2.1 Hz, 2H). ^{13}C NMR (100 MHz, CDCl$_3$): δ 45.1, 115.9 (q, *J* = 33.8 Hz), 117.7, 123.7 (q, *J* = 268.4 Hz), 129.6, 135.0 (q, *J* = 6.8 Hz), 148.2; ^{19}F NMR (282 MHz, CDCl$_3$): δ −63.5 (d, *J* = 6.7 Hz). IR (KBr): ν 2774, 1661, 1506, 1329, 1281, 1099, 986, 962, 644, 419 cm^{-1}. MS (EI): *m/z* 352 (100, M$^+$), 337 (15), 268 (34), 254 (21). Anal. Calcd for C$_{16}$H$_{18}$F$_6$N$_2$: C, 54.54; H, 5.15. Found: C, 54.56; H, 5.13.

Synthesis of 1,4-bis(2-methylpropenyl)-2,5-dipiperidinobenzene (3)
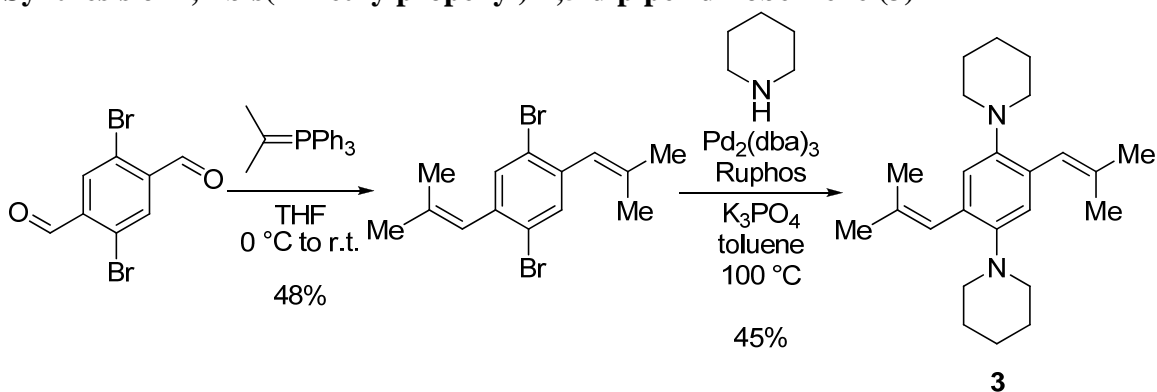
1,4-Dibromo-2,5-bis(2-methylpropenyl)benzene. A Schlenk tube (20 mL) was charged with isopropyltriphenylphosphonium bromide (1.18 g, 3.0 mmol) and THF (12 mL) under an argon atmosphere. To the solution was added a hexane solution of *n*-BuLi (1.6 M, 1.92 mL, 3.1 mmol) dropwise at 0 °C. The resulting solution was stirred at 0 °C for 30 min before the addition of 2,5-dibromoterephthalaldehyde (0.44 g, 1.5 mmol) portionwise. The resulting mixture was stirred at 0 °C for 1 h and then at room temperature for 1 h. To the tube was added AcOEt (5 mL) and silica gel (5.0 g). The organic solvents were removed under reduced pressure to give a residue which was purified by column chromatography on silica gel (hexane) followed by recrystallization from hexane to give 1,4-dibromo-2,5-bis(2-methylpropenyl)benzene (0.25 g, 48%) as colorless prisms. Mp: 60.7–61.3 °C. R_f 0.64 (hexane). ^{1}H NMR (400 MHz, CDCl$_3$): δ 1.80 (s, 6H), 1.94 (s, 6H), 6.18 (s, 2H), 7.44 (s, 2H); ^{13}C NMR (100 MHz, CDCl$_3$): δ 19.5, 26.3, 122.1, 123.4, 133.7, 137.5, 137.6. IR (KBr): ν 2968, 2906, 1651, 1464, 1442, 1433, 1377, 1344, 1203, 1066, 1045, 902, 821, 808, 449, 434 cm^{-1}. MS (EI): *m/z* 346 (50, M$^+$+4), 344 (100, M$^+$+2), 342 (50, M$^+$), 265 (15), 263 (15), 184 (63). Anal. Calcd for C$_{14}$H$_{16}$Br$_2$: C, 48.87; H, 4.69. Found: C, 48.95: H, 4.55.

1,4-Bis(2-methylpropenyl)-2,5-dipiperidinobenzene (3). A vial tube (15 mL) equipped with a magnetic stirring bar was charged with Pd$_2$(dba)$_3$ (0.10 g, 0.11 μmol) and Ruphos (0.22 g, 0.47 mmol). The vial tube was then capped with a rubber septum, evacuated for 5 min and charged with argon. The evacuation–purge operation was

repeated twice. Toluene (6 mL) was added to the vial at room temperature under an argon atmosphere and the resulting mixture was stirred at room temperature for 5 min. To the solution were added 1,4-dibromo-2,5-bis(2-methylpropenyl)benzene (0.54 g, 1.57 mmol), piperidine (1.52 mL, 15.7 mmol), and K_3PO_4 (4.47 g, 15.7 mmol). The mixture was stirred at 100 °C for 5 h and then allowed to cool to room temperature. The reaction mixture was passed through a short pad of neutral alumina (activated level I). The filtrate was then concentrated under reduced pressure to give the crude product which was purified by column chromatography on neutral alumina (activated level I, hexane). The following recrystallization from a mixture of toluene/hexane gave **1** (0.25 g, 45%) as colorless prisms. Mp: 216.5–216.9 °C. T_d (5 w%): 203.6 °C. R_f 0.11 (hexane). ^{1}H NMR (400 MHz, CDCl$_3$): δ 1.54–1.56 (m, 4H), 1.63–1.67 (m, 8H), 1.88 (s, 6H), 1.92 (s, 6H), 2.81–2.83 (m, 8H), 6.32 (s, 2H), 6.82 (s, 2H); ^{13}C NMR (100 MHz, CDCl$_3$): δ 19.8, 24.6, 26.7, 53.5, 119.9, 123.5, 130.6, 132.4, 146.2. IR (KBr): ν 2951, 2390, 2791, 2737, 1492, 1446, 1410, 1371, 1307, 1267, 1226, 1203, 1153, 1134, 1111, 1053, 1033, 947, 893, 853, 715, 536 cm^{-1}. MS (EI): m/z 353 (36, M$^+$+1), 352 (100, M$^+$), 337 (10), 296 (32). Anal. Calcd for C$_{24}$H$_{36}$N$_2$: C, 81.76; H, 10.29. Found: C, 81.76: H, 10.47.

Synthesis of 1,4-dipiperidino-2,5-divinylbenzene (4)

4
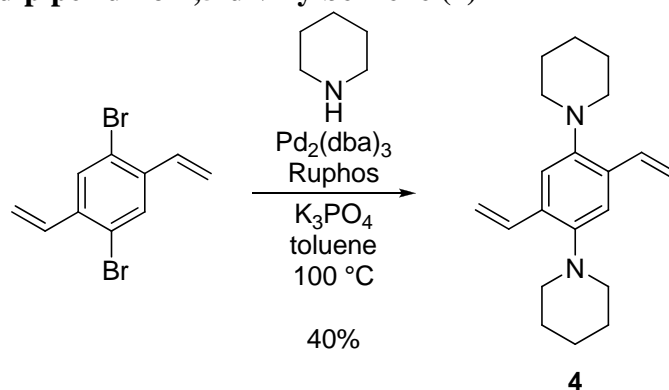
A vial tube (15 mL) equipped with a magnetic stirring bar was charged with Pd$_2$(dba)$_3$ (0.12 g, 0.13 mmol) and Ruphos (0.24 g, 0.52 mmol). The vial tube was then capped with a rubber septum, evacuated for 5 min, and charged with argon. The evacuation–purge operation was repeated twice. To the vial was added toluene (9 mL) at room temperature under an argon atmosphere and the resulting mixture was stirred at room temperature for 5 min. To the solution were added 1,4-dibromo-2,5-divinylbenzene (0.50 g, 1.7 mmol), piperidine (0.51 mL, 5.2 mmol), and K_3PO_4 (5.08 g, 5.2 mmol). The reaction mixture was stirred at 100 °C for 18 h and then allowed to cool to room temperature. The mixture was passed through a short pad of neutral alumina (activated level I). The filtrate was concentrated by rotary evaporator to give a residue which was purified by column chromatography on neutral alumina (activated level I, hexane/Et$_2$O 30:1) followed by recrystallization from Et$_2$O/hexane, giving rise to **4** (0.21 g, 40%) as pale yellow prisms. Mp: 133.4–134.2 °C. R_f 0.66 (hexane/AcOEt 20:1). ^{1}H NMR (400 MHz, CDCl$_3$): δ 1.56–1.68 (m, 4H), 1.68–1.73 (m, 8H), 2.85–2.87 (m, 8H), 5.20 (dd, J = 10.8, 1.6 Hz, 2H), 5.66 (dd, J = 17.6, 1.6 Hz, 2H), 7.07 (dd, J = 17.6, 10.8 Hz, 2H), 7.16 (s, 2H); ^{13}C NMR (100 MHz, CDCl$_3$): δ 24.4, 26.6, 54.1, 112.5, 116.3, 132.0, 133.9, 147.1. IR

(KBr): ν 2933, 2843, 2808, 2539, 1815, 1602, 1494, 1423, 1381, 1219, 1201, 1105, 1028, 1001, 933, 904, 877, 860, 667, 503 cm^{-1}. MS (EI): *m/z* 297 (92, M$^+$+1), 296 (100, M$^+$), 281 (68), 239 (56). Anal. Calcd for C$_{20}$H$_{28}$N$_2$: C, 81.03; H, 9.52. Found: C, 80.97: H, 9.58.

Synthesis of 1,4-bis[(*E*)-2-(ethoxycarbonyl)ethenyl]-2,5-dipiperidinobenzene (5)

5
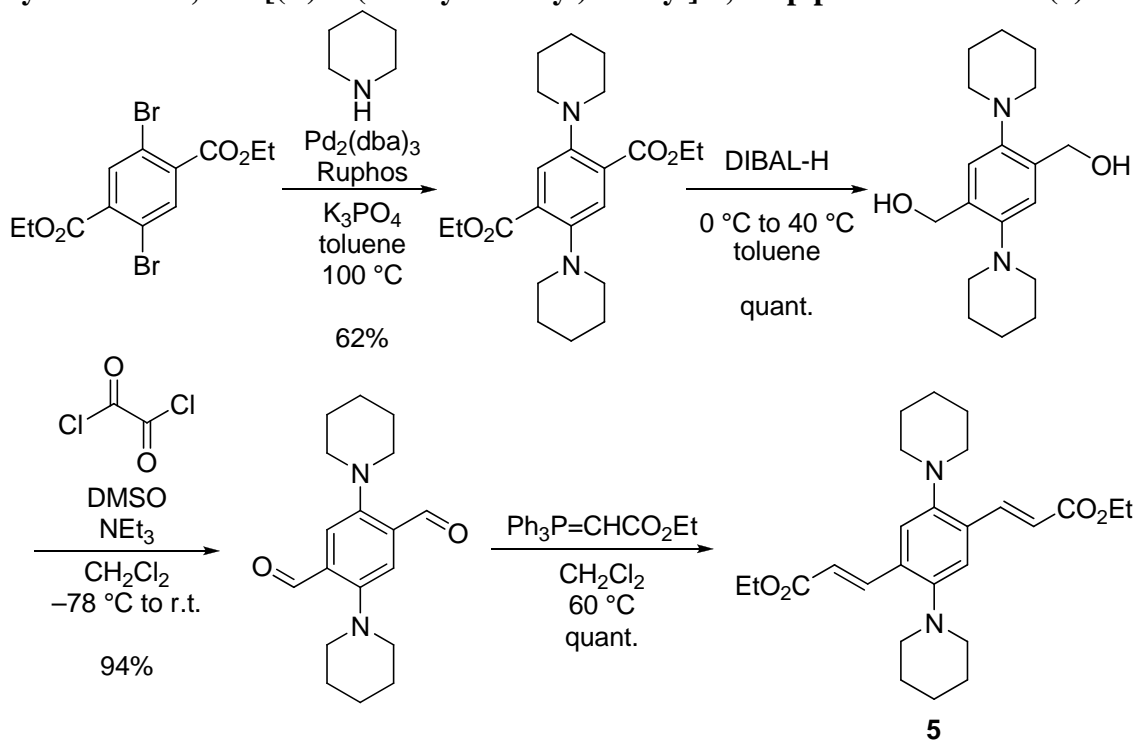
Diethyl 2,5-dipiperidinoterephthalate. A vial tube (5 mL) equipped with a magnetic stirring bar was charged with Pd$_2$(dba)$_3$ (6.7 mg, 7.5 μmol) and Ruphos (14 mg, 30 μmol). The vial tube was then capped with a rubber septum, evacuated for 5 min, and charged with argon. The evacuation–purge operation was repeated twice. Toluene (0.4 mL) was added to the vial at room temperature under argon and the resulting solution was stirred at room temperature for 5 min. To the solution were added diethyl 2,5-dibromoterephthalate (37 mg, 0.10 mmol), piperidine (99 μL, 1.0 mmol), and K$_3$PO$_4$ (0.29 g, 1.0 mmol). The reaction mixture was stirred at 100 °C for 5 h and then allowed to cool to room temperature. The mixture was passed through a short pad of neutral alumina (activated level I) and concentrated under reduced pressure. The residue was purified by column chromatography on neutral alumina (activated level I, hexane/AcOEt 20:1) followed by recrystallization from hexane to give diethyl 2,5-dipiperidinoterephthalate (19 mg, 62%) as bright yellow prisms. Mp: 174.9–175.5 °C. R$_f$ 0.33 (hexane/AcOEt 10:1). ^{1}H NMR (400 MHz, CDCl$_3$): δ 1.40 (t, *J* = 7.2 Hz, 6H), 1.52–1.55 (m, 4H), 1.65–1.71 (m, 8H), 2.91–2.93 (m, 8H), 4.36 (q, *J* = 7.2 Hz, 4H), 7.28 (s, 2H); ^{13}C NMR (100 MHz, CDCl$_3$): δ 14.4, 24.2, 26.3, 54.1, 61.1, 121.4, 129.0, 146.7, 168.0. IR (KBr): ν 2939, 2810, 703, 1498, 1446, 1410, 1381, 1286, 1247, 1215, 1195, 1031, 941, 781 cm^{-1}. MS (EI): *m/z* 389 (29, M$^+$+1), 388 (100, M$^+$), 360 (19), 359 (67), 343 (11). Anal. Calcd for C$_{22}$H$_{32}$N$_2$O$_4$: C, 68.01; H, 8.30. Found: C, 68.01: H, 8.25.

1,4-Bis(hydroxymethyl)-2,5-dipiperidinobenzene. A Schlenk tube (20 mL) equipped with a stirring bar was charged with diethyl 2,5-dipiperidinoterephthalate (0.12 g, 0.30 mmol) and toluene (1 mL) under argon. To the solution was added a toluene solution of DIBAL-H (1.50 M, 1.64 mL, 2.46 mmol) dropwise at 0 °C. The solution was gradually warmed to 40 °C and stirred for 15 min at 40 °C. The solution was then allowed to cool to 0 °C and diluted with toluene (1 mL). Methanol (3 mL) was slowly added to the tube at 0 °C. The reaction mixture was further diluted with toluene (3 mL) and allowed to warm to room temperature with vigorous stirring, resulting in formation of precipitate. The precipitate was filtered off through a pad of Celite and washed with methanol. The filtrate was concentrated under reduced pressure to give a residue which was purified by recrystallization from a toluene/hexane mixture, giving rise to 2,5-bis(hydroxymethyl)-1,4-dipiperidinobenzene (9.2 mg, quant.) as colorless needles. Mp: 178.8–179.6 °C. R_f 0.71 (MeOH). ^{1}H NMR (400 MHz, CDCl$_3$): δ 1.55–1.57 (m, 4H), 1.71–1.74 (m, 8H), 2.84–2.88 (m, 8H), 4.75 (d, J = 4.4 Hz, 2H), 6.02 (brs, 2H), 6.95 (s, 2H); ^{13}C NMR (100 MHz, CDCl$_3$): δ 24.0, 26.8, 53.9, 65.0, 120.7, 134.9, 148.0. IR (KBr): ν 3315, 2924, 2848, 2785, 2360, 1629, 1500, 1446, 1408, 1232, 1197, 1111, 1043, 1030, 991, 937, 877, 669, 449 cm^{-1}. MS (FAB): m/z 305 (100, M$^+$+H), 304 (95, M$^+$). HRMS (FAB) Calcd for C$_{18}$H$_{28}$N$_2$O$_2$: M$^+$ 304.2151. Found: 304.2139.

2,5-Dipiperidinoterephthalaldehyde. A Schlenk tube (20 mL) equipped with a stirring bar was charged with SMe$_2$ (0.19 mL, 2.58 mmol) and CH$_2$Cl$_2$ (4 mL). The solution was cooled to −78 °C and oxalyl chloride (0.14 µL, 1.64 mmol) was added dropwise. The resulting solution was stirred at −78 °C for 15 min before the addition of a solution of 1,4-bis(hydroxymethyl)-2,5-dipiperidinobenzene (54 mg, 0.17 mmol) in CH$_2$Cl$_2$ (2 mL). The reaction mixture was stirred at −78 °C for additional 30 min. To the tube was added Et$_3$N (0.24 mL, 1.69 mmol) dropwise and the solution was allowed to warm to room temperature. The mixture was stirred for 1 h at room temperature before the addition of H$_2$O (5 mL). The aqueous layer was extracted with CH$_2$Cl$_2$ (5 mL × 3 times) and washed with sat. aq. NaCl (10 mL). The combined organic layer was dried over MgSO$_4$ and concentrated under reduced pressure. The residue was purified by column chromatography on neutral alumina (activated level I, CH$_2$Cl$_2$) followed by recrystallization from CH$_2$Cl$_2$/hexane to give 2,5-dipiperidinoterephthal-aldehyde (50 mg, 94%) as red prisms. Mp: 158.7–159.6 °C. R_f 0.60 (CH$_2$Cl$_2$). ^{1}H NMR (400 MHz, CDCl$_3$): δ 1.58–1.61 (m, 4H), 1.72–1.77 (m, 8H), 2.99–3.01 (m, 8H), 7.55 (s, 2H), 10.34 (s, 2H); ^{13}C NMR (100 MHz, CDCl$_3$): δ 23.9, 26.2, 55.7, 119.1, 133.0, 151.6, 191.4. IR (KBr): ν 2935, 2918, 1676, 1485, 1467, 1413, 1383, 1222, 1128, 1109, 808 cm^{-1}. MS (EI): m/z 301 (21, M$^+$+1), 300 (100, M$^+$), 272 (8), 244 (21). Anal. Calcd for C$_{18}$H$_{24}$N$_2$O$_2$: C, 71.97; H, 8.05. Found: C, 71.84: H, 8.07.

1,4-Bis[(E)-2-(ethoxycarbonyl)ethenyl]-2,5-dipiperidinobenzene (5). A vial tube (5 mL) equipped with a magnetic stirring bar was charged with 2,5-dipiperidinoterephthalaldehyde (35 mg, 0.11 mmol), (carbethoxymethylene)triphenyl phophorane (81 mg, 0.24 mmol), and CH$_2$Cl$_2$ (2 mL) under argon. The resulting mixture was stirred at 60 °C for 6 h and then allowed to cool to room temperature. The solution was passed through a short pad of neutral alumina. The filtrate was concentrated under reduced pressure to give the crude

product which was purified by column chromatography on neutral alumina (activated level I, CH$_2$Cl$_2$) followed by recrystallization from hexane gave **4** (48 mg, quant.) as bright orange prisms.   Mp: 174.0–174.9 °C.   R$_f$ 0.40 (hexane/AcOEt 4:1). ^{1}H NMR (400 MHz, CDCl$_3$): δ 1.36 (t, J = 7.2 Hz, 6H), 1.57–1.60 (m, 4H), 1.72–1.78 (m, 8H), 2.84–2.87 (m, 8H), 4.27 (q, J = 7.2 Hz, 4H), 6.42 (d, J = 16.4 Hz, 2H), 7.19 (s, 2H), 8.05 (d, J = 16.4 Hz, 2H); ^{13}C NMR (100 MHz, CDCl$_3$): δ 14.4, 24.2, 26.4, 54.6, 60.4, 117.93, 117.95, 131.0, 141.5, 148.8, 167.1.   IR (KBr): ν 2935, 1701, 1492, 1415, 1271, 1247, 1215, 1205, 1045, 883 cm^{-1}.   MS (EI): m/z 441 (31, M$^+$+1), 440 (100, M$^+$), 412 (5), 385 (5).   Anal. Calcd for C$_{26}$H$_{36}$N$_2$O$_4$: C, 70.88; H, 8.24. Found: C, 70.66: H, 8.25.

Synthesis of 1,4-bis(2,2-diacetylethenyl)-2,5-dipiperidinobenzene (6)
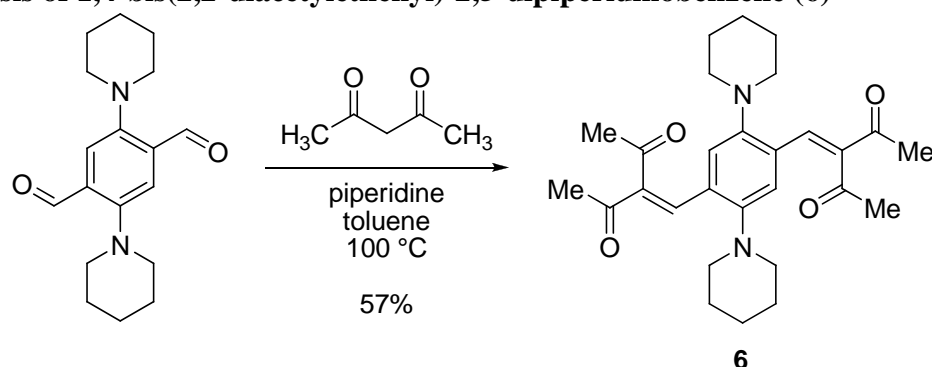
6

A vial (5 mL) equipped with a stirring bar was charged with 2,5-dipiperidinoterephthalaldehyde (35 mg, 0.11 mmol), pentane-2,4-dione (78 mg, 0.69 mmol), piperidine (3.5 μL, 23 μmol), and toluene (1 mL) under argon.   The solution was stirred at 100 °C for 5 h and then allowed to cool to room temperature.   The organic solvent was concentrated under reduced pressure to give the crude product which was purified by column chromatography on neutral alumina (activated level I, CH$_2$Cl$_2$) followed by recrystallization from CH$_2$Cl$_2$/hexane gave **5** (31 mg, 57%) as orange-red needles.   Mp: 203.8–204.6 °C.   R$_f$ 0.24 (CH$_2$Cl$_2$). ^{1}H NMR (400 MHz, CDCl$_3$): δ 1.58–1.60 (m, 4H), 1.70–1.74 (m, 8H), 2.28 (s, 6H), 2.47 (s, 6H), 2.81–2.84 (m, 8H), 6.98 (s, 2H), 7.83 (s, 2H); ^{13}C NMR (100 MHz, CDCl$_3$): δ 24.0, 26.7, 31.2, 31.6, 54.4, 120.5, 129.7, 137.6, 141.8, 148.5, 196.7, 204.6.   IR (KBr): ν 2945, 1705, 1666, 1608, 1491, 1417, 1375, 1240, 1217, 1168, 949, 916, 418 cm^{-1}.   MS (EI): m/z 465 (32, M$^+$+1), 464 (100, M$^+$), 421 (35), 378 (11).   Anal. Calcd for C$_{28}$H$_{36}$N$_2$O$_4$: C, 72.39; H, 7.81. Found: C, 72.18: H, 7.84.

UV–vis and fluorescence spectra of 1–6 in cyclohexane

UV–vis and fluorescence spectra of **1–6** in cyclohexane were measured with 1 × 10^{-5} M solution prepared from degassed spectroscopic-grade cyclohexane.

A typical procedure for preparation of spin-coated films 1–6

In a tube glass, solid sample of **4** (1.01 mg) was dissolved in THF (0.40 mL). The resulting solution was dropped onto a quartz plate (10 mm × 10 mm) and spin-coated at 100 rpm over a period of 300 sec.   The deposited film was dried under reduced pressure at room temperature for 2 h.

A typical procedure for preparation of PMMA and PS films doped with 1–6

In a tube glass, 1.1 mg of solid sample **3** (EXSTAR 6000 TG/DTA, Seiko Instruments Inc., was used for weighing sample) was dissolved in a saturated benzene solution of polystyrene (PS) (0.50 mL). The resulting solution was dropped onto a quartz plate (10 mm × 10 mm) and spin-coated at 300 rpm for 20 sec followed by further spin-coat at 100 rpm over a period of 280 sec. The deposited film was dried under reduced pressure at room temperature for 1.5 h.

Crystallographic data for 1a, 1c, and 2a

Table 6. Crystal data and structure refinement for **1a** (see Figures 2 and 3).

Empirical formula	$C_{22} H_{26} F_6 N_2$
Formula weight	432.45
Temperature	300(2) K
Wavelength	0.71073 Å
Crystal system	Triclinic
Space group	P–1
	$a = 8.245(3)$ Å, $\alpha = 107.877(5)°$
Unit cell dimensions	$b = 11.365(4)$ Å, $\beta = 104.822(5)°$
	$c = 12.935(4)$ Å, $\gamma = 93.533(5)°$
Volume	1102.2(6) Å^3
Z	2
Density (calculated)	1.303 Mg/m^3
Absorption coefficient	0.112 mm^{-1}
F(000)	452
Crystal size	$0.50 \times 0.50 \times 0.50$ mm^3
Theta range for data collection	1.73 to 25.50°
Index ranges	$-9<=h<=9, -11<=k<=13, -15<=l<=10$
Reflections collected	6040
Independent reflections	4029 [R(int) = 0.0160]
Completeness to theta = 25.50°	98.2 %
Absorption correction	Empirical
Max. and min. transmission	0.9461 and 0.9461
Refinement method	Full-matrix least-squares on F^2
Data / restraints / parameters	4029 / 72 / 327
Goodness-of-fit on F^2	1.075
Final R indices [I>2sigma(I)]	$R_1 = 0.0534$, $wR_2 = 0.1497$
R indices (all data)	$R_1 = 0.0629$, $wR_2 = 0.1587$
Largest diff. peak and hole	0.329 and –0.241 e.Å^{-3}

Table 7. Crystal data and structure refinement for **1c** (see Figures 4 and 5).

Empirical formula	$C_{16}H_{18}F_6N_2$
Formula weight	352.32
Temperature	300(2) K
Wavelength	0.71073 Å
Crystal system	Monoclinic
Space group	P2(1)/c
Unit cell dimensions	$a = 9.8553(11)$ Å, $\alpha = 90°$
	$b = 8.8354(10)$ Å, $\beta = 92.521(2)°$
	$c = 20.060(2)$ Å, $\gamma = 90°$
Volume	1745.0(3) Å^3
Z	4
Density (calculated)	1.341 Mg/m^3
Absorption coefficient	0.125 mm^{-1}
F(000)	728
Crystal size	$0.50 \times 0.50 \times 0.50$ mm^3
Theta range for data collection	2.03 to 25.49°
Index ranges	$-11<=h<=11, -10<=k<=9, -16<=l<=24$
Reflections collected	9236
Independent reflections	3240 [R(int) = 0.0172]
Completeness to theta = 25.50°	99.7 %
Absorption correction	None
Max. and min. transmission	0.9403 and 0.9403
Refinement method	Full-matrix least-squares on F^2
Data / restraints / parameters	3240 / 36 / 249
Goodness-of-fit on F^2	1.101
Final R indices [I>2sigma(I)]	$R_1 = 0.0667$, $wR_2 = 0.2058$
R indices (all data)	$R_1 = 0.0783$, $wR_2 = 0.2161$
Largest diff. peak and hole	0.366 and -0.267 e.Å^{-3}

Table 8. Crystal data and structure refinement for **2a** (see Figures 6 and 7, CCDC–719745).

Empirical formula	$C_{22}H_{26}F_6N_2$
Formula weight	432.45
Temperature	300(2) K
Wavelength	0.71073 Å
Crystal system	Triclinic
Space group	P–1
Unit cell dimensions	$a = 5.3317(9)$ Å, $\alpha = 76.137(2)°$
	$b = 9.9067(16)$ Å, $\beta = 75.647(3)°$
	$c = 10.6769(18)$ Å, $\gamma = 86.166(3)°$
Volume	530.42(15) Å^3
Z	1
Density (calculated)	1.354 Mg/m^3

Absorption coefficient	0.116 mm^{-1}
F(000)	226
Crystal size	0.50 × 0.50 × 0.50 mm^3
Theta range for data collection	2.02 to 25.50°
Index ranges	−6<=h<=4, −11<=k<=11, −12<=l<=12
Reflections collected	2877
Independent reflections	1935 [R(int) = 0.0161]
Completeness to theta = 25.50°	97.8 %
Absorption correction	Empirical
Max. and min. transmission	0.9441 and 0.9441
Refinement method	Full-matrix least-squares on F^2
Data / restraints / parameters	1935 / 0 / 136
Goodness-of-fit on F^2	1.076
Final R indices [I>2sigma(I)]	R_1 = 0.0478, wR_2 = 0.1304
R indices (all data)	R_1 = 0.0508, wR_2 = 0.1330
Largest diff. peak and hole	0.262 and −0.242 e.Å^{-3}

Molecular orbital calculations.

Molecular structures were optimized by DFT methods at the B3LYP/6-31G(d) level using Gaussian 03 package[3] with the Cartesian coordinates obtained from X-ray crystallography of **1a**, **1c**, and **2a** as an initial structure.   As for **1b**, **1d**, **2b**, and **2c**, the initial Cartesian coordinates were obtained by substitution of piperidino and dimethylamino groups of the initial structure of **1a**, **1c**, and **2a** with the corresponding amino groups.   Energy levels of molecular orbitals were calculated at the B3LYP/6-31G(d) level.   Absolute energies (in hartree) of calculated compounds are as follows: −1562.541512 (**1a**), −1483.898569 (**1b**), −1329.056610 (**1c**), −1250.451525 (**1d**), −1562.539256 (**2a**), −1483.897862 (**2b**), −1329.054389 (**2c**), −1045.728223 (**3**), −888.458133 (**4**), −1422.862833 (**5**), and −1499.032606 (**6**).   Detail results on TD-DFT calculations of **2a** and **3**–**6** are shown in Table 34.

Table 9.   Cartesian coordinates of the initial structure of **1a**.

C	0.647332	0.372881	−0.408557	C	−4.761059	−2.018294	−1.783707	H	0.664631	1.231337	5.191838
H	1.463308	0.858705	−0.935266	H	−5.767854	−2.080410	−1.352229	H	0.994437	−0.350376	5.905676
C	1.472272	1.444517	1.689877	H	−4.776217	−1.218915	−2.535599	C	0.239862	−0.429373	3.888402
H	1.063506	1.949187	2.562096	C	−3.765727	−1.633841	−0.681799	H	1.220828	−0.376951	3.412207
C	2.756665	1.658929	1.370974	H	−4.019474	−0.652414	−0.269904	H	−0.021521	−1.501000	3.976820
H	3.252133	1.156617	0.544760	H	−3.837395	−2.368938	0.143384	F	3.013460	3.171802	3.179690
C	3.633508	2.601078	2.122756	C	−2.098878	0.189164	3.591482	F	4.080640	3.605663	1.329078
C	−1.979728	−2.861286	−1.797999	H	−2.449690	−0.856817	3.688813	F	4.737811	1.972193	2.598032
H	−1.972120	−3.633173	−1.005077	H	−2.781610	0.702013	2.907268	F	1.630668	−1.440269	−5.320030
H	−0.955341	−2.766241	−2.163124	C	−2.130023	0.858052	4.971189	F	−0.335314	−0.500111	−5.366684
C	−2.915171	−3.295850	−2.928567	H	−1.905119	1.925257	4.848093	F	1.468423	0.723639	−5.365203
H	−2.595752	−4.276608	−3.302083	H	−3.144115	0.783522	5.383245	N	−0.748466	0.251234	3.027676
H	−2.821242	−2.585811	−3.760710	C	−1.109513	0.218392	5.921629	N	−2.407261	−1.568812	−1.225656
C	−4.370916	−3.345938	−2.446288	H	−1.416938	−0.814573	6.142084				
H	−5.046548	−3.573030	−3.279527	H	−1.089282	0.751750	6.879507				
H	−4.483146	−4.162010	−1.717283	C	0.284539	0.205103	5.280474				

Table 10.   Cartesian coordinates of the initial structure of **1b**.

N	1.303783	0.201096	−2.511502	C	1.535245	−0.032201	2.433681	F	4.706089	−0.215993	3.680905
C	1.373450	0.150000	−0.050601	H	1.081367	−0.605911	3.238328	C	3.502783	0.367221	3.906913
H	2.455640	0.207679	−0.075886	F	2.857514	−0.386195	4.823386	C	1.312479	−0.988868	−3.386867
C	0.663537	0.108202	−1.254903	C	0.747579	0.036061	1.198600	H	0.297291	−1.288426	−3.656156

H	1.785970	−1.841801	−2.869714
C	2.732931	0.531718	2.640256
H	3.224405	1.158103	1.900956
F	3.762752	1.566935	4.483429
C	2.661422	0.741678	−2.589361
H	3.389946	0.119870	−2.036055
H	2.695273	1.752745	−2.171239
C	2.159390	−0.547012	−4.599430
H	1.520786	−0.271655	−5.443809
H	2.809888	−1.360046	−4.935126
C	2.966553	0.682482	−4.094226
H	2.615173	1.596129	−4.582936
H	4.039882	0.594638	−4.287127

N	−1.303618	−0.201337	2.511511
C	−1.373262	−0.150033	0.050632
H	−2.455458	−0.207615	0.075958
C	−0.663333	−0.108351	1.254952
C	−1.535095	0.032264	−2.433625
H	−1.081198	0.605962	−3.238271
F	−2.857499	0.386562	−4.823212
C	−0.747407	−0.036106	−1.198559
F	−4.706028	0.216292	−3.680668
C	−3.502741	−0.366921	−3.906780
C	−1.312479	0.988700	3.386851
H	−0.297350	1.287004	3.657798
H	−1.783944	1.842189	2.868837

C	−2.732841	−0.531541	−2.640168
H	−3.224335	−1.157918	−1.900874
F	−3.762754	−1.566581	−4.483391
C	−2.660979	−0.742621	2.589426
H	−3.390060	−0.121043	2.036592
H	−2.694366	−1.753590	2.171027
C	−2.162046	0.548237	4.598280
H	−1.525686	0.276792	5.445602
H	−2.815394	1.360858	4.929423
C	−2.965369	−0.684048	4.094323
H	−2.610245	−1.596375	4.582819
H	−4.038819	−0.599907	4.288217

Table 11. Cartesian coordinates of the initial structure of **1c**.

	2.556157	−2.653845	−2.217835
H	2.669572	−2.618249	−1.133993
H	3.549577	−2.772655	−2.663791
H	1.952349	−3.541628	−2.474205
C	1.801602	−1.433622	−4.165495
H	1.132660	−2.231415	−4.535386
H	2.788673	−1.598017	−4.610623
H	1.423716	−0.469175	−4.514498
C	−2.939856	−0.271129	−3.732891
H	−2.231209	0.432506	−4.177332
H	−3.953578	0.049725	−3.995288
H	−2.779047	−1.267559	−4.182567
C	−3.822375	−1.104897	−1.640733
H	−3.740888	−2.156888	−1.965067
H	−4.821304	−0.740166	−1.903369

H	−3.720455	−1.072466	−0.555647
C	−0.427888	−0.820047	−2.484637
H	−0.616676	−1.221101	−3.472153
C	−1.505467	−0.314656	−1.744734
C	−1.273424	0.162283	−0.425412
C	0.027842	0.087671	0.081782
H	0.227150	0.539742	1.048722
C	1.110773	−0.418895	−0.643561
C	0.870371	−0.894082	−1.962177
C	2.477211	−0.339997	−0.121291
H	3.258337	−0.251700	−0.872863
C	2.833214	−0.358174	1.171055
H	2.118649	−0.493846	1.978121
C	4.243956	−0.203910	1.627880
C	−2.341650	0.833416	0.319140

H	−3.118383	1.288687	−0.290995
C	−2.432771	0.937625	1.652664
H	−1.724584	0.469633	2.330758
C	−3.515901	1.699106	2.337646
F	−3.014007	2.717037	3.079727
F	−4.411573	2.232974	1.478665
F	−4.206168	0.906906	3.196157
F	4.647600	−1.278646	2.351135
F	4.387382	0.874620	2.437067
F	5.117110	−0.058961	0.607128
N	1.943449	−1.418784	−2.717039
N	−2.811082	−0.259495	−2.283124

Table 12. Cartesian coordinates of the initial structure of **1d**.

H	0.207069	−3.993366	0.108309
C	1.122885	−4.466237	1.920616
H	2.216090	−4.357821	1.837292
H	0.859650	−5.502452	1.694767
H	0.837019	−4.267258	2.959323
C	2.945407	−0.306292	4.015758
H	2.296854	−0.931535	4.639141
H	3.450661	0.407496	4.670961
H	3.706633	−0.954005	3.552350
H	2.543675	1.328638	2.786857
C	1.269000	−1.579531	2.032756
H	1.807754	−2.178928	2.753853
C	1.397786	−0.183716	2.072031

C	0.732409	0.612249	1.091069
C	−0.019258	−0.050420	0.117183
H	−0.586669	0.552115	−0.585881
C	−0.164890	−1.438679	0.057191
C	0.505499	−2.220229	1.046295
C	−1.038026	−2.074712	−0.927531
H	−1.516956	−3.003867	−0.622076
C	−1.325887	−1.611281	−2.154050
H	−0.873702	−0.712160	−2.562757
C	−2.285942	−2.282441	−3.074083
C	0.772810	2.071383	1.165251
H	0.899473	2.501842	2.157558
C	0.639975	2.927123	0.139389

H	0.540343	2.598372	−0.891119
C	0.613298	4.406340	0.311446
F	−1.694183	−2.609840	−4.250649
F	−3.328130	−1.473170	−3.386861
F	−2.804183	−3.420848	−2.559265
N	0.390794	−3.598332	1.018664
N	2.157490	0.433925	3.049233
F	0.799230	4.792905	1.594248
F	1.578570	5.006567	−0.430013
F	−0.564910	4.937030	−0.099858

Table 13. Cartesian coordinates of the initial structure of **2a**.

N	−2.473388	1.375266	−0.000539
C	−0.003079	1.375266	−0.000538
H	−0.001990	2.305232	−0.000538
C	−1.219457	0.706831	0.007254
C	2.486298	1.431074	−0.090487
H	3.186228	1.017265	−0.540446
F	4.951031	2.609565	−0.292526
C	1.213601	0.702050	−0.008230
F	3.899704	4.435590	−0.463254
C	4.003534	3.331172	0.283894
C	−3.193491	1.311294	−1.278220
H	−3.136294	0.412370	−1.638271
H	−2.781379	1.916861	−1.914233
C	2.718471	2.623988	0.420441
H	2.034048	3.040258	0.892726
F	4.472337	3.751378	1.444353
C	−2.494083	2.729350	0.544818
H	−2.081665	3.342584	−0.083249
H	−1.988938	2.757484	1.373233

C	−4.642129	1.688493	−1.090144
H	−5.075032	1.031306	−0.524473
H	−5.090040	1.687112	−1.950471
C	−4.766500	3.063598	−0.456498
H	−4.468236	3.739107	−1.086403
H	−5.696035	3.238854	−0.242400
C	−3.933414	3.144989	0.803935
H	−4.317704	2.566957	1.480652
H	−3.949966	4.053944	1.140917
N	2.473077	−1.374955	0.000207
C	0.002769	−1.374955	0.000191
H	0.002653	−2.305736	0.000776
C	1.219146	−0.706520	−0.007626
C	−2.485634	−1.431579	0.090809
H	−3.185863	−1.016819	0.540869
F	−4.951339	−2.609255	0.292233
C	−1.213612	−0.702686	0.007881
F	−3.900009	−4.435430	0.464375
C	−4.003168	−3.330733	−0.283458

C	3.194152	−1.311804	1.278513
H	3.136953	−0.412882	1.638569
H	2.781065	−1.916559	1.913900
C	−2.718781	−2.623680	−0.420734
H	−2.034060	−3.040903	−0.893121
F	−4.472348	−3.752029	−1.444742
C	2.493773	−2.729036	−0.545156
H	2.081654	−3.343221	0.082806
H	1.989601	−2.757982	−1.372947
C	4.642116	−1.689135	1.089713
H	5.075021	−1.031946	0.524047
H	5.090025	−1.687757	1.950041
C	4.766864	−3.063157	0.456893
H	4.468600	−3.738668	1.086796
H	5.695725	−3.238698	0.243477
C	3.933782	−3.144544	−0.803543
H	4.317699	−2.567592	−1.481086
H	3.949959	−4.054580	−1.141357

Table 14. Cartesian coordinates of the initial structure of **2b**.

N	1.303783	0.201096	−2.511502	H	3.389946	0.119870	−2.036055	C	−3.502741	−0.366921	−3.906780
C	1.373450	0.150000	−0.050601	H	2.695273	1.752745	−2.171239	C	−1.312479	0.988700	3.386851
H	2.455640	0.207679	−0.075886	C	2.159390	−0.547012	−4.599430	H	−0.297350	1.287004	3.657798
C	0.663537	0.108202	−1.254903	H	1.520786	−0.271655	−5.443809	H	−1.783944	1.842189	2.868837
C	1.535245	−0.032201	2.433681	C	2.809888	−1.360046	−4.935126	C	−2.732841	−0.531541	−2.640168
H	1.081367	−0.605911	3.238328	C	2.966553	0.682482	−4.094226	H	−3.224335	−1.157918	−1.900874
F	2.857514	−0.386195	4.823386	H	2.615173	1.596129	−4.582936	F	−3.762754	−1.566581	−4.483391
C	0.747579	0.036061	1.198600	H	4.039882	0.594638	−4.287127	C	−2.660979	−0.742621	2.589426
F	4.706089	−0.215993	3.680905	N	−1.303618	−0.201337	2.511511	H	−3.390060	−0.121043	2.036592
C	3.502783	0.367221	3.906913	C	−1.373262	−0.150033	0.050632	H	−2.694366	−1.753590	2.171027
C	1.312479	−0.988868	−3.386867	H	−2.455458	−0.207615	0.075958	C	−2.162046	0.548237	4.598280
H	0.297291	−1.288426	−3.656156	C	−0.663333	−0.108351	1.254952	H	−1.525686	0.276792	5.445602
H	1.785970	−1.841801	−2.869714	C	−1.535095	0.032264	−2.433625	H	−2.815394	1.360858	4.929423
C	2.732931	0.531718	2.640256	H	−1.081198	0.605962	−3.238271	C	−2.965369	−0.684048	4.094323
H	3.224405	1.158103	1.900956	F	−2.857499	0.386562	−4.823212	H	−2.610245	−1.596375	4.582819
F	3.762752	1.566935	4.483429	C	−0.747407	−0.036106	−1.198559	H	−4.038819	−0.599907	4.288217
C	2.661422	0.741678	−2.589361	F	−4.706028	0.216292	−3.680668				

Table 15. Cartesian coordinates of the initial structure of **2c**.

N	1.400025	−0.019332	−2.474575	F	3.694798	1.463913	4.554681	C	−3.390241	−0.257880	−4.014165
C	1.381581	0.023758	−0.005441	C	2.745196	0.539807	−2.482234	C	−1.338351	1.285744	3.211815
H	2.464923	−0.021759	0.005520	H	3.502374	−0.117649	−2.017980	H	−0.315407	1.665439	3.236061
C	0.710848	−0.002855	−1.231464	H	2.751439	1.501407	−1.961868	H	−1.985441	2.059722	2.762861
C	1.444008	−0.051958	2.490825	H	1.666309	−1.118808	−4.243640	C	−2.681111	−0.413148	−2.711069
H	0.910236	−0.531382	3.307774	C	3.048229	0.708191	−3.521337	H	−3.251576	−0.950620	−1.958577
F	2.668740	−0.421323	4.930858	N	−1.400039	0.019411	2.474566	F	−3.695383	−1.463984	−4.554338
C	0.707721	0.021663	1.224261	C	−1.381582	−0.023701	0.005440	C	−2.745219	−0.539704	2.482211
F	4.566423	−0.398504	3.857905	H	−2.464926	0.021802	−0.005526	H	−3.502374	0.117762	2.017934
C	3.390254	0.257803	4.014163	C	−0.710852	0.002932	1.231466	H	−2.751471	−1.501311	1.961859
C	1.338346	−1.285684	−3.211786	C	−1.443999	0.051956	−2.490830	H	−1.666237	1.118826	4.243687
H	0.315384	−1.665336	−3.236096	H	−0.910233	0.531373	−3.307787	H	−3.048270	−0.708066	3.521313
H	1.985372	−2.059679	−2.762768	F	−2.668484	0.420683	−4.931092				
C	2.681155	0.413060	2.711050	C	−0.707720	−0.021607	−1.224260				
H	3.251648	0.950497	1.958555	F	−4.566097	0.399019	−3.858005				

Table 16. Cartesian coordinates of the initial structure of **3**.

N	1.375299	−0.000529	−2.473373	C	3.145022	0.803944	−3.933398	H	−3.738635	1.086804	4.468616
C	1.375299	−0.000529	−0.003063	H	2.566990	1.480662	−4.317688	H	−3.238665	0.243486	5.695741
H	2.305265	−0.000529	−0.001974	H	4.053977	1.140927	−3.949950	C	−3.144511	−0.803535	3.933798
C	0.706864	0.007263	−1.219442	N	−1.374922	0.000215	2.473093	H	−2.567559	−1.481078	4.317716
C	1.431107	−0.090478	2.486314	C	−1.374922	0.000200	0.002784	H	−4.054546	−1.141349	3.949975
H	1.017298	−0.540438	3.186244	H	−2.305702	0.000785	0.002669	C	−3.314068	−1.202428	−1.585690
C	0.702083	−0.008221	1.213617	C	−0.706487	−0.007617	1.219162	H	−2.609916	−1.867124	−1.130441
C	3.363301	0.277707	4.061874	C	−1.431545	0.090819	−2.485618	H	−3.682584	−0.516213	−0.852066
C	1.311327	−1.278210	−3.193475	H	−1.016785	0.540878	−3.185848	H	−4.129409	−1.767079	−1.987297
H	0.412403	−1.638262	−3.136279	C	−0.702653	0.007890	−1.213596	C	3.313382	1.202573	1.585056
H	1.916895	−1.914224	−2.781363	C	−1.311771	1.278522	3.194168	H	3.680219	0.516696	0.850275
C	2.624021	0.420450	2.718468	H	−0.412849	1.638577	3.136969	H	2.609099	1.868254	1.131454
C	2.729383	0.544828	−2.494067	H	−1.916526	1.913908	2.781081	H	4.129798	1.766192	1.985926
H	3.342617	−0.083240	−2.081649	C	−2.623647	−0.420724	−2.718765	C	−3.363084	−0.277161	−4.061978
H	2.757518	1.373242	−1.988922	C	−2.729003	−0.545148	2.493789	H	−4.246509	0.320881	−3.979483
C	1.688526	−1.090134	−4.642113	H	−3.343189	0.082814	2.081669	H	−2.779684	0.188352	−4.828687
H	1.031340	−0.524463	−5.075017	H	−2.757949	−1.372939	1.989617	H	−3.704217	−1.217479	−4.441884
H	1.687145	−1.950461	−5.090024	C	−1.689102	1.089721	4.642132	H	2.779755	−0.188431	4.828091
C	3.063631	−0.456489	−4.766484	H	−1.031914	0.524056	5.075037	H	3.703862	1.218216	4.441821
H	3.739141	−1.086393	−4.468220	H	−1.687724	1.950049	5.090042	H	4.246874	−0.320038	3.978806
H	3.238887	−0.242390	−5.696021	C	−3.063124	0.456902	4.766880				

Table 17. Cartesian coordinates of the initial structure of **4**.

N	1.375271	−0.000494	−2.473413	C	2.729355	0.544864	−2.494107	N	−1.374950	0.000252	2.473053
C	1.375271	−0.000493	−0.003104	H	3.342589	−0.083204	−2.081689	C	−1.374949	0.000236	0.002744
H	2.305237	−0.000493	−0.002014	H	2.757490	1.373278	−1.988962	H	−2.305730	0.000825	0.002628
C	0.706836	0.007299	−1.219482	C	1.688498	−1.090099	−4.642154	C	−0.706515	−0.007581	1.219122
C	1.431079	−0.090441	2.486274	H	1.031312	−0.524428	−5.075057	C	−1.431573	0.090854	−2.485659
H	1.017269	−0.540401	3.186204	H	1.687118	−1.950426	−5.090065	H	−1.016813	0.540914	−3.185888
C	0.702055	−0.008185	1.213577	C	3.063604	−0.456453	−4.766524	C	−0.702681	0.007926	−1.213637
C	1.311300	−1.278175	−3.193515	H	3.739113	−1.086358	−4.468261	C	−1.311800	1.278558	3.194127
H	0.412376	−1.638226	−3.136318	H	3.238860	−0.242355	−5.696060	H	−0.412877	1.638614	3.136929
H	1.916867	−1.914188	−2.781403	C	3.144995	0.803980	−3.933438	H	−1.916555	1.913945	2.781040
C	2.623992	0.420487	2.718446	H	2.566962	1.480697	−4.317728	C	−2.623674	−0.420689	−2.718805
H	3.040263	0.892772	2.034024	H	4.053949	1.140963	−3.949990	H	−3.040898	−0.893075	−2.034085

C	−2.729031	−0.545112	2.493748	H	−1.687753	1.950086	5.090001	H	−2.567587	−1.481041	4.317675
H	−3.343217	0.082851	2.081629	C	−3.063152	0.456938	4.766839	H	−4.054575	−1.141313	3.949934
H	−2.757977	−1.372903	1.989576	H	−3.738663	1.086841	4.468574	H	3.070743	0.334226	3.530262
C	−1.689131	1.089758	4.642092	H	−3.238694	0.243522	5.695701	H	−3.070520	−0.333933	−3.530517
H	−1.031942	0.524092	5.074996	C	−3.144539	−0.803498	3.933758				

Table 18. Cartesian coordinates of the initial structure of **5**.

N	−2.812254	0.284033	−0.140641	H	−5.597553	−0.829301	1.148200	H	5.134110	0.975531	0.343264
C	−0.744733	−0.117769	1.150226	N	2.811791	−0.283490	0.140902	H	5.597867	0.829983	−1.148557
H	−1.245684	−0.198344	1.929581	C	0.744272	0.118327	−1.149963	C	1.559241	−1.224283	4.894638
C	−1.402761	0.130207	−0.046414	H	1.246425	0.198239	−1.929584	O	2.662637	−0.804125	5.240389
C	1.316819	−0.439087	2.512198	C	1.402304	−0.129624	0.046681	O	0.840992	−1.929671	5.804560
H	2.166901	−0.074897	2.603464	C	−1.316085	0.438898	−2.512215	C	−1.559549	1.223966	−4.894557
C	0.637572	−0.249903	1.223465	C	−2.166939	0.074577	−2.602857	O	−2.662224	0.802236	−5.240697
C	−3.264107	1.662508	−0.365906	C	−0.637271	0.250496	−1.223837	O	−0.842047	1.930498	−5.804181
H	−2.698348	2.084810	−1.031151	C	3.264844	−1.662666	0.365887	C	1.558690	−2.039523	7.036526
H	−3.188089	2.168255	0.458413	H	2.699084	−2.084972	1.031130	C	1.347631	−3.389978	7.654973
C	0.820858	−1.082166	3.550690	H	3.187631	−2.167709	−0.458162	H	1.202746	−1.231356	7.720766
H	−0.019606	−1.471034	3.466015	C	−0.821321	1.082670	−3.550438	H	2.641973	−1.866099	6.825751
C	−3.609962	−0.365690	0.895172	H	0.019916	1.471672	−3.466387	H	1.908152	−3.476230	8.617340
H	−3.538550	0.131534	1.724800	C	3.609500	0.366239	−0.894907	H	0.264219	−3.563066	7.865530
H	−3.277779	−1.264524	1.050043	H	3.538862	−0.130848	−1.725158	H	1.703450	−4.197952	6.970395
C	−4.697221	1.680664	−0.837134	H	3.278512	1.264373	−1.050047	C	−1.559575	2.039540	−7.036318
H	−4.756380	1.251901	−1.704282	C	4.697532	−1.679990	0.836768	C	−1.346118	3.388565	−7.657060
H	−4.993036	2.599243	−0.934583	H	4.756690	−1.251233	1.703917	H	−2.643172	1.868494	−6.825191
C	−5.601082	0.959209	0.147967	H	4.993346	−2.598570	0.934213	H	−1.205171	1.229534	−7.719172
H	−5.658652	1.471423	0.970389	C	5.601048	−0.959502	−0.147361	H	−1.906410	3.474141	−8.619620
H	−6.493124	0.884815	−0.225282	H	5.658618	−1.471713	−0.969785	H	−1.700574	4.198316	−6.973876
C	−5.062499	−0.422196	0.449622	H	6.492620	−0.885643	0.225188	H	−0.262397	3.559417	−7.867850
H	−5.133795	−0.974855	−0.343617	C	5.062467	0.421905	−0.449010				

Table 19. Cartesian coordinates of the initial structure of **6**.

N	1.375376	−0.000629	−2.473342	C	−1.374845	0.000101	0.002814	C	−3.363007	−0.277261	−4.061948
C	1.375376	−0.000629	−0.003033	H	−2.305626	0.000685	0.002699	O	−4.473447	−0.763809	−4.252996
H	2.305342	−0.000629	−0.001944	C	−0.706410	−0.007716	1.219192	C	3.363378	0.277608	4.061904
C	0.706941	0.007164	−1.219411	C	−1.431468	0.090719	−2.485588	O	4.474301	0.763270	4.252399
C	1.431183	−0.090577	2.486344	H	−1.016708	0.540778	−3.185817	C	3.313458	1.202474	1.585086
H	1.017374	−0.540536	3.186275	C	−0.702576	0.007791	−1.213566	O	4.423245	1.708839	1.720266
C	0.702159	−0.008320	1.213647	C	−1.311695	1.278422	3.194197	C	−2.616477	0.517445	−5.149485
C	1.311405	−1.278310	−3.193444	H	−0.412773	1.638478	3.136999	H	−2.245328	1.430358	−4.732666
H	0.412480	−1.638362	−3.136248	H	−1.916450	1.913809	2.781111	H	−1.798108	−0.064903	−5.518323
H	1.916972	−1.914324	−2.781332	C	−2.623570	−0.420824	−2.718735	H	−3.287305	0.739046	−5.953092
C	2.624097	0.420351	2.718517	C	−2.728927	−0.545247	2.493819	C	−2.519807	−1.305871	−0.270292
C	2.729460	0.544728	−2.494036	H	−3.343112	0.082715	2.081699	H	−1.474024	−1.365051	−0.488780
H	3.342694	−0.083339	−2.081618	H	−2.757872	−1.373038	1.989647	H	−2.710324	−0.441035	0.330260
H	2.757595	1.373142	−1.988891	C	−1.689026	1.089622	4.642162	H	−2.823269	−2.183330	0.261569
C	1.688603	−1.090234	−4.642083	H	−1.031837	0.523957	5.075067	C	2.616000	−0.515000	5.150389
H	1.031417	−0.524563	−5.074946	H	−1.687648	1.949950	5.090087	H	1.794049	0.065844	5.513591
H	1.687222	−1.950561	−5.089994	C	−3.063047	0.456803	4.766909	H	2.249903	−1.431254	4.736440
C	3.063709	−0.456588	−4.766453	H	−3.738559	1.086705	4.468645	H	3.284766	−0.730299	5.957419
H	3.739218	−1.086493	−4.468190	H	−3.238589	0.243387	5.695772	C	2.517727	1.306935	0.270742
H	3.238964	−0.242490	−5.695989	C	−3.144434	−0.803634	3.933828	H	2.706572	0.442025	−0.330230
C	3.145180	0.803845	−3.933367	H	−2.567482	−1.481177	4.317746	H	1.472285	1.367176	0.490561
H	2.567067	1.480562	−4.317657	H	−4.054471	−1.141448	3.950005	H	2.821449	2.184185	−0.261317
H	4.054054	1.140827	−3.949919	C	−3.313990	−1.202528	−1.585660				
N	−1.374845	0.000116	2.473123	O	−4.423379	−1.709484	−1.721896				

Table 20. Cartesian coordinates of the optimized structure of **1a**.

C	0.907107	−0.395551	−4.844365	C	1.472272	1.444517	1.689877	H	−4.483146	−4.162010	−1.717283
C	0.912263	−0.369386	−3.353936	H	1.063506	1.949187	2.562096	C	−4.761059	−2.018294	−1.783707
H	1.905024	−0.329863	−2.914317	C	2.756665	1.658929	1.370974	H	−5.767854	−2.080410	−1.352229
C	−0.210166	−0.403202	−2.621578	H	3.252133	1.156617	0.544760	H	−4.776217	−1.218915	−2.535599
H	−1.162406	−0.491828	−3.139044	C	3.633508	2.601078	2.122756	C	−3.765727	−1.633841	−0.681799
C	−0.301570	−0.324958	−1.162256	C	−1.979728	−2.861286	−1.797999	H	−4.019474	−0.652414	−0.269904
C	−1.437558	−0.853861	−0.488829	H	−1.972120	−3.633173	−1.005077	H	−3.837395	−2.368938	0.143384
C	−1.567748	−0.644427	0.890772	H	−0.955341	−2.766241	−2.163124	C	−2.098878	0.189164	3.591482
H	−2.408076	−1.088378	1.409013	C	−2.915171	−3.295850	−2.928567	H	−2.449690	−0.856817	3.688813
C	−0.609139	0.056002	1.635544	H	−2.595752	−4.276608	−3.302083	H	−2.781610	0.702013	2.907268
C	0.529111	0.587805	0.968327	H	−2.821242	−2.585811	−3.760710	C	−2.130023	0.858052	4.971189
C	0.647332	0.372881	−0.408557	C	−4.370916	−3.345938	−2.446288	H	−1.905119	1.925257	4.848093
H	1.463308	0.858705	−0.935266	H	−5.046548	−3.573030	−3.279527	H	−3.144116	0.783522	5.383245

C	−1.109513	0.218392	5.921629	C	0.239862	−0.429373	3.888402	F	1.630668	−1.440269	−5.320030
H	−1.416938	−0.814573	6.142084	H	1.220828	−0.376951	3.412207	F	−0.335314	−0.500111	−5.366684
H	−1.089282	0.751750	6.879507	H	−0.021521	−1.501000	3.976820	F	1.468423	0.723639	−5.365203
C	0.284539	0.205103	5.280474	F	3.013460	3.171802	3.179690	N	−0.748466	0.251234	3.027676
H	0.664631	1.231337	5.191838	F	4.080640	3.605663	1.329078	N	−2.407261	−1.568812	−1.225656
H	0.994437	−0.350376	5.905676	F	4.737811	1.972193	2.598032				

Table 21. Cartesian coordinates of the optimized structure of **1b**.

C	2.556457	−2.653341	−2.217716	H	−3.720581	−1.071436	−0.555383	H	−3.118577	1.288764	−0.291111
H	2.669881	−2.617564	−1.133873	C	−0.427814	−0.819752	−2.484555	C	−2.433149	0.937921	1.652662
H	3.549898	−2.772032	−2.663672	H	−0.616631	−1.220941	−3.472031	H	−1.724959	0.470037	2.330854
H	1.952800	−3.541269	−2.473960	C	−1.505386	−0.314277	−1.744700	C	−3.516638	1.699011	2.337613
C	1.801376	−1.433728	−4.165534	C	−1.273345	0.162768	−0.425388	F	−3.015195	2.716964	3.079983
H	1.132491	−2.231725	−4.535059	C	0.027982	0.088198	0.081766	F	−4.412384	2.232809	1.478641
H	2.788387	−1.598113	−4.610808	H	0.227321	0.540318	1.048695	F	−4.206849	0.906539	3.195890
H	1.423289	−0.469437	−4.514775	C	1.110947	−0.418435	−0.643564	F	4.647837	−1.279431	2.350878
C	−2.939767	−0.271349	−3.732895	C	0.870480	−0.893715	−1.962161	F	4.388414	0.873862	2.437195
H	−2.231067	0.432059	−4.177627	C	2.477471	−0.339741	−0.121331	F	5.117784	−0.059631	0.607106
H	−3.953459	0.049497	−3.995425	H	3.258555	−0.251619	−0.872994	N	1.943503	−1.418452	−2.717086
H	−2.779042	−1.267961	−4.182176	C	2.833662	−0.358164	1.170977	N	−2.811001	−0.259168	−2.283102
C	−3.822306	−1.104414	−1.640482	H	2.119138	−0.493807	1.978109				
H	−3.740630	−2.156542	−1.964313	C	4.244517	−0.204444	1.627787				
H	−4.821234	−0.739913	−1.903469	C	−2.341762	0.833739	0.319136				

Table 22. Cartesian coordinates of the optimized structure of **1c**.

C	2.556457	−2.653341	−2.217716	H	−3.720581	−1.071436	−0.555383	H	−3.118577	1.288764	−0.291111
H	2.669881	−2.617564	−1.133873	C	−0.427814	−0.819752	−2.484555	C	−2.433149	0.937921	1.652662
H	3.549898	−2.772032	−2.663672	H	−0.616631	−1.220941	−3.472031	H	−1.724959	0.470037	2.330854
H	1.952800	−3.541269	−2.473960	C	−1.505386	−0.314277	−1.744700	C	−3.516638	1.699011	2.337613
C	1.801376	−1.433728	−4.165534	C	−1.273345	0.162768	−0.425388	F	−3.015195	2.716964	3.079983
H	1.132491	−2.231725	−4.535059	C	0.027982	0.088198	0.081766	F	−4.412384	2.232809	1.478641
H	2.788387	−1.598113	−4.610808	H	0.227321	0.540318	1.048695	F	−4.206849	0.906539	3.195890
H	1.423289	−0.469437	−4.514775	C	1.110947	−0.418435	−0.643564	F	4.647837	−1.279431	2.350878
C	−2.939767	−0.271349	−3.732895	C	0.870480	−0.893715	−1.962161	F	4.388414	0.873862	2.437195
H	−2.231067	0.432059	−4.177627	C	2.477471	−0.339741	−0.121331	F	5.117784	−0.059631	0.607106
H	−3.953459	0.049497	−3.995425	H	3.258555	−0.251619	−0.872994	N	1.943503	−1.418452	−2.717086
H	−2.779042	−1.267961	−4.182176	C	2.833662	−0.358164	1.170977	N	−2.811001	−0.259168	−2.283102
C	−3.822306	−1.104414	−1.640482	H	2.119138	−0.493807	1.978109				
H	−3.740630	−2.156542	−1.964313	C	4.244517	−0.204444	1.627787				
H	−4.821234	−0.739913	−1.903469	C	−2.341762	0.833739	0.319136				

Table 23. Cartesian coordinates of the optimized structure of **1d**.

H	0.207069	−3.993366	0.108309	C	0.732409	0.612248	1.091068	H	0.540343	2.598372	−0.891119
C	1.122885	−4.466238	1.920616	C	−0.019258	−0.050420	0.117183	C	0.613298	4.406339	0.311446
H	2.216090	−4.357821	1.837292	H	−0.586669	0.552115	−0.585881	F	−1.694183	−2.609841	−4.250648
H	0.859650	−5.502452	1.694767	C	−0.164890	−1.438679	0.057190	F	−3.328130	−1.473171	−3.386861
H	0.837019	−4.267259	2.959323	C	0.505500	−2.220230	1.046295	F	−2.804183	−3.420848	−2.559265
C	2.945407	−0.306293	4.015759	C	−1.038026	−2.074713	−0.927532	N	0.390795	−3.598333	1.018664
H	2.296854	−0.931536	4.639141	H	−1.516956	−3.003867	−0.622076	N	2.157490	0.433924	3.049232
H	3.450661	0.407495	4.670961	C	−1.325887	−1.611281	−2.154051	F	0.799230	4.792904	1.594248
H	3.706633	−0.954006	3.552350	H	−0.873702	−0.712160	−2.562757	F	1.578570	5.006567	−0.430013
H	2.543675	1.328637	2.786856	C	−2.285942	−2.282442	−3.074084	F	−0.564910	4.937029	−0.099858
C	1.269000	−1.579532	2.032756	C	0.772818	2.071382	1.165251				
H	1.807754	−2.178929	2.753853	H	0.899473	2.501841	2.157558				
C	1.397786	−0.183717	2.072031	C	0.639975	2.927122	0.139389				

Table 24. Cartesian coordinates of the optimized structure of **2a**.

N	1.389792	−0.028463	−2.479286	H	0.313244	−1.704319	−3.147968	C	3.107967	−0.456131	−4.797161
C	1.382242	0.016625	−0.010531	H	2.001998	−2.046710	−2.747874	H	3.870814	−1.164063	−4.440916
H	2.465420	−0.034578	−0.003598	C	2.691219	0.403143	2.705047	H	3.347020	−0.236519	−5.844641
C	0.707102	−0.008010	−1.234486	H	3.268528	0.930126	1.950304	C	3.170177	0.822022	−3.950465
C	1.450189	−0.052057	2.486226	F	3.718738	1.459239	4.537704	H	2.504944	1.583649	−4.377270
H	0.911985	−0.521553	3.305959	C	2.737362	0.546725	−2.505455	H	4.185452	1.237871	−3.949171
F	2.657527	−0.401947	4.935596	H	3.477621	−0.127793	−2.032298	N	−1.389797	0.028451	2.479313
C	0.712087	0.020177	1.221122	H	2.725673	1.476432	−1.927604	C	−1.382229	−0.016629	0.010565
F	4.558990	−0.427559	3.869284	C	1.722394	−1.106009	−4.683951	H	−2.465405	0.034563	0.003631
C	3.394137	0.251898	4.011670	H	0.971688	−0.468506	−5.169377	C	−0.707090	0.008015	1.234522
C	1.327890	−1.305356	−3.218336	H	1.705000	−2.075699	−5.196743	C	−1.450153	0.052014	−2.486203

H	−0.911907	0.521432	−3.305952	C	−2.691183	−0.403173	−2.705052	H	−1.705204	2.075734	5.196716
F	−2.657044	0.401067	−4.935905	H	−3.268536	−0.930119	−1.950318	C	−3.108093	0.456103	4.797112
C	−0.712073	−0.020177	−1.221088	F	−3.719610	−1.459185	−4.537209	H	−3.870953	1.163998	4.440822
F	−4.558422	0.428511	−3.869504	C	−2.737350	−0.546781	2.505445	H	−3.347178	0.236503	5.844589
C	−3.394081	−0.251878	−4.011680	H	−3.477613	0.127703	2.032246	C	−3.170211	−0.822068	3.950440
C	−1.327976	1.305362	3.218344	H	−2.725606	−1.476498	1.927610	H	−2.504961	−1.583656	4.377287
H	−0.313344	1.704366	3.148019	C	−1.722539	1.106030	4.683948	H	−4.185467	−1.237962	3.949110
H	−2.002092	2.046679	2.747839	H	−0.971835	0.468565	5.169425				

Table 25. Cartesian coordinates of the optimized structure of **2b**.

N	1.303782	0.201096	−2.511501	H	3.389945	0.119870	−2.036055	C	−3.502742	−0.366921	−3.906780
C	1.373450	0.150000	−0.050600	H	2.695273	1.752745	−2.171238	C	−1.312480	0.988700	3.386851
H	2.455640	0.207679	−0.075886	C	2.159389	−0.547012	−4.599429	H	−0.297351	1.287004	3.657799
C	0.663537	0.108201	−1.254902	H	1.520785	−0.271655	−5.443808	H	−1.783945	1.842189	2.868837
C	1.535244	−0.032201	2.433682	H	2.809887	−1.360046	−4.935125	C	−2.732842	−0.531541	−2.640168
H	1.081366	−0.605911	3.238329	C	2.966552	0.682482	−4.094225	H	−3.224335	−1.157918	−1.900874
F	2.857513	−0.386195	4.823387	H	2.615172	1.596129	−4.582935	F	−3.762754	−1.566581	−4.483390
C	0.747579	0.036061	1.198601	H	4.039882	0.594638	−4.287127	C	−2.660980	−0.742621	2.589427
F	4.706089	−0.215993	3.680906	N	−1.303619	−0.201337	2.511512	H	−3.390060	−0.121043	2.036592
C	3.502782	0.367221	3.906913	C	−1.373262	−0.150033	0.050633	H	−2.694366	−1.753590	2.171027
C	1.312478	−0.988868	−3.386867	H	−2.455458	−0.207615	0.075958	C	−2.162047	0.548237	4.598281
H	0.297290	−1.288426	−3.656155	C	−0.663333	−0.108351	1.254953	H	−1.525686	0.276792	5.445603
H	1.785969	−1.841801	−2.869714	C	−1.535096	0.032264	−2.433625	H	−2.815395	1.360858	4.929423
C	2.732930	0.531718	2.640256	H	−1.081199	0.605962	−3.238271	C	−2.965370	−0.684048	4.094324
H	3.224405	1.158103	1.900956	F	−2.857500	0.386562	−4.823212	H	−2.610245	−1.596375	4.582819
F	3.762751	1.566935	4.483430	C	−0.747407	−0.036107	−1.198558	H	−4.038819	−0.599907	4.288218
C	2.661422	0.741678	−2.589361	F	−4.706028	0.216292	−3.680667				

Table 26. Cartesian coordinates of the optimized structure of **2c**.

N	1.400025	−0.019332	−2.474574	F	3.694797	1.463911	4.554680	C	−3.390241	−0.257878	−4.014163
C	1.381581	0.023758	−0.005440	C	2.745196	0.539807	−2.482234	C	−1.338352	1.285744	3.211817
H	2.464923	−0.021759	0.005521	H	3.502374	−0.117649	−2.017980	H	−0.315407	1.665439	3.236062
C	0.710848	−0.002855	−1.231463	H	2.751439	1.501407	−1.961867	H	−1.985441	2.059722	2.762862
C	1.444008	−0.051958	2.490825	H	1.666308	−1.118807	−4.243639	C	−2.681111	−0.413148	−2.711069
H	0.910236	−0.531383	3.307774	H	3.048228	0.708191	−3.521337	H	−3.251577	−0.950619	−1.958576
F	2.668740	−0.421324	4.930859	N	−1.400039	0.019410	2.474566	F	−3.695385	−1.463983	−4.554338
C	0.707721	0.021663	1.224262	C	−1.381582	−0.023701	0.005441	C	−2.745219	−0.539704	2.482211
F	4.566422	−0.398505	3.857906	H	−2.464926	0.021802	−0.005525	H	−3.502374	0.117762	2.017935
C	3.390254	0.257802	4.014163	C	−0.710852	0.002932	1.231467	H	−2.751472	−1.501312	1.961860
C	1.338346	−1.285684	−3.211787	C	−1.443999	0.051957	−2.490830	H	−1.666237	1.118825	4.243686
H	0.315384	−1.665336	−3.236095	H	−0.910233	0.531373	−3.307787	H	−3.048270	−0.708066	3.521313
H	1.985372	−2.059678	−2.762768	F	−2.668485	0.420685	−4.931091				
C	2.681155	0.413059	2.711050	C	−0.707720	−0.021607	−1.224260				
H	3.251647	0.950497	1.958555	F	−4.566097	0.399019	−3.858005				

Table 27. Cartesian coordinates of the optimized structure of **3**.

N	1.331040	−0.061072	−2.511160	C	3.112160	0.747427	−4.004922	H	−3.740537	1.255556	4.521227
C	1.376197	−0.024504	−0.043630	H	2.463350	1.532504	−4.414647	H	−3.228086	0.300426	5.911172
H	2.455723	−0.115090	−0.068587	H	4.140005	1.132015	−4.017404	C	−3.112130	−0.747474	4.004885
C	0.667729	−0.034296	−1.250140	N	−1.331018	0.061050	2.511128	H	−2.463310	−1.532546	4.414607
C	1.517723	−0.087527	2.464939	C	−1.376174	0.024498	0.043598	H	−4.139972	−1.132074	4.017362
H	1.035085	−0.709009	3.219775	H	−2.455701	0.115063	0.068553	C	−3.448142	−1.472633	−1.940658
C	0.749796	0.014794	1.212170	C	−0.667705	0.034288	1.250108	H	−2.844877	−1.859801	−1.116328
C	3.345524	0.170903	4.121068	C	−1.517709	0.087824	−2.464962	H	−4.358589	−1.026343	−1.514183
C	1.213911	−1.324127	−3.260049	H	−1.035049	0.708923	−3.219844	H	−3.781392	−2.322603	−2.551819
H	0.185413	−1.681878	−3.179717	C	−0.749772	−0.014791	−1.212199	C	3.448055	1.472831	1.940841
H	1.868352	−2.096668	−2.810205	C	−1.213903	1.324104	3.260021	H	4.358517	1.026640	1.514298
C	2.694129	0.482929	2.795053	H	−0.185410	1.681867	3.179693	H	2.844769	1.860100	1.116575
C	2.692908	0.471050	−2.555752	H	−1.868353	2.096639	2.810182	H	3.781275	2.322725	2.552124
H	3.423811	−0.227940	−2.101944	C	−2.694160	−0.482887	−2.795002	C	−3.345577	−0.170917	−4.121019
H	2.720849	1.394947	−1.969180	C	−2.692878	−0.471087	2.555715	H	−4.347965	0.258027	−3.976781
C	1.592243	−1.124773	−4.730513	H	−3.423789	0.227898	2.101911	H	−2.757601	0.540313	−4.709579
H	0.856317	−0.455318	−5.195256	H	−2.720810	−1.394980	1.969139	H	−3.484427	−1.082115	−4.720481
H	1.533649	−2.087536	−5.254107	C	−1.592234	1.124739	4.730485	H	2.757576	−0.540410	4.709553
C	2.996312	−0.520321	−4.861652	H	−0.856301	0.455290	5.195226	H	3.484293	1.082064	4.720603
H	3.740545	−1.255612	−4.521256	H	−1.533651	2.087502	5.254084	H	4.347943	−0.257963	3.976830
H	3.228102	−0.300482	−5.911205	C	−2.996299	0.520270	4.861619				

Table 28. Cartesian coordinates of the optimized structure of **4**.

N	1.378125	−0.015213	−2.487739	H	1.708658	−2.073807	−5.194417	C	−2.720485	−0.406333	−2.688216
C	1.378996	0.007941	−0.017834	C	3.111465	−0.454526	−4.792385	H	−3.279781	−0.937136	−1.921485
H	2.462016	−0.046883	−0.017595	H	3.870831	−1.161051	−4.425651	C	−2.725326	−0.556771	2.508498
C	0.695116	−0.001493	−1.237268	H	3.359266	−0.241631	−5.839584	H	−3.464927	0.116007	2.030428
C	1.480700	−0.057940	2.480691	C	3.167909	0.827676	−3.951418	H	−2.712622	−1.487391	1.932089
H	0.949534	−0.536301	3.302177	H	2.504515	1.586609	−4.386180	C	−1.724461	1.102190	4.684578
C	0.722647	0.009406	1.221401	H	4.183197	1.244130	−3.946470	H	−0.979298	0.463733	5.177692
C	1.317726	−1.292985	−3.220535	N	−1.378127	0.015216	2.487737	H	−1.708659	2.073810	5.194415
H	0.299719	−1.684373	−3.157470	C	−1.378998	−0.007937	0.017833	C	−3.111462	0.454526	4.792387
H	1.984356	−2.038146	−2.743804	H	−2.462018	0.046887	0.017593	H	−3.870830	1.161047	4.425651
C	2.720489	0.406315	2.688216	C	−0.695117	0.001495	1.237267	H	−3.359261	0.241631	5.839587
H	3.279805	0.937091	1.921483	C	−1.480708	0.057949	−2.480690	C	−3.167905	−0.827679	3.951420
C	2.725326	0.556769	−2.508497	H	−0.949557	0.536340	−3.302170	H	−2.504508	−1.586610	4.386180
H	3.464924	−0.116011	−2.030424	C	−0.722649	−0.009403	−1.221402	H	−4.183191	−1.244134	3.946476
H	2.712625	1.487391	−1.932089	C	−1.317729	1.292988	3.220532	H	3.216032	0.276796	3.646050
C	1.724461	−1.102187	−4.684580	H	−0.299721	1.684376	3.157465	H	−3.216041	−0.276809	−3.646043
H	0.979301	−0.463727	−5.177694	H	−1.984359	2.038149	2.743801				

Table 29. Cartesian coordinates of the optimized structure of **5**.

N	−2.831565	0.236297	−0.049441	H	−5.624892	−1.211332	1.243278	H	5.116897	1.193048	0.450989
C	−0.730543	−0.246842	1.147979	N	2.831459	−0.235993	0.049552	H	5.624805	1.211594	−1.243173
H	−1.284951	−0.383152	2.069776	C	0.730439	0.247126	−1.147889	C	1.695361	−1.413953	4.747069
C	−1.419477	0.108912	−0.014180	H	1.284847	0.383430	−2.069688	O	2.845877	−1.038311	4.883706
C	1.364214	−0.627275	2.451982	C	1.419370	−0.108615	0.014272	O	1.001277	−2.056343	5.720957
H	2.393347	−0.278604	2.505603	C	−1.364313	0.627524	−2.451906	C	−1.695440	1.414113	−4.747027
C	0.668309	−0.355549	1.196313	H	−2.393449	0.278863	−2.505520	O	−2.846125	1.038925	−4.883484
C	−3.350317	1.612211	−0.178311	C	−0.668414	0.355832	−1.196227	O	−1.001095	2.055814	−5.721184
H	−2.731411	2.156371	−0.895432	C	3.350214	−1.611897	0.178497	C	1.712676	−2.274031	6.957015
H	−3.264786	2.139012	0.791776	H	2.731296	−2.156024	0.895636	C	0.772210	−2.994664	7.905198
C	0.867192	−1.254167	3.535865	H	3.264702	−2.138747	−0.791565	H	2.036215	−1.306525	7.355323
H	−0.132711	−1.676425	3.566718	C	−0.867272	1.254349	−3.535821	H	2.614475	−2.859735	6.748960
C	−3.596735	−0.542846	0.926583	H	0.132639	1.676585	−3.566692	H	1.276054	−3.180987	8.859999
H	−3.549136	−0.091467	1.937059	C	3.596643	0.543115	−0.926490	H	−0.122978	−2.394956	8.099340
H	−3.154093	−1.541785	0.993049	H	3.549067	0.091694	−1.936947	H	0.457659	−3.956855	7.488127
C	−4.811668	1.602651	−0.634570	H	3.154000	1.542050	−0.993007	C	−1.712409	2.273303	−6.957325
H	−4.861931	1.194235	−1.652171	C	4.811554	−1.602309	0.634785	C	−0.771345	2.992352	−7.906114
H	−5.181253	2.634746	−0.680072	H	4.861794	−1.193846	1.652366	H	−2.613611	2.860048	−6.749594
C	−5.676488	0.758141	0.311027	H	5.181146	−2.634400	0.680344	H	−2.036944	1.305833	−7.354904
H	−5.738859	1.257320	1.283470	C	5.676392	−0.757838	−0.310833	H	−1.275127	3.178550	−8.860971
H	−6.702319	0.681798	−0.069240	H	5.738781	−1.257060	−1.289223	H	−0.455762	3.954500	−7.489730
C	−5.064931	−0.637381	0.494237	H	6.702212	−0.681474	0.069447	H	0.123206	2.391607	−8.099977
H	−5.117016	−1.192713	−0.450894	C	5.064834	0.637673	−0.494118				

Table 30. Cartesian coordinates of the optimized structure of **6**.

N	1.225768	−0.213819	−2.552464	C	−1.384757	−0.008776	0.106785	C	−3.442599	−0.365480	−4.019426
C	1.384705	0.008714	−0.106588	H	−2.463331	0.040779	0.161402	O	−4.523397	−0.881825	−4.281979
H	2.463276	−0.040897	−0.161243	C	−0.623051	0.105378	1.271946	C	3.442749	0.365987	4.019380
C	0.622999	−0.105449	−1.271749	C	−1.589558	−0.076342	−2.394799	O	4.523451	0.882692	4.281632
C	1.589525	0.076331	2.394990	H	−1.067118	0.438105	−3.199770	C	3.611967	1.482548	1.751628
H	1.067107	−0.437955	3.200080	C	−0.795967	−0.112539	−1.164896	O	4.107098	1.045418	0.727232
C	0.795912	0.112448	1.165094	C	−1.106441	1.532566	3.205667	C	−2.762425	0.534513	−5.041464
C	1.106393	−1.532649	−3.205468	H	−0.092612	1.911120	3.054844	H	−2.601906	1.542818	−4.644342
H	0.092565	−1.911204	−3.054641	H	−1.797771	2.252646	2.728312	H	−1.784340	0.137548	−5.338021
H	1.797723	−2.252726	−2.728110	C	−2.807719	−0.599230	−2.689811	H	−3.406361	0.591118	−5.920770
C	2.807730	0.599204	2.689764	C	−2.584054	−0.330499	2.689117	C	−3.747306	−2.939241	−2.143019
C	2.584006	0.330417	−2.688926	H	−3.333766	0.331054	2.217823	H	−2.753999	−3.394261	−2.248740
H	3.333722	−0.331125	−2.217621	H	−2.627490	−1.288648	2.163716	H	−4.317852	−3.470505	−1.377877
H	2.627437	1.288578	−2.163543	C	−1.421717	1.433297	4.700648	H	−4.253137	−3.012327	−3.110179
C	1.421670	−1.433389	−4.700448	H	−0.655916	0.811327	5.184372	C	2.762818	−0.533793	5.041749
H	0.655873	−0.811421	−5.184177	H	−1.360026	2.432181	5.150331	H	1.784695	−0.136884	5.338260
H	1.359978	−2.432276	−5.150126	C	−2.807221	0.816113	4.931625	H	2.602410	−1.542232	4.644925
C	2.807177	−0.816213	−4.931427	H	−3.577650	1.514730	4.574170	H	3.406828	−0.590042	5.921021
H	3.577602	−1.514830	−4.573960	H	−2.989609	0.667080	6.002739	C	3.746272	2.939263	2.141457
H	2.989569	−0.667186	−6.002540	C	−2.935674	−0.510011	4.169870	H	4.317636	3.469987	1.376555
C	2.935631	0.509915	−4.169681	H	−2.260017	−1.257012	4.606998	H	2.752574	3.393901	2.245213
H	2.259976	1.256915	−4.606814	H	−3.955468	−0.905649	4.250496	H	4.250666	3.013621	3.109267
H	3.955426	0.905550	−4.250307	C	−3.611916	−1.482937	−1.751992				
N	−1.225816	0.213738	2.552663	O	−4.106266	−1.046445	−0.726941				

Table 31. Results on TD-DFT calculations of **2a** and **3–6**.

8	excited state	ΔE (eV, nm)[a]	f^{b}	transitions (CI expansion coefficients)
3	1	3.6310 341.46	0.1734	96→98 (–0.18025)
				96→99 (0.11000)
				97→98 (0.64026)
	2	4.4352 279.55	0.3348	96→98 (0.52536)
				97→98 (0.16016)
				97→99 (–0.39297)
	4	4.7569 260.64	0.6105	93→98 (0.14690)
				96→98 (0.36749)
				97→99 (0.51640)
4	1	3.4425 360.16	0.1021	80→82 (–0.18621)
				80→83 (0.11606)
				81→82 (0.64314)
	3	4.4756 277.02	0.2781	80→82 (0.54557)
				81→82 (0.14398)
				81→83 (–0.34606)
	4	4.8131 257.60	0.5354	77→82 (–0.17890)
				77→83 (0.10920)
				80→82 (0.30946)
				81→83 (0.54001)
2a	1	3.1524 393.30	0.1107	111→114 (–0.12003)
				113→114 (0.66053)
	3	4.5118 274.80	0.2751	111→114 (0.52646
				113→116 (–0.40271)
	5	4.8208 257.18	0.6832	110→114 (0.16101)
				110→116 (–0.11769)
				111→114 (0.36679)
				113→116 (0.50160)
5	1	2.6978 459.57	0.1547	118→120 (–0.14437)
				119→120 (0.65528)
	3	3.8430 322.63	0.8713	118→120 (0.63098)
				119→122 (–0.11672)
	6	4.2497 291.75	0.0119	115→120 (0.65237)
				116→121 (0.22333)
	7	4.6069 269.13	0.2443	113→120 (–0.40728)
				118→122 (0.11772)
				119→122 (0.52106)
6	1	2.5164 492.71	0.1225	124→126 (0.12272)
				125→126 (0.66127)
	3	3.2922 376.60	0.0391	119→126 (0.10445)
				120→127 (–0.10080)
				121→126 (0.52281)
				122→127 (0.22280)
				124→126 (0.34653)
	6	3.6273 341.81	0.4703	119→126 (–0.26879)
				120→127 (0.14542)
				121→126 (–0.24681)
				124→126 (0.52288)
	8	3.9244 315.93	0.2113	119→126 (0.53565)
				120→127 (–0.18507)
				121→126 (–0.28057)
				122→129 (–0.11213)
				124→126 (0.16296)

[a] Excitation energy. [b] Oscillator strength.

References

(1) Kobayashi, T.; Eda, T.; Tamura, O.; Ishibashi, H. *J. Org. Chem.* **2002**, *67*, 3156.

(2) Wolfe, J. P.; Buchwald, S. L. *J. Org. Chem.* **2000**, *65*, 1144.

(3) Frisch, M. J.; Trucks, G. W.; Schlegel, H. B.; Scuseria, G. E.; Robb, M. A.; Cheeseman, J. R.; Montgomery, J. A., Jr.; Vreven, T.; Kudin, K. N.; Burant, J. C.; Millam, J. M.; Iyengar, S. S.; Tomasi, J.; Barone, V.; Mennucci, B.; Cossi, M.; Scalmani, G.; Rega, N.; Petersson, G. A.; Nakatsuji, H.; Hada, M.; Ehara, M.; Toyota, K.; Fukuda, R.; Hasegawa, J.; Ishida, M.; Nakajima, T.; Honda, Y.; Kitao, O.; Nakai, H.; Klene, M.; Li, X.; Knox, J. E.; Hratchian, H. P.; Cross, J. B.; Bakken, V.; Adamo, C.; Jaramillo, J.; Gomperts, R.; Stratmann, R. E.; Yazyev, O.; Austin, A. J.; Cammi, R.; Pomelli, C.; Ochterski, J. W.; Ayala, P. Y.; Morokuma, K.; Voth, G. A.; Salvador, P.; Dannenberg, J. J.; Zakrzewski, V. G.; Dapprich, S.; Daniels, A. D.; Strain, M. C.; Farkas, O.; Malick, D. K.; Rabuck, A. D.; Raghavachari, K.; Foresman, J. B.; Ortiz, J. V.; Cui, Q.; Baboul, A. G.; Clifford, S.; Cioslowski, J.; Stefanov, B. B.; Liu, G.; Liashenko, A.; Piskorz, P.; Komaromi, I.; Martin, R. L.; Fox, D. J.; Keith, T.; Al-Laham, M. A.; Peng, C. Y.; Nanayakkara, A.; Challacombe, M.; Gill, P. M. W.; Johnson, B.; Chen, W.; Wong, M. W.; Gonzalez, C.; Pople, J. A. *Gaussian 03*, revision C.02; Gaussian, Inc.: Wallingford, CT, 2004.

(4) Zhao, C.; Wakamiya, A.; Inukai, Y.; Yamaguchi, S. *J. Am. Chem. Soc.* **2006**, *128*, 15934.

(5) (a) Zachariasse, K.; Grobys, M.; Haar, T.; Hebecker, A.; Jiang, Y.; Morawski, O.; Kuhnle, W. *J. Photochem. Photobiol. A: Chemistry A* **1996**, *102*, 59. (b) Yang, J.; Liau, K.; Li, C.; Chen, M. *J. Am. Chem. Soc.* **2007**, *129*, 13183.

(6) (a) Yang, B.; Liu, L.; Lin, D.; Ma, Y.; Ceng, G.; Liu, S. *J. Phys. Org. Chem.* **2005**, *18*, 962. (b) Wang, Z.; Li, Y.; Hanif, M.; Yang, G.; Ma, Y. *J. Phys. Chem. B* **2006**, *110*, 20993. (c) Tong, H.; Dong, Y.; Ha¨usler, M.; Wong, K. S.; Tang, B. Z. *J. Phys. Chem. B* **2007**, *111*, 2000.

(7) (a) Chen, C. T. *Chem. Mater.* **2004**, *16*, 4389. (b) Song, Y. H.; Yeh, S. J.; Chen, C. T.; Chi, Y.; Liu, C. S.; Yu, J. K.; Hu, Y. H.; Chou, P. T.; Peng, S. M.; Lee, G. H. *Adv. Funct. Mater.* **2004**, *14*, 1221. (c) Chiang, C. L.; Wu, M. F.; Dai, D. C.; Wen, Y. S.; Wang, J. K.; Chen, C. T. *Adv. Funct. Mater.* **2005**, *15*, 231. (d) Tung, Y. L.; Lee, S. W.; Chi, Y.; Tao, Y. T.; Chien, C. H.; Cheng, Y. M.; Chou, P. T.; Peng, S. M.; Liu, C. S. *J. Mater. Chem.* **2005**, *15*, 460. (e) Wakamiya, A.; Mori, K.; Yamaguchi, S. *Angew. Chem. Int. Ed.* **2007**, *46*, 4273. (f) Lee, Y. T.; Chiang, C. L.; Chen, C. T. *Chem. Commun.* **2008**, 217. (g) Wakamiya, A.; Sugita, N.; Yamaguchi, S. *Chem. Lett.* **2008**, *37*, 1094.

(8) AIE: (a) Luo, J.; Xie, Z.; Lam, J. W. Y.; Cheng, L.; Chen, H.; Qiu, C.; Kwok, H. S.; Zhan, X.; Liu, Y.; Zhu, D.; Tang, B. Z. *Chem. Commun.* **2001**, 1740. (b) Itami, K.; Ohashi, Y.; Yoshida, J. *J. Org. Chem.* **2005**, *70*, 2778. (c) Tong, H.; Hong, Y.; Dong, Y.; Häussler, M.; Lam, J. W. Y.; Li, Z.; Guo, Z.; Guo, Z.; Tang, B. Z. *Chem. Commun.* **2006**, 3705. (d) Kim, S.; Zheng, Q.; He, G. S.; Bharali, D. J.; Pudavar, H. E.; Baev, A.; Prasad, P. N. *Adv. Funct. Mater.* **2006**, *16*, 2317. (e) Ning, Z.; Chen, Z.; Zhang, Q.; Yan, Y.; Qian, S.; Cao, Y.; Tian, H. *Adv. Funct. Mater.* **2007**, *17*, 3799. (f) Dong, Y.; Lam, J. W. Y.; Qin, A.; Sun, J.; Liu, J.; Li, Z.; Sun, J.; Sung, H. H. Y.; Williams, I. D.; Kwok, H. S.; Tang, B. Z. *Chem. Commun.* **2007**, 3255.

(9) Xie, Z.; Yang, B.; Liu, L.; Li, M.; Lin, D.; Ma, Y.; Cheng, G.; Liu, S. *J. Phys. Org.*

Chem. **2005**, *18*, 962.

(10) Fagerlund, U. H. M.; Idler, D. R. *J. Am. Chem. Soc.* **1957**, *79*, 6473.

(11) Bonifacio, M. C.; Robertson, C. R.; Jung, J.-Y.; King, B. T. *J. Org. Chem.* **2005**, *70*, 8522.

(12) Kobayashi, T.; Eda, T.; Tamura, O.; Ishibashi, H. *J. Org. Chem.* **2002**, *67*, 3156.

(13) Liu, B.; Yu, W.-L.; Lai, Y.-H.; Huang, W. *Chem. Mater.* **2001**, *13*, 198.

List of Publications

I. Parts of the present Thesis have been or are to be published in the following journals.

Chapter 2

Facile Synthesis of Trifluoromethyl-substituted Enynes: Remarkable Reactivity and Stereoselectivity of Tributyl(3,3,3-trifluoropropynyl)stannane in Carbostannylation of Alkynes

Shimizu, M.; Jiang, G.; Murai, M.; Takeda, Y.; Nakao, Y.; Hiyama, T., Shirakawa, E. *Chem. Lett*. **2005**, *34*, 1700–1701.

Novel Generation of 3,3,3-Trifluoropropynyllithium and Transformation of the Carbonyl Adducts to Trifluoromethyl-substituted Allenes

Shimizu, M.; Higashi, M.; Takeda, Y.; Jiang, G.; Murai, M.; Hiyama, T. *Synlett*, **2007**, 1163–1165.

New Preparation and Synthetic Reactions of 3,3,3-Trifluoropropynyllithium, -borate and –stannane: Facile Synthesis of Trifluoromethylated Allenes, Arylacetylenes and Enynes

Shimizu, M.; Higashi, M.; Takeda, Y.; Murai, M.; Jiang, G.; Asai, Y.; Nakao, Y.; Shirakawa, E.; Hiyama, T. *Future Med. Chem.* **2009**, *1*, 921–945.

Chapter 3

Preparation, Structure, and Diels–Alder Reaction of Phenyl(trifluoromethanesulfonate)(3,3,3-trifluoropropynyl)-λ^3-iodane

Shimizu, M.; Takeda, Y.; Hiyama, T. *Chem. Lett.* **2008**, *37*, 1304–1305.

Chapter 4

Straightforward Synthesis of CF$_3$-Substituted Triarylethenes by Stereoselective Threefold Cross-coupling Reactions

Takeda, Y.; Shimizu, M.; Hiyama, T. *Angew. Chem. Int. Ed.* **2007**, *46*, 8659–8661.

Chapter 5

Synthesis, Structure, and Photophysical Properties of Dimethoxybis(3,3,3-trifluoropropenyl)benzenes

Shimizu, M.; Takeda, Y.; Higashi, M.; Hiyama, T. manuscript in preparation.

Chapter 6

1,4-Bis(alkenyl)-2,5-dipiperidinobenzenes: Minimal Fluorophores Exhibiting Highly Efficient Emission in the Solid State

Shimizu, M.; Takeda, Y.; Higashi, M.; Hiyama, T. *Angew. Chem. Int. Ed.* **2009**, *48*, 3653–3656.

II. Following publication is not included in this Thesis.

Stereoselective Preparation and Cope Rearrangement of 2-CF$_3$-*Cis*-2,3-bis(alkenyl)oxiranes: A Facile Route to 2-CF$_3$-Substituted Oxacycles

Shimizu, M.; Fujimoto, T.; Liu, X.; Takeda, Y.; Hiyama, T. *Heterocycles* **2008**, *76*. 329–351.

Acknowledgment

Youhei Takeda

Department of Material Chemistry

Graduate School of Engineering

Kyoto University